INVESTIGATION OF DOCETAXEL AND DOXORUBICIN RESISTANCE IN MCF-7 BREAST CARCINOMA CELL LINE

A THESIS SUBMITTED TO
THE GRADUATE SCHOOL OF NATURAL AND APPLIED SCIENCES
OF
MIDDLE EAST TECHNICAL UNIVERSITY

BY

ÖZLEM DARCANSOY İŞERİ

IN PARTIAL FULFILLMENT OF THE REQUIREMENTS
FOR
THE DEGREE OF DOCTOR OF PHILOSOPHY
IN
BIOTECHNOLOGY

FEBRUARY 2009

Approval of the thesis:

INVESTIGATION OF DOCETAXEL AND DOXORUBICIN RESISTANCE IN MCF-7 BREAST CARCINOMA CELL LINE

submitted by **ÖZLEM DARCANSOY İŞERİ** in partial fulfillment of the requirements for the degree of **Doctor of Philosophy in Biotechnology Department, Middle East Technical University** by,

Prof. Dr. Canan Özgen _____
Dean, Graduate School of **Natural and Applied Sciences**

Prof. Dr. Gülay Özcengiz _____
Head of Department, **Biotechnology**

Prof. Dr. Ufuk Gündüz _____
Supervisor, **Biological Sciences Dept., METU**

Prof. Dr. Fikret Arpacı _____
Co-Supervisor, **Oncology Dept.,**
Gülhane Military School of Medicine

Examining Committee Members:

Prof. Dr. Semra Kocabıyık _____
Biological Sciences Dept., METU

Prof. Dr. Ufuk Gündüz _____
Biological Sciences Dept., METU

Prof. Dr. Ali Uğur Ural _____
Hematology Dept.,
Gülhane Military School of Medicine

Assist. Prof. Dr. Sreeparna Banerjee _____
Biological Sciences Dept., METU

Assist. Prof. Dr. Dilek Şendil Keskin _____
Engineering Sciences Dept., METU

Date: 13.02.2009

I hereby declare that all information in this document has been obtained and presented in accordance with academic rules and ethical conduct. I also declare that, as required by these rules and conduct, I have fully cited and referenced all material and results that are not original to this work.

Name, Last name : Özlem DARCANSOY İŞERİ

Signature :

ABSTRACT

INVESTIGATION OF DOCETAXEL AND DOXORUBICIN RESISTANCE IN MCF-7 BREAST CARCINOMA CELL LINE

Darcansoy İşeri, Özlem
Ph.D., Department of Biotechnology
Supervisor: Prof. Dr. Ufuk Gündüz
Co-Supervisor: Prof. Dr. Fikret Arpacı

February 2009, 239 pages

Multidrug resistance phenotype of tumor cells describes resistance to wide range of structurally unrelated anticancer agents and is a serious limitation to effective chemotherapy. It is a multifactor yet not fully elucidated phenomenon by the involvement of diverse cellular pathways.

Aim of this study was to investigate the resistance mechanisms developed against docetaxel and doxorubicin that are widely used in the treatment of breast cancer in model cell line MCF-7. Resistant sublines were developed by application of drugs in dose increments and effect of docetaxel and doxorubicin on drug applied cells were investigated by cell viability assays. Expression analysis of *P-gp, MRP1, BCRP, Bcl-2, Bax* and *β-tubulin* isotypes were performed by RT-PCR, qPCR, Western blot and immunocytochemistry. Genome-wide expression analysis was also performed by cDNA microarray.

According to cell viability assays, drug applied cells developed varying degree of resistance to docetaxel and doxorubicin. Gene expression analysis demonstrated that *de novo* expression of P-gp contributed significantly to drug resistance. Expression levels of

class II, III and V *β-tubulin* isotypes increased in docetaxel resistant sublines. According to microarray analysis, a variety of genes showed significantly altered expression levels particularly drug metabolizing and detoxification enzymes (*i.e.* increased *GPX1* and *GSTP1* with decreased *POR*), survival proteins (*e.g.* decreased TRAIL together with increased decoy receptors and CD40), extracellular matrix components (*e.g.* increased integrin signaling), growth factors and cytokines (*e.g. EGFR1, FGFR1, CTGF, IL6, IL8* and *IL18* overexpression), epithelial-mesenchymal transition proteins (*i.e.* increased vimentin and N-cadherin with decreased E-cadherin and occludin) and microtubule dynamics related proteins (*e.g.* increased *MAP1B* and decreased *MAP7*).

Development of cross-resistance and combined drug effects on resistant sublines were also studied. Results demonstrated that docetaxel and doxorubicin resistant cells developed cross-resistance to paclitaxel, vincristine, ATRA, tamoxifen and irradiation. Finally, modulatory effects of verapamil and promethazine in combined drug applications were investigated and verapamil and promethazine were shown to decrease *MDR1* expression level thus reverse the MDR. They also showed synergic and additive effects in combined docetaxel and doxorubicin applications.

Identification of resistance mechanisms may personalize chemotherapy potentially increasing efficacy of chemotherapy and life quality of patients.

Keywords: Multidrug resistance, Docetaxel, Doxorubicin, Breast Cancer

ÖZ

MCF-7 MEME KANSERİ HÜCRE HATTINDA DOSETAKSEL VE DOKSORUBİSİN DİRENÇLİLİĞİNİN İNCELENMESİ

Darcansoy İşeri, Özlem
Doktora, Biyoteknoloji Bölümü
Tez Yöneticisi: Prof. Dr. Ufuk Gündüz
Ortak Tez Yöneticisi: Prof. Dr. Fikret Arpacı

Şubat 2009, 239 sayfa

Tümör hücrelerinde yapısal olarak farklı antikanser ajanlara direnç oluşması çoklu ilaç dirençliliği olarak tanımlanmakta ve kanser kemoterapisinin başarısını kısıtlamaktadır. Pekçok hücre yolağını içeren ve çok etkenli bir olgu olan çoklu ilaç dirençliliği henüz moleküler düzeyde tam olarak anlaşılamamıştır.

Bu çalışmada amaç, meme kanseri tedavisinde sıkça kullanılan dosetaksel ve doksorubisine karşı geliştirilen ilaç dirençliliğinin model MCF-7 hücre hattında incelenmesidir. Hücrelere artan dozlarda ilaç uygulanmasıyla dirençli hatlar geliştirilmiş ve direnç gelişimi sitotoksisite analizleri ile gösterilmiştir. Dirençli hücre hatlarında *MDR1, MRP1, BCRP, Bcl-2, Bax* ve *β-tubulin* isotiplerinde gen ve protein düzeylerindeki değişimler GT-PZR, eş zamanlı PZR, Western blot ve immunositokimya yöntemleri ile incelenmiştir. cDNA mikrodizin analizi ile dosetaksel ve doksorubisine dirençli seçilmiş hatlarda tüm genom ifade düzeyleri incelenmiş ve duyarlı MCF-7 hattı ile karşılaştırılmıştır.

Elde edilen sonuçlar değerlendirildiğinde, hücrelerin uygulanan ilaçlara çeşitli derecelerde direnç gösterdikleri saptanmıştır. Dirençli hücrelerde, özellikle *MDR1* ifadesinin yüksek düzeyde tetiklendiği ve dosetaksele dirençli hücrelerde *β-tübülin* izotiplerinin farklı düzeylerde (*β-tübülin II, III*, *V* izotiplerinde artan ifade düzeyleri) ifade edildikleri belirtilmiştir. Mikrodizin analiz sonuçlarına göre, ilaçları metabolize eden enzimleri (*GPX1* ve *GSTP1* ifadelerindeki artış ve *POR* ifedesindeki azalma), sağ kalım proteinlerini (TRAIL proteinini kodlayan gen ifadesinde azalma ve apoptozu engelleyen DcR2 ve DcR3 ile CD40 reseptörlerini kodlayan gen ifadelerinde artış), hücre dışı matris proteinlerini (reseptör ve ligand artışına bağlı integrin yolağında artış), büyüme faktörleri ve sitokinleri (*EGFR1, FGFR1, CTGF, IL6, IL8* ve *IL18* ifadelerinde artış) ifade eden genlerin düzeylerinde anlamlı değişimler olduğu saptanmıştır. Bunların yanısıra, yüksek N-kaderin ve vimentin ile azalan E-kaderin ve okludin ifadesi bulunan dirençli hücrelerin epitel hücre özelliklerini kaybederek mesenkimal hücre özelliği kazandıkları saptanmıştır.

Dosetaksel ve doksorubisine dirençli hatlarda çapraz direnç gelişimi incelenmiş ve dirençli hücrelerin paklitaksel, vinkristin, all-trans retinoik asit (ATRA), tamoksifen ve radyasyona karşı çapraz direnç geliştirdikleri görülmüştür. Bazı kombine ilaç uygulamalarının ise dirençli hücrelerde sitotoksik etkiyi arttırdıkları ve sinerji gösterdikleri belirlenmiştir. Verapamil ve prometazinin, dosetaksel ve doksorubisin ile kombine uygulandığında çoklu ilaç dirençlilğinin geri çevrilmesinde etkin olduğu saptanmıştır. Ayrıca, verapamil ve prometazinin *MDR1* gen ifade düzeyini azaltarak ilaç dirençliliğini geri çevirdiği de belirlenmiştir.

Çoklu ilaç dirençliliği mekanizmalarının belirlenmesi, kişiye bağlı kemoterapi yöntemlerinin geliştirilerek kanser kemoterapisinde başarının artırılması açısından önem taşımaktadır.

Anahtar Kelimeler: Çoklu ilaç dirençliliği, Dosetaksel, Doksorubisin, Meme kanseri

To my beloved husband Aykut İnan and precious son İlke İnan

ACKNOWLEDGEMENTS

First of all, I would like to express my deepest gratitude to my supervisor Prof. Dr. Ufuk Gündüz for her great advises, support and guidance throughout this study. I would also thank to my co-supervisor Prof. Dr. Fikret Arpacı for his valuable contributions, support and encouragement in this research.

I feel great appreciation to Prof. Dr. Ali Uğur Ural for his sincere guidance and confidence throughout our researches.

I would like to thank Prof. Dr. Hüseyin Avni Öktem for his support and contributions. Examining committee members Prof. Dr. Semra Kocabıyık, Assist. Prof. Dr. Sreeparna Banerjee and Assist. Prof. Dr. Dilek Şendil Keskin are also greatly acknowledged for their participation and valuable comments.

I am grateful to Meltem Demirel Kars for her friendship and pleasant collaboration in this study. I also thank to Gökhan Kars for his friendship and technical help. I also give my special thanks to my friends Betul Deçani Yol, Murat Yol and Abdullah Tahir Bayraç.

Esra Güç, Sevilay Akköse, Pelin Mutlu, Ogan Abaan, Bala Gür, Dr. Can :Atalay, Yaprak Dönmez, Uğur Eskiocak, Gülşah Pekgöz, Pelin Sevinç, Esra Kaplan, Petek Şen, Zelha Nil and special project students that we have worked with are greatly acknowledged for their friendship and contributions throughout this study.

I would like to express my great appreciation to my family members Emel-Naci Önelge, Dilek-Hüseyin Yavuz and Emel-Aslı-Aper-Celal Çağlar for their physical and moral support and encouragement in my life.

I am deeply indebted to my mother Ender Dinçer and sister Gizem Darcansoy for their endless love, trust and support in every step of my life. I am also greatful to my father Ender Darcansoy for his support.

Lastly, I am thankful to my husband Aykut more than expressed in words for his endless love and physical help in my thesis, and also to my little son İlke for his precious existence in our life.

This study was supported by the Research Fund of METU Grant No: BAP-2003-07-0200-64 and TÜBİTAK Grant No: 106S019. In addition, scholar of TÜBİTAK-BİDEB is acknowledged.

TABLE OF CONTENTS

LIST OF TABLES

TABLES

LIST OF FIGURES

FIGURES

LIST OF SYMBOLS AND ABBREVIATIONS

DOC	Docetaxel
DOX	Doxorubicin
MDR	Multidrug Resistance
ABC	ATP-Binding Cassette
P-gp/MDR1	P-glycoprotein
MRP1	Multidrug Resistance Protein 1
BCRP	Breast Cancer Resistance Protein
TNF	Tumour Necrosis Factor
TUBB	Beta Tubulin
EGFR	Epidermal Growth Factor Receptor
IL	Interleukin
ECM	Extracellular Matrix
MMPs	Matrix Metalloproteinases
ADAMs	A Disintegrin And Metalloproteinases
ROS	Reactive Oxygen Species
ER	Estrogen Receptor
MCF-7/S	Sensitive MCF-7
MCF-7/30nM DOC	30nM docetaxel resistant MCF-7 subline
MCF-7/120nM DOC	120nM docetaxel resistant MCF-7 subline
MCF-7/1000nM DOC	1000nM doxorubicin resistant MCF-7 subline
ATRA	All-Trans Retinoic Acid
dH_2O	Distilled Water
RT	Room Temperature
DMSO	Dimethly Sulfoxide
EDTA	Ethylene-Diamine-Tetra-Acetic Acid
IC_{50}	Inhibitory Concentration 50
t_d	Doubling Time
SEM	Standar Error of the Means

NaOH	Sodium Hydroxide
EtOH	Ethyl Alcohol
SDS	Sodium Dodecyl Sulfate
TEMED	N, N, N', N'-Tetramethylethylenediamine
PCR	Polymerase Chain Reaction
RT-PCR	Reverse Transcriptase-Polymerase Chain Reaction
qPCR	Quantitative Real-Time Polymerase Chain Reaction
dNTP	Deoxy Nucleotide Triphosphate
EtBr	Ethidium Bromide
PBS	Phosphate Buffered Saline
GAPDH	Glyceraldehyde-3-Phosphate Dehydrogenase
ATRA	All-Trans Retinoic Acid
FIX	Fractional Inhibitory Index
Vp	Verapamil
PRM	Promethazine
cGy	Centi-Gray
NS	Not significant
EMT	Epithelial-Mesenchymal Transition
PI3K	Phosphotidylinositol 3-Kinase
TGFBR	Transforming Growth Factor Beta Receptor
FGFR	Fibroblast Growth Factor Receptor
LRP	Lung Resistance Protein

CHAPTER 1

INTRODUCTION

1.1 Breast Cancer

Cancer is a group of diseases characterized by uncontrolled growth and spread of abnormal cells originated from normal body cells. The transformation from a normal cell into an abnormal tumor cell is a multistage process, typically a progression from a pre-cancerous lesion to malignant tumors. The localization of the progression can be any single cell of the body, so cancer can arise in many sites and behave differently depending on its site of origin.

According to World Health Organization (WHO), in 2007 around 13% of all deaths (7.9 million people) worldwide were because of cancer, making it a leading cause of death (www.who.int/mediacentre/factsheets/fs297/en/). It was also reported by WHO, in July 2008 that deaths from cancer worldwide continued rising, with an estimated 12 million deaths in 2030. The main types of cancer leading to overall cancer mortality each year are; lung (1.4 million deaths), stomach (866,000 deaths), liver (653,000 deaths), colon (677,000 deaths) and breast (548,000 deaths). It was reported as the most frequent cancer among women (23% of all cancers) worldwide (Parkin *et al.*, 2005). The risk factors associated with the disease onset and progress is complex. Briefly, risk factors are hormones, reproductive factors and lifestyle factors (e.g. weight gain and sedentary lifestyle have negative effects) which are overviewed in Figure 1.1.

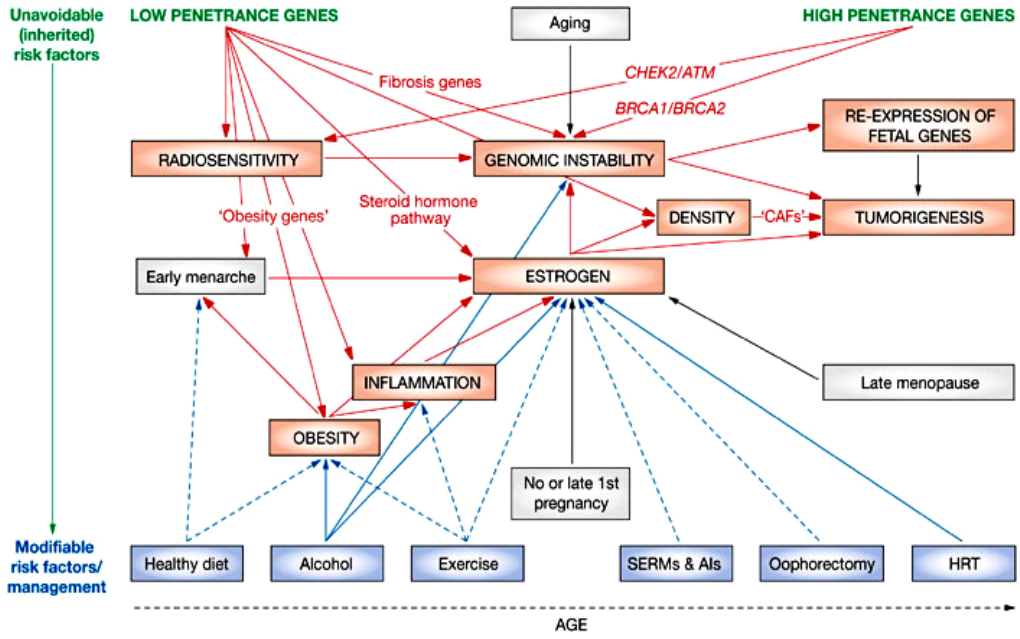

Figure 1.1 Overview of the many complex risk factors associated with breast cancer (Howell *et al*., 2005).

Breast cancer begins in breast tissue, which is made up of glands for milk production, called lobules, and the ducts that connect lobules to the nipple. The remainder of the breast is made up of fatty, connective, and lymphatic tissue. Theoretically, any type of tissue in the breast can form cancer but origin of tumor is usually either the ducts (called ductal carcinoma) or the glands (called lobular carcinoma). Breast cancer usually begins with the formation of a small, confined tumor (lump) and then spreads through channels to the lymph nodes or through the blood stream to other organs. When abnormal cells of lobules or ducts break out into the surrounding breast tissue, invasive breast cancer develops. Metastasis occurs when these cancer cells break away from the site of primary tumor and spread to other organs of the body through either the blood stream or the lymphatic system.

In order to evaluate prognosis and constitute a conventional guideline for treatment, breast cancer is staged into different groups. Cancer stage is based on the size of the tumor, whether the cancer is invasive or non-invasive, whether lymph nodes are involved, and whether the cancer has spread beyond the breast. Accordingly a nomenclature system was developed by American Joint Committee on Cancer (AJCC) and defined in the AJCC Manual for Staging of Cancer. In TNM staging all aspects of cancer distribution in terms of

primary tumor (T), regional lymph nodes (N), and distant metastasis (M) is included and further they are grouped into numerical stages (Table 1.1). In brief (www.imaginis.com/breasthealth/staging.asp):

- **T: Tumor size**

TX: Tumor cannot be assessed

T0: No evidence of a tumor

T1: Tumor is 2 cm or less in diameter. This group is divided into three subcategories as 1a, 1b and 1c.

T2: Tumor is between 2 and 5 cm in diameter

T3: Tumor is more than 5 cm in diameter

T4: Tumor is any size, has attached itself to the chest wall and spread to the pectoral (chest) lymph nodes. This group is divided into four subcategories as 4a, 4b, 4c and 4d.

- **N: Palpable Nodes**

NX: Lymph nodes cannot be assessed

N0: Cancer has not spread to lymph nodes

N1: Cancer has spread to the movable ipsilateral axillary lymph nodes (underarm lymph nodes on same side of breast cancer)

N2: Cancer has spread to ipsilateral (same side of body as breast cancer) lymph nodes fixed to one another or to other structures under the arm. This group is divided into two subcategories as 2a, and 2b.

N3: Cancer has spread to the ipsilateral mammary lymph nodes or the ipsilateral (same side of body as breast cancer) supraclavicular lymph nodes. This group is divided into three subcategories as 3a, 3b and 3c.

- **M: Metastasis**

MX: Metastatis cannot be assessed

M0: No distant metastasis to other organs

M1: Distant metastatis to other organs

Table 1.1 Stage grouping of breast cancer
www.imaginis.com/breasthealth/staging.asp.

Stage	Tumor (T)	Node (N)	Metastasis (M)
Stage 0	Tis	N0	M0
Stage 1	T1	N0	M0
Stage IIA	T0	N1	M0
	T1	N1	M0
	T2	N0	M0
Stage IIB	T2	N1	M0
	T3	N0	M0
Stage IIIA	T0	N2	M0
	T1	N2	M0
	T2	N2	M0
Stage IIIB	T3	N1, N2	M0
	T4	any N	M0
	any T	N3	M0
Stage IV	any T	any N	M1

1.2 Treatment of Breast Cancer

In order to determine a treatment strategy for a breast cancer patients, factors such as the size of the tumor, location of the tumor, stage of the cancer and some personal variables such as age and menopausal status, hormone receptor status, expression, mutation and gene amplification of the certain genes that affect treatment are considered. Based on the assessment of these factors, one of the treatment strategies of surgery, radiation therapy, chemotherapy, and hormone therapy and/or in a combination of them is selected. Use of an additional treatment with combination of chemotherapy drugs, radiation, and hormone therapy in addition to primary therapy for destruction of remaining cancer cells, prevent spread or recurrence is known as adjuvant therapy. It can either be local or systemic depending on the aim of use. Neoadjuvant chemotherapy, on the other hand, is also called primary or induction therapy and given is prior to the surgery. (/www.pharmacology.unmc.edu/cancer).

1.2.1 Surgery

If the tumor is not matastatic, surgery is usually the first line of attack against breast cancer. Types of breast cancer surgery are lumpectomy and mastectomy. Additionally, removal of lymph nodes, or axillary lymph node dissection, can take place during lumpectomy and mastectomy if the biopsy shows that breast cancer has spread outside the milk duct. In lumpectomy, breast tumor is surgically removed along with a small margin of the surrounding normal breast tissue. Lumpectomy is often performed on Stage 0, Stage I, or Stage II (occasionally Stage III) breast cancers with or without lymph node removal. Mastectomy is the surgical removal of the affected breast. Types of mastectomy include simple, modified radical, and radical (www.imaginis.com/breasthealth/treatment.asp). Removal of some or all of the underarm lymph nodes may be included. Mastectomy is common treatment for women with Stage 0, Stage I, Stage II, or Stage III (occasionally Stage IV) breast cancers.

1.2.2 Radiotherapy

In radiotherapy ionizing radiation (x-rays, gamma rays or electrons) is used to destroy cancer cells. Radiation therapy is often used to destroy any remaining tumor cells in the breast, chest wall, or underarm area after surgery. Occasionally, radiation therapy is used before surgery to shrink the size of a tumor.

In principle, direct effect of radiation at molecular level is breakage of chemical bonds or tautomeric shifts in the molecules of cells, primarily in DNA. An indirect effect is produced by generation of secondary charged particles, usually electrons, by excitation and ionization. High concentrations of reactive species like molecular free radicals, hydrated electrons, hydrogen radicals and hydroxy radicals are generated in irradiated tissues. They are derived primarily from water and react with O_2 to produce oxygen radical anion (superoxide), peroxy radicals and other longer-lived reactive species that bind covalently to molecules of cell. When they bind to DNA, single and double strand breaks, base damages ad adduct formation occur rendering the radiation-induced damage largely irreparable. Selective effect of radiation on tumor cells is explained by differential radiosensitivity of tumor cells and normal cells of the body. As explained by Bergonié and Tribondeau

(Bergonié and Tribondeau, 2003), highly proliferative cells are more sensitive to effects of radiation.

Radiation therapy is delivered by external beam, internal irradiation via an implant, or combination of the two. The most common type of radiation therapy for breast cancer is external beam radiation. External beam radiation is delivered from a source outside the body to the site of tumor. X-rays and gamma rays are the sources of irradiation. X- rays are focused on the site of cancer by linear accelerators and betatrons producing increasingly greater energy. The higher the energy of the X-ray beam, the deeper the x-rays can go into the target tissue. Gamma rays are produced spontaneously as elements such as radium, uranium, and cobalt 60 release radiation as they decompose, or decay. Each element decays at a specific rate and gives off energy in the form of gamma rays and other particles. X-rays and gamma rays have the same effect on cancer cells (www.meds.com/pdq/radio.html).

Another technique for delivering radiation to cancer cells is, internal radiotherapy, to place radioactive implants directly in a tumor (brachytherapy) or surrounding tissues (interstitial irradiation), or within body cavities (intracavitary irradiation) (www.utmb.edu/otoref/grnds/Radiation-oncology-2003-1203/Radiation-oncology-20031203 .htm). Internal radiotherapy has the advantage of delivering the radiation from a close distance, and thereby delivering a higher dose of radiation while not causing as much damage to other structures. Some of the radioactive substances used for internal radiation treatment include cesium, iridium, iodine, phosphorus, and palladium.

A course of radiotherapy is usually delivered using a shrinking field technique. In principle, tumor cell killing by radiation is an exponential function of dose and that the dose required for a particular tumor control probability is proportional to the logarithm of the number of viable cells in the tumor (www.utmb.edu/otoref/grnds/Radiation-oncology-2003-1203/Radiation-oncology-2003-1203.htm).

Side effects of radiotherapy are mainly dependent on the area of body being treated. However, skin irritation, extreme tiredness and temporary change of skin color in the treated area are commonly encountered.

1.2.3 Chemotherapy

Anticancer drugs selectively destroy cancer cells by preventing growth or division at one or more points in their growth cycle. Uncontrolled and rapid growth is characteristic of cancer cells. Drugs are designed to inflict greater damage on cancer cells than on normal cells, thereby typically drugs that affect a cell's ability to grow are used. Chemotherapy is systemic administration of anticancer drugs for the treatment of cancer. The goal of chemotherapy is to shrink primary tumors, slow the progression of tumor growth, destroy cancer cells that may have spread (metastasized) to other parts of the body from the site of the primary tumor and occasionally relieve the symptoms. Drugs are given by injection into the vein (intravenously) or as tablets (orally). When chemotherapy treatment is applied intravenously, it is in sessions followed by a rest period of a few weeks to allow body to rest.

There are many types of chemotherapeutics with different action mechanisms, selectivity and toxicity. They can be natural, synthetic or semi-synthetic according to their nature. According to their mechanism of action; alkylating agents, topoisomerase I and II inhibitors, antimetabolites, mitotic spindle inhibitors, angiogenesis inhibitors, hormones or hormone mimicking drugs for hormone therapy, drugs of targeted therapy and immunosuppressants are different types of compounds used as chemotherapeutics (Figure 1.2).

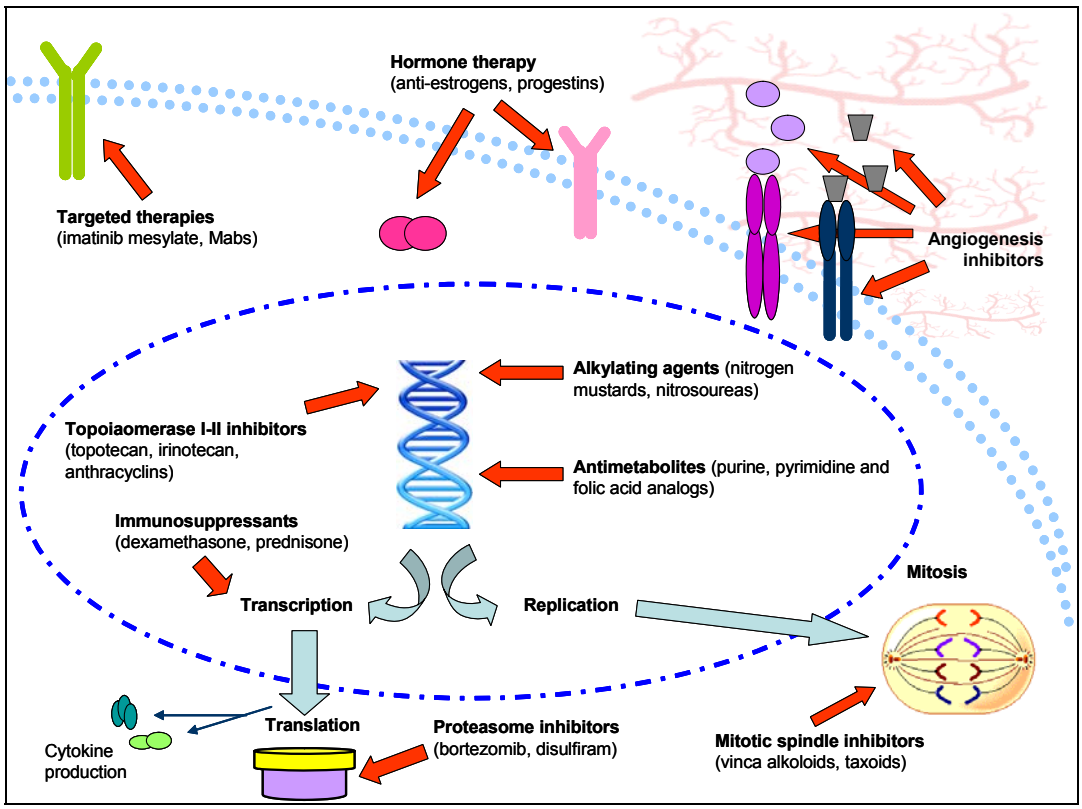

Figure 1.2 Mechanism of action of anticancer drugs.

Alkylating agents bind to nucleic acids alkylating it at the N7 position of guanine and interfere with DNA replication and transcription. Abnormal base pairing with thymine leades to miscoding, alternatively depurination by excision of guanine residues causes strand breakage. Alkylating agents are of two types; nitrogen mustards (*e.g.* cyclophosphamides, melphalan) and nitrosoureas (*e.g.* carmustine). The process of chromosome condensation and segregation during mitosis requires the activity of topoisomerase II (topo II), whereas other topological modifications of the DNA molecule, such as DNA relaxation, can be performed by topoisomerase I (topo I) (Robert and Larsen, 1998). Topoisomerase I and II inhibitors covalently bind to these enzymes causing irreversible stabilization of protein-DNA complex and inhibition of strand separation. Examples for topo I inhibitors are topotecan and irinotecan, where topo II inhibitors are anthracyclins (doxorubicin) and mitoxantrone. Antimetabolite drugs, unfuntional analogs of metabolites, are used to antagonize metabolic activities. Three types of compounds, purine (*e.g.* 6-Mercaptopurine, fludarabine) and pyrimidine (*e.g.* 5-fluorouracil (5-FU) and arabinosylcytosine) analogues, and folic acid analogues (*e.g.* methotrexate), are used for

this purpose. Mitotic spindle inhibitors act on cells by distruption of microtubule equilibrium in the direction of either destabilization, inhibiting the formation of mitotic spindles, *i.e. Vinca* alkoloids (*e.g.* vincristine and vinblastine) or stabilization causing irreversible stabilization of mitotic spindles, *i.e.* Taxoids (*e.g.* taxol and taxotere). Sex hormones, or hormone-like drugs, that alter the action or production of female or male hormones are used in hormone therapy. These are anti-estrogens (*e.g.* tamoxifen and toremifene), aromatase inhibitors (*e.g.* anastrozole and exemestane), progestins, estrogens and anti-androgens. Angiogenesis inhibitors exert their effect on expression of pre-angiogenic factors and increased tumor vascularization *i.e.* thalidomide (reduction of TNF-α) and bevacizumab (monoclonal antibody against vascular endothelial growth factor). Immunosupressive anticancer drugs are commonly used in hematological maligninties to suppress the rampant growth of the cancerous white blood cells. Some examples are corticosteroids (*e.g.* prednisone), cyclophosphamide and mercaptopurine. Targeted chemotherapy has been recently arised to increase selective toxicity thereby decreasing side effects. Most attack mutant versions of certain genes expressed in tumor cells, or particular genes that are abundantly expressed in tumor cells. For example, imatinib mesylate is a protein-tyrosine kinase inhibitor of signal transduction targeting the fusion protein bcr-abl encoded by Philadelphia chromosome in chronic myelogenous leukemia. In breast cancer, HER1 and HER2 targeting tyrosine kinase inhibitors are in use. Trastuzumab (Herceptin®) and Lapatinib (Tykerb®) are prescribed in the treatment of HER2/neu positive metastatic breast cancers. Gefitinib (Iressa®), epidermal growth factor receptor (EGFR/HER1) inhibitor is used for HER2 negative metastatic breast tumors.

The prescription of more than one drug in cancer chemotherapy is known as combination chemotherapy. Anticancer drugs are most commonly administered as combination therapy. During combination therapy, two different drugs having additive or synergistic effects are prescribed at the same time in relatively smaller doses when compared with their single applications. In general, anticancer drugs selected for combination chemotherapy are active against the tumor when used alone, have different mechanisms of action and have minimally overlapping toxicities. Thereby, occurrence of side effects is considerably reduced with increased effectiveness of the therapy. Combination therapy also reduces the risk of developing resistance to chemotherapy drugs, which can develop with prolonged use of a particular drug.

Table 1.2 Selected drug combinations used in breast cancer chemotherapy (Luqmani, 2005).

CMF	Cyclophosphamide, methotrexate, 5-FU
AC	Doxorubicin, cyclophosphamide
CAF	Cyclophosphamide, doxorubicin, 5-FU
AC→T	Doxorubicin, cyclophosphamide, paclitaxel
CEF	Cyclophosphamide, epirubicin, 5-FU
CMFVP	Cyclophosphamide, methotrexate, 5-FU, vincristine, prednisone
AT	Doxorubicin, docetaxel
AC→T	Doxorubicin, cyclophosphamide, docetaxel

Despite diverse action of anticancer drugs used, targeting of rapidly dividing cells is common feature. However, together with tumor cells, normal cells also divide, some being quite rapidly such as those in the bone marrow and those lining the mouth and intestine. Thus, all chemotherapy drugs affect normal cells to some extent and cause side effects. Common side effects are:

- nausea and vomiting
- loss of appetite
- hair loss
- anemia and fatigue
- infection
- easy bleeding or bruising
- sores in the mouth and throat
- neuropathy and other damage to the nervous system
- kidney damage

1.2.3.1 Docetaxel (Taxotere®)

Microtubules are protein polymers that are responsible for various aspects of cellular shape and movement. The major component of microtubules is the polymer

tubulin, a protein containing two nonidentical subunits (α and β) (Nogales *et al.*, 1998). Antimitotic microtubule inhibitory drugs are widely used in chemotherapy for the suppression of microtubule dynamics in treatment of variety of tumors including metastatic breast cancer (Clemons *et al.*, 1997; Enju *et al.*, 2005). Many plant alkaloids are used as antimicrotubule drugs disturbing the equilibrium between free tubulin dimers and assembled polymers. Equilibrium can be disturbed by inhibition of either polymerization of free tubulin dimers (vinca alkaloids) or depolymerization of tubulin heterodimers (taxanes). Distortion of polymerization-depolymerization dynamics results in mitotic arrest and growth inhibition (Yvon *et al.*, 1999). Upon binding of vinca alkaloids to β-tubulin of free tubulin dimers available for microtubule assembly, for example, effectively decreases resulting in a shift of the equilibrium toward disassembly. Formation of paracrystalline aggregates by vinca-bound tubulin dimers shifts the equilibrium even further toward disassembly and microtubule shrinkage. They block mitosis with metaphase arrest (Wilson and Jordan, 1995).

Taxane drugs, paclitaxel (Taxol®) and its semisynthetic derivative docetaxel (Taxotere®), have emerged as critically important antimicrotubule drugs in the treatment of patients with breast cancer. In contrast to other microtubule antagonists, both paclitaxel and docetaxel disrupt the equilibrium between free tubulin and microtubules (Figure 1.3) by shifting it in the direction of assembly, rather than disassembly, by binding to β–tubulin subunits (Kumar, 1981). As a result, taxane treatment causes the stabilization of microtubules against depolymerization and the formation of abnormal bundles of microtubules. Abnormal bundles resist physiologic disassembly, accumulate within tumor cells and inhibit cell proliferation leading to cell cycle arrest at G2/M, apoptosis, cytotoxicity and cell death (Clarke *et al.*, 1999). The cellular target for docetaxel is the taxane binding site on β-tubulin (Figure 1.4). This site on microtubules is only present in assembled tubulin. This pocket lies within a hydrophobic cleft near the surface of β-tubulin and allows for taxanes to interact with proteins via hydrogen bonding and hydrophobic contact (reviewed in McGrogan *et al.*, 2008).

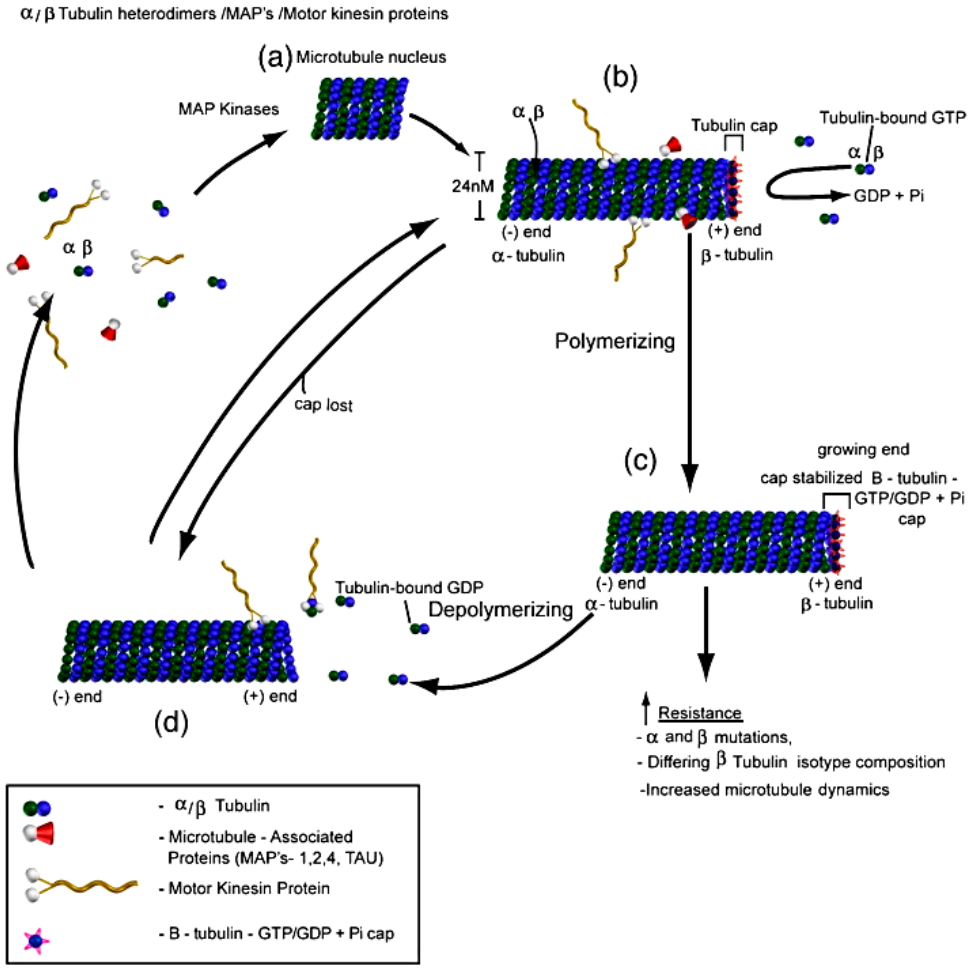

Figure 1.3 Polymerization and depolymerization microtubule dynamics: (a) Microtubule nucleus forms when α/β heterodimers associate, (b) Microtubules consisting of α/β heterodimers elongate to form cylindrical microtubules of 13 protofilaments with a plus (+) end and minus (−) end. Tubulin-bound GTP binds to plus (+) end of microtubule and GTP is hydrolyzed to GDP + Pi forming a GTP cap, (c) The GTP cap stabilizes the microtubules plus (+) end and stabilization is further enhanced by addition of the taxanes, (d) Depolymerization occurs when the tubulin − GTP / GDP + Pi cap is lost, Pi is released from tubulin, destabilization occurs and the tubulin-bound GDP dissociates from the plus (+) end causing depolymerization (McGrogan *et al.*, 2008).

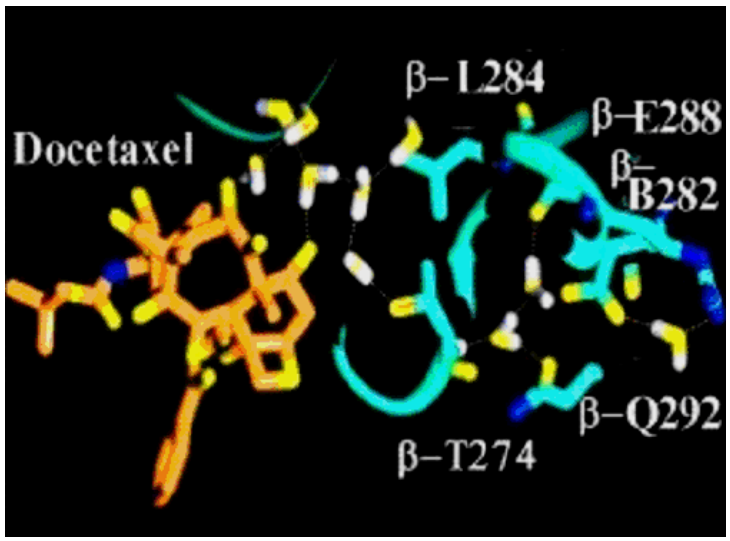

Figure 1.4 Binding site of docetaxel on β-tubulin (www.21cecpharm.com/px/action.htm).

Docetaxel ((2R,3S)-N-carboxy-3-phenylisoserine, N-tert-butyl ester, 13-ester with 5, 20-epoxy-1, 2, 4, 7, 10, 13-hexahydroxytax-11-en-9-one 4-acetate 2-benzoate, trihydrate; $C_{43}H_{53}NO_{14}$, MW: 807.879 g/mol) is a semi-synthetic analogue of paclitaxel, an extract from the rare Pacific yew tree *Taxus brevifolia*. Inactive taxoid precursor (10-deacetyl baccatin III) of docetaxel, on the other hand, is extracted from the needles of the the readily available European yew tree, *Taxus baccata*. Docetaxel differs from paclitaxel at two positions in its chemical structure. It has a hydroxyl functional group on carbon 10, where paclitaxel has an acetate ester, and a tert-butyl substitution exists on the phenylpropionate side chain (Figure 1.5). The carbon 10 functional group change causes docetaxel to be more water soluble than paclitaxel (Clarke *et al.*, 1999).

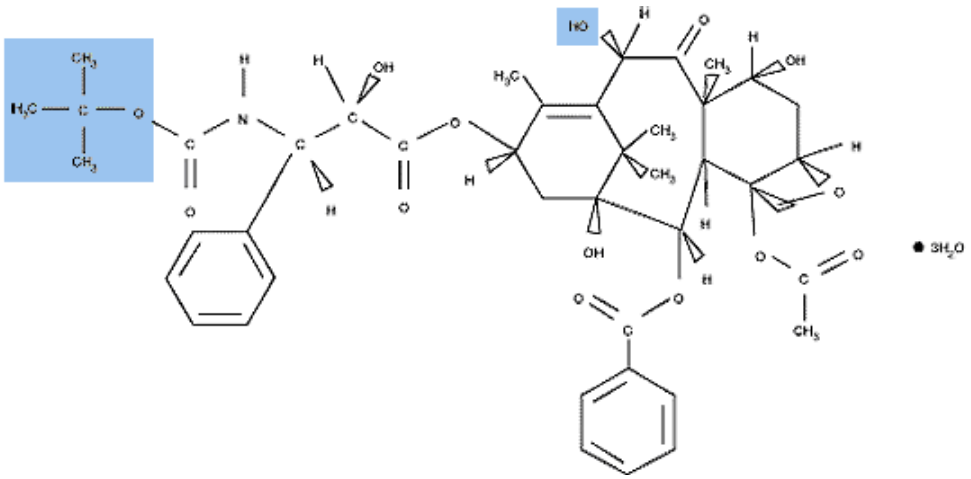

Figure 1.5 Docetaxel (Taxotere®) (www.taxotere.com/oncology/about_Taxotere/clinical_ pharmacology.aspx).

Docetaxel was approved by the Food and Drug Administration (FDA) for the treatment of breast cancer in 1996. Since then outcomes for breast cancer patients in the metastatic, adjuvant and neoadjuvant settings have been substantially improved in docetaxel containing regimens (Crown *et al.*, 2004).

1.2.3.2 Doxorubicin (Adriamycin®)

Doxorubicin (Adriamycin®) (Figure 1.6) is an anthracyclin type antibiotic. All anthracyclines bind to double stranded DNA and intercalate it, and thereby are called as intercalating agents. Anthracyclines have a number of important effects in the cytotoxic actions of these drugs. Firstly all anthracyclines can intercalate and interfere with DNA and RNA synthesis. Secondly, they interfere with a single step of the catalytic cycle of Topoisomerase II (Topo II) by stabilizing it in cleavable complex (Robert and Larsen, 1998). DNA strand breakages may be formed due to inhibition of break rejoining activity of Topo II. Thirdly, anthracyclines can also cause the formation of reactive oxygen species (ROS) and free radical damage on cells contributes to antitumor activity of the drug (Figure 1.7). The anthracycline chromophore contains a hydroxyquinone which is a well-described iron chelating structure. The drug-Fe complex catalyzes the transfer of electrons from glutathione to oxygen, resulting in the formation of ROS and free radicals in the cell. Superoxide and hydroxyl radicals are produced by the reductive semiquinone species.

Peroxidation of unsaturated membrane lipids causes disturbance of membrane structure and dysfunction of mitochondria which is, in particular, related to extensive cardiotoxicity of doxorubicin (Muraoka et al., 2004). The drug-Fe complex can also cause single-strand breakages in DNA. Collectively, the effects are inhibition of cell proliferation, induction G2–M cell arrest (Kwok et al., 1994) or apoptosis (Walker et al., 1991). Although the effect of doxorubicin on cells is not phase specific, cells in the S and G_2 phases are more sensitive than cells in G1.

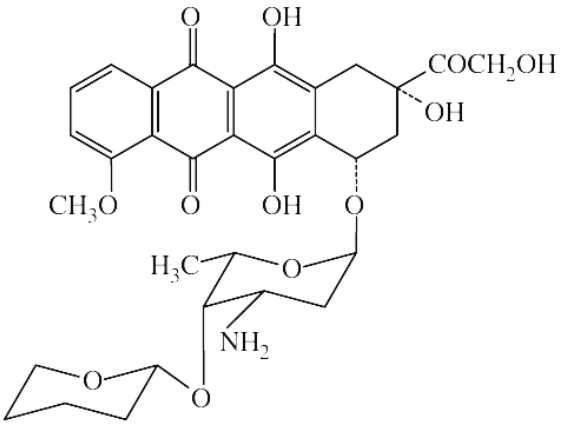

Figure 1.6 Doxorubicin (home.caregroup.org/clinical/altmed/interactions/Images/Drugs/doxorubi.gif).

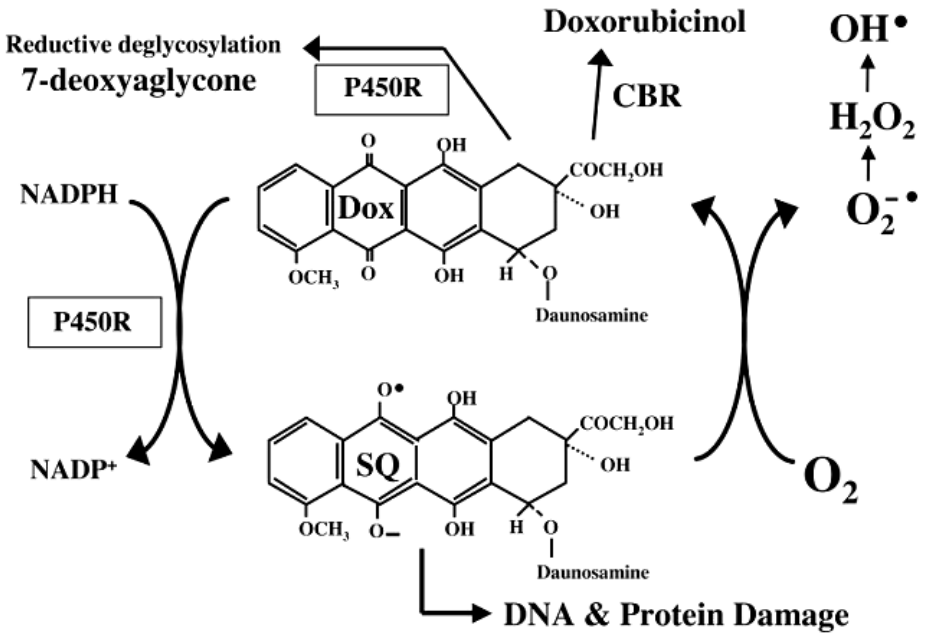

Figure 1.7 Doxorubicin biotransformation and effect (Riddick *et al.*, 2005).

Doxorubicin is most active against solid tumors, particularly breast cancer. Others are ovary, bladder, and lung carcinomas. It is also active in the treatment of Non-Hodgkin's lymphoma and Hodgkin's disease. In patients with advanced breast cancer, docetaxel and doxorubicin have the greatest activity as single agents (Nabholtz, 2003).

1.3 Multidrug Resistance (MDR)

Most patients with breast carcinoma respond to initial chemotherapy, but many have disease recurrence. Commonly patients who are refractory to disease show resistance to multiple anticancer agents of different structure and mode of action due to emergence of drug resistant tumor cells (Dalton *et al.*, 1997). The phenomenon, the major cause of the failure of chemotherapy, is defined as multidrug resistance (MDR) and involves cellular resistance to a broad spectrum of natural products used in cancer chemotherapy (Young *et al.*, 2003).

MDR may be intrinsic, making the malignant cells resistant to various unrelated drugs before they are exposed to any drugs, or may be acquired after exposure to chemotherapy (Krishan *et al.*, 1997). MDR is particularly seen in tumor cells of breast, ovarian, and renal cancers in leukemias and lymphomas (Sanfilippo *et al.*, 1991; Slovak *et al.*, 1988). Tumor cells with MDR phenotype also tend to be cross-resistant to a number of structurally and functionally unrelated drugs.

There are several mechanisms by which cancer cells develop resistance to cytotoxic agents. Its cause of development is multifactorial and may be affected by the cell cycle stage and proliferation status, biochemical mechanisms such as detoxification, cellular drug transport (influx, efflux and retention), and DNA replication and repair mechanisms (Young *et al.*, 2003) (Figure 1.8). Mechanisms of MDR include:

- Decreased intracellular drug levels which could result from increased drug efflux or decreased inward transport *e.g*., increased levels of ATP-binding cassette (ABC) family of membrane transport ATPases (Bodo *et al.*, 2003; Lage *et al*., 2003)
- Altered target type *e.g.*, differential expression pattern of *β-tubulin* isotypes or mutations in the protein resulting in decreased affinity for antimicrotubules (Drukman *et al.*, 2002; Giannakakau *et al.*, 2000)
- Altered expression of genes for survival *i.e.*, differential expression levels of the apoptotic/antiapoptotic genes (Lilling *et al.*, 2000)
- Altered amount of target *e.g.*, decreased sensitivity to topoisomerase II inhibitors is related to decreased topoisomerase II levels (Robert *et al.*, 1998)
- Decreased conversion of drug to its active form *e.g.,* alkylating agent cyclophosphamide require metabolic activation in the body and an alteration of the metabolic conversion can lead to reduced activity of the drug (Giaccone and Pinedo, 1996)
- Enhanced repair of the drug-induced defect *i.e.*, increased repair of DNA damage induced by alkylating agents or topoisomerase inhibitors (Giaccone and Pinedo, 1996)
- Increased cellular drug detoxification *e.g.*, glutathione S-transferase (GST) protects cells from damage due to free radicals is involved in the metabolic biotransformation of many anticancer drugs (Krishna and Mayer, 2000)

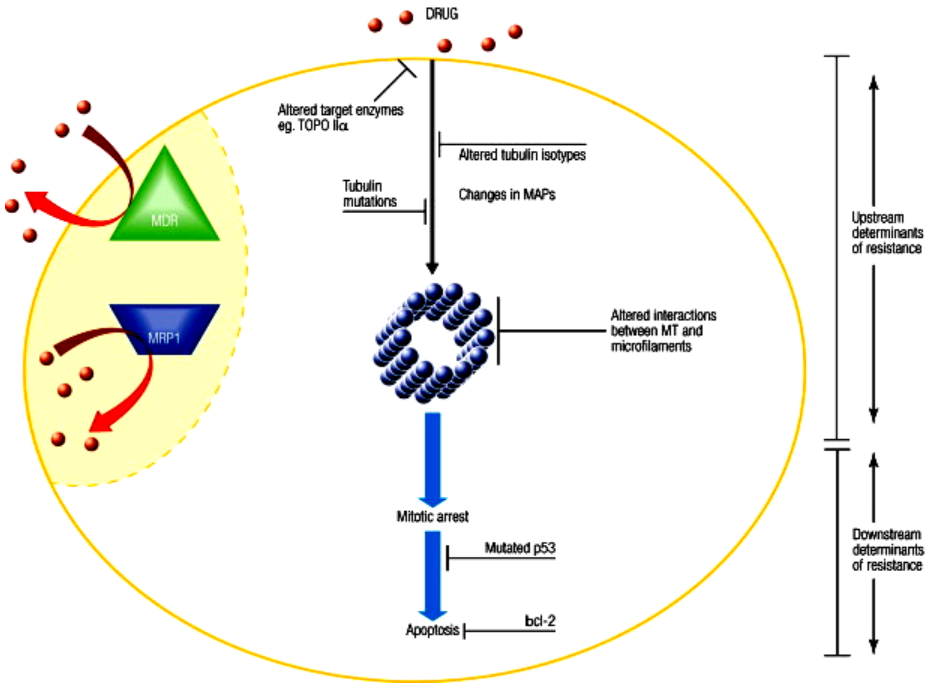

Figure 1.8 Some of the mechanisms of MDR (Coley, 2008).

1.3.1 Decreased Intracellular Drug levels Due To Increased Drug Efflux

The ATP-binding cassette (ABC) transporter family contains membrane proteins that translocate a variety of substrates across extra- and intra-cellular membranes. The ABC genes represent the largest family of transmembrane proteins. These ATPase proteins bind ATP and use the energy to drive the transport of various molecules across cellular membranes. Proteins are classified as ABC transporters based on the sequence and organization of their ATP-binding domains, also known as nucleotide-binding folds (NBF). The NBFs contain characteristic motifs, Walker A and B, separated by 90-120 amino acids, find in all ATP-binding proteins. ABC genes also contain an additional element, the signature C motif, located just upstream of the Walker B site (Dean *et al.*, 2001). The functional protein typically contains two NBFs and transmembrane domains (TMDs). TMDs contain membrane-spaninng hydrophobic α-helices (Figure 1.12) and provide the specificity for the substrates. The NBFs are located in the cytoplasm and transfer the energy to support the substrate across the membrane. ABC pumps are mostly unidirectional. In eukaryotes, most ABC pumps move compounds from the cytoplasm to the outside of cell

or into and extracellular compartment (endoplasmic reticulum, mitochondria, peroxisome) (Schinkl and Jonker; 2003). ABC genes are dispersed widely in eukaryotic genomes and are highly conserved between species. The genes can be divided into seven major subfamilies based on similarity in gene structures, order of the domains, and on sequence homology in the NBF and TMDs. A few genes do not fit into these subfamilies, and several of the subfamilies can be further divided into subgroups (Table 1.3).

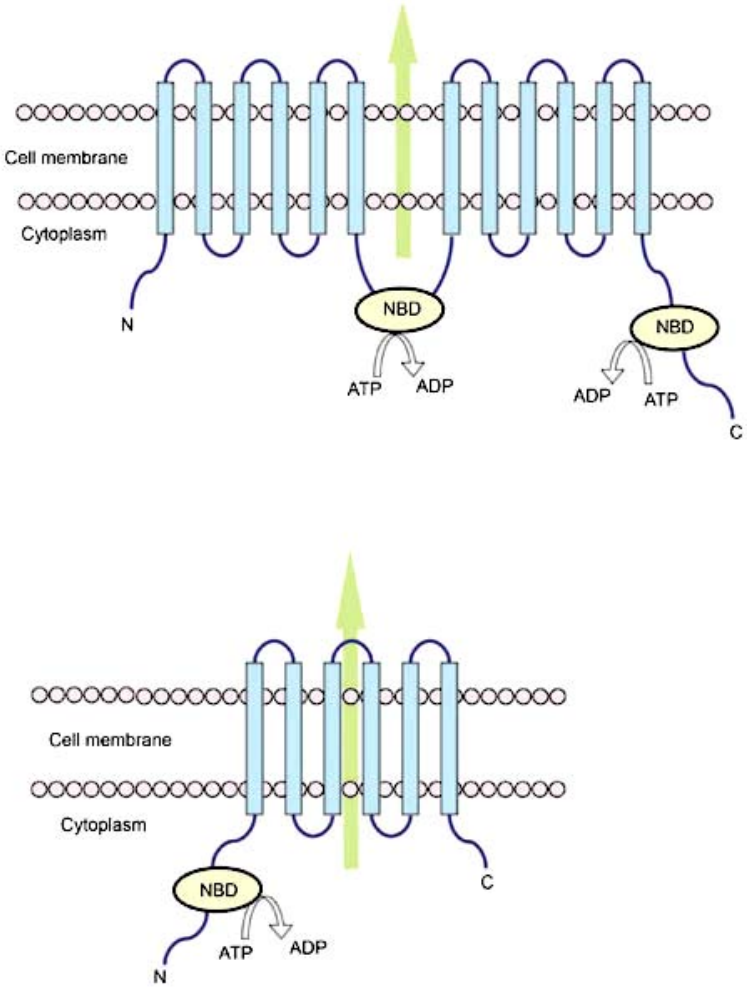

Figure 1.9 Structural features of full-length (top) and half (bottom) ABC transporters (Lin *et al*., 2006).

Table 1.3 List of Human ABC Genes and their chromosomal locations (Dean et al., 2001)

Symbol	Alias	Location	Expression	Function
ABCA1	ABC1	9q31.1	Ubiquitous	Cholesterol efflux onto HDL
ABCA2	ABC2	9q34	Brain	Drug resistance
ABCA3	ABC3, ABCC	16p13.3	Lung	
ABCA4	ABCR	1p22.1;–p21	Rod photoreceptors	N-retinylidiene-PE efflux
ABCA5		17q24	Muscle, heart, testes	
ABCA6		17q24	Liver	
ABCA7		19p13.3	Spleen, thymus	
ABCA8		17q24	Ovary	
ABCA9		17q24	Heart	
ABCA10		17q24	Muscle, heart	
ABCA12		2q34	Stomach	
ABCA13		7p11;–q11	Low in all tissues	
ABCB1	PGY1, MDR	7p21	Adrenal, kidney, brain	Multidrug resistance
ABCB2	TAP1	6p21	All cells	Peptide transport
ABCB3	TAP2	6p21	All cells	Peptide transport
ABCB4	PGY3	7q21.1	Liver	PC transport
ABCB5		7p14	Ubiquitous	
ABCB6	MTABC3	2q36	Mitochondria	Iron transport
ABCB7	ABC7	Xq12;–q13	Mitochondria	Fe/S cluster transport
ABCB8	MABC1	7q36	Mitochondria	
ABCB9		12q24	Heart, brain	
ABCB10	MTABC2	1q42	Mitochondria	
ABCB11	SPGP	2q24	Liver	Bile salt transport
ABCC1	MRP1	16p13.1	Lung, testes	Drug resistance
ABCC2	MRP2	10q24	Liver	Organic anion efflux
ABCC3	MRP3	17q21.3	Lung, intestine, liver	Drug resistance
ABCC4	MRP4	13q32	Prostate	Nucleoside transport
ABCC5	MRP5	3q27	Ubiquitous	Nucleoside transport
ABCC6	MRP6	16p13.1	Kidney, liver	
ABCC7	CFTR	7q31.2	Exocrine tissues	Chloride ion channel
ABCC8	SUR	11p15.1	Pancreas	Sulfonylurea receptor
ABCC9	SUR2	12p12.1	Heart, muscle	
ABCC10	MRP7	6p21	Low in all tissues	
ABCC11		16q11;–q12	Low in all tissues	
ABCC12		16q11;–q12	Low in all tissues	
ABCD1	ALD	Xq28	Peroxisomes	transport regulation
ABCD2	ALDL1, ALDR	12q11;–q12	Peroxisomes	
ABCD3	PXMP1, PMP70	1p22;–p21	Peroxisomes	

Table 1.3 (continued).

ABCD4	PMP69, P70R	14q24.3	Peroxisomes	
ABCE1	OABP, RNS4I	4q31	Ovary, testes, spleen	Oligoadenylate binding protein
ABCF1	ABC50	6p21.33	Ubiquitous	
ABCF2		7q36	Ubiquitous	
ABCF3		3q25	Ubiquitous	
ABCG1	ABC8, White	21q22.3	Ubiquitous	Cholesterol transport?
ABCG2	ABCP, MXR, BCRP	4q22	Placenta, intestine	Toxin efflux, drug resistance
ABCG4	White2	11q23	Liver	
ABCG5	White3	2p21	Liver, intestine	Sterol transport
ABCG8		2p21	Liver, intestine	Sterol transport

Decreased drug accumulation in tumor cells is due to increased drug efflux, reduced drug uptake or increased intracellular detoxification. ATP-dependent efflux of chemotherapeutics from tumor cells, which constitutes the major part of MDR phenotype, is related to the expression of some of the ABC transporters. The ABC transporters responsible for the decreased intracellular drug levels in cells conferring resistance to multiple drugs are P-glycoprotein (P-gp), multidrug resistance proteins (MRP1, MRP2, MRP3, MRP4 and MRP5), and breast cancer resistance protein (BCRP) (Table 1.3). The *ABCB1*, *ABCC1* and *ABCG2* genes and proteins encoded by these genes (P-gp, MRP1 and BCRP, respectively) are the most important ones among them for their overexpression in cells that display resistance to a wide variety of drugs and clinical relevance in patient studies.

1.3.1.1 P-glycoprotein (P-gp/MDR/PGY1)

The *ABBC1* (*MDR1*) gene is located on choromosome 7q21.12 (Table 1.2). The gene has 28 exons encoding for 170 kDa P-gp (MDR1/PGY1) protein (1280 aa) with 12 TMSs organized into 2 TMDs and *N*-glycosylation branches (which is not related to transport function of the pump but rather to stability in the plasma membrane) (Figure 1.10). It was first characterized by Endicottaland and Ling (Endicottaland and Ling, 1989) in resistant cancer cells as the ATP-dependent transporter responsible for the efflux of chemotherapeutic agents. P-gp prevents accumulation of toxic substances in the

environment and diet from entering the body and removes them by excretion into the bile and urine in normal human tissues, such as the intestine, liver, pancreas, and kidney (reviewed in Loo and Clarke, 2005). Furthermore, expression of P-gp in apical membranes of normal brain capillary endothelial cells contributes to the blood-brain barrier.

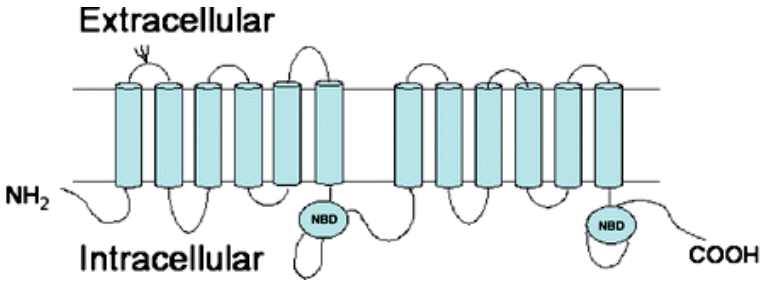

Figure 1.10 Schematic membrane topology of P-gp (Pal and Mitra, 2006).

Structurally unrelated molecules are transported by P-gp. Despite its broad range of substrate specifity, in common, they are hydrophobic molecules. Additionally, most of them are organic molecules sizes ranging from 200 to 1900 Da (Schinkl and Jonker, 2003). The hydrophobic nature of the substrates contributes to drug translocation mechanism *i.e.* transported molecules are inserted into the inner leaflet, flipped to the outer leaflet then released into the extracellular medium. The binding of a substrate to the high-affinity binding site results in ATP hydrolysis, causing a conformational change that shifts the substrate to a lower affinity binding site and then releases it into the extracellular space. In particular, proposed transport cycle of P-gp (Loo and Clarke, 2005) is based on the cross-linking pattern of Cys332 in TM6 which can be cross-linked to Cys856 in TM10 in the absence of ATP or drug substrate (Figure 1.11). Substrates diffuse into the lipid bilayer and enter the solvent-filled common drug-binding pocket through gates/portals formed by TMs 2 and 11 at one end and TMs 5 and 8 at the other end of the pocket. The cross-linking pattern is affected by the structure of the drug substrate via induced-fit mechanism. Binding of drug substrate changes the structure of the NBDs, resulting in stimulation of ATP hydrolysis. ATP binding and hydrolysis cause rearrangement of the drug-binding pocket such as rotation/lateral movement of the TM segments and simultaneous efflux of drug substrate out of the cell or possibly into the outer leaflet with very hydrophobic substrates. ATP hydrolysis promotes interaction between the extracellular ends of TM6 and TM12

such that Cys332 in TM6 can be cross-linked to Cys975 in TM12 with a cross-linker. After efflux of substrate, P-gp returns to its initial resting state (Loo and Clarke, 2005).

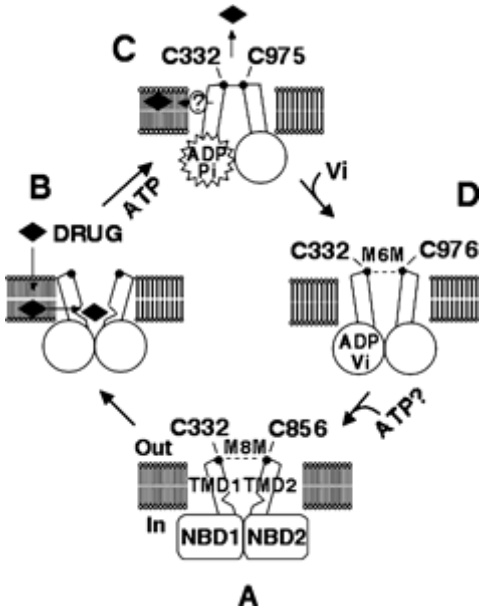

Figure 1.11 Transport mechanism of P-gp (Loo and Clarke, 2005).

Expression of P-gp was detected in various hematological malignanties and tumors which were also correlated to clinical outcome of patients. Examples include AML, myeloma, and breast, lung, ovarian, bladder, cervical, central nervous system cancers (reviewed in Leonard et al., 2003). P-gp is responsible for the development of resistance to a variety of anticancer agents. Some of its substrates are anthracyclins (doxorubicin, daunorubicin, and epirubicin), anthracenes (bisantrene, mitoxantrone), epipodophyllotoxins (etoposide, teniposide), actinomycinD, and paclitaxel (reviewed in Schinkl and Jonker, 2003).

Verapamil was the first agent discovered for its P-gp inhibitory function. Other first-generation agents together with verapamil, such as phenothiazine derivatives, cyclosporine, amiodarone, and tamoxifen were also employed in clinical trials for the reversal of drug resistance. More potent and less toxic second-generation agents were developed for the reversal of drug resistance mediated by Pgp. Some examples are PSC833,

VX-710, GG918, V-104, and PluronicL6 (Sparreboom *et al*., 2003; Schinkl and Jonker, 2003).

1.3.1.2 Multidrug Resistance Protein 1 (MRP1)

The *ABCC1* (*MRP1*) gene is located on choromosome 16p13.1 (Table 1.2). The gene has 31 exons encoding for a 190 kDa (1531 aa) MRP1 protein with 3 TMDs (17 TMSs), with a linker loop (L_0) binding TMD_0 and TMD_1, and 2 NBDs (Figure 1.12). The *ABCC1* gene was first identified in the small cell lung carcinoma cell line NCI-H69, a doxorubicin selected multidrug resistant cell line that did not overexpress P-gp (Cole *et al.*, 1992). In normal tissues, MRP1 localizes to the basolateral membrane of epithelial cell layers (Young *et al*., 2003) and substrates are therefore transported towards the basolateral side of epithelia. It has important pharmacological and toxicological functions. Its normal tissue expression is ubiquitous since it is the major leukotriene C4 transporter. Particularly, it is highly expressed in human placenta for protection of the fetus from xenobiotics, in blood brain barrier, intestine, and kidney (Young *et al*., 2003; Schinkl and Jonker, 2003; Eisenblätter *et al.*, 2003).

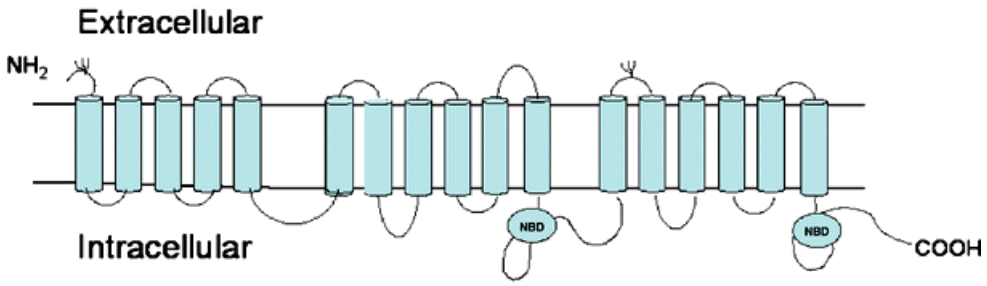

Figure 1.12 Schematic membrane topology of MRP1 (Pal and Mitra, 2006).

MRP1 is mainly able to transport lipophilic anions. In addition, MRP1 functions in the transport of hydrophobic drugs or other compounds (*e.g.* the inflammatory mediator leukotriene C4) that are conjugated or complexed to the anionic tripeptide glutathione (GSH), to glucuronic acid, or to sulfate (reviewed in Schinkl and Jonker, 2003). Therefore,

efficient transport of non-anionic anticancer drugs by MRP1 is mainly dependent on a normal cellular supply of GSH (Figure 1.13).

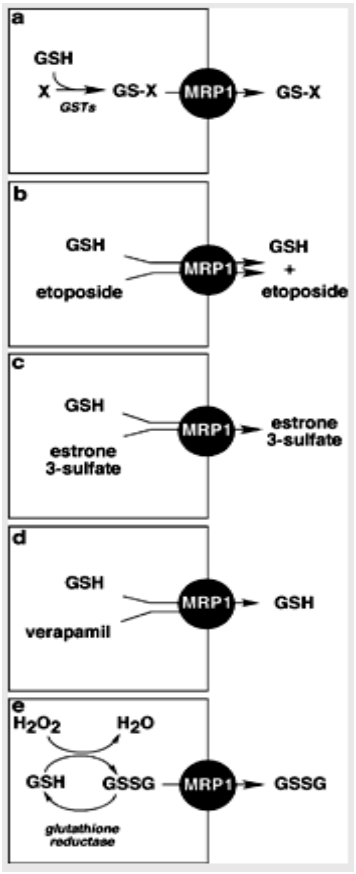

Figure 1.13 Involvement of glutathione in MRP1-mediated transport (Kruh and Belinsky, 2003): (a) Transport of hydrophobic compounds that are enzymatically conjugated to glutathione, (b) Cotransport of etoposide with glutathione, (c) Stimulation of transport by glutathione where glutathione is not cotransported, (d) Stimulation of glutathione transport by verapamil where verapamil is not cotransported, and (e) Transport of oxidized glutathione (GSSG).

Since MRP1 is expressed ubiquitously in normal human tissues, it is potentially present in most tumor types (Borst *et al.*, 2000). It plays a role in MDR conferring resistance to several compounds. There are several reports on the expression of MRP1 in cancers that are treated with anthracyclines, camptothecins, cisplatin and etoposide, such as leukemia (Plasschaert *et al.*, 2003) and breast (Burger *et al.*, 2003), lung cancers (Triller *et*

al., 2006), and in some cases correlations between clinical outcome and expression have also been drawn (Ohishi *et al.*, 2002; Triller *et al.*, 2006).

A variety of inhibitors of MRP1 has also been described. Some examples are the LTC_4 analogue MK571, LTC_4 itself, S-deacylglutathione, sulfinpyrazone, benzbromarone, and probenecid (reviewed in Schinkl and Jonker, 2003). Cyclosporine A and PSC 833 also inhibit MRP1 but only with low affinity and poor specificity. For specific *in vivo* inhibition of MRP1 the general organic anion transporter inhibitors are also not very suitable, as they extensively affect organic anion uptake systems. Moreover these inhibitor compounds need to be used at relatively high concentrations.

1.3.1.3 Breast Cancer Resistance Protein (BCRP)

Breast cancer resistance protein (BCRP)/placenta-specific ABC transporter (ABCP)/mitoxantrone resistance protein (MXR) was initially cloned by Doyle *et al*. (Doyle *et al.*, 1998) from a highly doxorubicin-resistant MCF7 breast cancer cell line. Importantly, transfection of the cloned BCRP Transfection of cDNA demonstrated that BCRP itself could confer resistance to mitoxantrone, doxorubicin, and daunorubicin through an ATP - dependent extrusion of its drug substrates. Furthermore, cDNA analysis revealed that BCRP is a 655 amino acid protein containing a single NH_2-terminal ABC transporter specific NBD followed by six TMSs (Figure 1.14). The human *BCRP* gene, containing 16 exons, is located on chromosome 4q22 (Dell *et al.*, 2001). Since other MDR related ABC transporters (P-gp and MRP subfamily members) contain multiple TMD structures with two times six TMSs (next to an NH_2-terminal 5 TMS extension present in MRP1 and MRP2), BCRP functions as a homo- or heterodimers (Allen and Schinkel, 2002).

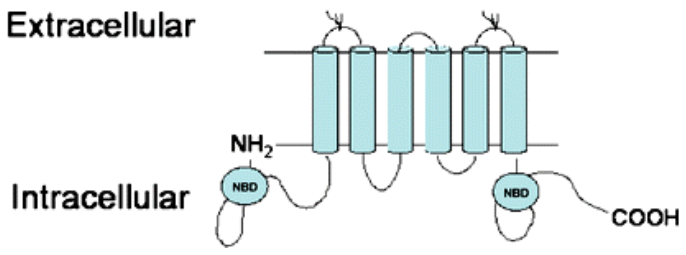

Figure 1.14 Schematic membrane topology of BCRP (Pal and Mitra, 2006).

ABCG2 is highly expressed in the trophoblast cells of the placenta, suggesting that the pump is responsible either for transporting compounds into the fetal blood supply or removing toxic metabolites (Young *et al.*, 2003). The gene is also highly expressed in the intestine and hemopoietic stem cells (Sarkadi *et al.*, 2004), and a lesser amount in the blood-brain barrier (Eisenblätter *et al.*, 2003). Subcellular localization of the protein is plasma membrane, polarity varying according to cell type.

BCRP confers resistance to mitoxantrone, anthracyclines, methotrexate, topotecan and topoisomerase I inhibitors (reviewed in Coley, 2008). In some drug-selected cell lines overexpressing *ABCG2*, a single amino acid change at position 482 occured. These mutants showed altered substrate specificity since they conferred increased mitoxantrone or doxorubicin resistance and rhodamine 123 transport capacities. They had increased transport and ATP hydrolytic activity with altered cross-resistance profiles (Honjo *et al*., 2001). Additionally, in mitoxantrone resistant cell lines overexpressing *BCRP,* the gene locus was found to be heavily amplified indicating that overexpression can result both from *in situ* gene activation and gene amplification (Knutsen *et al.*, 2000).

1.3.2 Altered Expression Levels of Genes for Survival

Apoptosis is an evolutionarily conserved form of cell death that was first described by Kerr *et al.* (Kerr *et al.*, 1972) in 1972. It may be a part of normal cell progression like embryonic development, is required for normal tissue specific events and cellular homeostasis. It may also be required for the destruction of cells that represents a threat to the integrity of the organism such as cells infected by viruses, cells that have damaged DNA, cells that have impaired mitosis or cancer cells.

Cells may enter apoptosis via stimulation by internal stress-induced signals, leading cells to enter the intrinsic or mitochondrial pathway, or stimulation by external ligand-induced signals, leading cells to enter the extrinsic or death receptor pathway (Figure 1.15).

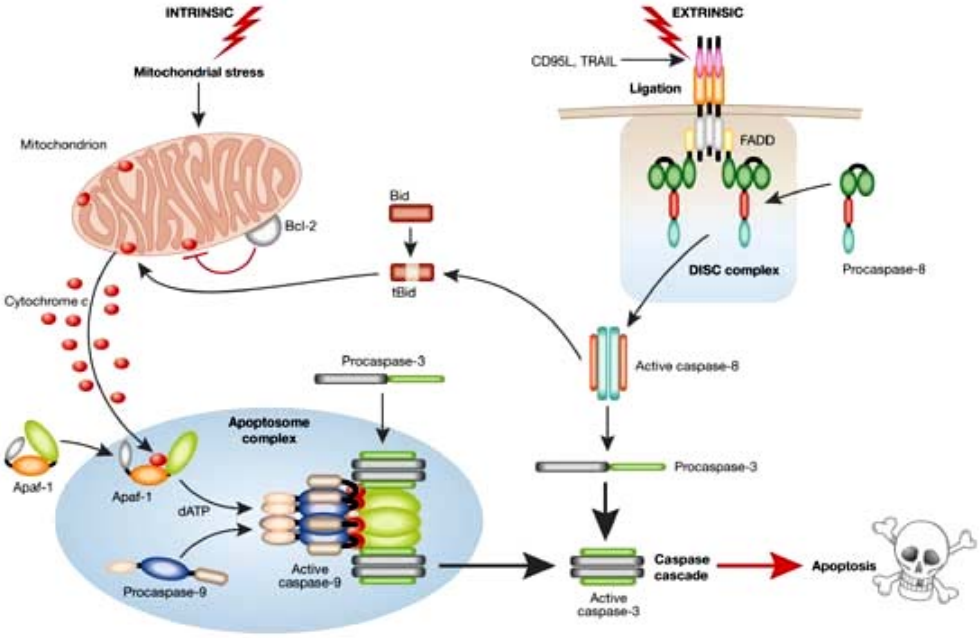

Figure 1.15 The intrinsic and extrinsic pathways for apoptosis (MacFarlane and Williams, 2004).

Fas, tumour necrosis factor (TNF) and TNF-related apoptosis-inducing ligand (TRAIL) receptors are involved in extrinsic or death receptor pathway. They are integral membrane proteins with their receptor domains exposed to the outer surface of the cell. Binding of the complementary death activator ligands (FasL, TNF and TRAIL, respectively) transmits a signal to the cytoplasm that leads to activation of caspase 8 via use of adaptor molecules for the recruitment, trimerized receptor–ligand complex (DISC), Fas-associated death domain protein (FADD) and TNF-receptor-associated death domain protein (TRADD). Caspase 8, in turn, cleaves and activates effector caspases such as caspase-3 and –7. This pathway can be regulated by c-FLIP, which inhibits upstream initiator caspases, and inhibitor of apoptosis proteins (IAPs), which affect both initiator and effector caspases. Sequential caspase activation creates an expanding cascade of proteolytic activity which leads to digestion of structural proteins in the cytoplasm, fragmentation of chromosomal DNA, and internal phagocytosis of the cell.

Intrinsic or mitochondrial pathway includes disruption of mitochondrial membrane via stimulation by stress-induced signals such as exposure to cytotoxic agents or radiation. Integral membranes proteins of the Bcl-2 family are expressed on the surface of outer membrane of mitochondria having C-terminal transmembrane domains that are inserted in the outer membrane of mitochondria. Products of the Bcl-2 gene family members are involved in regulation of apoptosis (Table 1.4) by homo/heterodimerization of pro/antiapoptotic members for alteration of the outer membrane integrity. Bcl-2 related proteins possess conserved Bcl-2 homolog domains (BH1-4) required for dimerization. The antiapoptotic members are more highly conserved, and each antiapoptotic member possesses a pocket that binds BH3 domains from selected proapoptotic members. Proapoptotic members can be further subdivided into the more fully conserved "multidomain" and "BH3-only" subsets (reviewed in Cory *et al.*, 2003). A proapoptotic cascade exists in which BH3-only members function as upstream death ligands that induce allosteric activation of multidomain Bax and Bak. 21 kDa Bax protein is a pro-apoptotic member of the Bcl-2 related proteins. On the contrary, antiapoptotic molecules such as Bcl-2, Bcl-X_L, and Mcl-1 sequester BH3-only molecules in stable complexes, preventing activation of Bax and Bak (Figure 1.16). Bcl-2 is a 26 kDa antiapoptotic protein inactive when phosphorylated on the serine residues (70 and 87) (Wang *et al.*, 1999). When activated Bcl-2 and/or another antiapoptotic member Bcl-X_L can block the pro-apoptotic effects of Bax by forming heterodimers. When not bound to an antiapoptotic member, Bax penetrates into mitochondrial membranes, changes mitochondrial outer membrane permeabilization (MOMP) causing cytochrome *c* to leak out from intermembrane space. Together with Bak, Bax constitute an obligate gateway to the intrinsic pathway of cell death, operating at both the mitochondria and endoplasmic reticulum (ER). Once released, cytochrome *c* binds to apoptotic protease-activating factor 1 (Apaf1), forms the Apaf1-caspase 9 'apoptosome' complex in the presence of dATP and activates caspse 9 (Figure 1.15). Activated caspase 9 triggers the sequential activation of the caspase cascade, leading to proteolytic degredation and cell death.

Table 1.4 Pro-survival/-apoptotic members of the Bcl-2 related proteins (Cory et al., 2003).

Category	Genes
Antiapoptotic (Pro-survival)	Bcl-2, Bcl-X_L, Bcl-w, A1/Bfl-1, Brag-1, Mcl-1, CED-9
Pro-apoptotic	Bcl-X_s, Bax, Bak, Bok/Mtd, Bad, Bid, Bik, Bim_L

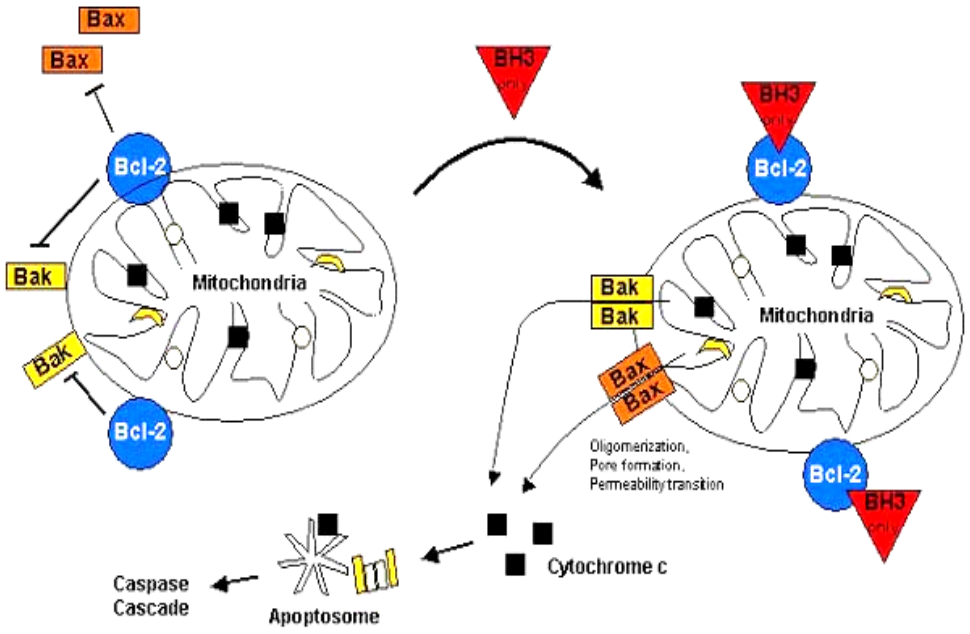

Figure 1.16 Role of Bcl-2 related proteins in apoptosis (www.celldeath.de/encyclo/index.html).

Overexpression of the Bcl-2 protein or of close family members blocks the release of cytochrome c, thus blocking the mitochondrial apoptotic pathway. Thus, the balance between pro- and antiapoptotic Bcl-2 related proteins expressed in the outer mitochondrial membrane is one of the determinant factors whether apoptotic cell death is initiated or the cell survives. On the other hand, Bax opposes the action of Bcl-2 and accelerates cell death

when overexpressed in mammalian cells. Therefore, altered expression levels of genes encoding the pro-/apoptotic members of the Bcl-2 related proteins is one of the mechanisms of multidrug resistance of to chemotherapeutic agents that mediate their action through apoptosis. For instance, Huang *et al*. (Huang *et al.*, 1997) reported that increase in the p26Bcl-2/p21Bax was one of the mechanisms of taxol resistance. They also demonstrated the positive effects of estrogen in estrogen receptor positive MCF-7 cells inhibiting the taxol-induced apoptosis. However, according to Del Bufalo *et al*. (Del Bufalo *et al.*, 2002), Bcl-2 had been shown to exert differing effects on the sensitivity of breast cancer cells depending on the antineoplastic drugs used together with drug accumulation and efflux. Chun and Lee (Chun and Lee, 2004) demonstrated that p26Bcl-2 was up-regulated in paclitaxel-treated sensitive Hep3B human hepatocellular carcinoma cells and paclitaxel-induced effects were p53 independent. These cells were shown to contain very low levels of Bcl-2 protein and to be more sensitive to paclitaxel-induced apoptosis when compared to another hepatocellular carcinoma cell line, SNU-38, that was resistant to paclitaxel containing very low levels of Bcl-X_s a much higher level of Bcl-2. Bcl-X_L expression was also shown to increase in dose-dependent manner in the same study concluding that both Bcl-2 and Bcl-X_L proteins exert a protective effect against apoptosis and might have mediated paclitaxel resistance.

1.3.3 Altered Target Type Due to Differential Expression of *β-tubulin* Isotypes

Distortion of polymerization-depolymerization dynamics due to antimicrotubule agent application results in mitotic arrest and growth inhibition (Yvon *et al.*, 1999). Docetaxel is an antimitotic agent that binds to microtubules, thereby stabilizing them against depolymerization and inhibiting cell replication by disrupting normal mitotic spindle formation. Docetaxel binds preferentially to the β subunit of the microtubule and it has its binding site on helix 1, between the residues 15-25 (Liu *et al.*, 2001). Tubulin is a heterodimer that consists of α- and β-tubulin subunits and constituting the microtubule. The genes that encode tubulin have been highly conserved throughout evolution, and even within species multiple α- and β-tubulin genes encode distinct tubulin gene products (Kavallaris *et al.*, 1997). There are seven β-tubulin isotypes in human tissues with differential tissue specific expression pattern (Verdier-Pinard *et al.*, 2003). Multiple tubulin

isotypes in cells has been correlated to their different physiological properties (Ludueńa, 1998). Some tubulin isotypes (Table 1.5) have differing assembly properties (Banerjee *et al.*, 1990; Bhattacharya and Cabral, 2004). Alterations in expression levels of the β-tubulin isotypes, differential expression of microtubule associated proteins (MAPs) and mutations in *TUBB* gene which encodes the predominant constitutive class I β-tubulin have been correlated to multiple drug resistance (MDR) developed against antimicrotubule agents (Kavallaris *et al.*, 2001; Giannakakou *et al*., 1997; Hasegawa *et al*., 2002).

Table 1.5 β-tubulin isotypes.

β-tubulin isotype classes	**Human gene[d]**	**Gene Bank accession number**	
		mRNA	**Protein**
βI[a] (tubulin, beta)[b]	*TUBB*	AF141349	AAD33873
βII[a] (tubulin, beta-2A/tubulin, beta-2B)[b]	*TUBB2A/TUBB2B*	BC001352	AAH01352
βIII[a] (tubulin, beta-3)[b]	*TUBB3*	BC000748	AAH00748
βIVa[a,c] (tubulin, beta-4)[b]	*TUBB4*	BC013683	AAH13683
βIVb[a,c] (tubulin, beta-2C)[b]	*TUBB2C*	BC004188	AAH04188
βV[a] (tubulin, beta-6)[b]	*TUBB6*	NM_032525	NP 115914

[a] βI, II, III, IVa, IVb,V-tubulin refer for names of different beta tubulin isotype proteins differentiated based on each carboxy terminal region of each protein.

[b] New protein names used in NCBI Entrez Protein database.

[c] Tubulin, beta-4 for the protein encoded by *TUBB4* gene and tubulin beta-2C for the protein encoded by *TUBB2C* gene are updated and preferred names by NCBI database.

[d] Updated and accepted gene names by HUGO Gene Nomenclature Committee.

Tumor cells resistant to paclitaxel, docetaxel and vinca alkaloids presented altered tubulin composition (Drukman and Kavallaris, 2002). Opposing tubulin alterations are responsible for taxoid and *vinca* alkaloid resistance. For example, decreased microtubule stability increases taxoid sensitivity where increased microtubule stability increases vincristine sensitivity of cells. βIII-tubulin has been previously characterized for its low polymerization rate (Banerjee *et al.*, 1990) and tumor cells overexpressing this isotype have been shown to overcome stabilizing effects of paclitaxel (Hari *et al.*, 2003). Alterations in expression levels of other isotypes have been correlated to paclitaxel, docetaxel (Liu *et al*., 2001; Banerjee, 2002; Hasegawa *et al.*, 2003; Shalli *et al*., 2005) and vincristine resistance

(Kavallaris *et al.*, 2001). However, the results demonstrating involvement of other tubulin isotypes in MDR are still controversial.

1.3.4 Involvement of Growth Factor and Cytokine Signaling in MDR

Growth factors and cytokines can affect cellular stress and DNA damage responses, and can act either as survival factors, providing drug resistance, or sensitizing factors, potentiating cytotoxicity. However, recent studies documented that inappropriate activation of growth factor signaling cascades, either through an enhanced supply of growth factor ligands, or via up-regulation and increased activation of their target growth factor receptors or their recruited downstream signaling elements, can promote failure of chemotherapy in breast cancer cells (Nicholson *et al.*, 2005). Alterations in epidermal growth factor (EGF) signaling pathway, which is involved in cell proliferation, cell cycle progression and DNA damage repair, occurs frequently in human cancer cells and subsequently, affect the cell survival towards chemotherapy. For instance a previous study demonstrated long-term exposure to EGF might induce drug resistance to doxorubicin, etoposide and amsacrine through the downregulation of topoisomerase II (Tsang *et al.*, 2006). In addition, growth factor signaling through the insulin-like growth factor-I (IGF-I) and –II activation of insulin-like growth factor-I receptor (IGFIR) plays a role in proliferation and survival, as well as its supportive role in EGFR driven proliferative signals through promoting the phosphorylation of the EGFR (Knowlden *et al.*, 2003). Furthermore, protection from drug-induced apoptosis by fibroblastic growth factor (FGF) and vascular endothelial growth factor (VEGF) is observed, with achievement of even greater level of protection when both growth factors are used (reviewed in Coleman, 2003).

Moreover, hormone receptor status has been correlated to prognosis and outcome in the clinic, *i.e.* ER negativity is associated with poor prognosis, precluding response to all categories of anti-hormones and associating with a more aggressive, proliferative phenotype (Nicholson *et al.,* 1993).

Acute inflammatory response is associated with many conditions including infection, injury, hypoxia and stress, and results in release of a few of the pro-inflammatory cytokines. Among them, IL-1β, IL-6 and TNF-α are the principle mediators. Downstream

effectors involved in signaling pathways of these cytokines are important in regulating gene expression of numerous glycoproteins *e.g.* cytochrome P450 drug metabolizing enzymes and ABC transporters through transcription factor activation as well as their putative roles in various cellular responses. Effects of cytokines on chemotherapy resistance are contradictory. In particular, Ho and Piquette-Miller (Ho and Piquette-Miller, 2006) reviewed modulatory effects of inflammatory response on MDR toward suppressed expression and activity of ABC transporters. On the other hand, elevated serum levels of cytokines (*e.g.* IL-6) have been documented in various studies of breast, prostate and ovarian cancer patients having poor respond to chemotherapy, metastasis and morbidity (Conze *et al.*, 2001; Scambia *et al.*, 1995). Moreover, the mechanism of this resistance was attributed to the activation of the CCAAT enhancer-binding protein family of transcription factors and induction of *MDR1* gene expression (Conze *et al.*, 2001). Another cytokine, transforming growth factor (TGF-) ß, which is released during an acute inflammatory reaction, also appears to influence *MDR1* gene expression in a complex manner depending on the duration of exposure (Sukhai and Piquette-Miller, 2000). Thus it is likely that the cytokines interact with *MDR1* gene expression resulting in unique effects dependent upon cytokine concentrations, cell type and health-disease status.

1.3.5 Involvement of Extracellular Matrix in MDR

Extracellular matrix (ECM) made up of collagens, fibronectin, laminins, proteoglycans and other macromolecules, controls many aspects of cells such as gene expression, differentiation and proliferation, and invasive/metastatic phenotype of tumor cells. Altered expression levels of these molecules in tumor cells was reported to affect their sensitivity to drug induced apoptosis and drug resistance through activation of survival pathways of cells (Hoyt *et al.*, 1996; Kraus *et al.*, 2002). Tumor cells remodel their microenvironment for survival and invasion. Differential expression of ECM components, matrix metalloproteinases (MMPs) and adamalysins (a disintegrin and metalloproteinases; ADAMs and a disintegrin and metalloproteinase with thrombospondin motifs; ADAMTSs) may contribute the remodeling of ECM, cancer invasion and metastasis. According to a previous report (Mitsumoto *et al.*, 1998) on invasive/metastatic behavior of drug resistant tumor cells, carboplatin resistant mouse epithelial cells had increased levels of ECM components (fibronectin, laminin, collagen type IV) with enhanced MMP-2 activity. Remodeling of ECM due to drug exposure has also been related to drug resistance that it

can affect tumor cell survival by preventing the penetration of the drug into the tumor in vivo. In addition, changes in ECM can also affect the sensitivity of the tumor cells to apoptosis through growth factors dependent on cell-matrix and cell-cell interactions through ECM-integrin signaling (Morin, 2003) as well as development of cell adhesion-mediated drug resistance (CAM-DR).

1.4 Modulation of MDR

MDR can be inhibited or reversed; a phenomenon also known as circumvention or modulation of MDR. The ability to overcome multidrug resistance is complicated since many human tumors simultaneously exhibit multiple resistance mechanisms. Thus, in order to effectively overcome multidrug resistance designing new strategies that combine multiple pharmacological and molecular approaches has become necessary.

The pharmacologically used compounds are so called reversal agents, inhibitors, modulators or chemosensitizers (Ugocsai *et al.*, 2005). Different modulators for different targets have been found and developed for the modulation of MDR. Transport of cytotoxic drugs and other substrates by MDR pumps (ABC transporters) can be inhibited by certain compounds. This type of modulation of MDR by chemical means includes:

- blocking drug binding site either competitively, non-competitively or allosterically
- interfering with ATP hydrolysis
- altering integrity of cell membrane lipids

Although many MDR inhibitors have been identified, none of them was being clinically useful without side effects. Efforts are in progress for the discovery of nontoxic MDR inhibitors also lacking pharmacokinetic interactions with anticancer drugs. The application of anticancer drugs with MDR modulators is acceptable in case the pharmokinetic interaction between modulator and anticancer drug is synergistic. Initially identified reversal agents, first-generation reversal agents, had other pharmacological activities than inhibition of MDR since they were not specifically developed for inhibiting MDR. Thus, their affinity was low for ABC transporters and necessitated the use of high doses, resulting in high toxicity which limited their application. These agents are calcium

channel blockers (*e.g.*, verapamil), calmodulin antagonists, steroidal agents, protein kinase C inhibitors, immunosuppressive drugs (*e.g.*, cyclosporine A), antibiotics (*e.g.*, erythromycin), antimalarials (*e.g.*, quinine), psychotropic phenothiazines and indole alkaloids (*e.g.*, fluphenazine and reserpine), steroid hormones and anti-steroids (*e.g.*, progesterone and tamoxifen), detergents (*e.g.*, cremophorEL) and surfactants (reviewed in Ozben, 2006). So studies on various synthetic and natural compounds have been emerged on different cell lines to identify the most effective resistance modifiers. For example, synthetic compounds such as cinnamylidene ketones and organosilicons were tested on different cancer cell lines for resistance reversal effects (Engi *et al.*, 2006; Molnar *et al.*, 2004). Second-generation chemosensitizers were designed to reduce the side effects of the first generation drugs. Limitations of the use of these agents also rose due to modulation of MDR protein in normal tissues, especially blood-brain barrier as well as their unpredictable effects on cytochrome P450 3A4-mediated drug metabolism and pharmacokinetic interactions with anticancer drugs used. Third-generation molecules have been developed to overcome the limitations of the second generation modulators as they are not metabolized by cytochrome P450 3A4 and they do not alter pharmacokinetics of anticancer drugs. They specifically and potently inhibit P-gp and do not inhibit other ABC transporters (Thomas and Coley, 2003).

Some natural compounds extracted from various fruits and vegetables were also used as chemopreventive agents (Zhu *et al.*, 2001). Paprika exracts containing carotenoids were proved to reverse MDR in drug resistant cells (Ford *et al.*, 1989). It was proved that, some flovanoids (Zhang *et al.*, 2004) and carotenoids exhibit anticarcinogenic and resistance modulating effects by modification of lipid bilayer in which P-gp is embedded and the transport activity of P-gp can slow down depending on the conformational changes induced by resistance modifiers (Molnar *et al.*, 2006).

One of the strategies to reverse MDR is to prevent the biosynthesis of resistance related genes by selectively inhibiting their expression. The aim of this strategy is to increase the chemosensitization of cancer cells while at the same time reducing toxicity and side effects of the chemosensitizers previously described. Antisense oligonucleotides (ASOs) and hammerhead ribozymes have been used for the specific inhibition of *ABCB1* (*MDR1*) gene expression and inhibiting the synthesis of the protein for the reversal of MDR phenotype. Motomura *et al*. (Motomura *et al*., 1998) demostrated that a lipopolyamine-coated phosphorothioate ASO complementary to *MDR1* (MDR1-AS) was effective in

inhibiting P-gp expression in acute myelogenous leukemia blast cells. Furthermore, modifications for the enhancement of cellular uptake and mRNA binding of ASOs have been performed by doxorubicin conjugation (Ren *et al*., 2004) in doxorubicin resistant cells. Ribozymes have been shown to decrease resistance to chemotherapeutic agents in leukemia, gastric carcinoma, hepatocellular carcinoma and breast carcinoma cells (Kobayashi *et al.*, 1999; Kowalski *et al.*, 2005; Huesker *et al.*, 2002; Peng *et al*., 2006). A variety of genes of regulators of apoptosis, cell growth, metastasis and angiogenesis have also been validated as molecular targets. For instance, two commercial ASOs in clinical trials are Genasense® inhibitor of Bcl-2 and Affinitak™ inhibitor of the protein kinase-Ca (PKCa) gene.

1.5 Use of Large-scale Gene Expression Analysis for Investigation of MDR

Genome wide expression analysis techniques may provide additional information on contribution of novel candidate genes to drug resistance. Microarrays for gene expression profiling are rapidly becoming important research tools. Particularly, large-scale expression analysis using high-density oligonucleotide cDNA microarrays enable researcher's assessment in a variety of conditions. Gene expression microarrays typically contain thousands of oligonucleotides or cDNAs, which correspond to transcripts of many different genes. cDNA microarrays for the investigation of gene expression profiles may be applied to basic laboratory research and studies of patient material. The high numbers enable to study expression of levels of genes under specific pre-defined circumstances such as studying expression profiles of drug resistant cells. The objective analysis of the expression level of thousands of genes almost automatically leads to identification of contribution of several genes to the development of drug resistance.

Beyond its application in research, these approaches offer the advantage of overcoming multidrug resistance. Since drug resistance is a multifactor phenomenon yet with undefined pathways, identifying key genes and new pathways involved in the molecular mechanisms of resistance can establish new drug targets and enable the rational

design of new anticancer drugs. Furthermore, a promising development may be the discovery of molecular markers of resistance, which would personalize chemotherapy with prior determination of potential responders or non-responders to anticancer drugs. Application of this approach in clinics may potentially increase efficacy of cancer chemotherapy and life quality of cancer patients.

1.6 Aim of the Study

Chemotherapy is one of the treatment strategies in cancer. It is administration of selective and specific cytotoxic anticancer agents to the patients. Multidrug resistance is a complex phenotype of tumor cells describing resistance to a wide range of structurally unrelated anticancer agents prescribed in cancer chemotherapy. Commonly patients, refractory to chemotherapy, develop multidrug resistance which seriously limits the efficacy of cancer chemotherapy. Multidrug resistance has been an extensive research area for its clinical implications. Since it is a multifactor yet not fully elucidated phenomenon with involvement of diverse cellular pathways, many comprehensive studies on the subject are required. The objectives of this study were:

- To develop docetaxel and doxorubicin resistant MCF-7 human breast carcinoma sublines by stepwise selection of resistant cells.
- To investigate gene expression levels of *MDR1, MRP1, BCRP, Bcl-2, Bax* and *β-tubulin* isotypes in response to increasing drug concentrations in resistant sublines.
- To determine expression of significantly altered genes at transcription level and at protein level.
- To perform genome wide expression analysis of resistant sublines by the use of high-density cDNA microarrays.
- To investigate development of cross-resistance to paclitaxel, vincristine, ATRA, tamoxifen and irradiation.
- To evaluate antiproliferative efficacy of combined drug applications on resistant cells.

- To determine the inhibitory effects of verapamil and promethazine on drug resistance.

In summary, this study aimed to elucidate the basic molecular mechanisms of docetaxel and doxorubicin resistance in breast carcinoma model cell line MCF-7 and to evaluate efficacy of reversal agents on resistant sublines.

CHAPTER 2

MATERIALS AND METHODS

2.1 Cell Culture

2.1.1 Growth Conditions

The parental MCF-7 cell line was donated by the ŞAP Institute, Ankara, Turkey. It is a model cell line for human mammary carcinoma which exhibits some features of differentiated mammary epithelium (Bacus *et al.*, 1990). MCF-7 cells were maintained as an attached type monolayer culture in commercially defined RPMI 1640 medium (Biochrom AG, Germany) (Appendix A) supplemented with 10% (v/v) heat-inactivated fetal bovine serum (FBS) (Biochrom AG) and 1% (v/v) gentamycin (Biological Industries, Israel). Incubation conditions at 37°C in a 95% (v/v) humidified atmosphere of 5% (v/v) CO_2 were maintained in a Heraeus incubator (Hanau, Germany). The solutions used were cell culture grade quality and the equipment used in cell culture were commercially presterilized and disposable.

2.1.2 Cell Harvesting (Passaging)

Cells were grown in either 25cm^2 or 75cm^2 attached types, filter cap culture flasks (Greiner Bio-One Germany). When attached cell concentration on flask surface exceeded 80% confluency, the cells were trypsinated with trypsin-EDTA (Biochrom AG). Medium was poured out and cells attached to flask surface were washed out with FBS-free growth medium. Trypsin-EDTA was added (1mL for 25cm^2 and 3mL for 75cm^2 flasks) and discarded immediately leaving small amount of trypsin-EDTA (~0.5mL in 25cm^2 and ~1mL in 75cm^2 flasks). The flasks then incubated at 37°C until detachment of cells was

observed from outside of the flasks. Growth medium (amount depending on downstream processes) was added and detached cells were homogenized and passed into new culture flasks or separated for further experiments or freezed.

2.1.3 Freezing and Thawing of Cells

Trypsinated and detached cells (concentration no more than $5x10^6$ cells/mL) were centrifuged at 800 rpm for 5 min in 15mL falcon tubes (Greiner). Supernatant was discarded and pellet of cells were resuspended in 1 mL of cold freezing medium (90% (v/v) FBS and 10% (v/v) DMSO (Sigma-Aldrich, USA)). The freezing medium was transferred into the cryovials (Greiner) and maintained on ice for 30 min. The cryovials were then kept in -20ºC freezer for 24 h and transferred to -80ºC freezer. For long-term storage they were immersed into liquid nitrogen container.

Cryovials were removed from -80ºC freezer or liquid nitrogen container and immediately transferred to 37ºC. When they were completely thawed, aliquots were transferred into the 15mL falcon tubes and cells were pelleted at 800 rpm for 5 min. Supernatant was discarded and pellet was resuspended in a volume of complete media appropriate for type of culture flask. Cells were maintained in defined growth conditions.

2.2 Drugs and Development of Resistant Sublines

Docetaxel (DOC) was purchased from Fluka (Switzerland) and stored as 0.05 M stock solution in DMSO at -20°C. Doxorubicin (DOX) was kindly provided by Prof. Dr. Fikret Arpacı (Gülhane Military Medical Academy, School of Medicine, Department of Oncology) and stored as 3.4 mM stock solution in pure distilled water at room temperature. These solutions were further diluted with cell culture medium and stored at -20°C. 1 nM DOC and 10 nM DOX of initial concentrations were directly applied to culture medium. Docetaxel and doxorubicin were applied to parental MCF-7 cells separately in culture flasks in dose increments for stepwise selection of resistant cells. Developed sublines were maintained by exposure to selective drug concentration. Cells capable of growing in

selection concentrations became resistant (Appendix B). Developed sublines were designated with their respective drug concentrations and maintained by exposure to selective drug concentration.

2.3 Cell Proliferation Assays

2.3.1 Viable Cell Count

Cells suspension with a concentration of $5.0x10^4$ cells/mL were prepared and distributed to 6-well attach type culture plates (Greiner) as dublicates. Every corresponding day counts were made by trypsinizing cells and staining with trypan blue (Sigma-Aldrich) with a 1: 9 ratio of tryphan blue to cell suspension. Cells were counted in in a Neubauer counting chamber (Bright-line, Hausser Scientic, USA) under light microscopy. Cells that were stained into dark blue were indicated as dead due to the impermeability of the dye to cell membrane. Cells were counted for 10 days for construction of growth curves.

2.3.2 XTT Cell Proliferation Assay

Antiproliferative effects of docetaxel and doxorubicin on parental MCF-7 cells and drug selected sublines were evaluated by means of the Cell Proliferation Kit (Biological Industries) according to manufacturer's instructions. Assay was a colorimetric test based on the reduction tetrazolium salt, XTT to colored formazan products by mitochondria of live cells. In brief, cells were seeded to 96-well microtiter plates (Greiner) at a concentration of $5.0x10^4$ cells/well and incubated for 72 h in medium containing horizontal dilutions of drugs. In each plate assay was performed with a column of blank medium control and a cell control coloumn. Then, XTT reagent was added and soluble product was measured at 500 nm with an Spectromax 340 96-well plate reader (Molecular Devices, USA).

2.3.3 Statistical Analysis

The results of viable cell counts and XTT cell proliferation assay were subjected to Student's t-test by using SPSS Software (SPSS Inc., USA) to determine the significant difference with $\alpha = 0.05$.

2.4 Reverse Transcription-Polymerase Chain Reaction (RT-PCR)

2.4.1 RNA Isolation

Prior to RNA isolation, all the plastic- and glassware were treated with DEPC-treated dH_2O (Appendix C) in order to inhibit RNases. Excess DEPC was vaporized under hood for over night and the equipment were autoclaved before RNA isolation and cDNA sysnthesis.

Total RNA was isolated according to modified and optimized 'Guanidum Thiocynate (GTC)' method (Chomczynski *et al.*, 1987). Cells were centrifuged at 800 rpm for 5 min; pellet was resuspended in a solution of 596 µL GTC solution (Appendix C) and 4µL 0.1 M β-mercaptoethanol (Sigma-Aldrich), and vortexed. 100µL sodium acetate solution (Appendix C), 1mL citrate saturated acid phenol (Appendix C) and 200µL choloroform were added and 2mL microcentrifuge tubes (Greiner) were reversed up and down for a couple of times. After centrifugation at 13,000 rpm, 4ºC for 15 min, total cellular RNA is collected from upper aqueous phase into new 1.5mL microcentrifuge tubes (as 5x100µL aliquots). Double volume of 98% (v/v) ethyl alcohol was added and centrifuged at 13,000 rpm, 4ºC for 15 min. RNA pellet was resuspended in 70% (v/v) ethyl alcohol and repelleted. RNA pellet was dried near flame and resuspended in 40µL RNAase-free water by incubation at 60ºC for 10 min. Isolated RNA was stored at -80ºC.

Isolated RNA was detected by horizontal agarose gel electrophoresis on 1% (w/v) agarose. For gel electrophoresis 1g agarose (Applichem, Germany) was dissolved in

100mL 1X TAE buffer (Appendix C) and boiled in a microwave oven. 7µL ethidium bromide solution (Appendix C) was added into the gel solution. The gel solution was poured into electrophoresis tray for solidification. 5µL of RNA sample was mixed with 2X loading buffer (Fermantas, Lithuania) and loaded. High Range RNA Ladder was also loaded (Fermantas). Electrophoresis was run with 1L of 1X TAE buffer at 70V, for 1.5 h. The gel was observed under UV light and photographed. Gels were evaluated in terms of intactness of RNA and DNA contamination.

Concentration and purity of isolated total RNA were determined by measuring optical density at 260 nm for nucleic acids and 280 nm for proteins. OD_{260} / OD_{280} were calculated which should be equal in between 1.6 and 2.1 for pure RNA. Concentration of total RNA was calculated for cDNA sysntesis as follows:

$$\mu g/mL\ RNA = 40 \times Dilution\ factor \times OD_{260} \qquad \text{[Equation 2.1]}$$

Concentrations of RNA samples were calculated to determine volume of aliquot required for 5µg of total RNA to use in cDNA synthesis.

2.4.2 cDNA Synthesis

cDNA synthesis was performed on ice. Aliquot from RNA samples containing 5µg of total RNA was mixed with 0.5 µg of gene specific primers. Reaction volume was completed to 11 µL with RNAase-free water and incubated at 70ºC for 5 min to disrupt secondary structures of RNA. 4µL from 5X reaction buffer (Fermentas), 2µL from 10mM dNTP mix were added and the volume was completed to 19.7µL with RNAase-free water. The reaction mix was incubated for 5 min at 37°C for annealing of primers. Finally, 0.3µL (40 units) Moloney-Murine Leukemia Virus Reverse Transcriptase (Fermentas) was added. Synthesis was performed at 42°C for 60 min and the reaction was stopped by heating to 70°C for 10 min. cDNA was stored at -20°C.

cDNA synthesis of *β tubulin* isotype classes II and V were performed according to protocol defined by Cobley *et al.* (Cobley *et al.*, 2002) to prevent amplification of contaminating DNA. 5' tags were added to cDNA during sysnthesis and unique sites on cDNA which were not present on genomic DNA were created. The methodology was

schematized in Figure 2.1 and the gene specific oligonucleotides used in cDNA synthesis with their T_m values are given in Table 2.1.

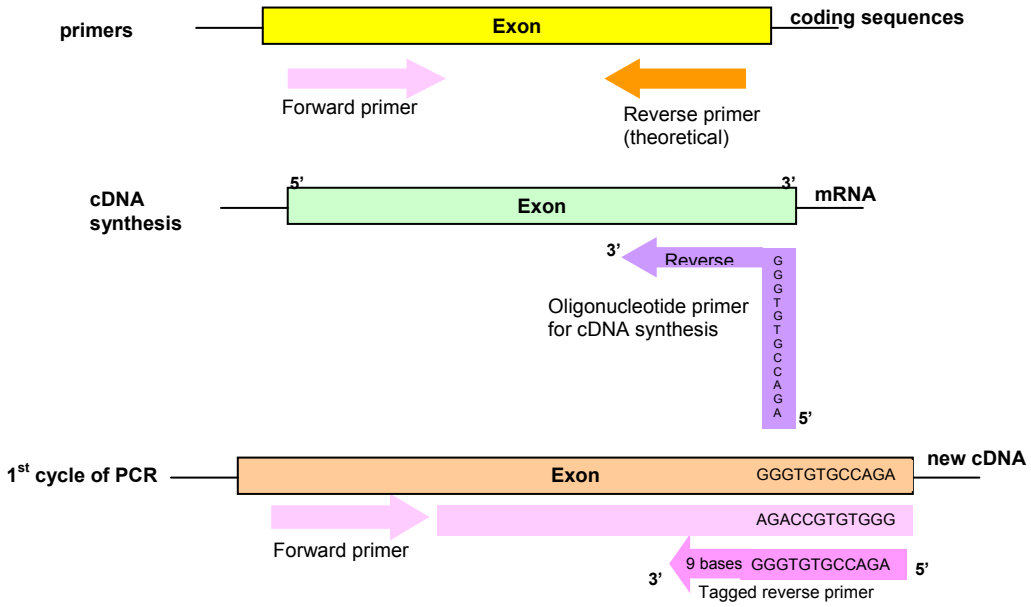

Figure 2.1 Schematic representation of 5'tagged primer synthesis.

Table 2.1 Oligonucleotides for *β tubulin* class II and V cDNA synthesis.

Class	Oligonucleotides	T_m
II	5'AGACCGTGTGGGTCGCCCTCCTCCTCCTCGA3'	75ºC
V	5'AGACCGTGTGGGCTGGGTAGAACCCGCAATTCTCT3'	74ºC

2.4.3 PCR

Synthesized cDNA was amplified for expression analysis by PCR. *β2-microglobulin* (*β2-m*) gene was used as internal control in expression analysis of other genes for its constitutive expression in mammalian cells. *MRP1, MDR1, Bcl-2, Bax* and *β2-*

m primer sets were designed from coding sequences of genes, by using the Primer3 Software (Rozen *et al.*, 2000) according to gene sequences obatained from the databases of 'National Center for Biotechnology Information (NCBI)' (www.ncbi.nlm.nih.gov). Left and right primers were designed to anneal on different exons to prevent amplification of contaminating DNA. Primers for *BCRP* and PCR conditions were previously described by Palissot *et al*. (Palissot *et al*.,2005). Primer sets specific to *β tubulin* isotypes were previously described (Dozier *et al.*, 2003) except for the *β tubulin* classes II and V. PCR conditions for these genes were modified and optimized. All primer sets for *β tubulin* isotypes were class specific and two primers annealed to different exons except for the *β tubulin* classes II and V. In PCR of these genes 5'tagged cDNA were synthesized as described above to prevent amplification of contaminating DNA. Primer sequences and amplicon sizes are given in Table 2.2. PCR was carried out in 50µL reaction volume. The reagents and optimized PCR conditions are given in Table 2.3.

Table 2.2 Primer sets for PCR.

Genes	Forward	Reverse	Amplicon sizes (bp)
β2-m	5'TCTCTCTTTCTGGCCTGGAG3' Exon 1	5'GGATGGATGAAACCCAGACA3' Exon2	122
MRP1	5'CTGGCATTCAAGACAAGGT3' Exon 6	5'ACCGGAGGATGTTGAACAAG3' Exon 7	217
MDR1	5'GAGCCTACTTGGTGGCACAT3' Exon 24	5'AGGCTCAGTCCCTGAAGCAC3' Exon 26	295
BCRP	5'TACAGTTCTCAGCAGCTCTTCG3' Exon 5	5'CAACTTGAAGATGGAATATCGAG3' Exon 7	356
Bcl-2	5'GGATTGTGGCCTTCTTTGAG3' Exon 1	5'TCTTCAGAGACAGCCAGGAGA3' Exon 2	219
Bax	5'TCTGACGGCAACTTCAACTG3' Exon 4	5'TTGAGGAGTCTCACCCAACC3' Exon 5	188
β tubulin I	5'CCCCATACATACCTTGAGGCGA3' Exon 1	5' GCCAAAAGGACCTGAGCGAA 3' Exon 3	289
β tubulin II	5' CATCTCCGAGCAGTTCACGG3' Exon 4	5' AGACCGTGTGGGTCGCCCTC 3' Exon 4	200
β tubulin III	5'ATGCGGGAGATCGTGCACAT3' Exon 1	5'CCCCTGAGCGGACACTGT3' Exon 3	238
β tubulin IVa	5'TCTCCGCCGCATCTTCCA3' Exon 1	5'GCTCTGGGGACATAATTTCCTCCT3' Exon 3	272
β tubulin IVb	5'GCTGTTTGTCTACTTCCTCCTGCT3' Exon 1	5'CAGTTGTTCCCAGCACCACTCT3' Exon 4	344
β tubulin V	5'CGGGGAGGAAGCTTTTGAGG3' Exon 4	5' AGACCGTGTGGGCTGGGTAG 3' Exon 4	256

Table 2.3 PCR conditions for:

A) *β2-m, MRP1, MDR1, BCRP, Bcl-2* and *Bax*

	β2-m	***MRP1***	***MDR1***	***BCRP***	***Bcl-2***	***Bax***
[$MgCl_2$]	2mM	2mM	2mM	2mM	2mM	2mM
[dNTP]	0.2mM of each	0.2mM of each	0.2mM of each	0.2mM of each	0.3mM of each	0.3mM of each
[primers]	0.5µM	0.5µM	0.5µM	2µM	0.5µM	0.5µM
[DMSO]	-	-	10%	-	-	-
Hot start	-	-	+	-	-	-
***Taq* polymerase**	1U	1.5U	2U	1U	1.5U	1.5U
Initial denaturation	94ºC, 5´	94ºC, 5´	94ºC, 5´	94ºC, 5´	94ºC, 5´	94ºC, 5´
Denaturation	94ºC, 30´´	94ºC, 30´´	94ºC, 30´´	94ºC, 50´´	94ºC, 30´´	94ºC, 30´´
Annealing	55ºC, 30´´	55ºC, 30´´	56ºC, 30´´	59ºC, 50´´	53ºC, 30´´	53ºC, 30´´
Extension	72ºC, 30´´	72ºC, 30´´	72ºC, 25´´	72ºC, 20´´	72ºC, 30´´	72ºC, 30´´
Final extension	72ºC, 10´	72ºC, 10´	72ºC, 10´	72ºC, 10´	72ºC, 10´	72ºC, 10´
# of cycles*	30	25	30		30	28

* Number of cycles were determined according to cycle optimization results given in Appendix D.

Table 2.3 (Continued)

B) *β tubulin* isotypes

Class	I	II	III	IVa	IVb	V
[$MgCl_2$]	3mM	1.5mM	2.5mM	2.5mM	2.5mM	2mM
[dNTP]	0.4mM of each	0.4mM of each	0.4mM of each	0.4mM of each	0.4mM of each	0.4mM of each
[primers]	1μM	0.5μM	1μM	1μM	1μM	0.5μM
[DMSO]	-	10%		10%	-	
Hot start	-	+	-	-	+	-
***Taq* polymerase**	2U	2U	2U	2U	2U	1U
Initial denaturation	94ºC, 5′	94ºC, 5′	94ºC, 5′	94ºC, 5′	94ºC, 5′	94ºC, 5′
Denaturation	94ºC, 45′′	94ºC, 1′	94ºC, 45′′	94ºC, 45′′	94ºC, 45′′	94ºC, 1′
Annealing	51ºC, 45′′	62ºC, 45′′	52ºC, 45′′	53ºC, 45′′	54ºC, 45′′	62ºC, 45′′
Extension	72ºC, 45′′	72ºC, 45′′	72ºC, 45′′	72ºC, 45′′	72ºC, 45′′	72ºC, 45′′
Final extension	72ºC, 10′	72ºC, 10′	72ºC, 10′	72ºC, 10′	72ºC, 10′	72ºC, 10′
# of cycles*	31	31	33		31	31

* Number of cycles was determined according to cycle optimization results given in Appendix D.

PCR products were detected by horizontal agarose gel elecrophoresis on 2% (w/v) agarose gels. Preparation of agarose gels were described above. For preparation of 2% agarose gel, 2g agarose was dissolved in 100mL 1X TAE buffer. 10µL of PCR sample was mixed with 2µL 6X loading buffer (Fermantas) and loaded. 50 bp DNA Ladder (Fermentas) was also loaded at each run. Electrophoresis was run with 1L of 1X TAE buffer at 90V, for 1 h. Gel was observed under UV light and photographed. Densitometric measurements of band intensities were performed using Scion Image Software (Scion Corporation, USA).

2.4.4 Statistical Analysis

The densitometric measurements of RT-PCR were subjected to student's t-test by using SPSS Software to determine the significanct difference with $\alpha = 0.05$.

2.5 Quantitative Real-Time Polymerase Chain Reaction (qPCR)

2.5.1 RNA Isolation and cDNA synthesis

RNA isolation was performed from parental and resistant MCF-7 cells using Tri Reagent™ RNA Isolation Reagent (Sigma, USA) according to manufacturer's instructions. In brief, cells were lysed by pipetting cell homogenate in Tri Reagent™ for several times. Chloroform was added, mixture was incubated 15 min on ice and centrifuged at 12,000g, 4°C for 15 min. Upper RNA phase was collected to a fresh tube; isopropanol was added and incubated 10 min at RT. After centrifugation at 12,000g, 4°C for 10 min RNA pellet was obtained. Pellet was washed with 75% (v/v) ethanol and repelleted at 12,000g, 4°C for 5 min. RNA pellet was dissolved in RNase free water and stored at -80°C. Qualification and quantification of the isolated RNA was performed as previously described in section 2.4.1.

cDNA synthesis was performed as described in section 2.4.2 with 5 µg of total RNA and 0.5 µg specific primer.

2.5.2 qPCR

For quantitative real-time PCR analysis, LightCycler® (Roche, Germany) and The LightCycler® Taqman® Master Kit (Roche) was used according to manufacturer's instructions. In brief, 20 µL reaction mix contained 7 µL cDNA, 0.5 µM from each forward and reverse primers and 0.2 µM hydrolysis probe. Conditions for qPCR are summarized in Table 2.4. The specific primers for amplification of *MDR1* and *MRP1* genes (Table 2.5) and probes (Universal probe library) were supplied by Roche. Each sample run was performed in duplicates with non template controls. For optimization of the runs, standard amplification curves were constructed by using known dilutions of *MDR1* and *MRP1* positive cDNA as template (Figure 2.2). The automated system run and the software analysis with calculations were performed according to instructions supplied by the instrument (Roche LightCycler®2.0). In brief, for quantification of RT-PCR results, fluorescent signal intensities (640nm) were plotted against the number of PCR cycles on a semi-logarithmic scale. Crossing point cycles (C_P) were determined for all samples in parallel with a standardization series of known dilutions (Table 2.6) of *MDR1* and *MRP1* positive cDNA as template. The C_P value of each sample was then compared to those in the standardization series, and the calculated concentration values corresponded to the expression level of the *MDR1* and *MRP1* genes.

Table 2.4 Conditions for qPCR.

	MDR1, MRP1
[primers]	0.5µM
[probe]	0.2µM
Pre-incubation	95ºC, 15´
Denaturation	95ºC, 10´´
Annealing	56ºC, 30´´
Extension	72ºC, 1´´
Cooling	40ºC, 30´
# of cycles	45

Table 2.5 Primer sets for qPCR.

Genes	Forward	Reverse	Amplicon sizes (bp)
MDR1	5'AAGGCATTTACTTCAAACTTGTCA3' Exon 16	5'GGATTCATCAGCTGCATTTTC3' Exon 17	77
MRP1	5'TGTGGGAAAACACATCTTTGA3' Exon 18	5'CTGTGCGTGACCAAGATCC3' Exon 19	80

Table 2.6 cDNA standard dilutions for qPCR optimizations.

Standard (STD)	Dilution (Copy Number)	Preparation
1	10^7	40 µL cDNA stock
2	$10^{6.5}$	10 µL STD1 + 21.6 40 µL dH_2O
3	10^6	4 µL STD1 + 36 µL dH_2O
4	$10^{5.5}$	10 µL STD3 + 21.6 40 µL dH_2O
5	10^5	4 µL STD3 + 36 µL dH_2O
6	$10^{4.5}$	10 µL STD5 + 21.6 40 µL dH_2O

A)

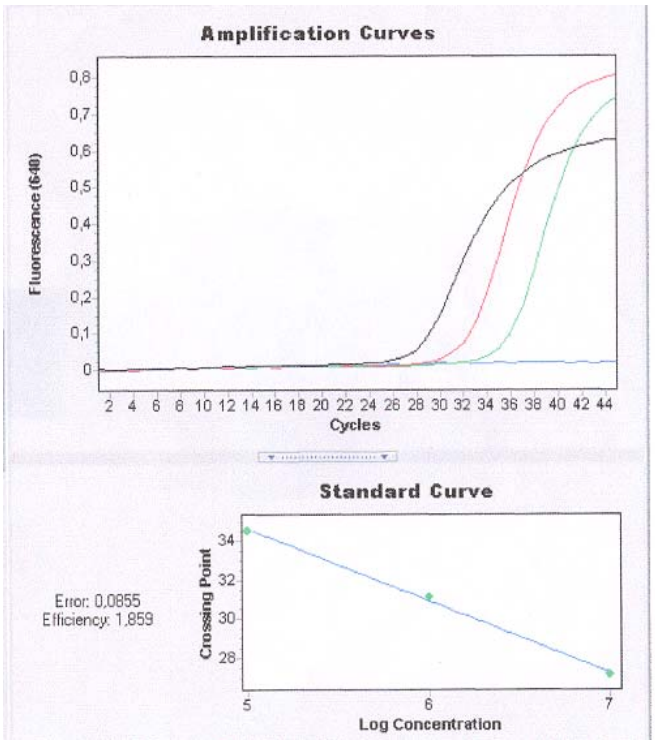

B)

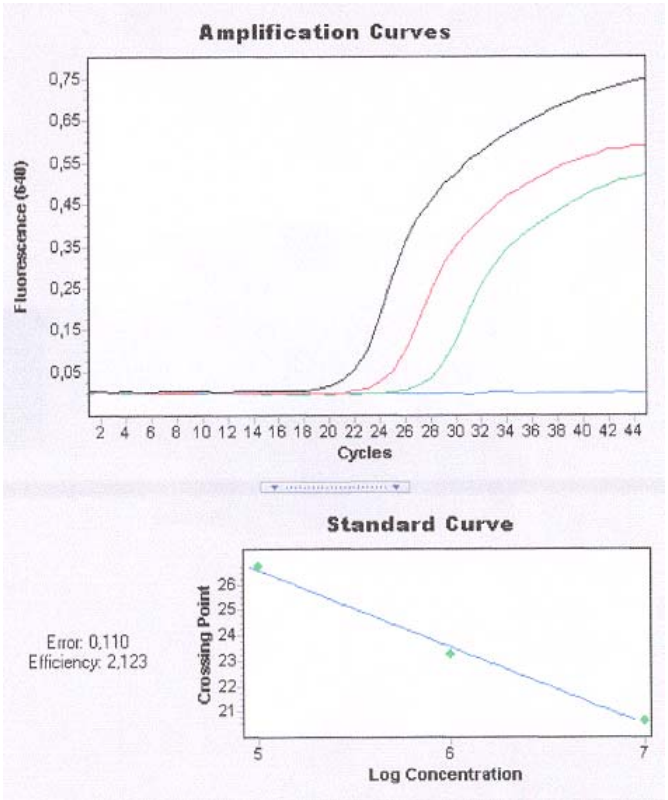

Figure 2.2 Standardization curve for A) *MDR1*, and B) *MRP1*.

2.6 Protein Isolation and Western Blotting

Protein isolation is performed according to modified and optimized procedure described by Kyu *et al.* previously (Kyu *et al*., 2002). A confluent 75 cm^2 flask of cells were tyripsinated and pelleted in phosphate buffered saline (PBS). Lysis buffer (Appendix C) containing a cocktail of protease inhibitors (1 mM phenylmethylsulphonyl fluoride (PMSF); 2 µg/mL aprotinin; 1 µg/mL pepstatin) was added on to the pellet. Following 30 min ice incubation, nuclei were pelleted at 3400 rpm for 5 min at 4ºC. Supernatant containing cell lysate was collected and Samples were stored at -80ºC. Protein concentration was measured by Bradford assay (Bradford *et al.*, 1976). In brief, 5X Bradford reagent (BR) (Appendix C) was diluted to 1X and filtered. 1mg of bovine serum albumin (BSA) (Sigma) was dissolved in 1mL of dH_2O freshly. A blank and six dilutions of Bradford solutions containing BSA solution were prepared in triplicates as described in Table 2.7:

Table 2.7 Preparation of Bradford solutions.

	dH_2O (µL)	BR (mL)	BSA (µL)	[BSA] (µg/mL)
Blank	500	5	-	-
1	495	5	5	0.91×10^{-3}
2	490	5	10	1.82×10^{-3}
3	480	5	20	3.64×10^{-3}
4	470	5	30	5.46×10^{-3}
5	450	5	50	9.01×10^{-3}
6	420	5	80	14.55×10^{-3}
Samples	480	5	20	-

Tubes were vortexed and incubated at room temperature for 10 min. Optical density (OD) was measured at 595 nm against blank by spectrophotometer. OD_{595nm} versus BSA concentration standard curve was plotted. Samples were measured and concentrations were calculated from the equation of the standard curve.

Total cell lysates were fractionated by SDS-PAGE. 7.5% (w/v) separating and 4% (w/v) polyacrylamide (Sigma) stacking gels were prepared as described in Table 2.8:

Table 2.8 Preparation of gel solutions.

	Seperating gel (mL)	Stacking gel (mL)
Gel solution (Appendix C)	7.5	2
dH_2O	21.86	12.67
Separating gel buffer (Appendix C)	10	-
Stacking gel buffer (Appendix C)	-	5
SDS (Appendix C)	0.4	0.2
Ammonium per sulfate (Appendix C)	0.2	0.1
TEMED (Sigma)	0.04	0.03"
Total volume	40	20

Midi gel apparatus (Sigma) was prepared and separating gel was poured in between the glasses. Isopropanol was added on top of the gel to fasten solidification. After the separating gel solidified, stacking gel was poured and the comb was placed. After solidification comb was removed, apparatus was filled with 1X electrode buffer (Appendix C) containing 0.1% (w/v) SDS and a pre-run was performed. For sample loading, 3X sample loading buffer (Appendix C) was diluted to 1X by mixing with samples and the sample mix was boiled for 90 sec. Samples and protein ladder (Fermentas) were loaded. Electrophoresis was performed at 20mA and 40mA during stack and separating gel runs, respectively. For western blotting, gels were soaked in blotting (transfer) buffer (Appendix C). In order to visualize total cell proteins on gel, gels were stained by Coomassie blue staining solution (Appendix C) for 1 h and then immersed in destain solution (Appendix C) overnight by renewing the solution 3-4 times. Gels were photographed by digital camera under visible light.

Proteins were electrophoretically transferred to a 0.45 µm nitrocellulose membrane (Protran BA 85, Schleicher & Schuell, UK) in blotting buffer (Appendix C) with a BioRad ElectroBlot System (Hercules, California, USA) at 30V overnight. After incubation in tris-buffered-saline-Tween-20 (TBST) buffer (Appendix C) for 10 min, the nonspecific binding sites were blocked by incubation in blocking buffer (Appendix C) for 1 h at room temperature in shaker. The membrane was then incubated with specific glyceraldehyde-3-phosphate dehydrogenase (GAPDH), Bcl-2, Bax monoclonal antibodies (Chemicon, Temecula, California, USA) and P-gp (JSB1), MRP1 antibodies for 2 h at room temperature. Working dilutions of antibodies were prepared in blocking buffer as 1:200 for anti GPADH, 4µg/mL for anti Bcl-2, 2µg/mL for anti Bax, for P-gp and for MRP1. The

membrane was washed with TBST for 5 min in shaker for three times and incubated with peroxidase conjugated goat anti mouse IgG secondary antibody (Chemicon) in blocking buffer for 1 h at room temperature in shaker. After washing with TBST for three times, DAB chromogen solution (Chemicon) was applied onto the membrane at dark until the dark brown bands were appeared. The membrane was photographed under visible light and the densitometric measurements of the blots were performed using Scion Image Software (Scion Corporation).

2.7 Immunocytochemistry

Cells were harvested and resuspended in serum free media and density of cell suspension was adjusted to $1x10^6$ cells/mL. 200 µL of cell suspension were cytocentrifugated (Cytospin-3 Shandon, Sweden) at 1000 rpm for 5 min according to manufacturer's instructions. The samples were fixed in cold acetone for 10 min and washed with PBS for 5 min. Endogenous peroxidases were quenched in 3% (v/v) H_2O_2 for 5 min. The samples were incubated with P-gp, MRP1 and LRP monoclonal primary antibodies (JSB1, anti MRP1 and anti LRP, respectively) for 30 min at room temperature. Sample preperations were washed in PBS buffer and incubated with horse-raddish peroxidase (HRP) conjugated secondary antibody for 30 min. The samples were washed in PBS. Diaminobenzidine (DAB; brown) were used as chromogen substance. Slides were counterstained with hematoxylin and mounted.

2.8 Microarray Analysis

2.8.1 RNA Isolation, cDNA Synthesis and Target Preparation

RNA isolation form MCF-7/S, MCF-7/30nMDoc, MCF-7/120nMDoc and MCF-7/1000nMDox were performed using Tri Reagent™ RNA Isolation Reagent (Sigma) as

previously described in section 2.5.2. Absorbance values (260nm, 280nm) were measured for RNA quantification by spectrophotometry and RNA intactness was checked by agarose (1% w/v) gel electrophoresis (70V, 90min) as previously described in section 2.4.1. RNA samples having a ratio of 1.8-2.0 containing at least 2.5µg of RNA in µL were considered for target preparation. All RNA samples were prepared as duplicates to provide biological replicates for microarray assay. Complete GeneChip® 3'-Expression Amplification Reagents (Affymetrix, USA) were used according to procedure as described in detail in the Affymetrix GeneChip® Expression Analysis Technical Manual. The flow chart of the procedure is given in Figure 2.3. The kit contains One-Cycle Target Labelling (IVT Labelling Kit, One-Cycle cDNA Synthesis Kit and Sample Cleanup Module) and Control Reagents (Poly-A RNA Control Kit and Hybridization Control Kit). cDNA was synthesized from 15µg of total RNA by One-Cycle Target Labelling Assay® (Affymetrix, USA) according to manufacturer's instructions. Poly-A RNA controls were also added to be amplified and labelled together with the samples and provided exogeneous positive controls to monitor the process. One-Cycle cDNA Synthesis Kit contained SuperSriptII™ enzyme and T7-Oligo(dT) primers for first strand cDNA sysnthesis and *E. coli* DNA Polymerase I *E. coli* DNA Ligase, Rnase H and T4 DNA Polymerase for second strand cDNA synthesis. Synthesized cDNA was puriffied with Sample Cleanup Module prior to labelling. Samples were amplified and biotinylated for generation of labelled cRNA targets with IVT Labelling Kit containing IVT Labelling Enzyme Mix. Labelled cRNA was cleanedup and quantified using spectrophotometry (260nm). cRNA yield was calulated:

$$cRNA = RNA_{measured} - (\text{initial total RNA})\,(\text{fraction of cDNA used in IVT}) \qquad \text{[Equation 2.2]}$$

20µg of cRNA was fragmented with Fragmentation Buffer supplied with Sample Cleanup Module. Fragmentation of cRNA was checked by agarose gel electrophoresis (1% (w/v) agarose, 70V, 90 min).

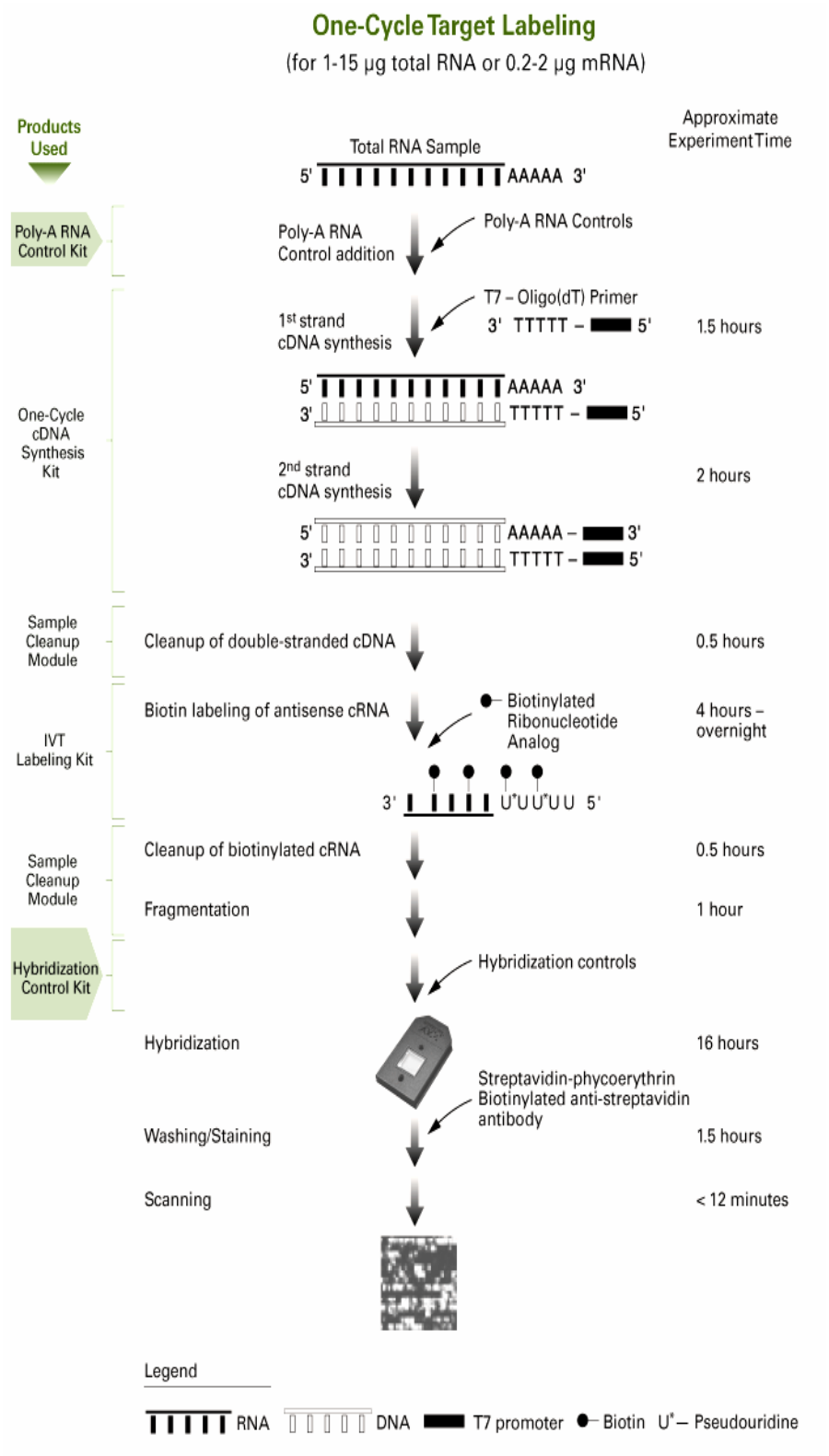

Figure 2.3 Schematic representation of Affymetrix GeneChip® Expression Analysis protocol (www.affymetrix.com/products/reagents/specific/one_cycle_target_control.affx).

2.8.2 Target Hybridization and Scanning

Biotin labelled and fragmented target cRNA samples were loaded in 300µL hybridization coctail (Appendix C) into 49/64 format type Affymetrix GeneChip® (Human Genome U133 Plus 2.0 Array) together with control cRNAs and oligo B2 provided by Hybridizatin Control Kit. Target hybridization and scanning procedures were performed in Molecular Biology and Biotechnology R & D Center (METU-Central Laboratory, Ankara, Turkey). Hybridization procedure was conducted at 45ºC, 60 rpm for 17 h in Affymetrix GeneChip® Hybridization Oven 640. Washing and staining (Appendix C) procedure was performed in Affymetrix GeneChip® Fuidics Station 450 with Euk Ge-WS2v5 fluidics script according to the instructions in Affymetrix GeneChip® Expression Analysis Technical Manual. Affymetrix GeneChip® Scanner 3000 device was used for array scanning according to the technical instructions.

2.8.3 Preliminary and Data Analysis

Preliminary analysis of the scanned chips was performed using Affymetrix GeneChip® Operating Software (GCOS). The quality of gene expression data was checked according to quality control criteria as previously described (Yılmaz *et al*., 2008). Parameters background and noise averages, percentage of present calls, presence of internal hybridization controls in increasing signals, presence of poly-A controls as decreasing signals and GAPDH to beta actin 3'/5' signal ratios. The raw data files in '.CEL' format were transferred using Data Tansfer Tool (Agilent Technologies, Inc., USA). Then, GeneSpring GX 7.3.1 Software (Agilent) was used for further data analysis and evaluation. Attributes of the arrays including detailed sample description and experimental parameters are given in Appendix E. The data was pre-processed according to robust multiarray average (RMA) normalization algorithms. In RMA normalization, the data for the variable considered as all are sampled from the same or similar distributions and the values for that variable are then normalized to a standard distribution. It normalizes a set of hybridizations at the probe level *i.e.* a measure of robust averaging of background correction, quantile normalization and log-transformation of perfect match probes (Irizarry *et al.*, 2003). Statistically significant data were selected by independent sample t-test (α=0.05) between duplicate data for resistant sublines with respect to data of the sensitive MCF-7. Significantly altered genes between resistant sublines and the sensitive MCF-7 were listed

and gene trees were constructed from these lists by standard correlation. Upregulated and downregulated genes were selected from gene trees. The genes were filtered by volcano plots and genes upregulated and downregulated more than 2-fold were considered in constructing gene lists. Gene lists were further classified according to gene ontology annotations of the software. These were 'biological processes' (*i.e.* cell growth and maintenance, death.) and 'molecular functions' (*i.e.* apoptosis regulator activity, binding activity, catalytic activity etc.) of the proteins that are encoded by the genes. Finally the genes that encode proteins related with cellular processes that may have contributed to develpment of drug resistance were selected from the gene lists and new lists were generated to evaluate the relation between multidrug resistance phenotype and these cellular processes.

2.9 Proliferation Assays for Cross–resistance Studies

2.9.1 Application of Other Anticancer Drugs

The effects of the chemotherapeutic agents and their combinations on the proliferation of sensitive and resistant MCF-7 cell lines were tested in 96-well microtiter plates. Antiproliferative effects of anticancer agents on parental MCF-7 cells and drug selected sublines were evaluated by means of the Cell Proliferation Kit as previously described in Section 2.3.2. IC_{50} values and the resistance indices were calculated to determine the degree of cross-resistance of each subline to different anticancer drugs. Vincristine (Oncovin®), doxorubicin, tamoxifen (Sigma) and all-trans retinoic acid (ATRA) (Sigma) were tested for development of cross-resistance in MCF-7/120nM DOC cells. Paclitxel, docetaxel, tamoxifen, and ATRA were also tested for development of cross-resistance in MCF-7/1000nM DOX cells.

2.9.2 Irradiation

Sensitive and resistant (MCF-7/120nM DOC and MCF-7/1000nM DOX) cells were seeded to 96-well microtiter plates (5000 cells/well) and after 24 h incubation in standard culture conditions irradiated with doses of 200 and 800 cGy by a Theratron 780 Cobalt 60 Teletherapy Unit (AECL Medical, Ontario, Canada). After irradiation, all plates were incubated at 37°C in a 5% CO_2 atmosphere for an additional 24 hour. Then cell proliferation was evaluated using Cell Proliferation Kit (Biological Industries) as previously described above. IC_{50} values represent inhibitory doses of irradiation in cGy to evaluate antiproliferative effects of irradiation on cells and were calculated from cell proliferation curves as described above.

2.10 Checkerboard Micro Plate Method for Evaluation of Drug Interactions

Checkerboard micro plate method was applied to study the effects of drug interactions between two anticancer drugs or drug-resistance modifier interactions on docetaxel and doxorubicin resistant MCF-7 cells. The dilutions of anticancer drugs (A) were made in horizontal direction and the dilutions of second anticancer drug (B) vertically in microtiter plates in 100 µL. Combined effects of vincristine, doxorubicin, tamoxifen, and ATRA were evaluated with docetaxel (agent A) on MCF-7/120nM DOC. Paclitaxel, docetaxel, tamoxifen and ATRA were applied in combinations with doxorubicin (agent A) on MCF-7/1000nM DOX. The cells were distributed to each well as 50 µL aliquots ($5x10^3$ cells) and incubated for 72h at 37ºC in CO_2 incubator. The cell growth was determined by means of Cell Proliferation Kit. Drug interactions were evaluated according to the following expressions:

FIC (fractional inhibitory concentration)$_A$= IC_{50}(A) in combination / IC_{50}(B) alone [Equation 2.3]

FIC_B= IC_{50}(B) in combination / IC_{50}(B) alone [Equation 2.4]

FIX (fractional inhibitory index) = $FIC_A + FIC_B$ [Equation 2.5]

Equation 2.5 demonstrates the combined effects of anticancer drugs. If FIX value is 0.51-1, it indicates an additive effect; if FIX value is less than 0.5 it is synergism. FIX value in between 1-2 is considered an indifferent effect while the value greater than 2 indicates antagonism (Eliopoulos *et al*., 1980).

SEM values were derived from the IC_{50} values of three independent experiments for cross-resistance studies and at least three FIX values for checkerboard micro plate method. The results were subjected to two-tailed t-test by using SPSS Software to determine significant difference between means of groups ($\alpha = 0.05$).

2.11 Reversal of MDR

Efficiency of verapamil (Isoptin®, Germany) and promethazine (denoted by Prof. Dr. Jozsef Molnàr, University of Szeged, Faculty of Medicine, 6720, Szeged, Hungary) for reversal of MDR were evaluated in terms of cell proliferation and expression levels of *MDR1* and *MRP1*.

2.11.1 Proliferation Studies

Antiproliferative effects of verapamil and promethazine on parental MCF-7 and MCF-7/120nM DOC and MCF-7/1000nM DOX were evaluated by Cell Proliferation Kit and IC_{50} values were calculated from cytotoxicity curves as previously described in Section 2.3.2.

Checkerboard micro plate method was applied to study the effects of drug interactions between drug-resistance modulator interactions on cells. The dilutions of anticancer drugs (A) were made in horizontal direction and the dilutions of second modulator (B) vertically in microtiter plates as previously above.

2.11.2 Expression Analysis of *MDR1* and *MRP1* by RT-PCR

Effects of verapamil and promethazine on gene expression levels of *MDR1* and *MRP1* were evaluated in different time intervals and concentrations. Verapamil was applied to MCF-7/120nM DOC and MCF-7/1000nM DOX cells at concentrations half of their IC_{50}. Accordingly, 40 µM and 60 µM verapamil were applied to MCF-7/120nM DOC and MCF-7/1000nM DOX cells, respectively for 48 and 72 hours. RNA was isolated from these cells, 5µg of total RNA was converted to cDNA and amplified by PCR as previously described in section 2.4. Significance of alterations between band intensity ratios were analyzed by two-tailed t-test with ($\alpha = 0.05$) using SPSS Software.

CHAPTER 3

RESULTS AND DISCUSSION

3.1 Development of Resistant Cell Lines and Cell Proliferation Assays

3.1.1 Viable Cell Count and Construction of Growth Curves

The cell count data were expressed as number of cells (cells/mL) and plotted against time to construct growth curves for parental MCF-7 and drug applied sublines (Figures 3.1 and 3.2).

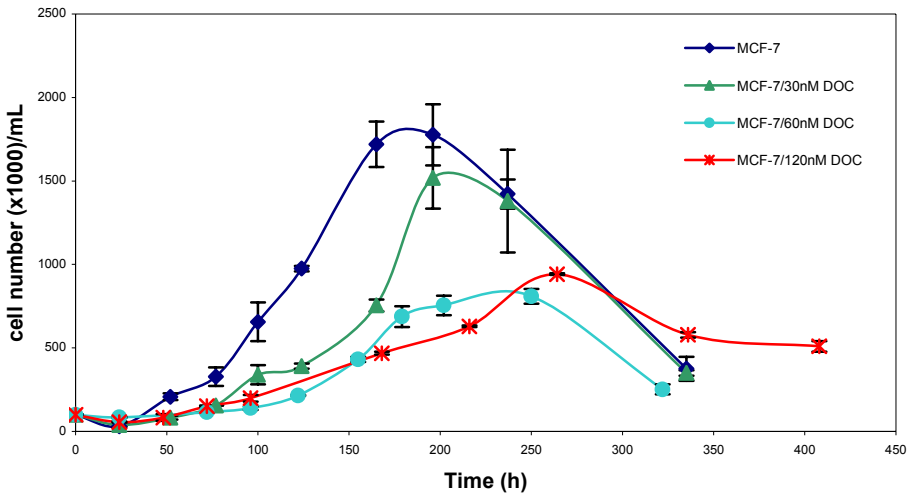

Figure 3.1 Growth curves of docetaxel applied MCF-7 cells.

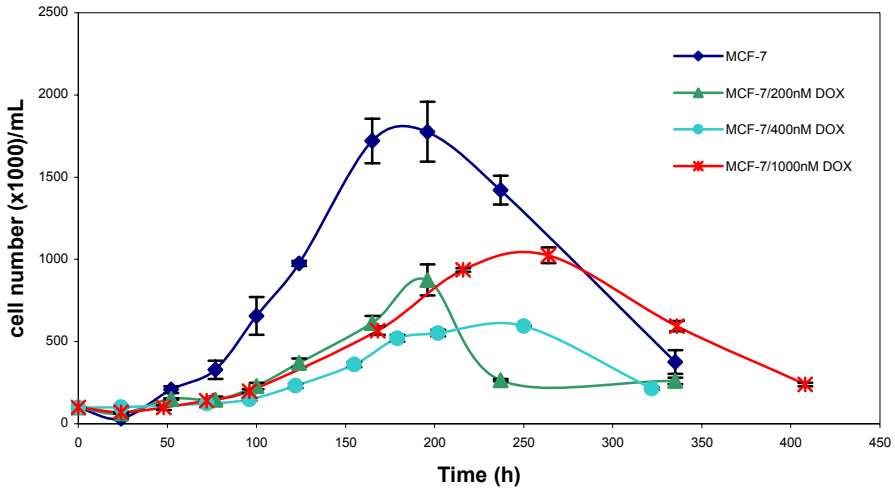

Figure 3.2 Growth curves of doxorubicin applied MCF-7 cells.

Doubling time (t_d), time required for cells to complete one cell cycle is calculated as follows:

$t_d = \ln 2 / \mu$ where μ is growth rate [Equation 3.1]

Growth rate is obtained from logarithmic phase of growth (Figures 3.1 and 3.2) *i.e.*, slope of ln (cell number/mL) vs time line (described in detail in Apendix F). Doubling times calculated from cell counts for docetaxel and doxorubicin applied cells are listed in Tables 3.1 A and 3.2 A, respectively.

Table 3.1 A) Doubling times (t_d) for docetaxel applied MCF-7 cells.

	Mean t_d (h) ± SEM[¥]
MCF-7	27.85 ± 0.65
MCF-7/30nM DOC	39.05 ± 0.55
MCF-7/60nM DOC	39.91 ± 0.21
MCF-7/120nM DOC	49.70 ± 0.54

[¥]SEM (standard error of the means) were derived from two independent experiments.

Table 3.1 (Continued)

B) Statistical analysis of t_d values for docetaxel applied MCF-7 sublines (α=0.05).

	MCF-7	**30nM DOC**	**60nM DOC**	**120nM DOC**
MCF-7		p<0.05 *	p<0.05 *	p<0.05 *
30nM DOC			p>0.05	p<0.05 *
60nM DOC				p<0.05 *
120nM DOC				

* Represents significant difference in t_d between groups of sublines.

Table 3.2 A) Doubling times (t_d) for doxorubicin resistant MCF-7 sublines.

	Mean t_d (h) ± SEM[¥]
MCF-7	27.85 ± 0.65
MCF-7/200nM DOX	47.25 ± 6.45
MCF-7/400nM DOX	49.65 ± 1.05
MCF-7/1000nM DOX	51.50 ± 0.80

[¥]SEM were derived from two independent experiments.

B) Statistical analysis of t_d values for doxorubicin applied MCF-7 sublines (α=0.05).

	MCF-7	**200nM DOX**	**400nM DOX**	**1000nM DOX**
MCF-7		p>0.05	p<0.05 *	p<0.05 *
200nM DOX			p>0.05	p>0.05
400nM DOX				p>0.05
1000nM DOX				

* Represents significant difference in t_d between groups of sublines.

According to Figures 3.1 and 3.2; doubling times of docetaxel and doxorubicin applied MCF-7 sublines were higher when compared to parental cell line. According to statistical analysis, doubling times of 30, 60 and 120nM docetaxel applied sublines were significantly higher than sensitve MCF-7 (p<0.05). On the other hand, doubling time of

200nM doxorubicin resistant cells was not significantly higher than the parental cells where values for 400nM and 1000nM resistant cells increased significantly when compared to parental cells ($p<0.05$). Statistical analysis of the doubling times with differences between each sublines were summarized in Tables 3.1 B and 3.2 B.

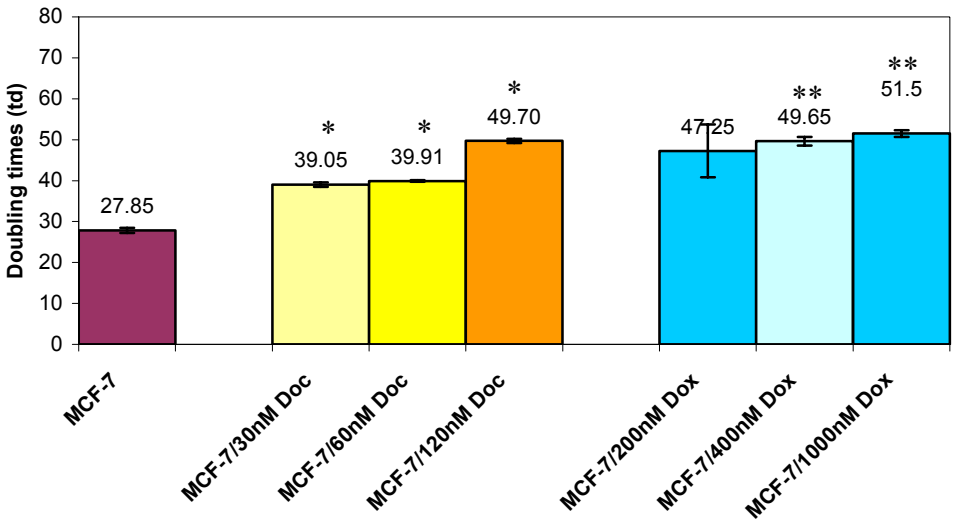

Figure 3.3 T_d for docetaxel and doxorubicin resistant MCF-7 cells; * represents significant difference ($p < 0.05$) in T_d of parental MCF-7 and docetaxel applied cells, ** represents significant difference ($p < 0.05$) in T_d of parental MCF-7 and doxorubicin applied cells.

According to viable cell counts, both docetaxel and doxorubicin applied MCF-7 cells had increased doubling times. Increse in t_d demonstrated that these sublines had different growth patterns (Figures 3.1 and 3.2) when compared to parental cells which may be an indication of development of drug resistance. Slower growth rate might provide survival advantage to drug applied cells since both docetaxel and doxorubicin target developing cells.

3.1.2 XTT Cell Proliferation Assay

Cell viability measurements obtained from Elisa Reader were converted to percent viability by setting the control wells as 100% cell viable. Averages of measurements obtained from three experiments were expressed as percentage of the control measurements and percent cell proliferation versus log (docetaxel and doxorubicin concentration) curves were constructed (Figures 3.4 and 3.5).

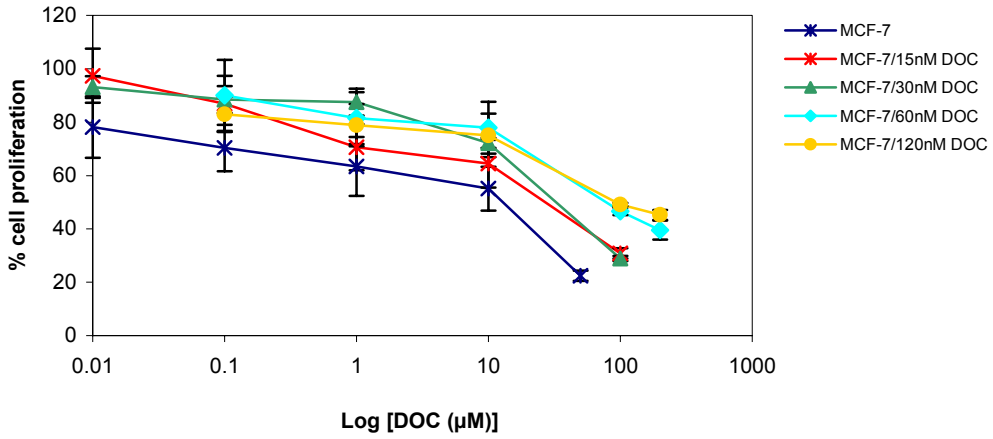

Figure 3.4 Antiproliferative effects of docetaxel on docetaxel applied MCF-7 sublines.

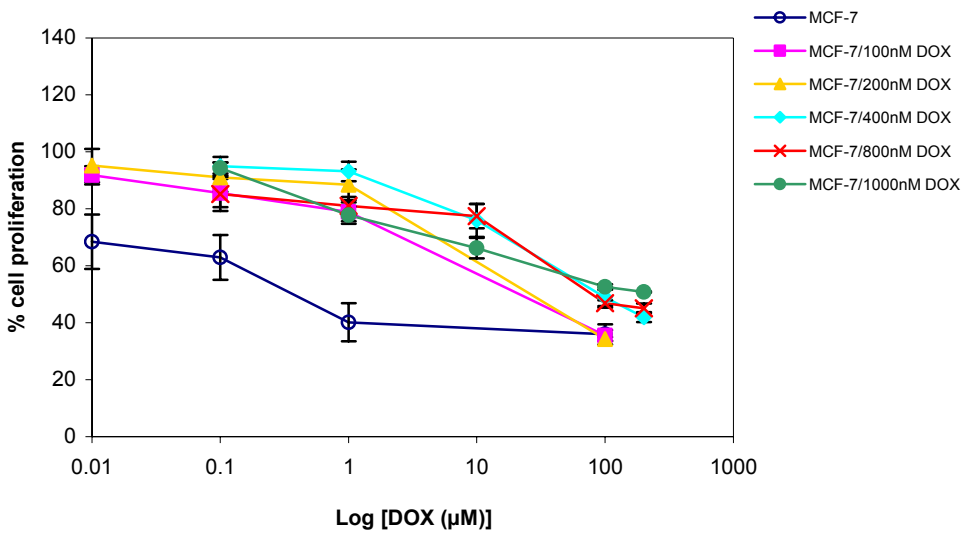

Figure 3.5 Antiproliferative effects of doxorubicin on doxorubicin applied MCF-7 sublines.

Inhibitory concentration (IC_{50}) value is the drug concentration at which 50% of cells are viable and calculated from the logarithmic trendline of the cytotoxicity graphs (as described in detail in Appendix F). IC_{50} values for docetaxel and doxorubicin applied sublines are summarized in Tables 3.3 A and 3.4 A, respectively. Significant differences between the calculated IC_{50} values were evaluated by two-tailed t-test. According to statistical analysis, IC_{50} of docetaxel applied sublines are significantly higher than that of sensitive MCF-7 ($p<0.05$) (Table 3.3 B). Similarly, IC_{50} of doxorubicin applied sublines are significantly higher than that of sensitive MCF-7 ($p<0.05$) (Table 3.3 B). IC_{50} of cells increased as the applied drug concentration increased (Figure 3.6) indicating that the amount of drug required to kill 50% of cells increased. Elevated levels of IC_{50} showed that drug applied cells acquired resistance to selective drugs.

Degree of resistance of developed sublines is evaluated in terms of "resistance index (R)" which is calculated according to:

$R = IC_{50}$ resistant subline / IC_{50} sensitive MCF-7 [Equation 3.2]

Resistance indices for docetaxel and doxorubicin resistant sublines are summerized in Tables 3.3 A and 3.4 A, respectively. R values demonstrated that, docetaxel and doxorubicin applied cells acquired resistance to their respective drugs. Degree of acquired resistance in these cells increased with increasing drug concentrations (Figure 3.6).

Table 3.3 A) IC_{50} and R values for docetaxel applied MCF-7 sublines.

	Mean IC_{50} (µM) ± SEM[¥]	**R**
MCF-7	3.49 ± 1.55	-
MCF-7/15nM DOC	13.36 ± 1.29	3.80
MCF-7/30nM DOC	46.57 ± 3.00	13.40
MCF-7/60nM DOC	93.33 ± 5.23	26.70
MCF-7/120nM DOC	163.21 ± 11.19	46.70

[¥] SEM were derived from three independent experiments.

Table 3.3 (Continued)

B) Statistical analysis of IC_{50} values for docetaxel applied MCF-7 sublines (α=0.05).

	MCF-7	**15nM DOC**	**30nM DOC**	**60nM DOC**	**120nM DOC**
MCF-7		$p<0.05$ *	$p<0.05$ *	$p<0.05$ *	$p<0.05$ *
15nM DOC			$p<0.05$ *	$p<0.05$ *	$p<0.05$ *
30nM DOC				$p<0.05$ *	$p<0.05$ *
60nM DOC					$p<0.05$ *
120nM DOC					

* Represents significant difference in IC_{50} between groups of sublines.

Table 3.4 A) IC_{50} and R values for doxorubicin applied MCF-7 sublines.

	Mean IC_{50} (μM) ± SEM[¥]	**R**
MCF-7	1.14 ± 0.30	-
MCF-7/100nM DOX	17.20 ± 1.65	15.10
MCF-7/200nM DOX	32.80 ± 2.87	28.80
MCF-7/400nM DOX	122.13 ± 6.25	107.10
MCF-7/800nM DOX	148.51 ± 2.28	130.30
MCF-7/1000nM DOX	183.11 ± 23.63	160.60

[¥] SEM were derived from three independent experiments.

B) Statistical analysis of IC_{50} values for doxorubicin applied MCF-7 sublines (α=0.05).

	MCF-7	**120nM DOX**	**200nM DOX**	**400nM DOX**	**800nM DOX**	**1000nM DOX**
MCF-7		p<0.05*	p<0.05*	p<0.05*	p<0.05*	p<0.05*
120nM DOX			p<0.05*	p<0.05*	p<0.05*	p<0.05*
200nM DOX				p<0.05*	p<0.05*	p<0.05*
400nM DOX					p<0.05*	p>0.05
800nM DOX						p>0.05
1000nM DOX						

* Represents significant difference in IC_{50} between groups of sublines.

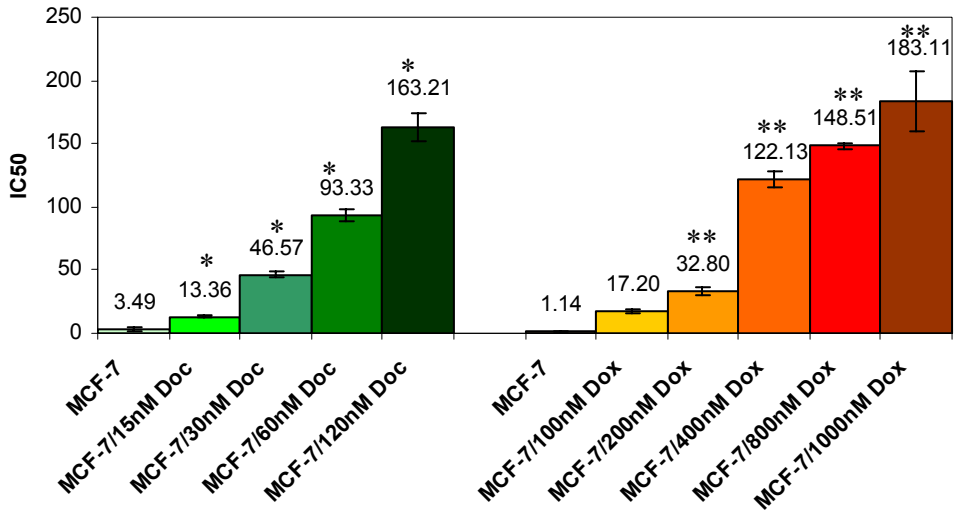

Figure 3.6 IC_{50} values for docetaxel and doxorubicin resistant MCF-7 sublines; * represents significant difference ($p < 0.05$) in IC_{50} values of sensitive MCF-7 and docetaxel resistant sublines, ** represents significant difference ($p < 0.05$) in IC_{50} values of sensitive MCF-7 and doxorubicin resistant sublines.

3.2 Reverse Transcription-Polymerase Chain Reaction (RT-PCR) Analysis

3.2.1 RNA Isolation

Isolated total RNA was visualized on 1% agarose gel (w/v) and photographed (Figure 3.7). Three bands referring to 28S (4770 bases), 18S (1990 bases) and 5S (150 bases) ribosomal RNA subunits indicated that intact total RNA was isolated without contaminating DNA. Since both tRNA and mRNA has lower abundancy in cells (~5% and ~15% of the total RNA, respectively) with respect to rRNA (~80%), it cannot be visualised and detected by agarose gel electrophoresis. However it is conventionally accepted that detection of three ribosomal RNA subunits on agarose gels is an indication of total RNA isolation.

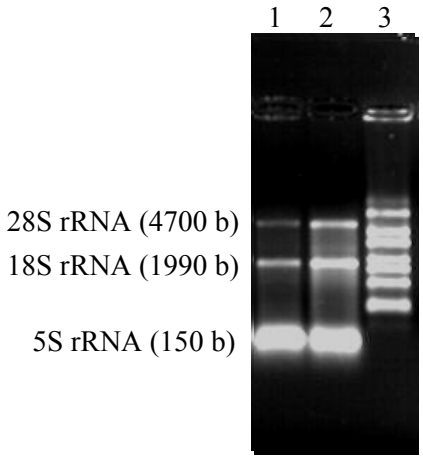

Figure 3.7 Total RNA isolated from sensitive MCF-7 cells (lanes 1 and 2) and RNA ladder (lane 3) (1% agarose gel).

3.2.2 Expression Analysis of ABC Transporter Genes (*MRP1, MDR1* and *BCRP*)

Expression of *MDR1, MRP1* and *BCRP* genes were analyzed in docetaxel and doxorubicin resistant sublines. The RT-PCR products were normalized with respect to *β2-microglobulin* products (Figures 3.8 and 3.10) and fold changes were calculated from band intensity measurements of dublicate experiments (Appendix G).

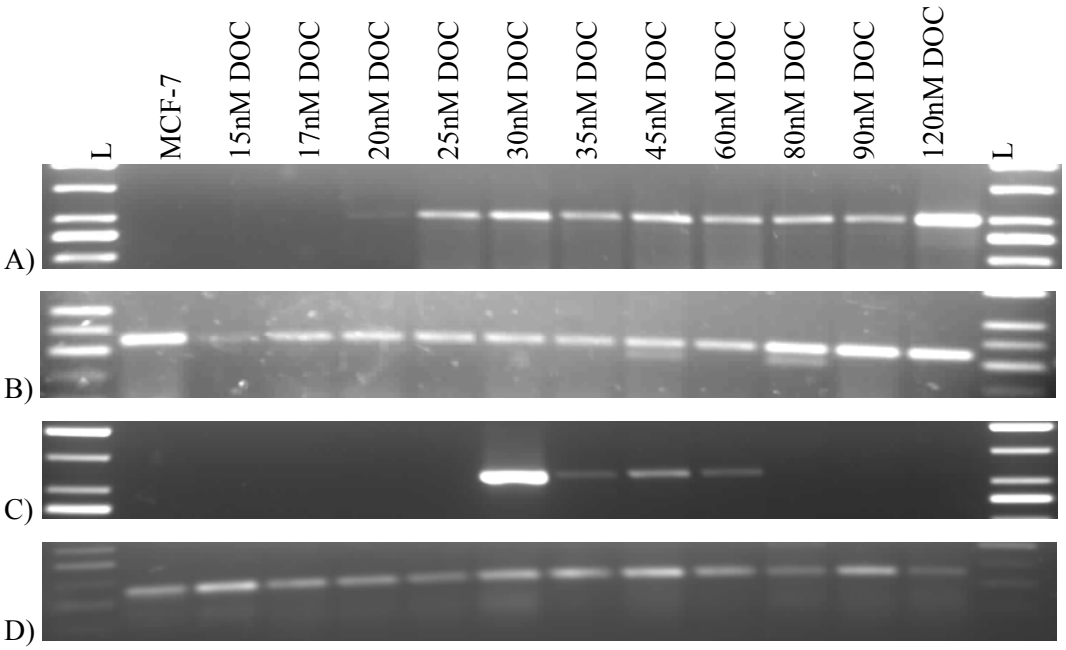

Figure 3.8 Expression levels of *MDR1, MRP1, BCRP and β2-m genes* in docetaxel resistant MCF-7 sublines (2% agarose gel); L: 50 bp ladder, A) *MDR1*, B) *MRP1*, C) *BCRP* and D) *β2-m* products.

Sensitive MCF-7 cells did not have intrinsic gene expression and *MDR1* expression was induced in MCF-7/20nM DOC (Figure 3.9). According to statistical analysis of band intensity ratios of docetaxel resistant sublines, *de novo* expression of *MDR1* is statistically significant with respect to sensitive cells. The gene expression levels were upregulated 1.37-, 1.40-, 1.40-, 1.41- and -2.17-fold in 25, 30, 35, 45 and 60nM docetaxel resistant cells, repectively (Appendix G). *MDR1* was upregulated 1.71-fold in MCF-7/80nM DOC and MCF-7/90nM DOC cells and 2.96-fold in MCF-7/120nM DOC. According to statistical analysis, increases in expression levels in 25-120nM docetaxel resistant cells were significant with respect to 20nM. Furthermore, increases in expression levels in 80-120nM docetaxel resistant cells were significant with respect to 25-60nM docetaxel resistant cells and increase of *MDR1* in MCF-7/120nM DOC cells was significant with respect to MCF-7/80nM DOC and MCF-7/90nM DOC cells. Conclusively, *MDR1* expression increased significantly due to 20nM, 80nM and 120nM drug applications and these drug applications may be important concentrations in terms of adaptation and resistance development. On the other hand, MCF-7 cells had intrinsic *MRP1* gene

expression at basal level. However, alterations in gene expression levels of *MRP1* were not statistically significant in docetaxel resistant sublines.

Interestingly, *BCRP* gene expression was induced in MCF-7/30nM DOC cells, downregulated in 35, 45 and 60nM docetaxel resistant cells (3.7-, 4.55- and 3.7-fold, respectively), and completely lost in more resistant sublines. BCRP gene has a a putative estrogen response element (ERE) in the 5'-flanking region and estrogen has been shown to enhance the expression of BCRP mRNA. According to microarray results MCF-7/120nM DOC cells had reduced estrogen receptor levels while in MCF-7/30nM DOC it remained same. Concordantly, a decrease in *BCRP* level may be correlated to decreased estrogen receptor levels in docetaxel resistant cells.

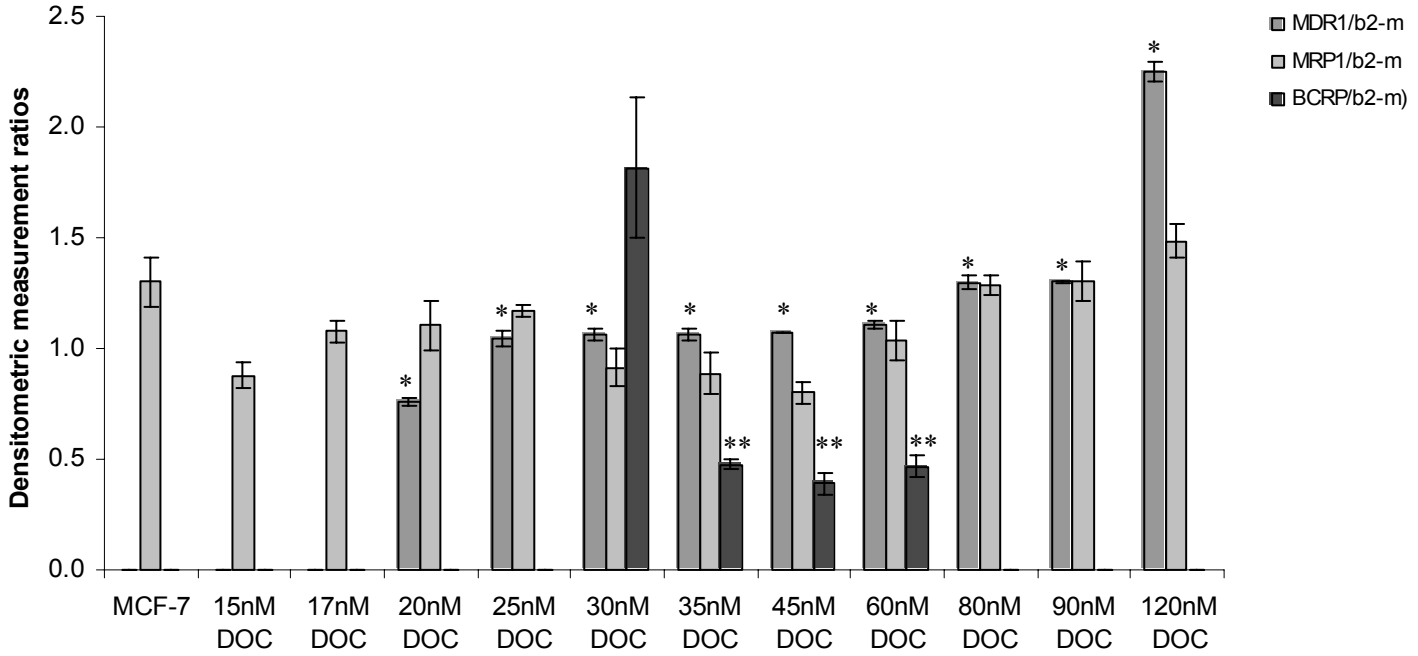

Figure 3.9 Expression of *MDR1, MRP1* and *BCRP* genes in docetaxel resistant sublines; * represents significant difference ($p<0.05$) in *MDR1* expression between sensitive and docetaxel resistant sublines, ** represents significant difference ($p<0.05$) in *BCRP* expression between 30nM docetaxel resistant subline and sublines resistant to higher docetaxel concentrations.

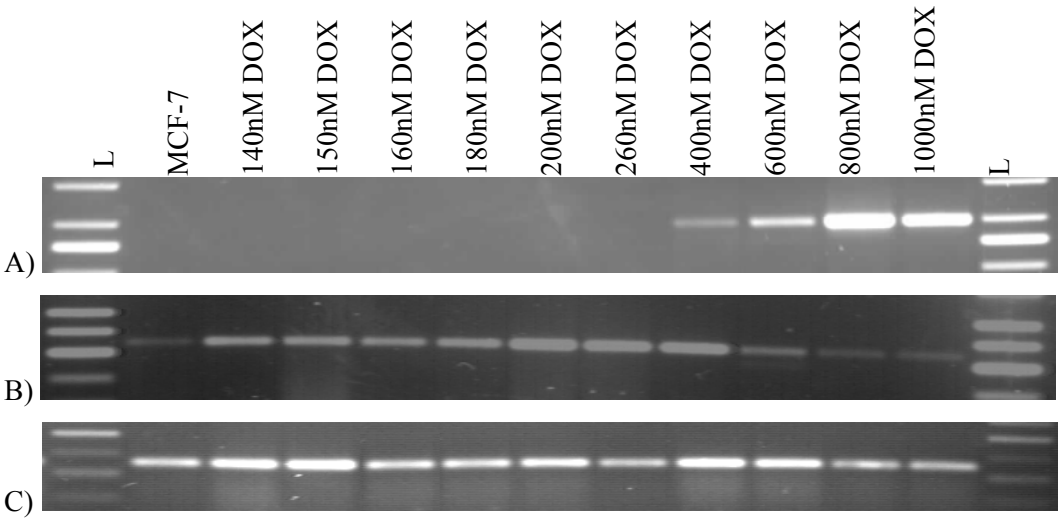

Figure 3.10 Expression levels of *MDR1, MRP1 and β2-m genes* in doxorubicin resistant MCF-7 sublines (2% agarose gel); L: 50 bp ladder, A) *MDR1*, B) *MRP1* and C) *β2-m* products.

MDR1 gene expression was induced in MCF-7/400nM DOX cells (Figure 3.10) and upregulated with increasing drug concentrations in 600, 800 and 100nM doxorubicin resistant cells (2.39-, 3.09- and 3.28-fold, respectively) (Appendix G). According to statistical analysis of band intensity ratios of doxorubicin resistant sublines, *de novo* expression of *MDR1* in 400nM resistant cells was not statistically significant ($p>0.05$) however differences in expression levels in 600nM, 800nM and 1000nM resistant cells (Figure 3.11) were significant with respect to sensitive cells. In addition, increases in expression levels of 800nM and 1000nM concentrations were also significantly greater than 400nM resistant cells. According to gene expression analysis of *MRP1* gene (Figure 3.11), alteration in expression levels of *MRP1* in resistant cells were not siginificant changes. However, increasing pattern of the gene expression up to 260nM doxorubicin resistant cells and following decreasing pattern in more resistant cells are apperant since in MCF-7/400nM DOX cells *MDR1* expression was induced. These alterations were confirmed by real-time RT-PCR and microarray analysis and, are further discussed in the respective sections. In addition, there was no BCRP expression in any of the doxorubicin resistant sublines.

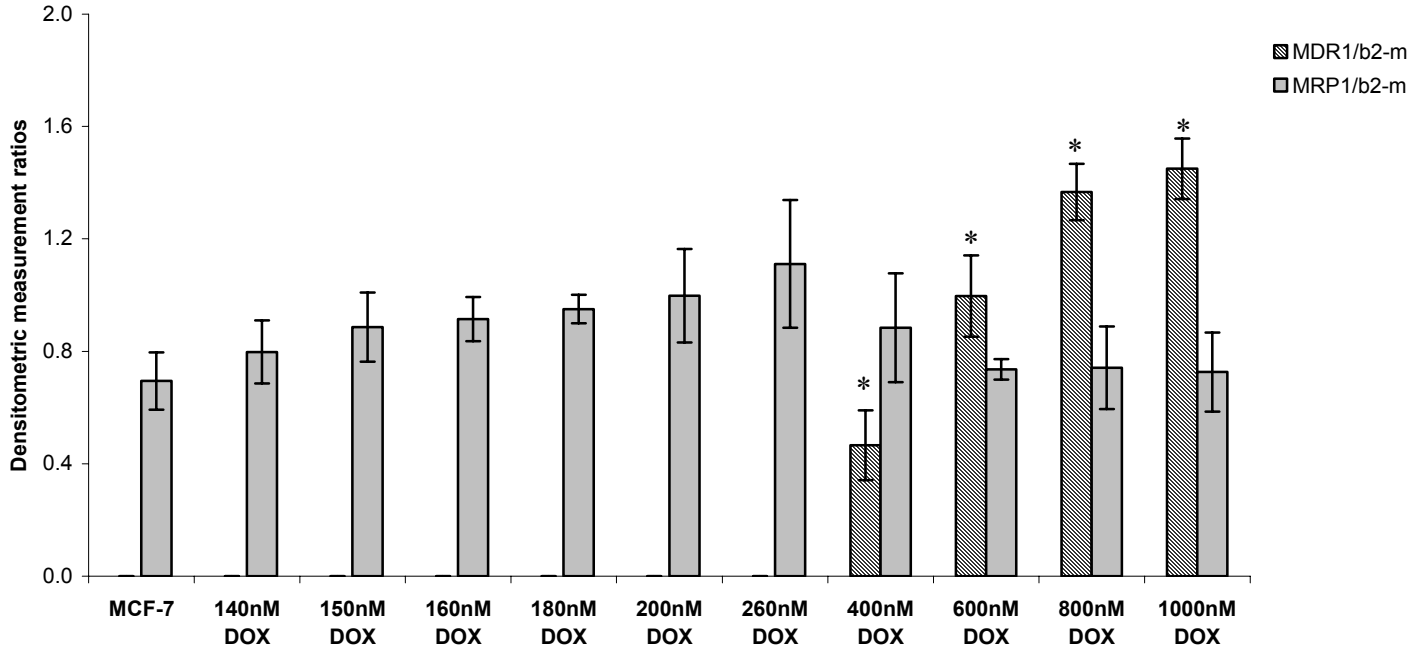

Figure 3.11 Expression of *MDR1* and *MRP1* genes in doxorubicin resistant sublines; * represents significant difference ($p<0.05$) in *MDR1* expression between sensitive and doxorubicin resistant sublines.

3.2.3 Expression Analysis of *Bcl-2* and *Bax*

Increase in expression levels of antiapoptotic genes and/or decrease in expression levels of proapoptotic genes may be two possible mechanisms of resistance to chemotherapeutic agents that mediate their action through apoptosis. Previously Huang *et al*. (Huang *et al*., 1997), defined *Bcl-2/Bax* ratio as a determinant of taxol resistance. Expression of *Bcl-2* and *Bax* genes were analyzed in doecetaxel and doxorubicin resistant sublines. The RT-PCR products were normalized with respect to *β2-microglobulin* products (Figure 3.12 and 3.14) and fold changes were calculated from band intensity measurements of dublicate experiments (Appendix G).

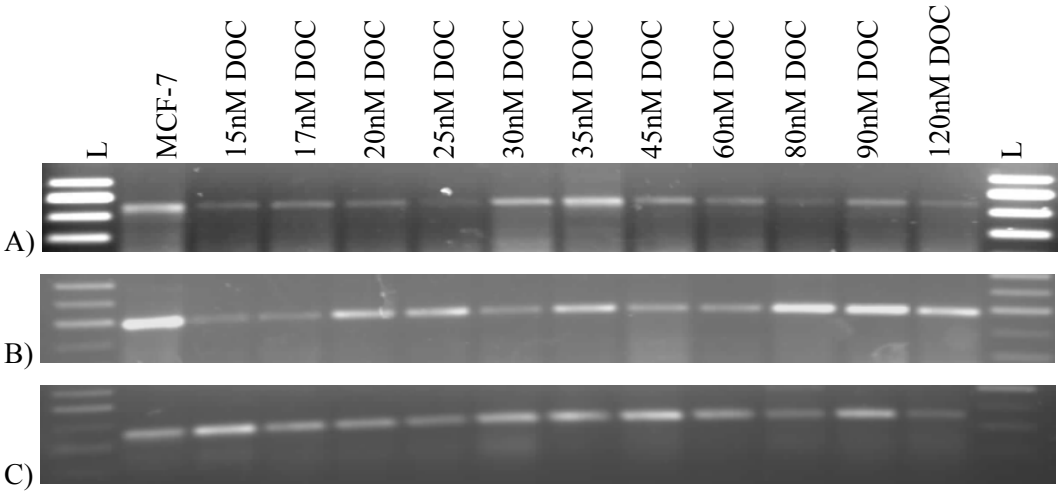

Figure 3.12 Expression levels of *Bcl-2, Bax and β2-m genes* in docetaxel resistant MCF-7 sublines (2% agarose gel); L: 50 bp ladder, A) *Bcl-2*, B) *Bax* and C) *β2-m* products.

Expression analysis of *Bcl-2* and *Bax* genes (Figures 3.12 and 3.14) demonstrated that MCF-7 cells had intrinsic gene expression. In evaluation of the results, ratio of antiapoptotic *Bcl-2* to proapoptotic *Bax* expression was considered as a survival parameter which may contribute to drug reistance (Figure 3.13). *Bcl-2/Bax* expression ratios were calculated (Appendix G) and RT-PCR results were evaluated on the basis of this ratio. According to Figure 3.13, *Bcl-2/Bax* ratio increased with initial 15nM and 17nM docetaxel

application (1.59- and 1.26-fold, respectively). In 20nM and 25nM, expression levels significantly decreased with respect to 15nM. Interestingly, 30nM docetaxel application caused another significant increase in the ratio. Expression levels were restored to levels of sensitive cells stepwise with increasing docetaxel concentrations. These fluctuating variances can be correlated with dose responses and acquirement of resistance. Some concentrations, such as 15 and 30nM docetaxel seem to be critical drug levels for cell survival. The cells which overcome these threshold drug concentrations seem to acquire resistance.

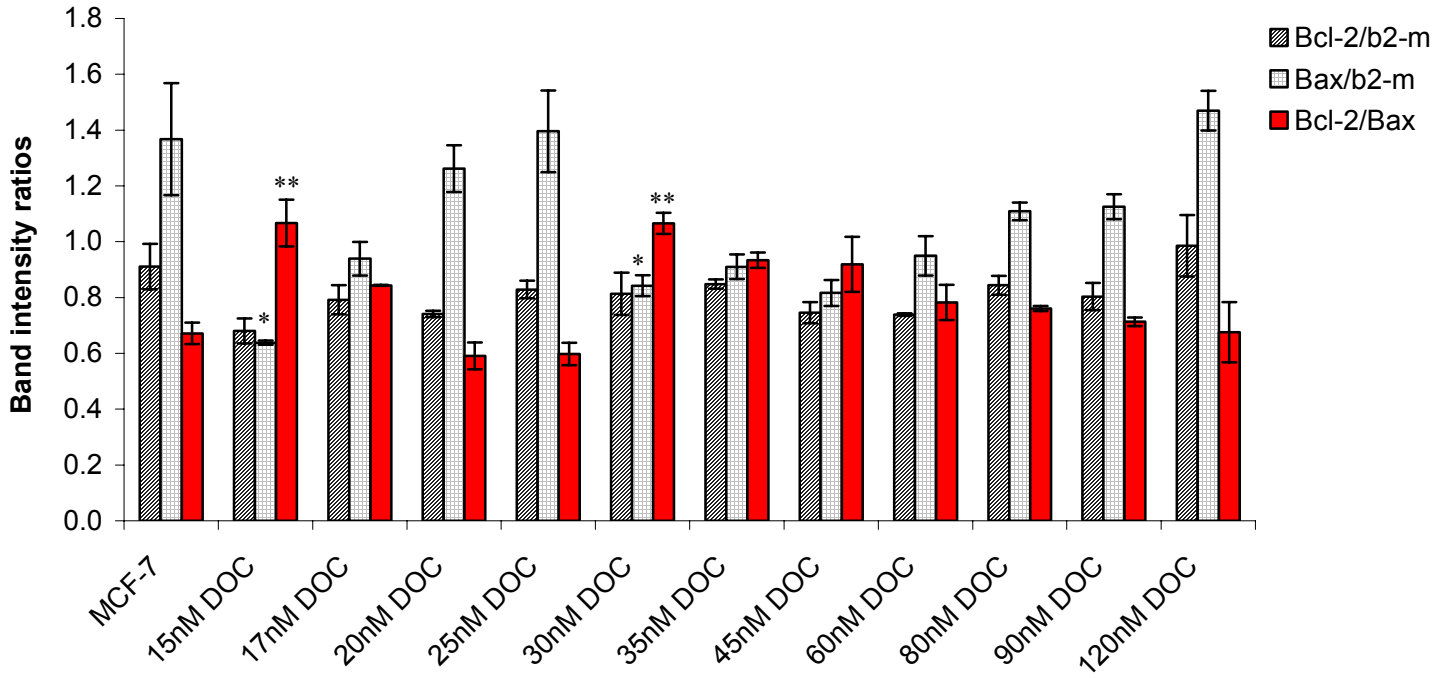

Figure 3.13 Expression of *Bcl-2* and *Bax* genes in docetaxel resistant MCF-7 sublines. * represents significant difference ($p<0.05$) in *Bcl-2/Bax* expression ratio between sensitive and docetaxel resistant sublines, ** represents significant difference ($p<0.05$) in *Bax* expression between sensitive and docetaxel resistant sublines.

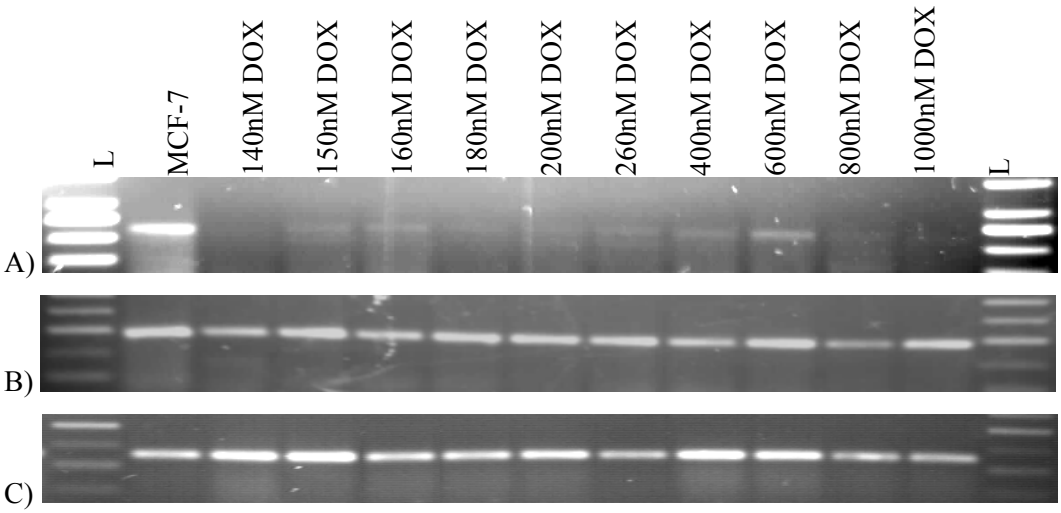

Figure 3.14 Expression levels of *Bcl-2, Bax and β2-m genes* in doxorubicin resistant MCF-7 sublines (2% agarose gel); L: 50 bp ladder, A) *Bcl-2*, B) *Bax* and C) *β2-m* products.

Bcl-2 and *Bax* expression levels which were determined by RT-PCR (Figure 3.14) in doxorubicin resistant sublines demonstrated that there were not significant changes in expression levels of these genes or *Bcl-2/Bax* ratios (Figure 3.15). Conclusively, alterations in apoptotic gene expression levels did not correlate to development of doxorubicin resistance in MCF-7 cells. The action mechanisms of these two drugs namely, docetaxel and doxorubicin, are quie different fom each other (see Sections 1.2.3.1 and 1.2.3.2). Therefore, it is not suprising that the metabolic responses of the resistant cells to these dugs are different from each other.

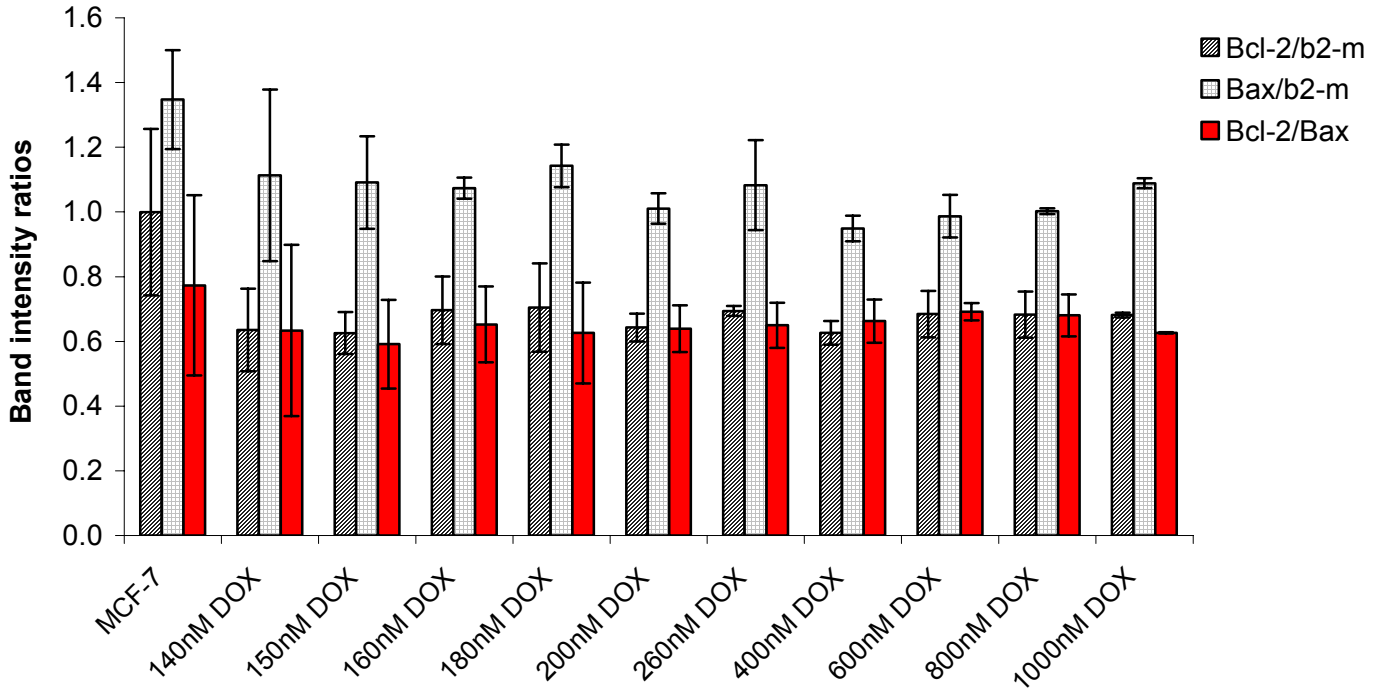

Figure 3.15 Expression of *Bcl-2* and *Bax* genes in doxorubicin resistant MCF-7 sublines.

3.2.4 Expression Analysis of *β-tubulin* Isotypes

Since docetaxel binds to β subunit of tubulins, *β-tubulin* isotype expression levels were investigated in docetaxel resistant sublines. Class I (βI), II (βII), III (βIII), IVa (βIVa), IVb (βIVb) and V (βV) tubulin mRNA levels were studied using gene specific primers by RT-PCR (Figure 3.16). Normalized expression levels and fold change calculations are presented in Appendix G.

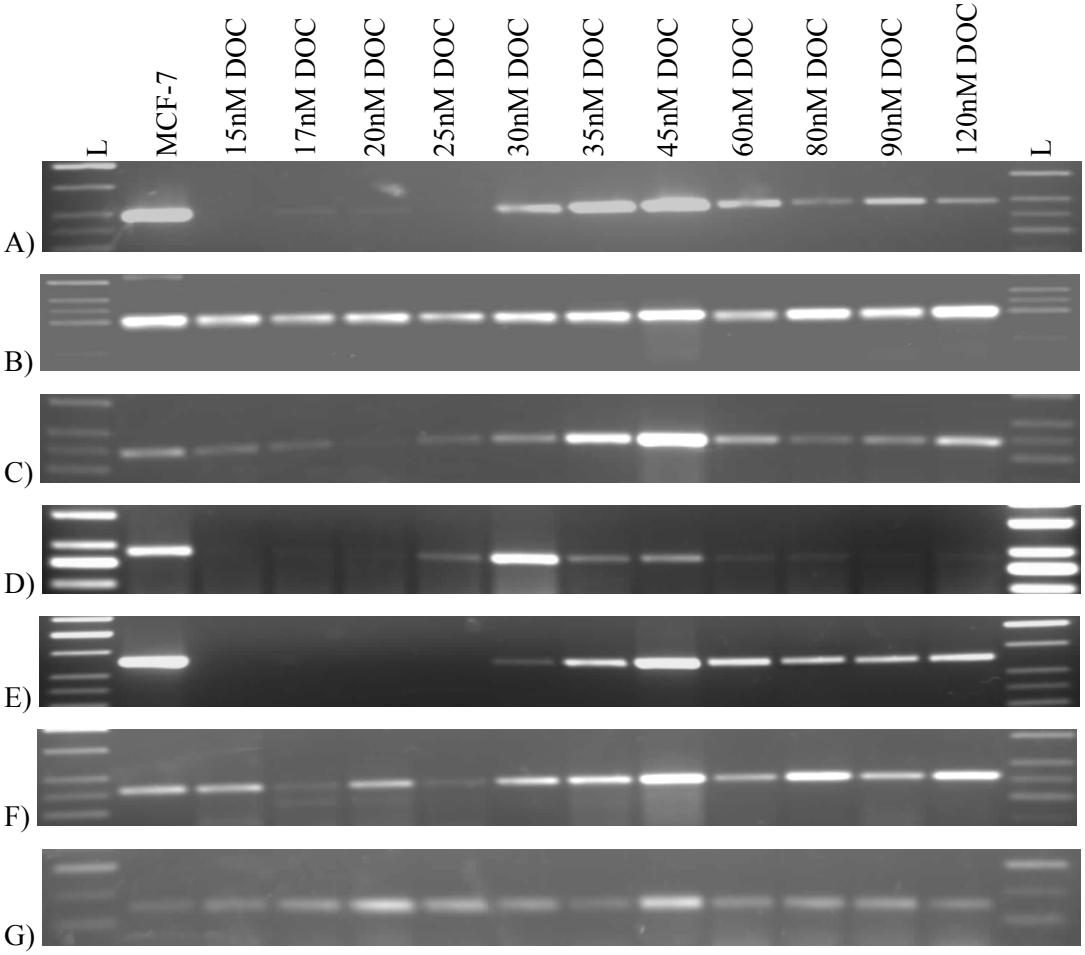

Figure 3.16 Expression levels of *β-tubulin* isotype genes in docetaxel resistant MCF-7 sublines (2% agarose gel); L: 50 bp ladder, A) *β-tubulin* isotype I, B) *β-tubulin* isotype II, C) *β-tubulin* isotype III, D) *β-tubulin* isotype IVa, E) *β-tubulin* isotype IVb, F) *β-tubulin* isotype V and G) *β2-m* product.

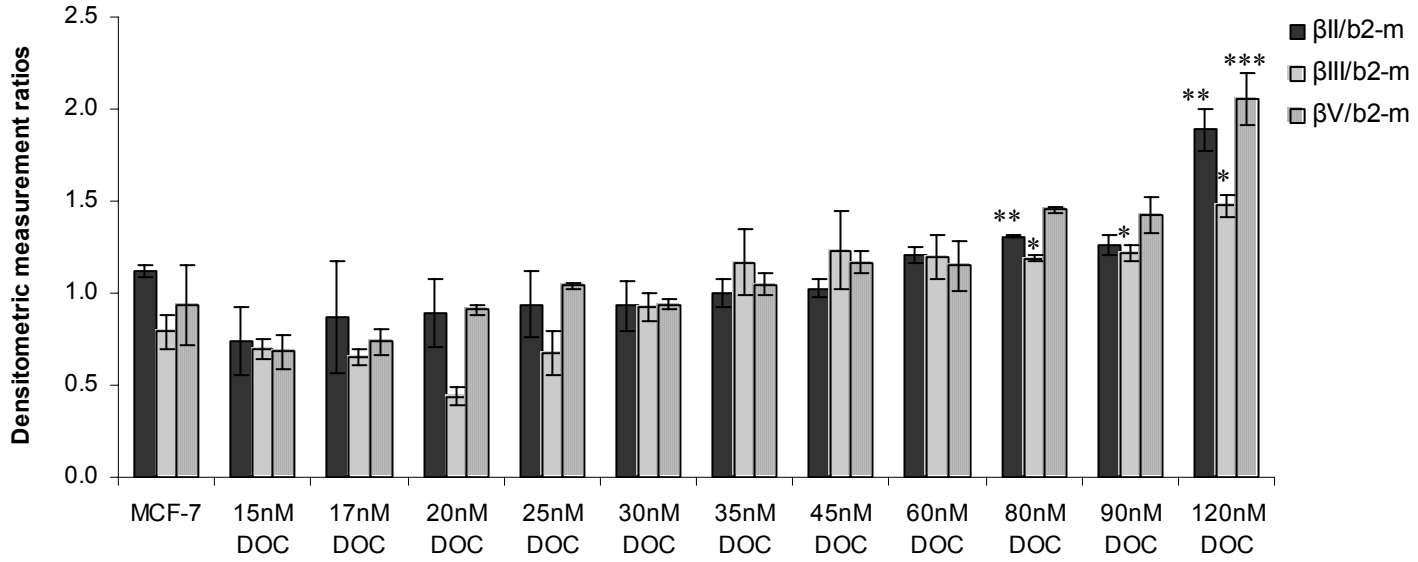

Figure 3.17 *β-tubulin* gene expression levels in docetaxel resistant MCF-7 sublines; * represents significant difference ($p<0.05$) in *βII-tubulin* expression between sensitive and docetaxel resistant sublines, ** represents significant difference ($p<0.05$) in *βIII-tubulin* expression between sensitive and docetaxel resistant sublines, *** represents significant difference ($p<0.05$) in *βV-tubulin* expression between sensitive and docetaxel resistant sublines.

The idea that changes in tubulin expression may confer resistance to microtubule targeting drugs comes from the fact that mammals have different tubulin proteins having differential assembly properties (Hari *et al.*, 2003). Gene expression analysis revealed that all the isotypes were intrinsically expressed in sensitive MCF-7 cells. Class II β-tubulin mRNA expression level significantly increased in MCF-7/120nM DOC cells (1.68-fold) with respect to original MCF-7 (Figure 3.17 A). It was previously reported (Bernard-Marty *et al.*, 2002) that increased mRNA expression levels of class II β-tubulin as a promising predictive marker of docetaxel response in breast cancer patients. Expression level of class III β-tubulin also significantly increased in 80, 90 and 120nM docetaxel resistant sublines (1.52-, 1.55- and 1.90-fold, respectively) (Figure 3.17). Decreased mRNA expression level of class III β-tubulin have been correlated with vincristine and vinblastine resistance in human leukemia cells (Kavallaris *et al.*, 2001) since class III β-tubulin has relatively higher microtubule-destabilizing potency (Banerjee *et al.*, 1990; Lu and Luduena, 1993; Kavallaris *et al.*, 1999). In addition, increased expression levels were also correlated with taxol resistance in previous studies (Hari *et al.*, 2003; Banerjee, 2002; Hasegawa *et al.*, 2003). Similarly, antisense reduction of class III beta tubulin mRNA and protein expression in Taxol resistant lung cancer cells corresponded to an increase in sensitivity (Kavallaris et al., 1999). Class V β-tubulin was significantly overexpressed in MCF-7/120nM DOC (1.90-fold) cells (Figure 3.17 A). Interestingly, it was previously reported that similar to class III β-tubulin, mouse class V β-tubulin had also destabilizing properties (Bhattacharya and Cabral, 2004). Furthermore, Horwitz *et al*. (Verdier-Pinard *et al.*, 2005) demonstrated a possible regulated balance between class III and V β-tubulin expressions in cells based on their similar topology that has been correlated to microtubule-destabilizing properties. However, alterations in expression of class V β-tubulin have not been correlated with antimicrotubule resistance, previously. Class I β-tubulin mRNA expression level decreased in resistant sublines. Similarly, class IVa β-tubulin levels decreased in resistant cells (Appendix G). Alterations in class IVb β-tubulin were not statistically significant. The results will be further discussed in Section 3.6.8.

3.3 Quantitative Real-Time Polymerase Chain Reaction (qPCR)

Expression analysis of *MDR1* and *MRP1* genes were performed in selected resistant sublines and sensitive MCF-7. Docetaxel and doxorubicin resistant sublines with moderate (MCF-7/30nM DOC and MCF-7/400nM DOX) and highest (MCF-7/120nM DOC and MCF-7/1000nM DOX) resistance indices were selected for qPCR. Complete qPCR data are given in Appendix G. *MDR1* was induced in MCF-7/30nM DOC cells and fluorescence intensity 1763-fold increased in MCF-7/120nM DOC cells wit respect to MCF-7/30nM DOC. qPCR results verifed that MCF-7 cells have intrinsic *MRP1* gene expression at basal level. *MRP1* was 1.69- and 2.44-fold downregulated in MCF-7/30nM DOC and MCF-7/120nM DOC when compared to sensitive cells (Figure 3.18 A). *MDR1* was induced in 400nM doxorubicin resistant cells and expression was 4558-fold upregulated in MCF-7/1000nM DOX cells. On the other hand, *MRP1* was significantly upregulated (2.08-fold) in MCF-7/400nM DOX cells where it was 3.85-fold downregulated in MCF-7/1000nM DOX cells (Figure 3.18 B). Interestingly, RT-PCR expression analysis (Figure 3.8 and 3.9) of *MDR1* and *MRP1* genes demonstrated that, *MRP1* was downregulated where *MDR1* was upregulated in docetaxel resistant cells. Furthermore *MRP1* was gradually upregulated until the emergence of *MDR1* gene in doxorubicin resistant cells (Figures 3.10 and 3.11 B). In other words, MRP1 was involved in low levels of resistance while P-gp showed intermediate to high levels of resistance doxorubicin resistant cells. Sequential emergence of these two pumps was not observed in docetaxel resistant cells since unlike doxorubicin it is not among the substrates of MRP1. So drug efflux through MRP1 is not one mechanisms of drug resistance in docetaxel resistant cells. Sequential emergence of *MDR1* and *MRP1* genes was demonstrated in etoposide selected small cell lung cancer and doxorubicin selected AML sublines previously (Brock *et al.*, 1995; Choi *et al.*, 1999). Similarly, Zhou et al. (Zhou *et al.*, 1996) reported MRP1 was an earlier event than P-gp in development of drug resistance in homoharringtonine selected K-562 cells and their expression was regulated at different levels depending on the concentration of selection. Progressive increase of expression levels of these pumps were negatively correlated dependent on the drug and selection concentration in MCF-7 cells in development of drug resistance.

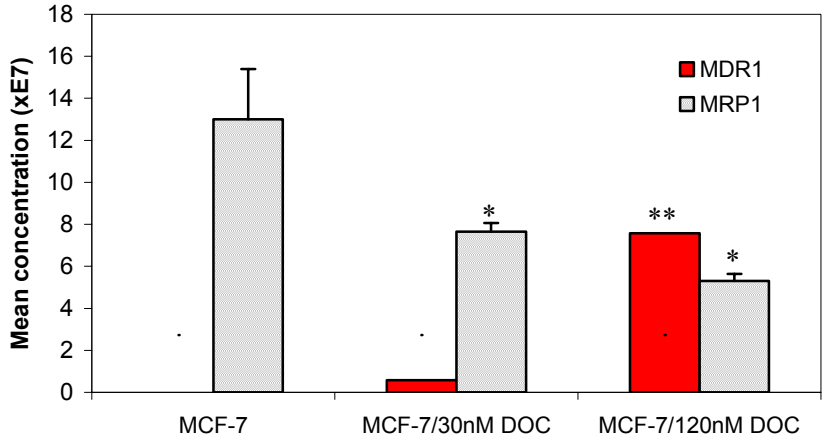

A)

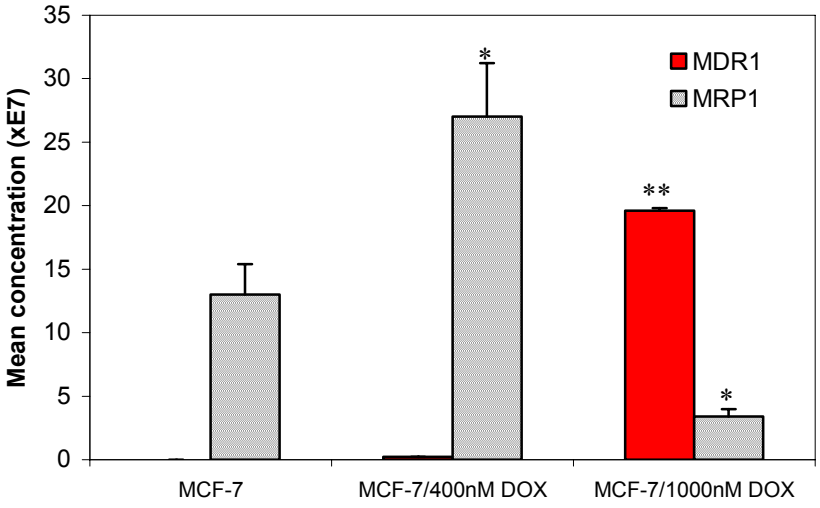

B)

Figure 3.18 QPCR results of expression analysis of *MDR1* and *MRP1* genes in; A) docetaxel, and B) doxorubicin resistant cells. * Represents significant difference ($p<0.05$) in expression level of *MRP1* between sensitive MCF-7 and resistant sublines, ** represents significant difference ($p<0.05$) in expression level of *MDR1* between resistant sublines.

3.4 Western Blotting

3.4.1 Protein Isolation

Total cell lysates were visualized on SDS-PAGE to determine cellular proteins (Figure 3.19).

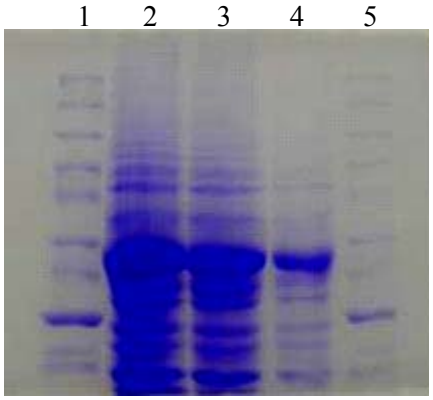

Figure 3.19 Fractionation of total cell proteins of MCF-7 cells (7.5% (w/v) polyacrylamide gel); lanes: (1 and 5) protein standard, (2) 50µg of protein, (3) 30µg of protein, (4) 10µg of protein.

3.4.2 Determination of P-gp and MRP1 Levels

P-gp and MRP1 protein levels were normalized according to loading control GAPDH. Figure 3.20 demonstrates western blot results of P-gp, MRP1 and GAPDH proteins in docetaxel and doxorubicin resistant MCF-7 sublines.

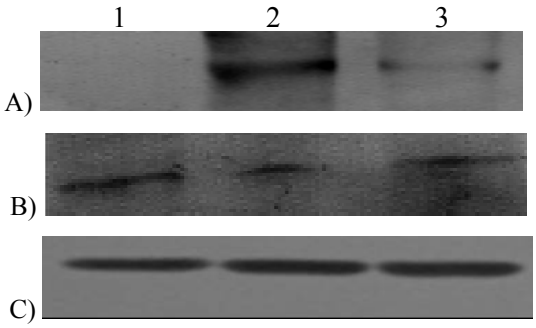

Figure 3.20 Western blots of docetaxel and doxorubicin resistant MCF-7 total cell proteins; A) 170kD P-gp, B) 190kD MRP1 and C) 36kD GAPDH; lanes (1) MCF-7, (2) MCF-7/MCF-7/80nM DOC, (3) MCF-7/600nM DOX.

Western blot results demonstrated *de novo* expression of P-gp in docetaxel and doxorubixin resistant cells. Concordant with the RT-PCR results MRP1 protein levels seemed to be unchanged in these sublines.

3.4.3 Determination of Bcl-2 and Bax Levels

Bcl-2 and Bax protein levels were normalized according to loading control GAPDH. Figures 3.21 and 3.22 demonstrate western blot results of Bcl-2, Bax and GAPDH proteins in docetaxel and doxorubicin resistant MCF-7 sublines.

According to densitometric measurements (Appendix G) of western blot results, Bcl-2 increased in MCF-7/15-20nM DOC cells and decreased in more resistant cells. Athough variations in fold change values were small, alterations in Bcl-2 protein level were concordant with RT-PCR results demonstrated above. RT-PCR results demonstrated that there was not significant change in *Bax* expression levels, Bax protein levels were determined only in six sublines in which changes in expression levels were relatively higher (Figure 3.13) and changes in Bax protein levels in these sublines seemed to be concordant.

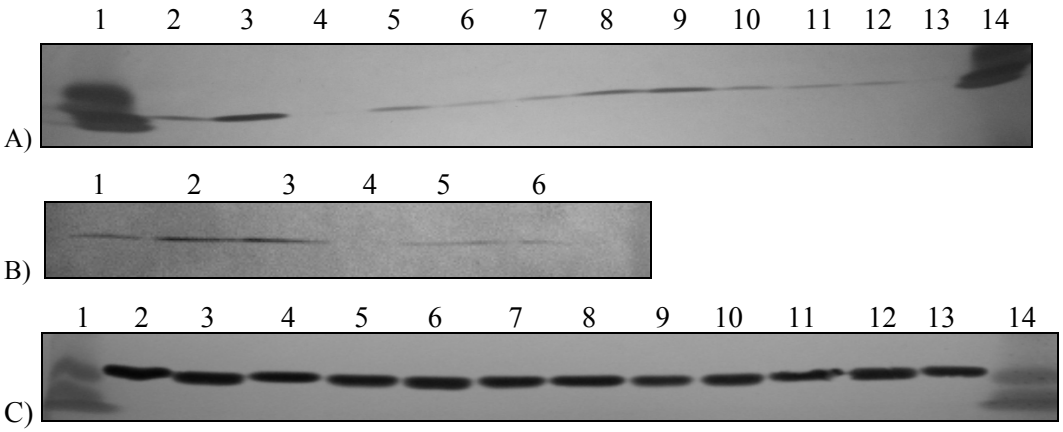

Figure 3.21 Western blots of docetaxel resistant MCF-7 total cell proteins; A) 26kD Bcl-2, B) 21kD Bax, C) 36kD GAPDH; lanes (1 and 14) protein standard, (2-13) MCF-7, MCF-7/15-120nM DOC sublines for A and B, and lanes (1 and 6) MCF-7, MCF-7/15-30nM DOC sublines for B.

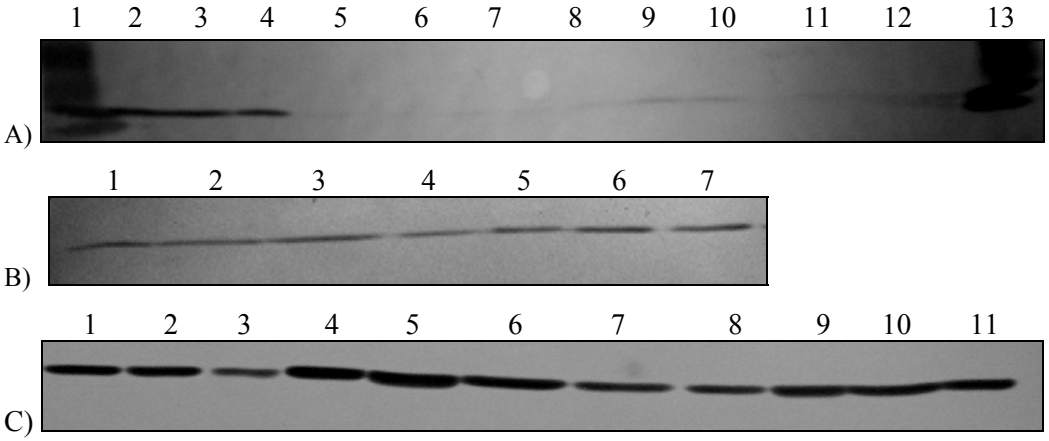

Figure 3.22 Western blots of doxorubicin resistant MCF-7 total cell proteins; A) 26kD Bcl-2 (50μg) (lanes 1 and 13 protein standard, 2-12 MCF-7, MCF-7/140-1000nM DOX sublines), B) 21kD Bax (50μg) (lanes 1-7 MCF-7, MCF-7/140-260nM DOX sublines, C) 36kD GAPDH (4μg) (lanes 1-11 MCF-7, MCF-7/140-1000nM DOX sublines).

Bcl-2 levels in doxorubicin resistant cells decreased (Figure 3.34). Accordingly, *Bcl-2* mRNA levels decreased in these cells (Figure 3.15). However Bax levels remained unchanged in MCF-7/140-260nM DOX cells.

3.5 Immunocytochemistry

Presence of P-gp and MRP1 on cell surface was confirmed by immunucytochemistry (Figures 3.23 and 3.24). According to photographs in Figure 3.23 P-gp expressing cells have red stains on their cellular membranes. Sensitive MCF-7 cells did not have P-gp on their membranes (Figure 3.35 A) where docetaxel and doxorubicin resistant cells (Figure 3.23 B and C, respectively) expressed P-gp on their cellular membranes.

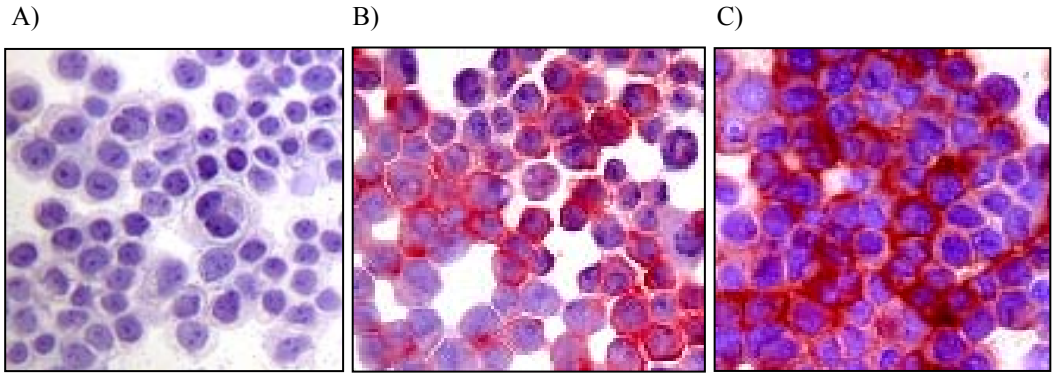

Figure 3.23 Cells labelled with anti P-gp and HRP-DAB staining (40X); A) MCF-7, B) MCF-7/80nM DOC and C) MCF-7/600nM DOX.

MRP1 protein was labeled as dark brown on cellular membranes (Figure 3.24). All sensitive and resistant cells had MRP1 labels on their cellular membranes. Presence of LRP was also assessed by immunucytochemistry. Neither of the sublines expressed LRP (Figure 3.25).

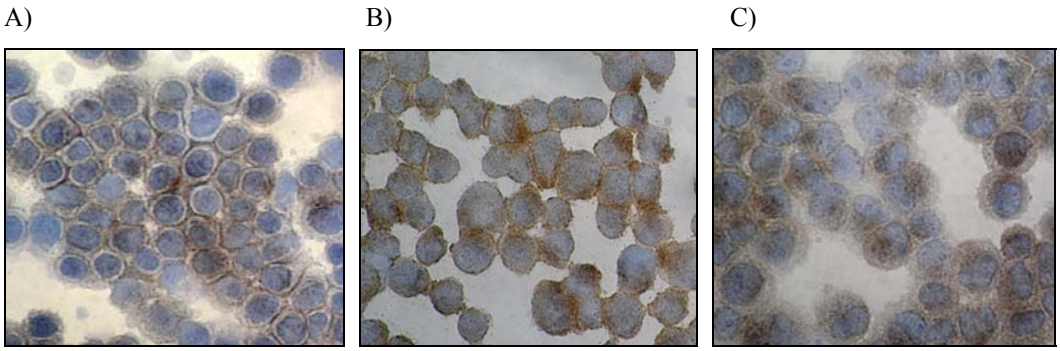

Figure 3.24 Cells labelled with anti MRP1 and HRP-DAB staining (40X); A) MCF-7, B) MCF-7/80nM DOC and C) MCF-7/600nM DOX.

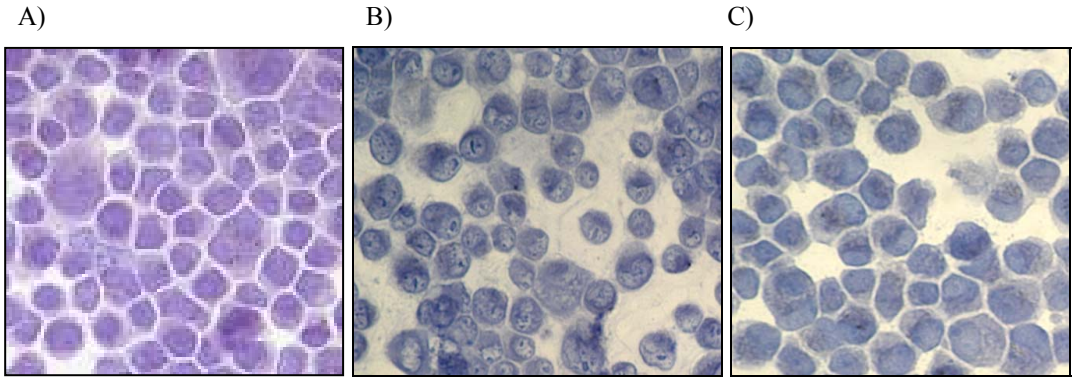

Figure 3.25 Immunocytochemistry of MCF-7 cells: anti LRP and HRP-DAB (40X); A) MCF-7, B) MCF-7/80nM DOC and C) MCF-7/600nM DOX.

3.6 Microarray Analysis

The hybridization of positive control cRNAs with respective probes provides appearance of an expression on the left top corner of all Affymetrix chips. Apperance of this image on signal scan files is the very initial assessment of success of hybridization and scanning. For example, the appearance expression "GeneChip HG-U133 Plus2" in Figure 3.26 demonstrated that the hybridization and scanning procedures worked successfully and the raw data could be subjected to preliminary analysis. The quality of scanned samples were assessed according to parameters described in Section 2.6.3 and expression data were

found to be in “good sample” range based on these criteria. The chips were comprised of 1,300,000 unique oligonucleotide probes covering over 47,000 transcripts and variants, which, in turn, represented approximately 25,000 of the characterized human genes (www.affymetrix.com/products/arrays/specific/hgu133plus.affx). All probe sets represented on the array included a set of human maintenance genes, which showed consistent level of expression independent of tissue types, to facilitate the normalization and scaling of array experiments.

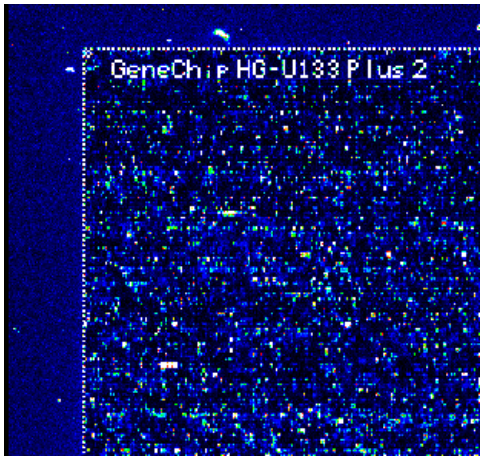

Figure 3.26 The image that was obtained after scanning of one of the chips.

In order to monitor differential expression profiles in sensitive and resistant cells, box plot (Figure 3.27) and line graph (Figure 3.28) were constructed. Accordingly, expression profiles of MCF-7 and MCF-7/30nM DOC were similar to each other. On the other hand, expression profiles of MCF-7/120nM DOC and MCF-7/1000nM DOX differed from MCF-7 and MCF-7/30nM DOC while the resistant profiles of these two were also similar. Concordantly, expression profiles changed gradually with increasing degree of resistance.

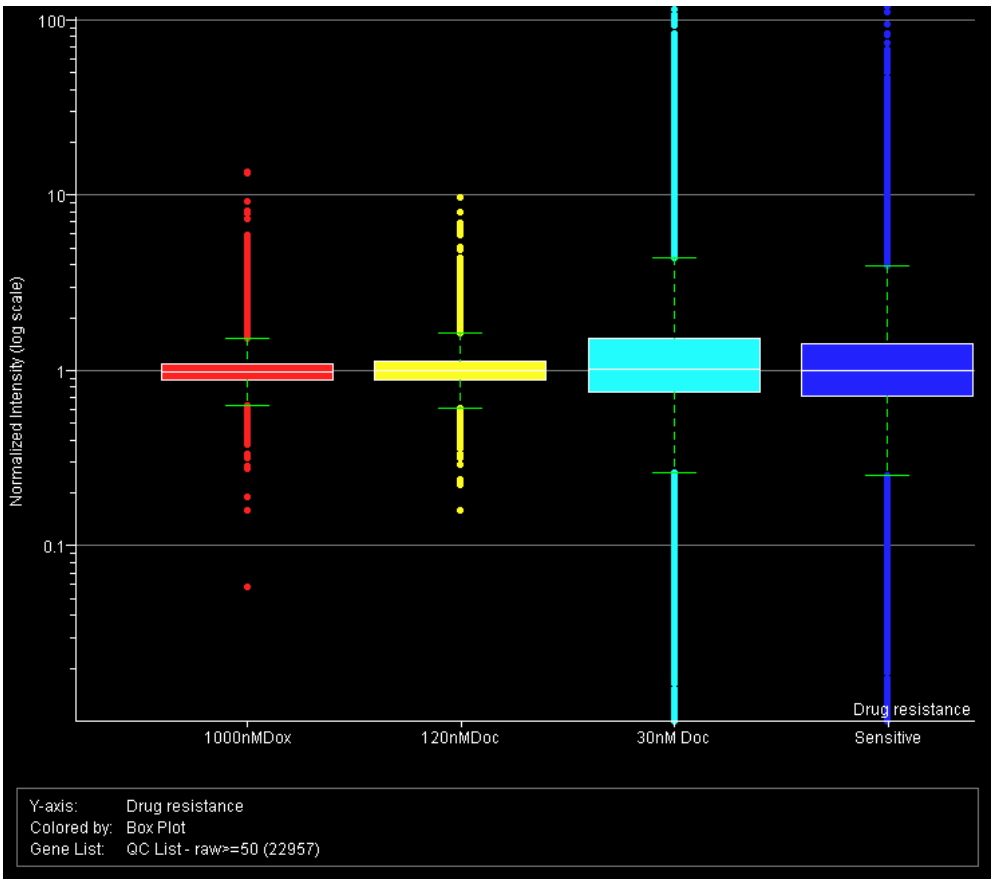

Figure 3.27 Box plot representation of data sets.

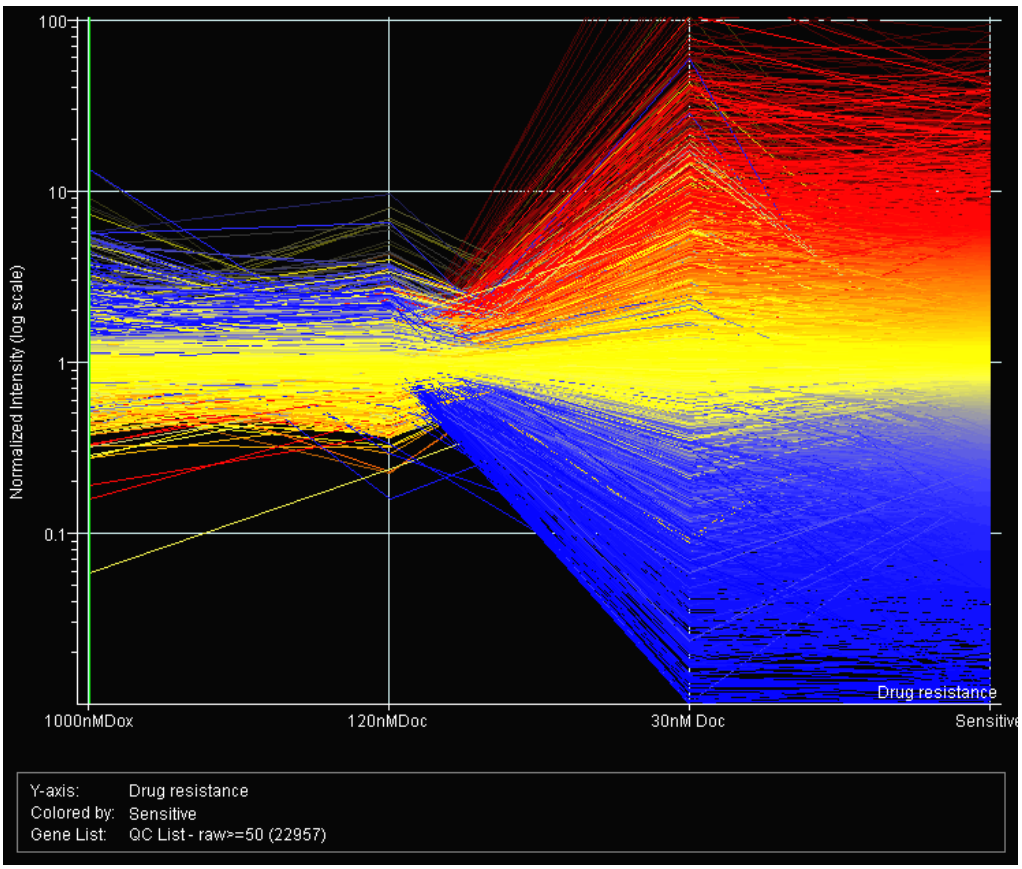

Figure 3.28 Line graph representation of data sets.

According to Venn diagram (Figure 3.29) representing the amount of genes altered in resistant sublines with respect to sensitive cells, alteration in expression level of approximately 500 genes was common in three resistant sublines. Expressions of aproximately 2300 genes were changed in both MCF-7/120 DOC and MCF-7/1000nM DOX while 850 genes were altered in common in two docetaxel resistant sublines. Similarly, 950 genes were changed both in MCF-7/30nM DOC and MCF-7/1000nM DOX. Results revealed that expression profiles showed similarity based on degree of resistance rather than based on selective drug.

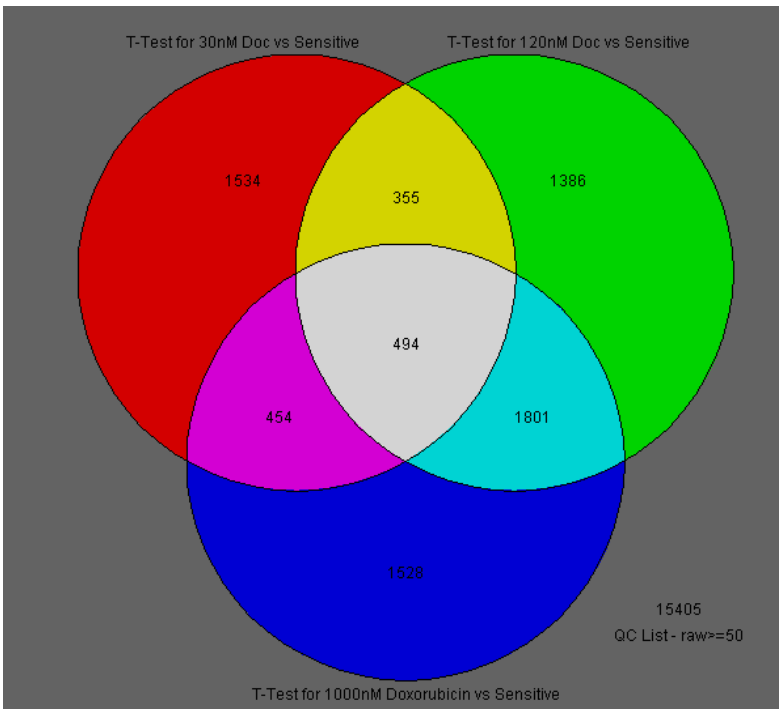

Figure 3.29 Venn diagram representing number of altered genes in sensitive MCF-7 and resistant sublines.

Changes in expression levels were analysed for significance as MCF-7 and resistant subline pairs. Significantly altered genes between resistant sublines and sensitive MCF-7 cells were listed and then gene trees were constructed (Figure 3.30 and 3.31) from these lists by standard correlation. Upregulated and downregulated genes were selected from gene trees. The genes were filtered by volcano plots (Figure 3.32 and 3.33) and significant fold change values greater than 2-fold upregulation and less than 2-fold downregulation were considered for evaluation and their contribution to drug resistance. The genes whose expression level changed in between 2-fold and -2-fold were considered as 'not significant (NS)'.

.

A)

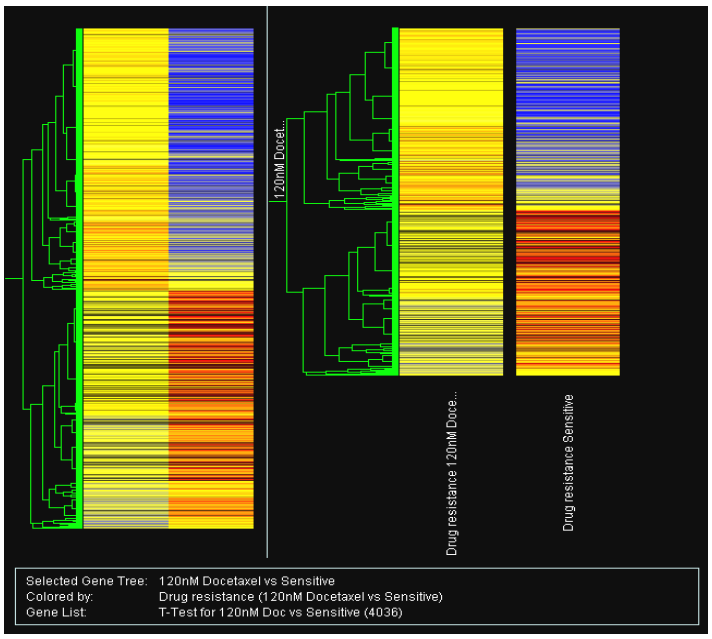

B)

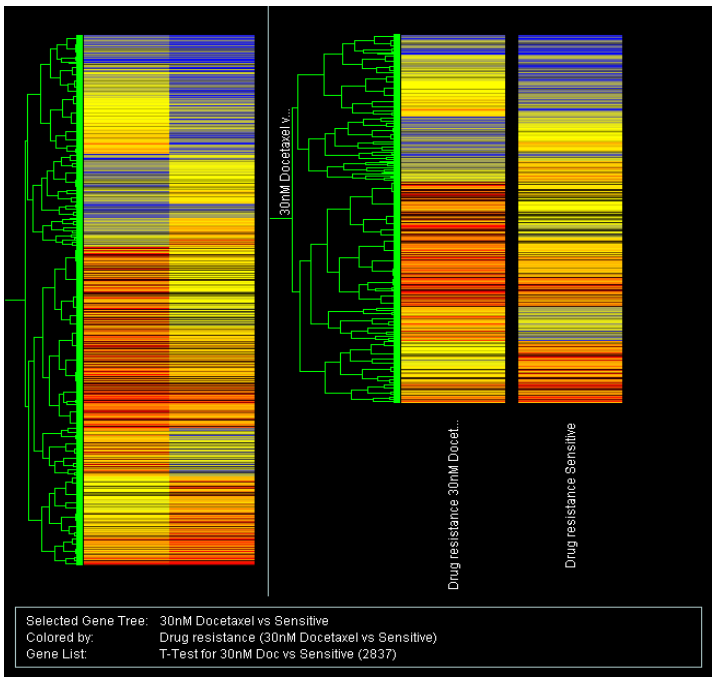

Figure 3.30 Gene tree for docetaxel resistant MCF-7 cells; A) MCF-7/120nM DOC and B) MCF-7/30nM DOC.

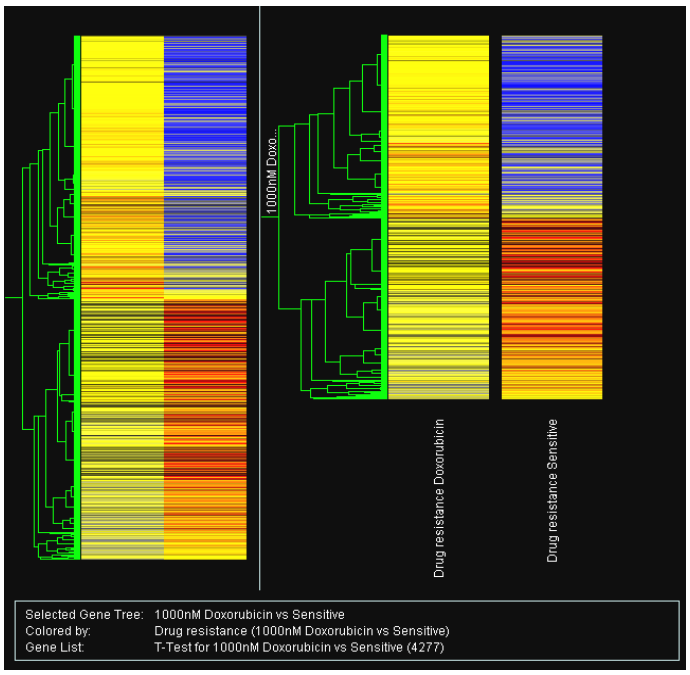

Figure 3.31 Gene tree for doxorubicin (1000nM) resistant MCF-7 cells.

A)

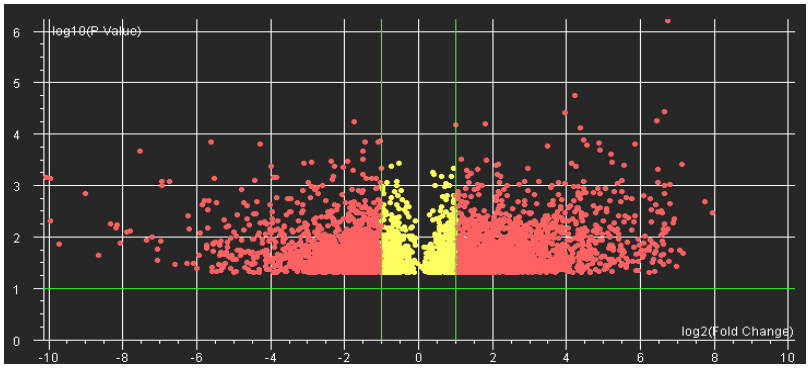

B)

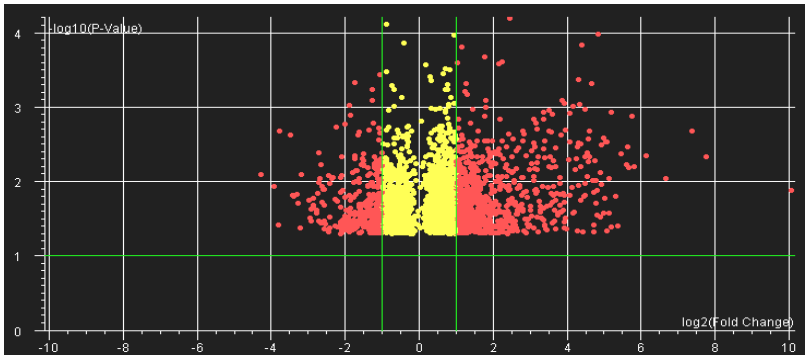

Figure 3.32 Volcano plots for docetaxel resistant MCF-7 cells; A) MCF-7/120nM DOC, and B) MCF-7/30nM DOC.

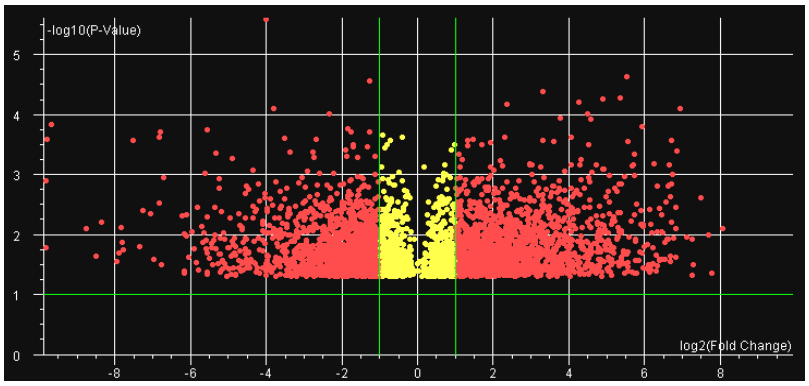

Figure 3.33 Volcano plot for doxorubicin (1000nM) resistant MCF-7 cells.

3.6.1 Alterations in ABC Transporter Family Genes

Changes in expression levels of the ABC transporter family genes in resistant sublines are listed in Table 3.5. The *ABCB4* gene is located on chromosome 17q21.1, 34 kb downstream of the *ABCB1* gene. The *ABCB1* and *ABCB4* genes are very similar. They both contain 27 introns and are inserted at identical positions in the coding sequence. The proteins encoded by these genes have virtually identical hydropathy plots; they are 77% identical and 82% similar in amino acid sequence. The ABCB4 P-gp is normally involved in the transport of phospholipids from liver hepatocytes into bile but is also involved in the transport of paclitaxel and vinblastine. ABCB4 is also inhibited by verapamil, a classic inhibitor of the ABCB1 protein, P-gp. ABCB4 expression was correlated negatively with clinical outcome. Previously it was reported that ABCB4 has lower transport rates for paclitaxel as compared with ABCB1 and it did not play as significant role in paclitaxel resistance as P-gp at least *in vitro* (Duan *et al.*, 2004). Furthurmore, *ABCB4* was found to be coamplified with *ABCB1,* so increased expression levels were correlated with increase in copy number of entire 7q21.12 region rather than its contribution to drug transport in paclitaxel resistant cells (Yabuki *et al.*, 2007). The four half transporters, ABCB6, ABCB7, ABCB8 and ABCB10 localize on mitochondria, where they function in iron metabolism and transport of Fe/S protein precursors (Ševkova *et al.*, 2004). D subfamily consists of four human proteins, all ABC half-transporters that require a partner half-transporter to form functional homo- or heterodimeric transporters. They are localized in the peroxisomal membrane, and mutations in these genes cause different peroxisomal disorders. The

ABCD1/ALD protein is located in the peroxisomal membrane and most likely plays a role in the transport of very long chain fatty acids. ABCB2/TAP1 and ABCB3/TAP2 are half-transporters, and form heterodimers in order to function as peptide transporters involved in the MHC-I-dependent antigen presentation. They are localized in the membrane of endoplasmic reticulum, and pump degraded cytoplasmic peptides into the ER lumen (Glavinas *et al.,* 2004).

Table 3.5 List of differentially expressed ABC transporter family genes in drug resistant MCF-7 sublines and fold changes of expression.

Gene Name	Gene Symbol	Gene Description	Gene Ontology	MCF-7/ 30DOC	MCF-7/ 120DOC	MCF-7/ 1000DOX
209994_s_at	ABCB1; ABCB4	ATP-binding cassette, sub-family B (MDR/TAP), member 1 ; ATP-binding cassette, sub-family B (MDR/TAP), member 4	BP[¥]: cell growth and maintanence; MF[†]: transporter activity	9.77	244.80	266.90
209993_at, 243951_at	ABCB1	ATP-binding cassette, sub-family B (MDR/TAP), member 1	BP: cell growth and maintanence; MF: transporter activity	10.55	215.20	205.90
1570505_at	ABCB4	ATP-binding cassette, sub-family B (MDR/TAP), member 4	BP: cell growth and maintanence; MF catalytic activity, transporter activity	NS	17.03	23.30
223320_s_at	ABCB10	ATP-binding cassette, sub-family B (MDR/TAP), member 10	MF: binding, catalytic activity, transporter avtivity	3.86	NS	NS
205142_x_at	ABCD1	ATP-binding cassette, sub-family D (ALD), member 1	MF: binding, catalytic activity, transporter activity	3.54	NS	NS
214033_at	ABCC6	ATP-binding cassette, sub-family C (CFTR/MRP), member 6	BP: cell growth and maintenence; MF: binding, catalytic activity, transporter activity	NS	NS	3.37
204769_s_at	TAP2	transporter 2, ATP-binding cassette, sub-family B (MDR/TAP)	BP: cell growth and maintenence; MF: binding, catalytic activity, defense and immunity, structural molecules, transporter activity	NS	NS	3.08

Table 3.5 (Continued)

202805_s_at	ABCC1	ATP-binding cassette, sub-family C (CFTR/MRP), member 1	BP: cell growth and maintanance; MF: binding, catalytic activity, transporter activity	-2.42	NS	NS
212772_s_at, 210100_s_at	ABCA2	ATP-binding cassette, sub-family A (ABC1), member 2	BP: cell growth and maintanence; MF: catalytic activity, transporter activity	NS	-2.73	-2.86
213353_at	ABCA5	ATP-binding cassette, sub-family A (ABC1), member 5	BP: cell growth and maintanence; MF: catalytic activity, transporter activity	NS	-4.149	-5.99
211113_s_at, 204567_s_at	ABCG1	ATP-binding cassette, sub-family G (WHITE), member 1	BP: cell growth and maintanence; MF: catalytic activity, transporter activity	NS	-39.22	-11.91

[¥] BP: Biological process

[†] MF: Molecular function

3.6.2 Alterations in Genes Encoding Glutathione Metabolism Related Proteins

According to Table 3.6, *GPX1* was drastically upregulated in MCF-7/120nM DOC and MCF-7/1000nM DOX (105.8- and 113.4-fold, respectively). Glutathione (GSH) is the most abundant intracellular nonprotein contributor of ROS defense. The major downstream effector of GSH-mediated ROS defense is the enzyme glutathione peroxidase 1 (GPX1), which reduces hydrogen peroxide to water at the expense of oxidizing GSH to its disulfide form GSSG. Overexpression of GPX1 and other antioxidant enzymes, as well as depletion of intracellular GSH, have been shown to suppress anthracycline induced apoptosis in several experimental systems, including cancer cell lines and tumor xenografts (Andreadis *et al.*; 2007). Glutathione S-transferase π (*GSTP1*) was also 55.5- and 57.6-fold upregulated in MCF-7/120nM DOC and MCF-7/1000nM DOX, repectively. Glutathione-S-transferases comprise a family of related proteins that can enzymatically conjugate GSH to electrophilic chemotherapeutic agents and able to facilitate their elimination through the ABC transporter MRP1. Besides GSH conjugation activity, GSTs have organic peroxidase activity and may also play a role in protection from ROS induced effects of anticancer drugs. Moreover, recent studies have demonstrated that GST subclasses π and μ have a regulatory role in the cell by binding to key members of the survival and death-signaling pathway, such as c-Jun N-terminal kinase 1 (JNK1) and apoptosis signal-regulating kinase 1 (ASK1) (Andreadis *et al.*; 2007)

Table 3.6 List of differentially expressed genes encoding glutathione metabolism related proteins in drug resistant MCF-7 sublines and fold changes of expression.

Gene Name	Gene Symbol	Gene Description	Gene Ontology	MCF-7/ 30DOC	MCF-7/ 120DOC	MCF-7/ 1000DOX
200736_s_at	GPX1	glutathione peroxidase 1	BP: cell growth and maintanence; MF: transporter activity	NS	105.80	113.40
200824_at	GSTP1	glutathione S-transferase pi	BP: cell growth and maintanence; MF: catalytic activity	NS	55.70	57.61
213170_at	GPX7	glutathione peroxidase 7	BP: cell growth and maintanence; MF: catalytic activity, transporter activity	NS	8.28	NS
201415_at, 211630_s_at	GSS	glutathione synthetase	BP: cell growth and maintenence; MF: binding, catalytic activity, transporter activity	NS	2.21	2.35

3.6.3 Alterations in Genes Encoding Cytochorome P450 Family Proteins

Table 3.7 summarizes the alterations in levels of the genes encoding cytochrome P450 enzymes. P450 oxireductase (POR) was noticeably downregulated in 120nM docatexel and 1000nM doxorubicin resistant cells. The enzyme is essential for cytochrome P450 activity in cells since it provides electrons used in P450-mediated reactions using NADPH as a cofactor. Overexpression of this enzyme in breast carcinoma cells was correlated to depletion of NADPH levels and increased ROS levels which increase cellular oxidative stress (see Figure 1.7). In addition transfection of these cells with P450 reductase caused increased 5-fluorouracil sensitivity with a slight increase in docetaxel sensitivity (Martinez *et al.*, 2008). In addition, it was reported that doxorubicin was predominantly metabolized to its active form by this enzyme (Cummings *et al.*, 1992). Moreover decreased levels of P450 reductase and enzyme activity were detected Adriamycin resistant MCF-7 cells, previously (Mimnaugh *et al.*, 1989).

CYP26B1 was 10-fold upregulated in both MCF-7/120nM DOC and MCF-7/1000nM DOX cells. CYP26s are the retinoic acid (RA) signaling enzymes of the P450s. Endogenous RA is an important effector of various cellular signaling pathways and is degraded by CYP26 enzymes (Reijntjes *et al.*; 2007). All-trans-RA (ATRA) is also used in chemotherapy for its antitumor activity. It is a natural ligand of nuclear retinoic acid receptors (RARs) which have effects on cell proliferation, differentiation and apoptosis so it is used in chemotherapy (Wu Q *et al.*; 1997). So the CYP26s are thought to be responsible for switching off the RA signal. Furthermore, CYP26A1, which is a RA hydroxylation enzyme, was also 2.9-fold upregulated in MCF-7/1000nM DOX cells. This subline was also found to be cross-resistant to ATRA as will be discussed in Section 3.7.

Interestingly, *CYP24A1* was 8.1-fold upregulated while *CYP1B1* was 3.03-fold downregulated only in MCF-7/30nM DOC cells. CYP24A1 catalyzes the catabolism of 1,25-$(OH)_2D_3$ (active vitamin D3) via C24- or C23-hydroxylation (Kutuzovaa et al.; 2007). Active vitamin D_3 exerts pleiotropic effects on cell proliferation, differentiation and the immune system via binding to vitamin D_3 receptor (VDR) and plays an important role in reducing the risk of prostate, colon and other cancers as well as autoimmune diseases.

Increase in the expression level of the *CYP24A1* gene may be an earlier event of protection from cytotoxic effects of docetaxel. Furthermore, several anticancer drugs (docetaxel, paclitaxel, mitoxantrone and flutamide) were identified as substrates for CYP1B1 (Rochat *et al,* 2001) and particularly, CYP1B1 was found to interact with docetaxel and reduce its cytotoxicity (Bournique and Lemarie, 2002). CYP1B1 is found in steroid-responsive tissues, such as the breast, uterus, and prostate since its expression is under hormonal control in many steroidogenic tissues. An elevated level of *CYP1B1* mRNA was detected in docetaxel selected MCF-7 cells (Martinez *et al.*, 2008). However, *CYP1B1* expression is dependent upon ER status of cells. For example expression levels of both *CYP1A1* and *CYP1B1* were investiated in ER+/- lineages of estrogen responsive and nonresponsive breast cancer cell lines. *CYP1B1* was found to be lower than basal level in ER positive cells lineages of estrogen responsive cells (Angus *et al*.; 1999). *ESR1* expression was downregulated in MCF-7/120nM DOC and MCF-7/1000nM DOX cells while it was not downregulated in MCF-7/30nM DOC cells (Table 3.10).

Table 3.7 List of differentially expressed genes encoding cytochrome P450 family proteins in drug resistant MCF-7 sublines and fold changes of expression.

Gene Name	Gene Symbol	Gene Description	Gene Ontology	MCF-7/ 30DOC	MCF-7/ 120DOC	MCF-7/ 1000DOX
208928_at	POR	P450 (cytochrome) oxidoreductase	BP: cell growth and maintanence; MF: catalytic activity, transporter activity	NS	-5.10	-6.45
219825_at	CYP26B1	cytochrome P450, family 26, subfamily B, polypeptide 1	BP: cell growth and maintanence; MF: catalytic activity, transporter activity	NS	10.66	10.09
206424_at	CYP26A1	cytochrome P450, family 26, subfamily A, polypeptide 1	BP: cell growth and maintenance; MF: binding, catalytic activity, transporter activity	NS	NS	2.88
206504_at	CYP24A1	cytochrome P450, family 24, subfamily A, polypeptide 1	MF: binding, catalytic activity	8.05	NS	NS
202436_s_at, 202435_s_at	CYP1B1	cytochrome P450, family 1, subfamily B, polypeptide 1	BP: cell growth and maintenance; MF: binding, catalytic activity, transporter activity	-3.06	NS	NS

3.6.4 Alterations in Expression Levels of Genes Encoding Proteins Related to Cell Survival and Cell Death

Fas and Tumor Necrosis Factor (TNF) are important death ligands that effectively induce apoptosis in cancer cells. TNF superfamily ligands and receptors are inveolved in membrane mediated apopotosis through FasL and TNF-Related Apoptosis-Inducing Ligand (TRAIL or Apo2L). Alterations in various TNF receptors (Table 3.8 A) and ligands (Table 3.8 B) have been observed in resistant cells. TRAIL selectively induces apoptosis in cancer cells by binding to either of its receptors, DR4 or DR5 (Figure 3.34). These receptors consist of an extracellular TRAIL binding domain and a cytoplasmic "death domain". Two other receptors, so called decoy receptors, contain an extracellular TRAIL-binding domain, a transmembrane domain, and a truncated cytoplasmic death domain. The protein encoded by *TNFRSF10D* gene, TRAIL-R4 or decoy receptor 2 (DcR2), is a member of the TNF-receptor superfamily. TRAIL-R4 is known to protect cells from apoptosis by acting both as a decoy receptor and an antiapoptotic signal provider. Expression of TRAIL-R4 decoy receptor was correlated with TRAIL resistance phenotype observed in MCF-7 cells and inhibition of NF-κB signaling pathway sensitized cells to TRAIL induced apoptosis (Sanlioglu *et al.*, 2005). Another decoy receptor gene *TNFRSF6B*, encoding the decoy receptor 3 (DcR3), had the highest fold change among the genes of interest in both MCF-7/120nM DOC and MCF-7/1000nM DOX (27.61 and 29.64, respectively). DcR3 can also inhibit FasL-dependent immune-cytotoxic attack by competing with Fas for binding to FasLigand, thereby blocking apoptosis (Pitti *et al.*, 1998). Concordantly, Mild *et al.* (Mild *et al.,* 2002*)* demonstrated that about 2/3 of colorectal cancer patients treated with FU/MMC adjuvant chemotherapy had elevted DcR3, and Takahama *et al.*, (Takahama *et al.*, 2002) reported its significance of overexpression for progression of gastric cancer in patients with gastric carcinomas.

As a member of the TNF receptor family, CD40 relies on interaction with TRAF proteins to mediate an intracellular signal in response to CD40L binding (Vonderheide *et al.,* 2007). The downstream pathway of TRAFs activates the transcription factor NF-κB through a kinase pathway involving MAP kinases, NIK (NF-κB inducing kinase) and I-kappa B kinases. In normal and certain malignant B cells, CD40 ligation rapidly rescues cells from apoptosis, an effect involving increased expression of Bcl-X_L, A20, and Bfl-1,

each downstream from CD40-mediated nuclear factor-κB activation. Transfection studies have confirmed the oncogenic effect of CD40 signaling which was was inhibited by the suppression of the NF-κB signaling pathway (Baxendale *et al.*, 2005). Furthermore, several preclinical studies have suggested that the CD40 signaling pathway plays a role in the modulation of chemosensitivity in breast cancer cells. For example, stimulation of the CD40 receptor inhibited paclitaxel-induced apoptosis in breast cancer cell lines (Stumm *et al.,* 2004). In addition, reduction of apoptosis caused by various drugs including doxorubicin and paclitaxel in cells co-cultured with CD40 ligand supports the idea that upregulation of CD40 in both MCF-7/120nM DOC and MCF-7/1000nM DOX might be a common cell survival response.

The *TNFRSF9* gene encodes CD137, a member of the tumor necrosis factor receptor family. It provides expansion and survival signal to T cells. Interestingly it was only upregulated in MCF-7/1000nM DOX cells. Palma *et al.* (Palma *et al.*, 2004) demonstrated that CD137/CD137L system ligation opposed the anticancer drug cytotoxic effects, reducing the apoptotic DNA fragmentation and stimulating proliferation of doxorubicin-escaped leukemia cells. On the other hand, ligation of CD137L on hepatocarcinoma cells with CD137 caused tumor cells to produce IL8 (Wang *et al.*, 2008). Interstingly, 1000nM doxorubicin resistant cells, but not docetaxel resistant cells, had elevated *IL8* levels.

TNF ligand family proteins were also differentially expressed in resistant cells (Table 3.8 B). TRAIL (or Apo2L), a transmembrane protein encoded by *TNFSF10* gene, is notable for its 12.66- and 10.19-fold downregulation in MCF-7/120nM DOC and MCF-7/1000nM DOX and unexpected 3.954-fold upregulation in MCF-7/30nM DOC. Ligation of TRAIL to its death receptors causes recruitment of the adaptor molecule FADD, activation of the extrinsic apoptosis pathway, resulting in Caspase-8 and Caspase-3 activation (Figure 3.34). TRAIL selectively induces apoptosis in tumor cells; wehereas nontrasformed cells remain TRAIL-resistant, due to expression of at least one of the TRAIL death receptors on tumor cells. This selective apoptotic activity made administration of recombinant human TRAIL a promising candidate for cancer therapy in combined applications with chemotherapeutic drugs. Recent studies have shown alternative functions of TRAIL in apoptosis-resistant cells. For instance, promotion of cell migration and invasion has been shown via induction of NF-κB activation in apoptosis-resistant cholangiocarcinoma cells with increased TRAIL expression (Ishimura *et al.*, 2006). Other

physiological roles of TRAIL were also elucidated. Secchiero *et al.* (Secchiero *et al.,* 2004) also demonstrated the proangiogenic activity of TRAIL together with its high expression levels in malignant vascular sacomas. Similarly, it has been reported to stimulate a proliferative response in endothelial cells by activating antiapoptotic PI3K/Akt pathway (Secchiero *et al.,* 2003). MCF-7/30nM DOC cells overexpressed antiapoptotic Bcl-2 gene (Table 3.9 A). Conclusively, effect of endogenous TRAIL expression on resistant cells most probably depends on antiapoptotic/apoptotic expression profiles and apoptosis resistance status of cells. MCF-7/120nM DOC and MCF-71000nM DOX cells seemed to be more sensitive to apoptosis as drug resistance in these cells was related to other mechanisms.

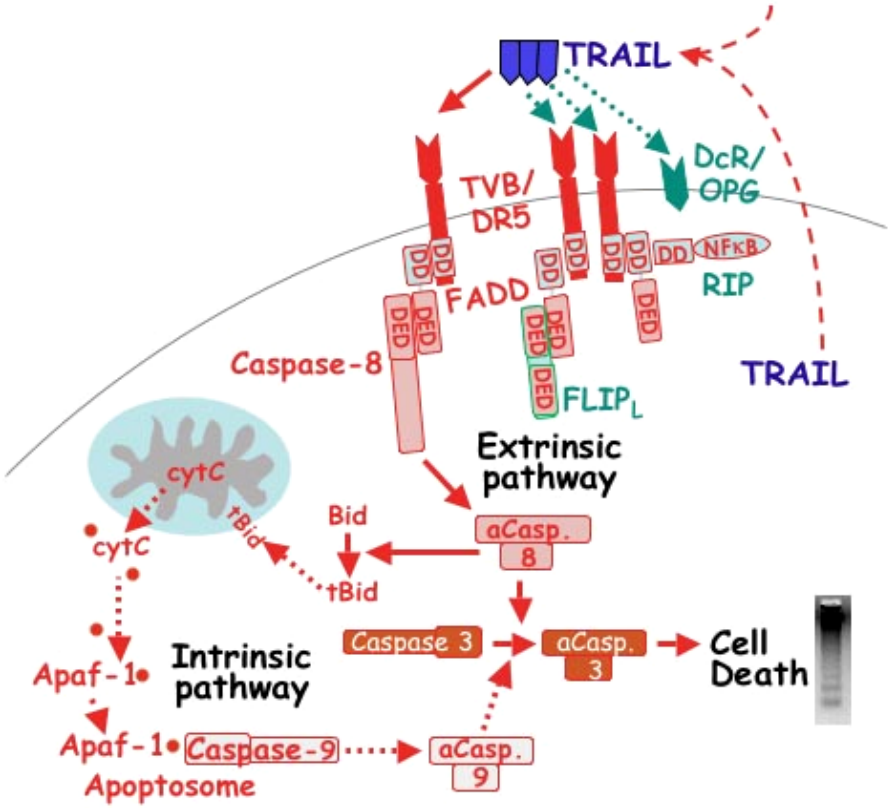

Figure 3.34 TRAIL induced apoptosis (Johnson *et al.*, 2007).

TNFSF13, also known as APRIL (A Poliferation Inducing Ligand), was 3.57-fold upregulated in MCF-7/30nM DOC cells. It is expressed in normal cells (*e.g.* monocytes, macrophages) whereas it is also strongly expressed in several types of tumors that it

stimulates cell proliferation *in vitro* and *in vivo* (Hahne *et al.*, 1998). A previous study also demonstrated that addition of APRIL to B-CLL cultures increased resistance to spontaneous or drug-induced apoptosis (Kern *et al.,* 2004). Concordantly, altered APRIL levels seem to be correlated to decreased apoptotic potential of MCF-7/30nM DOC cells (Table 3.8 B).

The CD70 protein encoded by *TNFSF7* gene is a cytokine that belongs to the TNF ligand family and it is a CD27 ligand. Its increased expression was observed in both MCF-7/120nM DOC and MCF-7/1000nM DOX. In addition to function of CD27-CD70 ligation in immune response, effect of this ligation on signaling and cellular responses has been explored. For example, ligand activated CD27 protects T cells from apoptosis upon T cell receptor stimulation (Borst *et al.*, 2005), induces activation of NF-κB signaling (Akiba *et al.*, 1998) and CD27 with CD40 co-stimulatory signals inhibits p53-independent apoptotic pathway primarily induced by B cell receptor ligation in B cells (Hase *et al.*, 2002). Moreover, Borst *et al.*, (Borst *et al.*, 2005) suggested control of CD27 by CD70 expression as a target for therapy.

Three members of the Akt (v-Akt Murine Thymoma Viral Oncogene)/PKB (protein kinase B) family serine/theronine kinases can regulate numerous cellular functions, including stimulation of cellular growth and inhibition of cellular death. The Akt family of protein kinases are activated downstream of phosphotidylinositol 3-kinase (PI3K) and collectively all Akt kinases phosphorylate various key cytoplasmic and nuclear substrates (Figure 3.35). In Nakatani *et al.* (Nakatani *et al.*, 1999), both the Akt3 enzymatic activity and mRNA were found to be elevated in breast cancer cell lines and tumors that lack the estrogen receptor as well as in prostate cancer cell lines that are androgen-insensitive. Moreover, in another study expression of active Akt-3 in MCF-7 cells resulted in estrogen independent tumor growth, and growth of tumors was inhibited estrogen E2 and enhanced by tamoxifen (Faridi *et al.*, 2003). However it was suggested in the study of Nakatani *et al.* (Nakatani *et al.*, 1999) that estrogen receptor did not directly repressed *AKT3* expression but via a more complex interaction involving estrogen receptor. Elevated levels of *AKT3* (Table 3.9 A) in MCF-7/120nM DOC and MCF-7/1000nM DOX may be related to lower estrogen receptor levels in these cells.

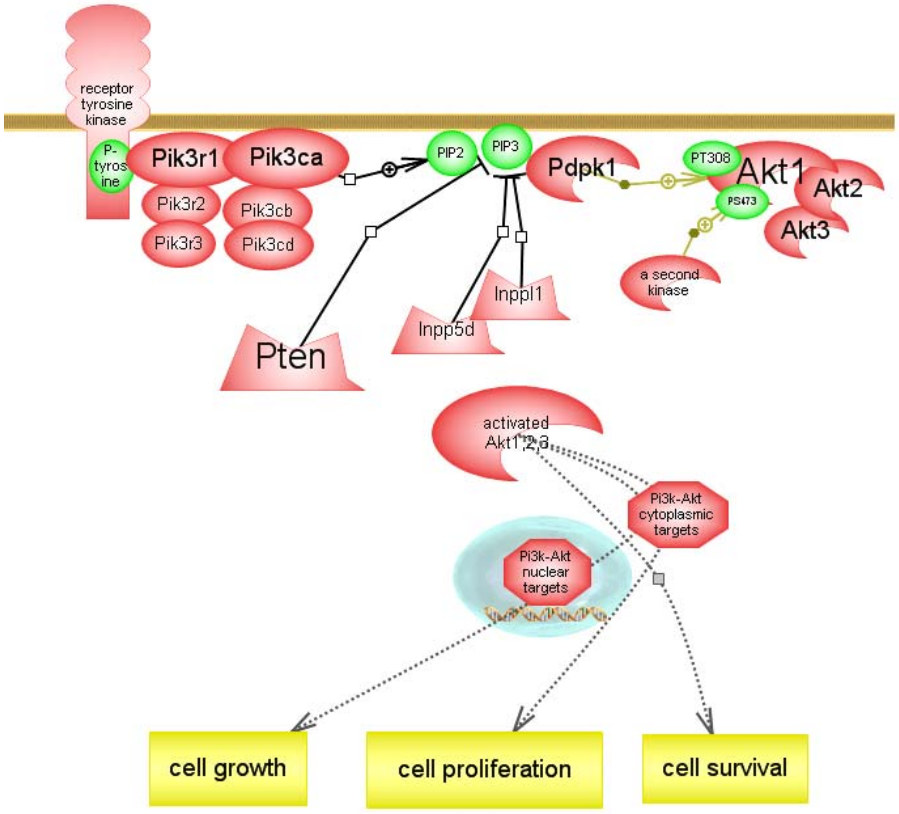

Figure 3.35 PI3K/Akt signaling cascade (rgd.mcw.edu/tools/ontology/ont_annot.cgi?ont_id=PW:0000232&ontology=wo)

BIRC5 gene, encoding the surviving protein, was upregulated in doxorubicin resistant cells (Table 3.9 A). Survivin is a member of the inhibitor of apoptosis protein (IAP) family. It has multiple functions, including cell-cycle regulation at mitosis, inhibition of apoptosis and caspase-independent cytoprotection. Previous studies indicated survivin to be a cellular factor potentially involved in the chemo- and radioresistant phenotypes of human tumours (reviewed in Zaffaroni and Daidone, 2002).

Antiapoptotic and proapoptotic BCL-2 family proteins share sequence homology within conserved Bcl-2 homology (BH) domains (reviewed in Daniel, 2007). They are the key regulatory proteins of cell survival. Antiapoptotic members *e.g.* Bcl-2 regulate mitochondrial outer membrane permeabilization together with cytochrome c release from mitochondria and prevent apoptosis. Bcl-2 was 5.78-fold upregulated in MCF-7/30nM DOC where there was not any significant change in expression level of the gene in other

resistant sublines (Table 3.9 A). Teixeira *et al.* (Teixeira *et al.*, 1995) reported that estrogen receptor positive MCF-7 cells had increased Bcl-2 levels in the presence of estrogen and depletion of estrogen from the medium results in loss of expression of the mRNA. Similarly, Bcl-2 expression showed association with estrogen receptor positive mammary tumors (Tang *et al.*, 2004). So unchanged levels of Bcl-2 in MCF-7/120nM DOC and MCF-7/1000nM DOX cells seems to be related to loss of estrogen receptor in these cells (Table 3.11). On the other hand, estrogen receptor level was not altered in MCF-7/30nM DOC. Bcl-2-associated athanogene (BAG)-family proteins are BAG domain-containing proteins that interact with the heat shock proteins 70 and Bcl-2. Therefore, anti-apoptotic activities of BAG-family proteins may be dependent on their interactions with Hsc70/Hsp70 and/or binding to Bcl-2 (reviewed in Doong *et al.*, 2002). BAG-1 and BAG-3/CAIR-1 have been shown to interact with the anti-apoptotic protein Bcl-2. Overexpression of *BAG1* or *BAG3* genes with *Bcl-2* was shown to strengthen and synergize anti-apoptotic effect of Bcl-2 (Takayama *et al.,* 1995; Lee *et al.*, 1999). Bcl-2 and BAG-1 expressions were associated and correlated to estrogen receptor status in breast cancer cells and patients (Tang *et al.*, 2004; Brimmell *et al.*, 1999). In concordance, increased expression levels of *BAG-1, BAG-3* and *BAG-5* in MCF-7/30nM DOC and decreased expression levels of these genes in MCF-7/120nM DOC and MCF-7/1000nM DOX may be related to estrogen receptor status of these cells.

Caspases are group of proteases that share a group of features distinguishable from other proteases. They all are synthesized as inactive zymogens that are activated through cleavage cascade. Although they are known to be involved in various cellular processes, simply they can functionally be classified into two subfamilies, pro-apoptotic and pro-inflammatory subfamilies. Pro-apoptotic caspases (caspase-2, -3, -6, -7, -8, -9, -10) are known to be mainly involved in mediating cell death signaling transduction, whereas pro-inflammatory caspases (caspase-1, -4, -5, -11, -12) regulate cytokine maturation during inflammation (Li and Yuan, 2008) *i.e.* caspase 1 activates proinflammatory cytokines interleukin(IL)-1beta, IL-18, and IL-33. Keller *et al.* (Keller *et al*., 2008) suggested that stress-induced activation of caspase-1 was linked to cytoprotection and cell survival through inflammatory processes. Concordantly, both *IL18* (Table 3.10) and *CASP1* (Table 3.9 B) genes were overexpressed in MCF-7/120nM DOC and MCF-71000nM DOX. Interestingly, *CASP4* was also upregulated in these cells. Similarly caspase 4 was also identified for its role in secretion of important cytokines and chemokines in human monocytic cells via NF-κB-dependent transcriptional up-regulation (Lakshmanan and

Porter, 2007). Additionally, *CASP4* lies in the downstream genomic region of *CASP1* on chromosome 11q22 which may suggest, in addition to functional similarity, a common transcriptional activation.

DAPK-1 belongs to a family of Ser/Thr kinases, death-associated protein kinases, and has cell death–associated tumor suppressor functions (reviewed in Bialik and Kimchi, 2006). It was surprisingly upregulated in MCF-7/120nM DOC and MCF-7/1000nM DOX cells. It was previously demonstrated that TGF-β induced the expression of the DAPK through promoter activation by the action of SMAD2, SMAD3 and SMAD4 (Jang *et al.*, 2002). Accordingly, *SMAD3* was also upregulated in these cells (Table 3.11). Although overexpression of the gene is correlated to increased cell death signals, death associated kinase activity is regulated various phosphorylation events under control of many signaling cascades (Bialik and Kimchi, 2006).

PDCD8, apoptosis-inducing factor (AIF), is localized in mitochondrial intermembrane space and released during initiation of apoptosis. AIF-dependent cell death, independent from cytochrome-c/Apaf-1/caspase-9 system, displays structural features of apoptosis (Joza *et al*., 2001). *PDCD4* encodes a tumor suppressor protein, interacting with eukaryotic initiation factor 4A of the translation initiation complex inhibits protein synthesis. Its expression is lost in in progressed carcinomas of lung, breast, colon, and prostate. Palamarchuk *et al.* (Palamarchuk *et al.*, 2005) showed that PDCD4 was phosphorylated by Akt *in vitro* and *in vivo*. The phosphorylation of PDCD4 by Akt inhibited the tumor suppressor function of the protein. It is one of the downstream effectors of the Akt/PI3K which is related to prosurvival and antiapoptotic signaling. *PDCD2* encodes a protein that is expressed in many human tissues, including lymphocytes. It was found to be target of transcriptional repressor protein; BCL6 suggesting that the interactions among BCL6, PDCD2, and other regulatory factors were likely to be very important in the development of human B and T cell lymphomas (Baron *et al.*, 2007). Furthermore, it was previously demonstrated that PDCD2 was expressed in decreased levels in a multidrug-resistant human colon carcinoma cell line (Fan *et al.*, 2004). *PDCD10*, is also known as murine TF1 cell apoptosis-related gene-15 (TFAR-15), was identified initially through screening for genes differentially expressed during the induction of apoptosis in the TF-1 premyeloid cell line (Wang *et al*., 1999). Bergametti *et al.* (Bergametti *et al.*, 2005) identified the *PDCD10* gene as the *CCM3* gene, mutations of which are responsible for cerebral cavernous malformations, a disorder characterized abnormally enlarged capillary

cavities without intervening brain parenchyma. It was drastically downregulated in MCF-7/120nM DOC and MCF-7/1000nM DOX. Although it was identified as a protein induced during apoptosis neither a direct correlation with cell survival or proliferation nor its apoptotic/proapoptotic effectors has been established to date.

Table 3.8 A) List of differentially expressed genes encoding tumor necrosis factor receptor superfamily members in drug resistant MCF-7 sublines and fold changes of expression.

Gene Name	Gene Symbol	Description	Gene Ontology	MCF-7/ 30DOC	MCF-7/ 120DOC	MCF-7/ 1000DOX
206467_x_at	TNFRSF6B ; RTEL1	tumor necrosis factor receptor superfamily, member 6b, decoy ; regulator of telomere elongation helicase 1	BP: cell growth and maintanence, cell death; MF: signal transducer, binding, catalytic activity, apoptosis regulator	NS	27.61	29.64
227345_at	TNFRSF10D	tumor necrosis factor receptor superfamily, member 10d, decoy with truncated death domain	BP: cell growth and maintanence, cell death; MF: signal transducer, binding, apoptosis regulator	NS	6.65	9.49
205153_s_at, 35150_at	CD40	CD40 antigen (TNF receptor superfamily member 5)	BP: cell growth and maintanence; MF: signal transducer, binding, catalytic activity, apoptosis regulator, defense and immunity:	NS	16.80	15.85
207536_s_at	TNFRSF9	tumor necrosis factor receptor superfamily, member 9	BP: cell growth and maintenence, cell death; MF: apoptosis regulator, binding, apoptosis regulator	NS	NS	4.55

Table 3.8 (Continued)

B) List of differentially expressed genes encoding tumor necrosis factor ligand superfamily members in drug resistant MCF-7 sublines and fold changes of expression.

202688_at, 202687_s_at	TNFSF10	tumor necrosis factor (ligand) superfamily, member 10 ; tumor necrosis factor (ligand) superfamily, member 10	BP: cell growth and maintanence, cell death; MF: signal transducer, binding, catalytic activity, apoptosis regulator	3.95	-12.66	-10.19
210314_x_at, 209499_x_at	TNFSF13, TNFSF12	tumor necrosis factor (ligand) superfamily, member 13 ; tumor necrosis factor (ligand) superfamily, member 12-member 13	BP: cell growth and maintanence, cell death; MF: apoptosis regulator, signal transducer	3.57	NS	NS
206508_at	TNFSF7	tumor necrosis factor (ligand) superfamily, member 7	BP: cell growth and maintanence, cell death; MF: signal transducer, binding, apoptosis regulator, defense and immunity:	NS	4.28	3.86
202644_s_at, 202643_s_at	TNFAIP3	tumor necrosis factor, alpha-induced protein 3	MF: apoptosis regulator, catalytic activity	5.97	NS	5.30

Table 3.9 A) List of differentially expressed genes encoding proteins related to cell survival in drug resistant MCF-7 sublines and fold changes of expression.

212607_at	AKT3	v-akt murine thymoma viral oncogene homolog 3 (protein kinase B, gamma)	BP: cell growth and maintanence, cell death; MF: apoptosis regulator, catalytic activity, binding, defense immunity poteins	NS	35.86	28.32
202094_at	BIRC5	baculoviral IAP repeat-containing 5 (survivin)	BP: cell growth and maintanence, cell death; MF: apoptosis regulator, binding, signal transducer	NS	NS	2.76
232210_at	BCL2	B-cell CLL/lymphoma 2	BP: cell growth and maintanence, cell death; MF: apoptosis regulator, binding	5.78	NS	NS
210347_s_at, 222891_s_at, 219497_s_at	BCL11A	B-cell CLL/lymphoma 11A (zinc finger protein)	BP: cell growth and maintenance; MF: binding, transcription regulator activity	NS	NS	12.98
222895_s_at	BCL11B	B-cell CLL/lymphoma 11B (zinc finger protein)	BP: cell growth and maintenance; MF: binding, transcription regulator activity	2.75	NS	NS
1558143_a_at	BCL2L11	BCL2-like 11 (apoptosis facilitator)	BP: cell death, MF: apoptosis regulator, binding	2.82	-2.55	-2.25

Table 3.9 (Continued)

229720_at	BAG1	BCL2-associated athanogene	BP: cell growth and maintanence, cell death; MF apoptosis regulator, catalytic activity, signal transducer	2.40	-2.63	-2.35
209406_at, 230879_at	BAG2	BCL2-associated athanogene 2	BP: cell growth and maintanence, cell death; MF: apoptosis regulator	NS	7.66	5.38
217911_s_at	BAG3	BCL2-associated athanogene 3	BP: cell death; MF: apoptosis regulator	4.09	-2.36	NS
219624_at	BAG4	BCL2-associated athanogene 4	BP: cell death; MF: apoptosis regulator, binding, signal transducer	2.57	NS	5.78
202984_s_at, 230427_s_at, 230427_s_at, 202985_s_at	BAG5	BCL2-associated athanogene 5	BP: cell death; MF: apoptosis regulator	2.56	-3.04	-3.03

Table 3.9 (Continued)

B) List of differentially expressed genes encoding proteins related to cell death in drug resistant MCF-7 sublines and fold changes of expression.

209970_x_at	CASP1	caspase 1, apoptosis-related cysteine peptidase (interleukin 1, beta, convertase)	BP: cell growth and maintanence, cell death; MF: apoptosis regulator, catalytic activity, binding	NS	2.44	3.86
209310_s_at	CASP4	caspase 4, apoptosis-related cysteine peptidase	BP: cell growth and maintanence, cell death; MF: apoptosis regulator, catalytic activity, binding	10.43	14.42	17.78
203139_at	DAPK1	death-associated protein kinase 1	BP: cell growth and maintanence, cell death; MF: apoptosis regulator, catalytic activity, binding	NS	21.46	24.13
213581_at	PDCD2	programmed cell death 2	BP: cell death; MF: apoptosis regulator	NS	-3.40	NS
212593_s_at, 202730_s_at	PDCD4	programmed cell death 4 (neoplastic transformation inhibitor)	BP cell death; MF: apoptosis regulator	3.23	-2.55	-2.78
205512_s_at	PDCD8	programmed cell death 8 (apoptosis-inducing factor)	BP: cell growth and maintanence, cell death; MF: binding, catalytic activity, apoptosis regulator	NS	-2.13	-2.01
210907_s_at	PDCD10	programmed cell death 10	BP: cell growth and maintanence, cell death; MF: binding, catalytic activity, apoptosis regulator	NS	-133.33	-113.90
204859_s_at	APAF1	apoptotic peptidase activating factor	BP cell growth and maintenance, cell death; MF: binding, catalytic activity, apoptosis regulator	NS	NS	4.41

3.6.5 Alterations in Genes Encoding Growth Factors and Cytokines

Alterations in expression levels of genes encoding growth factors and cytokines were summarized in Table 3.10. *EGFR* was 18-fold upregulated in both MCF-7/120nM DOC and MCF-7/1000nM DOX. Its elevated levels in resistant cells seem to be an important mechanism of resistance since it is one of ErbB family of receptor tyrosine kinases (also known as ErbB-1/HER1) and a cell surface and nuclear receptor that plays an important role in intracellular signaling pathways including cell proliferation/survival, migration, tumor cell invasion and inhibition of apoptosis (Figure 3.36). Binding of EGF and TGF-α to receptor causes receptor activation as well as transactivation of other Erb family receptors. Several pharmacological attempts have been emerging in order to inhibit receptor mediated promotion of cell survival and transformation in tumor cells. Elevated EGFR expression and activity frequently correlate with tumor resistance to radiotherapy in patients (Chen *et al.*, 2007). Reports on its role in chemoresistance have also been emerging. For example, treatment of head and neck squamous cell carcinoma cells with *EGFR* siRNA in combination with cisplatin, 5-FU and docetaxel showed enhanced chemosensitivity with a significant increase in apoptosis (Nozawa *et al.*, 2006). Selective inhibition of *EGFR* in Adriamycin resistant MCF-7 cells was found to overcome taxane resistance in these cells and inhibit cell proliferation (Ciardiello *et al.*, 2002). Concept of chemosensitization of drug resistant cells by selective inhibition of *EGFR* and downstream signaling pathways in combined drug treatments has been demonstrated although mechanism of action is still under investigation (reviewed by Schmidt *et al*., 2002).

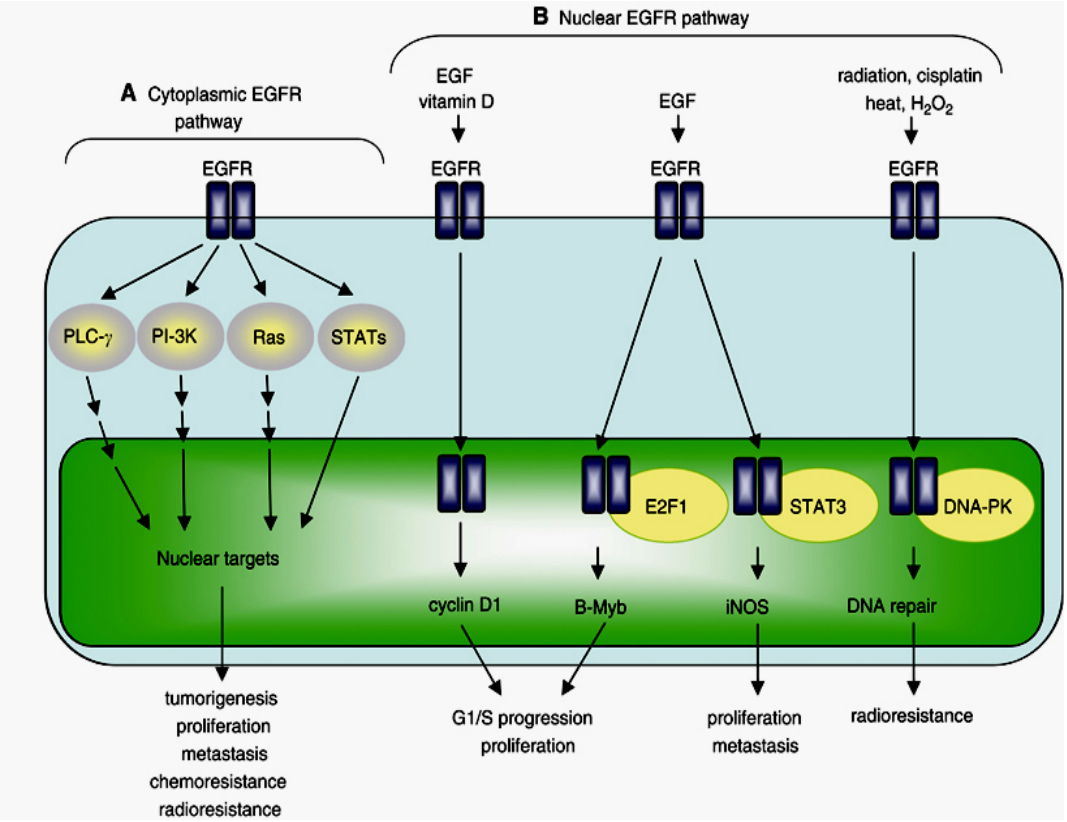

Figure 3.36 EGFR pathways (Lo *et al.*, 2006).

CTGF belongs to CCN family molecules. They are secreted, extracellular matrix-associated proteins and involved in internal and external cellular signaling to regulate cell adhesion, migration, mitogenesis, differentiation, and survival. Gene expression of CTGF is induced by TGFβ signaling resulting in proliferation and stimulation of production of fibronectin and collagen in fibroblasts (Duncan *et al.*, 1999). It promotes continuous inactivation of p38 MAPK by downregulating the expression of *SMAD7* and upregulating the expression of *MKP-1*, thus preventing the phosphorylation of Bcl-2, preserving its anti-apoptotic function and promoting cell survival (Wahab *et al.*, 2007). Consistent with its functions, it is overexpressed in various malignancies including breast, melanoma, pancreas and ALL (Xie *et al.*, 2001; Kubo *et al.,* 1998; Wenger et al., 1999; Sala-Torra *et al*., 2007). In these studies, it is elevated levels were correlated with advanced stages of tumor progression and lesser survival. It was 126.5-fold upregulated only in MCF-7/120nM DOC cells. Drastic increase of the gene in docetaxel resistant cells adresses the question whether elevated levels of the gene or downstream effectors prevent cells from docetaxel induced cytotoxicty.

ECGF1, also known as thymidine phosphorylase (TP), is an angiogenic factor which also stimulates *in vitro* growth of a variety of endothelial cells. It was previously demonstrated that TP confers resistance to apoptosis induced by hypoxia (Kitazono *et al.*, 1998) which is deprived oxygen condition of tumor cells. Although hypoxic conditions promote apoptosis, it is also correlated to poor outcome of patients for its effect on chemoresistance of cells. Drug uptake under hypoxic conditions decreases due to acidity of hypoxic medium, as well as cytotoxicity of drugs due to decreased oxygen levels and low ROS generation and adaptation of tumor cells to hypoxic conditions with altered gene expression levels. For instance, TP was shown to produce 2-deoxy-d-ribose from thymidine which can suppress expression of BNIP3, a proapoptotic factor mediating hypoxia induced apoptosis (Ikeda *et al.*, 2008).

PDGFD is a ligand of PDGF receptor signaling pathway which supports a variety of cell processes including proliferation, survival, movement, ECM deposition and tissue remodeling. PDGFR activation promotes downstream effectors phosphoinositol-3 kinase (PI3K), an inhibitor of apoptosis (Grünert *et al.*, 2003). Its overexpression was also correlated to EMT with enhanced invasive behaviours in prostate cancer cells (Kong *et al.*, 2008).

Retinoic acid (RA) receptors (RARα, -β and -γ) and retinoid X receptors (RXRα, --β and -γ) are nuclear receptors and transcription factors that function as RAR-RXR heterodimers or RXR homodimers. In response to retinoid binding, these dimers control gene expression by binding to specific retinoic acid response elements. Intracellular RA levels, important for regulation of cell proliferation, differentiation and apoptosis, are regulated by binding of retinol to cellular retinol binding proteins (CRBPs) and to retinoic acid binding proteins (CRABPs). Szondy et al. (Szondy *et al*., 1997) presented an RARγ-dependent retinoid effect *i.e.* all-trans, 9-cis RA and RAR-selective RA analogs induce apoptosis. RARγ (RARG) was -3.57-fold downregulated only in MCF-7/120nMDOC cells. Interestingly, there is a report demonstrating the dose dependent inhibitory effects of microtubule interfering agents including Taxol on gene expression levels of RARγ in primary rat hepatocytes although the mechanism of action was not elucidated (Dvorák *et al*., 2007). An implication of these retinoic acid related alterations in expression levels on cross-ressistance to ATRA is further discussed in Section 3.7.

IL6 was 88-fold upregulated in doxorubicin resistant cells. It is an inflammatory cytokine that provokes a broad range of cellular and physiological responses. Binding of IL6 to its receptor initiates cellular events including activation of JAK kinases and activation of Ras-mediated signaling. IL6 has been shown to block apoptosis induced by p53 (Yonish-Rouach *et al.*, 1991) and certain cancer chemotherapeutic compounds. For example, IL6 secretion was demonstrated to protect the hormone-resistant prostate tumor cells against the cytotoxic effects of cisplatin and etoposide and its neutralization sensitizes cells to cytotoxicity (Borsellino *et al.,* 1995). Elevated levels of IL6 and IL8 were also reported in drug resistant ovarian cancer cells and it was proposed tha elevated levels of IL6 in the tumor microenvironment leaded to local chemotherapy resistance (Duan *et al.*, 1999). *IL8* (CXCL8) was also 36-fold upregulated in doxorubicin resistant cells. It is a pro-inflammatory CXC-chemokine whose expression is primarily regulated by the AP-1 and NF-κB transcription factors (Brat *et al.*, 2005). Wilson *et al*., (Wilson *et al*., 2008) reported that reinforcement of NF-κB signaling caused survival of metastatic prostate cancer cells via increased expression of anti-apoptotic proteins and IL8. They also stated that chemotherapy-induced IL8 signalling conferred resistance to oxaliplatin. *IL18* was upregulated in MCF-7/120nM DOC and MCF-7/1000nM DOX (38.37- and 62.85-fold, respectively). It has a PI3K/Akt pathway dependent anti-apoptotic function and augments expression of anti-apoptotic proteins, Bcl-2, XIAP and glucose regulated protein78/BiP (Hosotani *et al.*, 2008). SOCS3 is an SH2-containing protein that binds to the activation loop of Janus kinases, inhibiting kinase activity and thereby suppressing cytokine signaling. It is a member of the suppressor of cytokine signaling (SOCS), family. The expression of the SOCS3 gene is induced by various cytokines, including IL6, IL10, and interferon (IFN)-gamma. SOCS expression is 10-fold increased in MCF-7/1000nM DOX cells where there is 90-fold upregulation of IL6 only in these cells.

IFI16, the interferon-inducible p200 family protein, inhibits cell proliferation, modulates p53-mediated apoptosis, and stimulates senescence in fibroblasts and epithelial cells (reviewed in Choubey *et al.*, 2008). However a recent report demonstrated its novel role in the signal transduction pathways regulating the inflammation processes by triggering expression of proinflammatory genes through activating the NF-κB complex (Caposio *et al.*, 2007). Expression of IFI16 was also shown in highly proliferative normal cells. Consistently, negative regulatory role of IFI16 on p53 tumor suppressor and its target genes was also proposed by Kwak *et al.* (Kwak *et al.*, 2003) with the result that IFI16 inhibition increased the half-life of p53. In the light of these previous studies, substantial

overexpression of the gene in resistant cells implies that IFI16 may act as either transcription factor or cofactor and promote expression of genes related to cell survival or cell cycle progress.

Table 3.10 List of differentially expressed genes encoding growth factors and cytokines in drug resistant MCF-7 sublines and fold changes of expression.

Gene Name	Gene Symbol	Description	Gene Ontology	MCF-7/ 30DOC	MCF-7/ 120DOC	MCF-7/ 1000DOX
201983_s_at, 224999_at, 201984_s_at	EGFR	epidermal growth factor receptor (erythroblastic leukemia viral (v-erb-b) oncogene homolog, avian)	BP: cell growth and maintanence; MF: signal transducer, binding, catalytic activity	NS	18.57	18.27
209101_at	CTGF	connective tissue growth factor	BP: cell growth and maintanence; MF: binding, signal transducer	NS	126.50	NS
204858_s_at	ECGF1	endothelial cell growth factor 1 (platelet-derived)	BP: cell growth and maintanence; MF: signal transducer, binding, catalytic activity	3.30	5.60	3.92
219304_s_at	PDGFD	platelet derived growth factor D	BP: cell growth and maintenance; MF: binding, catalytic activity	NS	NS	9.41
204188_s_at	RARG	retinoic acid receptor, gamma	BP: cell growth and maintanence; MF: transcription regulation, signal transducer, binding	NS	-3.62	NS
202575_at, 202575_at	CRABP2	cellular retinoic acid binding protein 2	BP: cell growth and maintanence; MF: transcription regulation, binding	NS	-4.90	NS
209651_at	TGFB1I1	transforming growth factor beta 1 induced transcript 1	BP: cell growth and maintenance; MF: binding	NS	NS	41.34
201506_at	TGFBI	transforming growth factor, beta-induced, 68kDa	BP: cell growth and maintanence	NS	95.38	62.40
205016_at	TGFA	transforming growth factor, alpha	BP: cell growth and maintanence	-5.78	NS	NS
205207_at	IL6	interleukin 6 (interferon, beta 2)	BP: cell growth and maintenence	NS	NS	87.96
211506_s_at	IL8	interleukin 8	BP: cell growth and maintenence	4.34	NS	35.96

Table 3.10 (Continued)

206295_at	IL18	interleukin 18 (interferon-gamma-inducing factor)	BP: cell growth and maintanence	NS	38.37	62.85
227697_at	SOCS3	suppressor of cytokine signaling 3	BP: cell growth and maintenence	NS	NS	10.46
208966_x_at, 206332_s_at	IFI16	interferon, gamma-inducible protein 16	BP: cell growth and maintanence	NS	61.83	32.15

3.6.6 Alterations in Expression Levels of Genes Encoding Epithelial-mesenchymal Transition (EMT) Related Proteins

Epithelial-mesenchymal transition (EMT) is an essential developmental process by which cells of epithelial origin lose epithelial characteristics and polarity, and acquire a mesenchymal phenotype with increased migratory behavior. EMT might also occur during tumor progression in carcinomas and changes related to EMT are often indicators of poor prognosis in clinical specimens (Thompson *et al.*, 2005). Expression levels of genes related to this process were evaluated in drug resistant cells in order to assess their involvement in drug resistance. The list of genes is given in Table 3.11 and cross-talk of these genes is schematically summarized in Figure 3.37.

Snail family proteins (Snail, Slug and Twist) are transcription factors and their altered expression levels are the key regulatory elements of EMT along with the control of expression of many genes, including cell-cell-adhesion, cell survival and apoptosis. Concordantly, their ectopic expression was associated with resistance to genotoxic effects induced by Adriamycin (Kajita *et al.*, 2004). Slug (also Snail2; encoded by *SNAI2*) promoter contains a Sp1 binding site so it is also one of the downstream mediators of TGFβ1 signalling (Choi *et al*., 2007).The estrogen receptor-α (ER, ERα, and ESR1) acts as a hormone dependent nuclear transcription factor. Upon entering the cell by passive diffusion, estrogen binds its receptor which subsequently dimerizes and translocates to the nucleus. Ligand activated ER binds specific sequences in the genome, called estrogen responsive elements (EREs), and recruits a number of cofactors that facilitate gene transcription. Interestingly it was reported that ligand-activated ERα suppressed transcription factor Slug expression by transcriptional repression and that the ER ligand activation pathway interacts with the E-cadherin/Slug EMT pathways directly by repression of Slug (Ye *et al.*, 2008).

Transforming growth fctor, beta receptor2 (TGFBR2) together with TGFBR1 form heterodimeric receptor complexes and promote TGFβ1 signalling through phosphorylated activation of SMAD2 and 3. Acivated SMAD2/3 complex corporate with cytoplasmic SMAD4 and translocate into the nucleus where they induce expression of target genes among which are the EMT inducing factors (reviewed in Zavadil and Böttinger, 2005). Ectopic expression of SMAD2 or 3 was shown to enhance TGFβ1 induced EMT.

Interestingly, amplified EGF signaling via receptor amplification and cros-talk between TGFβ1 stimulated pathways exhibit characteristics of EMT (Wilkins-Port *et al.*, 2007). Concordantly, as mentioned above elevated levels of *EGFR* (Table 3.10) could also be considered in this respect. Inconsistent to increased levels of TGFBR3 observed in resistant cells (Table 3.11), downregulation of this receptor in a variety of cancers including breast cancer (Dong *et al.*, 2007) and its regulatory role in invasion/metastasis (Finger *et al*., 2008) have been reported. Hempel *et al*. (Hempel *et al*., 2008) demonstrated that TGFβ1 downregulated TGFBR3 expression, while TGFBR1 and TGFBR2 remain unaffected, at physiologically relevant concentrations. However elevated TGFBR2 in drug resistant cells may cause decerased free TGFβ1 levels which in turn disregulate repressive effect of TGFβ1 on TGFBR3 levels.

Downregulation of E-cadherin and occludins with upregulation of mesenchymal markers like vimentin are initial determinants of EMT which lead to increase in motility, invasiveness, and metastasic capabilities (Sarrió *et al*., 2008). Vimentin expression, which causes cytoskeletal reorganization, may promote cancer migration and/or invasion for *in vitro* and *in vivo* models, and its expression is associated with a poor prognosis and/or a tendency to develop metastasis in breast cancer (Sarrió *et al.*, 2008). In addition to E-cadherin downregulation, upregulation of mesenchymal cadherin N-cadherin is also characterized, a phenomenon known as “cadherin switch” (reviewed in Christofori *et al.*, 2003). Cadherins family of cell-surface glycoproteins promote calcium-dependent cell-cell adhesion and serve as the transmembrane components of cell–cell adherens junctions. E-cadherin is a calcium dependent adhesion molecule which has also growth suppressive functions and it is repressed in a number of human cancer types. Although molecular mechanism of cadherin switch is currently under investigation, E-cadherin is transcriptionaly repressed of by Snail family proteins. Among them elevated levels of Slug was correlated with transcriptionally repressed levels of E-cadherin in breast and oesophageal cell lines (Hajra *et al.*, 2002; Jethwa *et al.*, 2008). Integral membrane proteins claudins and occludin, localized at tight junctions, are responsible for establishing and maintaining epithelial cell polarity. Occludin (*OCLN*) is a direct downstream target gene of Slug in epithelial cells that it is repressed by Slug at its promoter region (Kajita *et al.*, 2004). Although the concurrent loss of claudins like both E-cadherin and occluding has been reported during the EMT, differential expression levels of claudin family proteins have also been reported and associated to EMT in various cancer types. For example, Dhawan *et al.* (Dhawan *et al.*, 2005) demonstrated that induced claudin-1 expression in

primary colon cancer cell lines promoted changes in cellular phenotype, with structural and functional changes in markers of EMT with significant effects on growth of xenografted tumors and metastasis in athymic mice. In addition, overexpression of *CLDN1* gene was also found to have a contribution to melanoma cell invasion as it increased MMP2 secretion and activation in a PKC regulated manner (Leotlela *et al.*, 2007). Knockdown of claudin-7 in squamous cell carcinoma cell lines led to decreased E-cadherin expression, increased cell growth, and enhanced invasion (Lioni *et al.*, 2007). Dysregulated expression of both claudin-7 and -4 were associated with with induced Snail expression and increased ionic permeability of tight junctions (Carrozzino *et al.*, 2005). In another report decreased claudin-4 expression was detected in invasive fronts and metastatic lesions in colorectal carcinomas, in which knockdown of the gene in cell lines shown to distrupt claudin-4 mediated tight junctions and increase cell motility (Ueda *et al.*, 2007).Additionally, high expression of *CLDN3, 4* and *7* were demonstrated in epithelial tissues and lower expression in other tissues such as brain (Hewitt *et al.*, 2006). Reports on claudin-3 expression levels in cancer progression, invasion/metastasis and EMT are rather controversial (reviewed in Kominsky SL, 2007). However claudin-3 was identified as one of the downregulated markers of EMT in a report of expression profiling of epithelial plasticity in tumor progression (Jechlinger *et al*., 2003). Claudin-11 was reported to be expressed in developing mesenchymal cells and its involvement in the cellular interactions with ECM (Bronstein *et al.*, 2000). Abberrant expression of claudin family proteins seem to be important in terms of invasive potential and EMT of epithelial cells but regulation and downstream events are most probably tissue specific as well as dependent on a complex molecular signaling.

In contrast to tumor suppressor effects of E-cadherin, N-cadherin associates with the fibroblast growth factor receptor1 (FGFR1) at the cell surface and attenuates ligand-induced receptor downregulation, leading to increased FGFR1 stability, persistent expression of FGFR1 at the cell surface (Suyama *et al*., 2002). FGFR1 is a transmembrane receptor tyrosine kinase. Like other FGFRs it has been implicated for mediating mammary gland development and transformation. Its induced activation was correlated to cellular proliferation, survival and migration of mammary epithelial cells (Xian *et al.*, 2005). Furthermore, targetting FGFRs in combined applications with chemotherapeutics has improved success of chemotherapy (Gowardhan *et al.*, 2005).

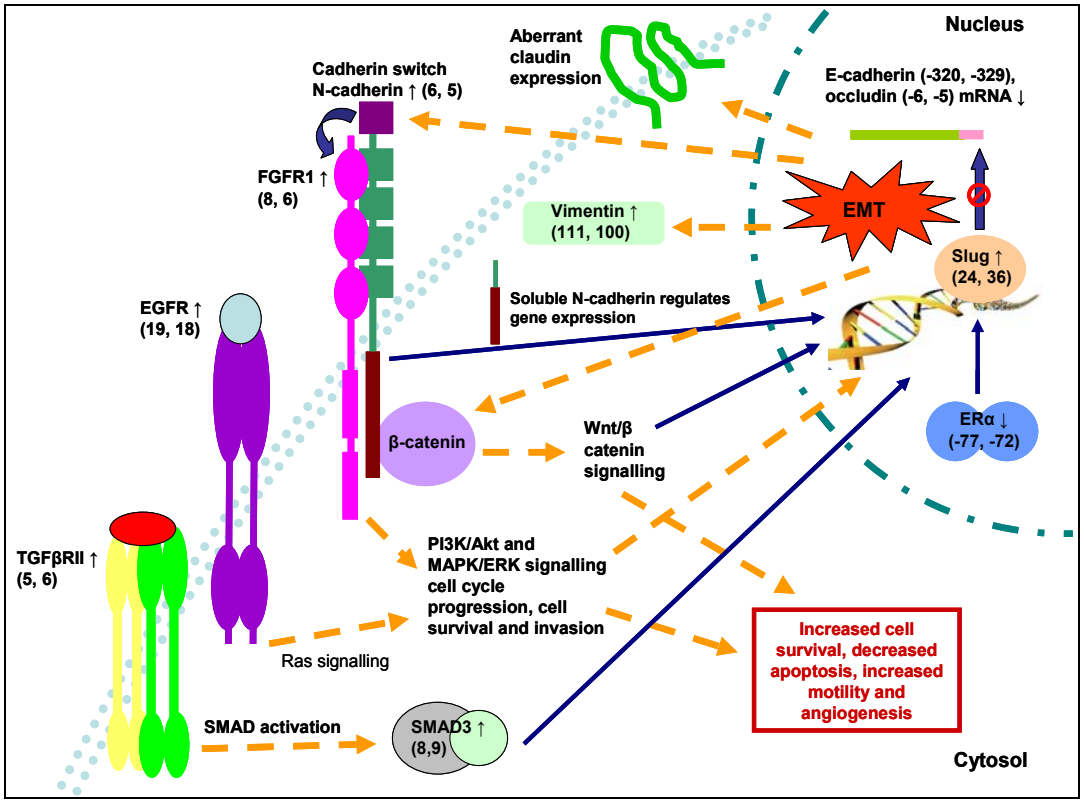

Figure 3.37 EMT related genes altered in drug resistant cells; numbers in parenthesis representing fold change values for MCF-7/120nM DOC and MCF-7/1000nM DOX, respectively. Dashed yellow arrows indicate a signaling cascade leading to a change in the target molecule where dark blue arrows indicate direct molecular interaction with the target.molecule.

Table 3.11 List of differentially expressed genes related to EMT in drug resistant MCF-7 sublines and fold changes of expression.

Gene Name	Gene Symbol	Description	Gene Ontology	MCF-7/ 30DOC	MCF-7/ 120DOC	MCF-7/ 1000DOX
213139_at	SNAI2	snail homolog 2 (Drosophila)	MF: transcription regulation, binding	NS	23.45	36.56
205397_x_at, 205398_s_at	SMAD3	SMAD, mothers against DPP homolog 3 (Drosophila)	MF: transcription regulation, binding	NS	7.81	8.65
208944_at	TGFBR2	transforming growth factor, beta receptor II (70/80kDa)	BP: cell growth and maintanence; MF: signl transducer, binding	NS	5.17	6.30
226625_at	TGFBR3	Transforming growth factor, beta receptor III (betaglycan, 300kDa)	BP: cell growth and maintanence; MF: signl transducer, binding	NS	3.99	8.69
222164_at, 210973_s_at	FGFR1	Fibroblast growth factor receptor 1 (fms-related tyrosine kinase 2, Pfeiffer syndrome)	BP: cell growth and maintanence; MF: signl transducer, binding	NS	7.70	6.04
205225_at	ER, ESR1	estrogen receptor 1	BP: cell growth and maintanence; MF: signl transducer, binding	NS	-76.92	-71.94
201131_s_at	CDH1	cadherin 1, type 1, E-cadherin (epithelial)	MF: cell adhesion molecule, binding, signal transducer	NS	-319.49	-328.95
203440_at 203441_s_at	CDH2	cadherin 2, type 1, N-cadherin (neuronal)	MF: cell adhesion molecule, binding, signal transducer	NS	6.09	5.15

Table 3.11 (Continued)

201426_s_at	VIM	vimentin	MF: structural molecule activity, binding	NS	110.90	99.99
209925_at	OCLN	occludin	MF: structural molecule activity, binding	2.206	-5.55	-5.08
201428_at	CLDN4	claudin 4	MF: cell adhesion molecule, structural molecule activity, binding, signal transducer	NS	-21.98	-29.33
202790_at	CLDN7	claudin 7	MF: cell adhesion molecule, structural molecule activity, binding, signal transducer	NS	-37.04	-34.01
228335_at	CLDN11	claudin 11 (oligodendrocyte transmembrane protein)	MF: cell adhesion molecule, structural molecule activity, binding, signal transducer	NS	42.79	39.45

3.6.7 Alterations in Genes Encoding Extracellular Matrix (ECM) Proteins

MCF-7 sublines overexpressed a variety of genes encoding ECM proteins (Table 3.12). These include integrins, collagens, laminins, fibronectins, claudin, glypican, keratin, syndecan, and microfibrils (fibrillins and fibulins). Integrins are membrane glycoproteins that mediate cell adhesion to ECM upon forming α/β heterodimers. Furthermore, integrin dependent cell attachment elicits integrin-mediated intracellular cell signaling which is among the survival pathways of normal and tumor cells. Collectively, α and β integrin subunits form distinct heterodimeric membrane receptors each having different ligand specificity. Laminins, collagens and fibronectins are among attachment proteins that mediate cell survival via integrin interactions (Ahmed *et al.*, 2005; Morin, 2003; Sethi *et al*. 1999). Among genes encoding the integrins, gene encoding the α6 integrin (*ITGA6*) was highly overexpressed in both 120nM docetaxel and 1000nM doxorubicin resistant sublines (24.66- and 27.92-fold, respectively).To a lesser extent genes encoding the α5 and β1 (in MCF-7/1000nM DOX) integrins (*ITGA5* and *ITGB1*, respectively) were also upregulated. Several reports have demonstrated differential expression of integrin subunits in drug resistant variants of tumor cell lines exhibiting altered binding efficiencies to ECM ligands such as fibronectin, laminin and collagen IV (Nista *et al.*, 1997; Narita *et al*., 1998; Liang *et al.*, 2001). In addition, Aoudjit *et al.*, (Aoudjit *et al.*, 2001) identified the inhibitory role of β1 integrin signaling in paclitaxel and vincristine induced apoptosis of breast carcinoma cells which was related to intgrin-mediated inhibition of cytochrome c release from mitochondria dependent on activation of the PI3-kinase/Akt pathway.

Among collagens *COL4A2, COL4A1, COL6A1* and *COL6A2* were overexpressed in drug resistant sublines, *COL4A2* having 55- and 115-fold overexpression in 120nM docetaxel and 1000nM doxorubicin resistant cells, respectively. Collagen IV and laminin are the main components of the basement membranes and important in ECM remodeling. They bind to integrin receptors and are involved in integrin-mediated adhesion, signaling and contribute to the invasive behavior of tumor cells as well as fibronectin. Interestingly, *COL12A1* was 21.33-fold upregulated in MCF-7/30nM DOC while expression was not changed in MCF-7/120nM DOC. It may be one of the early resistance development genes considering its lower fold chage value (4.57-fold) in MCF-7/1000nM DOX. Laminin

molecules are heterotrimers assembled from alpha-, beta-, and gamma-chains each having different forms. *LAMA1* gene encoding the α1 chain of laminin was drastically overexpressed in MCF-7/120nM DOC and MCF-7/1000nM DOX (84- and 87-fold, respectively). The laminin α1 is known to interact with ECM molecules and integrin receptors with its implications in cellular processes and assembly of the basement membrane. Other genes encoding laminin chains were also substantially upregulated in resistant cells, demonstrating a collective increase in mRNA levels of distinct laminin molecules. Fibronectin is composed of three homologous repeating modules, type I, II and III. Type I modules are involved in fibrin and collagen binding whereas type III modules are involved in integrin and heparin binding. *FN1* gene encoding the type I domain of fibronectin was substantially upregulated in MCF-7/120nM DOC and MCF-7/1000nM DOX. Fibronectin was shown to upregulate MMP9 expression, activity, and invasiveness in a concentration dependent manner in different cell types (Shibata *et al.*, 1997; Esparza *et al.*, 1999). It was also found to enhance activation of Ras and downstream Erk and Akt pathways (Ahmed et al., 2005).

Increase in expression levels of *GPC6*, encoding the glypican 6, was common in all three resistant sublines (Table 3.12). Although there is evidence that some glypicans have critical role in the regulation of cell proliferation and survival based on their capacity to modulate the activity of various growth and survival factors (Filmus and Selleck, 2001), this gene has not been correlated to these functions, yet. Syndecans are heaparan sulfate proteoglycan transmembrane components of ECM. Members of the family are co-receptors of growth factor binding and cellular interactions having diverse functions in cell adhesion, migration and proliferation. *SDC2* gene encodes the syndecan 2 protein. It was highly upregulated in 120nM docetaxel (49-fold) and 1000nM doxorubicin resistant cells (27-fold). Reports on syndecan 2 are contradicting. Modrowski *et al.* (Modrowski *et al.*, 2005) reported that overexpression of syndecan 2 induced osteoblastic cell apoptosis through the JNK/Bax apoptotic pathway. The same group also demonstrated sensitization of the human osteosarcoma cells to chemotherapy-induced apoptosis upon overexpression of syndecan 2 supporting tumor-suppressor functon of the gene (Orosco *et al.*, 2007). However, syndecan-2 interacts with cytokines and growth factors that stimulate angiogenesis (*e.g.* interleukin-8, VEGF, bFGF, and TGF) and these factors with MMPs may also stimulate syndecan-2 shedding which in turn promotes angiogenic processes (Fears *et al.*, 2006) and TGFβ induced increased matrix deposition in fibroblasts (Chen *et al.*, 2004). Collectively, molecular interactions of syndecan-2 and downstream effects can differ according to cell

type *i.e.* it may have an apoptotic effect on particular cell types depending on tissue specific expression of interacting molecules or expression profiles of other cell surface and ECM molecules. Fibrillins and fibulins are the microfibrils of ECM. Fibrillins 1 and 2 (*FBN1* and *FBN2*) are the major building blocks of extracellular microfibrils. *FBN1* was upregulated in MCF-7/120nM DOC and MCF-7/1000nM DOX while *FBN2* was highly upregulated only in MCF-7/1000nM DOX (80-fold). Although fibrillins have not been correlated to proliferation of tumor cells before, being key components of ECM they may function in remodeling of ECM as well as growth factor shedding (Chaudhry *et al.*, 2007). Fibulins upon binding to other ECM molecules functions as the bridges in the organization of ECM. *FBLN1* gene encoding the fibulin-1 had increased mRNA levels in all drug resistant cells. Pupa *et al.* (Pupa *et al.*, 2007), reported that it can promote survival of breast cancer cells during doxorubicin treatment although its modulation of expression was result of doxorubicin-induced stress rather than development of chemoresistance. Similarly, tumor promoting function for fibulin 5 was identified in developing and progressing breast cancers which might be related to its ability to enhance MMP expression correlated with *FBLN5* overexpression (Lee *et al.*, 2008). The upregulation of *FBLN5* only in MCF-7/1000nM DOX may be correlated to doxorubicin-induced cytotoxicity. *ECM1* gene, upregulated in 120nM docetaxel and 1000nM doxorubicin resistant cells, encodes the extracellular matrix protein 1. Stimulatory effect of ECM1 on proliferation of endothelial cells and angiogenesis of breast carcinoma cells with its increased expression was identified (Han *et al*., 2001).

Matrix metalloproteinases (MMPs) play role on cell behavior such as cell proliferation, migration, differentiation, angiogenesis, apoptosis, and metastasis and invasion since they are involved in the cleavage of cell surface receptors, the release of apoptotic ligands, and chemokine in/activation. *MMP14* was 3.5-fold upregulated in docetaxel resistant cells (Table 3.13). It is expressed in fibroblast cells during both wound healing and human cancer progression. Pro MMP2 and -13, pro TNF-α are among substrates of MMP14 and it takes place in angiogenesis. MMP23A and B are gelatinases that take role in degredation of ECM.

Adamalysins (ADAMs) family proteases are characterized by the presence of a cytoplasmic domain that in many family members specifies binding sites for various signal transducing proteins. Through binding to integrin, ADAMs modulate extracellular matrix-integrin interactions, and thus they can indirectly promote proliferation through integrin

signaling. *ADAM9* was overexpressed in all drug resistant sublines (Table 3.13). It binds to α2β1, α6β1, α6β4, α9β1 and αVβ5 integrins and digest fibronectin and gelatin. In addition, it can modulate EGF receptor activity upon shedding of heparin-binding EGF, cause transactivation of EGFR which in turn activates pathways to promote cell survival (Fischer *et al.*, 2004). Interestingly, unlike other metalloproteases, *ADAM15* was down regulated in MCF-7/120nM DOC. The protein encoded by *ADAM15* is unique among ADAM proteins since it contains the integrin binding motif Arg-Gly-Asp (RGD) within its disintegrin region (Krätzschmar *et al.*, 1996). Trochon-Joseph *et al.* (Trochon-Joseph *et al.*, 2004) previously produced recombinant human disintegrin domain of ADAM15 and identified this domain as a potent intrinsic inhibitor of angiogenesis, tumor growth, and metastasis in breast carcinoma cells and mice. Furthermore, they have concluded that it could be a promising tool for use in anticancer treatment. Moreover, Beck *et al.* (Beck *et al.*, 2005) reported ADAM15 as a natural binding partner of integrin αvβ3 which loosens tumor cell adhesion to the underlying matrix and regulated tumor cell migration and invasion. The adamalysins also contain the ADAMTS family proteinases; members having a variable number of thrombospondin-like (TS) motifs. *ADAMTS3* was 13.63-fold upregulated in MCF-7/120nM DOC. Although its function remains unclear, it's one of the ECM degrading enzymes of procollagen type.

Four tissue inhibitors of metalloproteinases (TIMPs) specifically inhibit matrix metalloproteinases and regulate extracellular matrix turnover and tissue remodeling by directly interacting with their active sites (Somerville *et al.*, 2003). Among genes encoding TIMPs, *TIMP3* was drastically downregulated in MCF-7/120nM DOC and MCF-7/1000nM DOX cells (-100- and -111-fold, respectively). In addition to its inhibitor activity, its proapoptotic function was also demonstrated by Ahonen *et al*. (Ahonen *et al.*, 1998). It was reported that overexpression of TIMP3 promoted apoptosis through stabilization of TNF-α receptors on the cell surface (Smith *et al.*, 1997). It is also known to inhibit TNF-α convertase enzyme; ADAM17 (Amour *et al.*, 1998). In contrast to *TIMP3*, *TIMP4* was 8.367-fold upregulated in MCF-7/1000nM DOX cells. TIMP4 has been shown to have antiapoptotic activity and tumor-stimulating effect in breast cancer cells and upregulate Bcl-2 and Bcl-X_L proteins (Jiang *et al.*, 2001).

Table 3.12 List of differentially expressed genes encoding extracellular matrix proteins in drug resistant MCF-7 sublines and fold changes of expression.

Gene Name	Gene Symbol	Description	Gene Ontology	MCF-7/ 30DOC	MCF-7/ 120DOC	MCF-7/ 1000DOX
215177_s_at	ITGA6	integrin, alpha 6	MF: binding, signal transducer, cell adhesion molecules	NS	24.66	27.92
201389_at	ITGA5	integrin, alpha 5 (fibronectin receptor, alpha polypeptide)	MF: binding, signal transducer, cell adhesion molecules	NS	4.91	4.04
1553678_a_at	ITGB1	integrin, beta 1 (fibronectin receptor, beta polypeptide, antigen CD29 includes MDF2, MSK12)	MF: binding, signal transducer, cell adhesion molecules	NS	NS	2.76
211964_at, 211966_at	COL4A2	collagen, type IV, alpha 2	MF: ECM structural constituent, structural molecule activity	NS	54.65	114.7
211981_at	COL4A1	collagen, type IV, alpha 1	MF: ECM structural constituent, structural molecule activity	NS	11.99	27.97
213428_s_at, 212937_s_at	COL6A1	collagen, type VI, alpha 1	MF: ECM structural constituent, cell adhesion molecules, structural molecule activity, binding	NS	19.10	12.03
209156_s_at, 213290_at	COL6A2	collagen, type VI, alpha 2	MF: ECM structural constituent, cell adhesion molecules, structural molecule activity, binding	NS	6.19	5.34

Table 3.12 (Continued)

231879_at	COL12A1	collagen, type XII, alpha 1	MF: ECM structural constituent, structural molecule activity, binding	21.33	NS	4.57
204345_at	COL16A1	collagen, type XVI, alpha 1	MF: structural molecule activity, cell adhesion molecules	NS	2.73	NS
227048_at	LAMA1	laminin, alpha 1	BP: cell growth and maintanance; MF: structural molecule activity, cell adhesion molecules, signal transducer activity	NS	84.30	86.86
211651_s_at	LAMB1	laminin, beta 1 ; laminin, beta 1	MF: structural molecule activity, binding, cell adhesion molecules	NS	16.72	14.58
209270_at	LAMB3	laminin, beta 3	MF: structural molecule activity, cell adhesion molecules	NS	7.76	NS
219407_s_at	LAMC3	laminin, gamma 3	MF: structural molecule activity, cell adhesion molecules, protein binding	NS	9.48	6.38
214701_s_at	FN1	fibronectin 1	BP: cell growth and maintanance; MF: ECM structural constituent, cell adhesion molecules, signal transducer activity	NS	33.94	11.23
227059_at	GPC6	glypican 6	BP: cell growth and maintenance; MF: binding	13.90	78.43	41.77
212236_x_at, 205157_s_at	KRT17	keratin 17	MF: structural molecule activity, binding	NS	NS	32.71

Table 3.12 (Continued)

212158_at	SDC2	syndecan 2 (heparan sulfate proteoglycan 1, cell surface-associated, fibroglycan)	BP: cell growth and maintanance, MF: protein binding	NS	48.98	27.15
213905_x_at, 201261_x_at, 201262_s_at	BGN ; SDCCAG33	biglycan ; serologically defined colon cancer antigen 33	MF: ECM structural constituent, transcription factor activity	NS	19.87	11.91
202766_s_at, 202765_s_at	FBN1	fibrillin 1 (Marfan syndrome)	MF: ECM structural constituent, transmembrane receptor activity, signal transducer activity	NS	37.19	43.44
203184_at, 203886_s_at	FBN2	fibrillin 2 (congenital contractural arachnodactyly)	MF: ECM structural constituent	NS	NS	79.54
202995_s_at, 201787_at	FBLN1	fibulin 1	MF: ECM structural constituent, binding	2.44	5.36	7.07
203088_at	FBLN5	fibulin 5	MF: ECM structural constituent, binding	NS	NS	4.73
209365_s_at	ECM1	extracellular matrix protein 1	MF: signal transducer activity, structural molecule activity	NS	21.56	14.29

Table 3.13 List of differentially expressed genes related to matrix metallopeptidases in drug resistant MCF-7 sublines and fold changes of expression.

Gene Name	Gene Symbol	Description	Gene Ontology	MCF-7/ 30DOC	MCF-7/ 120DOC	MCF-7/ 1000DOX
202827_s_at	MMP14	matrix metallopeptidase 14 (membrane-inserted)	BP: cell growth and maintenance; MF: binding, catalytic activity	NS	3.49	NS
207118_s_at	MMP23B; MMP23A	matrix metallopeptidase 23B ; matrix metallopeptidase 23A	MF: catalytic activity, defense and immunity, structural molecule activity	NS	11.71	14.38
1555326_a_at 202381_at	ADAM9	ADAM metallopeptidase domain 9 (meltrin gamma)	MF: binding, catalytic activity	2.55	5.75	5.51
217007_s_at	ADAM15	ADAM metallopeptidase domain 15 (metargidin	MF: catalytic activity, cell adhesion molecules	NS	-2.15	NS
214913_at	ADAMTS3	ADAM metallopeptidase with thrombospondin type 1 motif, 3	BP: cell growth and maintenance; MF: binding, catalytic activity	NS	13.64	NS
201150_s_at	TIMP3	TIMP metallopeptidase inhibitor 3	BP: cell death; MF: signal transducer activity	NS	-97.09	-109.05
206243_at	TIMP4	TIMP metallopeptidase inhibitor 4	BP: cell death; MF: signal transducer	NS	NS	8.37

3.6.8 Alterations in Expression Levels of Genes Encoding Proteins Related to Microtubule Dynamics

According to microarray analysis (Table 3.14), class II β-tubulin, expression level significantly increased in MCF-7/30nM DOC and MCF-7/120nM DOC cells (3- and 11-fold, respectively). As previously discuused in Section 3.2.4., class III β-tubulin has relatively higher microtubule-destabilizing potency (Banerjee *et al.*, 1990; Lu and Luduena, 1993; Kavallaris *et al.*, 1999) and its expression significantly increased in 120nM docetaxel resistant and to a lower extent in 30nM docetaxel resistant sublines. Similar to class III β-tubulin, mouse class V β-tubulin had also destabilizing properties (Bhattacharya and Cabral, 2004) which was also 11-fold overexpressed in MCF-7/120nM DOC. Results obtained from RT-PCR analysis of class I, IVa and IVb were not consistent with microarray analysis results. Alterations in these isotypes were lower and statistically not significant in some of them (*e.g.* class IVa and IVb). Different gene expression patterns may be because of heterogenic cell populations expressing these isotypes. During stepwise dose selection cells acquire a resistant phenotype with gradual changes at gene expression levels and these changes may variate in a cell population (Kars *et al.*, 2006). Alterations in expression levels of these genes might be related to higher resistance indices or be a more sudden transient changes rather than their direct correlation to drug resistance. In addition, direct functional relevance of these isotypes with microtubule stabilizing and/or destabilizing agents still remains unclear

Microtubule-associated proteins (MAPs) are thought to be involved in microtubule dynamics, both stabilizing and destabilizing microtubules, guiding microtubules towards specific cellular locations, cross-linking microtubules and mediating the interactions of microtubules with other proteins in the cell. Product of the *MAP7* gene is a microtubule-associated protein that is predominantly expressed in cells of epithelial origin. It was 22-fold downregulated in MCF-7/120nM DOC. In concordance, the protein has been shown to stabilize microtubules, and may serve to modulate microtubule functions (www.ncbi.nlm.nih.gov/sites/entrez?Db=gene&Cmd=retrieve&dopt=full_report&list_uids =9053&log$=genesensorsearch&logdbfrom=pubmed). MAP1B is a major, component of the neuronal cytoskeleton (Bloom *et al.*, 1985). It is enriched in the distal region of the growing axons which have higher polymer turnover (Black *et al.*, 1994.). Thus, MAP1B is

different from other MAPs, such as MAP2 and Tau, which strongly suppress turn over when present at high levels on microtubules (Pryer *et al.*, 1992; Umeyama *et al.*, 1993) as well as its relatively lower binding affinity to microtubules. In concordance with the previous reports, 21-fold upregulation of the MAP1B gene in MCF-7/120nM DOC (and 2-fold in MCF-7/30nM DOC) might provide a shift in microtubule stability caused by docetaxel. Moreover, phosphorylation of MAPs interferes with their microtubule-stabilizing capacity *e.g.* in mitotic cells, MAPs exhibit a several-fold higher degree of phosphorylation as well as their incresed microtubule dynamics. Tau tubulin kinase 2 phosphorylates Tau, a microtubule stabilizing MAP. The *TTBK2* gene was 4-fold upregulated in MCF-7/120nM DOC cells. Evans *et al.* (Evans *et al*., 2000) demonstrated that phosphorylation of microtubule-associated tau results in tau dissociation from the microtubules and tubulin depolymerization. MARK family of proteins also phosphorylates Tau, MAP2, and MAP4 on their microtubule-binding domain, causing their dissociation from microtubules and increased microtubule dynamics (Drewes *et al.*, 1997).

Tubulin-tyrosine ligase (TTL) catalyses the ATP-dependent post-translational addition of a tyrosine to the carboxy terminal ends of detyrosinated alpha-tubulin. In cultured cells, detyrosinated tubulin is enriched in stable microtubules exhibiting little dynamic behavior (Gundersen *et al*., 1984; Wehland and Weber, 1987), whereas dynamic microtubules display tyrosinated tubulin.

Tubulin-specific chaperone e (TBCE) is an α-tubulin-binding protein involved in the formation of the tubulin dimer and in microtubule dynamics, through the regulation of tubulin heterodimer dissociation. Kortazar et al., (Kortazar *et al.*, 2006) demonstrated that excess of purified TBCE dissociated tubulin heterodimers producing a highly unstable TBCE-alpha-tubulin complex, which formed aggregates. It was 4-fold upregulated in MCF-7/120nM DOC cells.

Table 3.14 List of differentially expressed genes encoding proteins related to microtubule dynamics in drug resistant MCF-7 sublines and fold changes of expression.

Gene Name	Gene Symbol	Description	Gene Ontology	MCF-7/ 30DOC	MCF-7/ 120DOC	MCF-7/ 1000DOX
214023_x_at	TUBB-PARALOG (TUBB2B)	tubulin, beta polypeptide paralog (βII tubulin)	BP: cell growth and maintenance, MF: structural molecule activity, binding	2.73	16.39	NS
209191_at	TUBB6	tubulin, beta 6 (βV tubulin)	BP: cell growth and maintenance, MF: structural molecule activity, binding	NS	11.45	NS
202154_x_at, 213476_x_at	TUBB3	tubulin, beta 3 (βIII tubulin)	BP: cell growth and maintenance, MF: structural molecule activity, binding	2.03	4.98	NS
213726_x_at, 208977_x_at	TUBB2 (TUBB2C)	tubulin, beta, 2 (βIVb tubulin)	BP: cell growth and maintenance, MF: structural molecule activity, binding	NS	2.99	15.57
209026_x_at, 211714_x_at	TUBB	tubulin, beta polypeptide (βI tubulin)	BP: cell growth and maintenance, MF: structural molecule activity, binding	NS	2.80	2.63
212233_at	MAP1B	Microtubule-associated protein 1B ; Homo sapiens, clone IMAGE:5535936, mRNA	BP: cell growth and maintenance, MF: structural molecule activity, binding	2.08	20.95	NS

Table 3.14 (Continued)

200836_s_at, 212567_s_at, 33850_at	MAP4	microtubule-associated protein 4	BP: cell growth and maintenance, MF: structural molecule activity, binding	NS	2.90	NS
202890_at	MAP7	microtubule-associated protein 7	BP: cell growth and maintenance, MF: structural molecule activity, binding	NS	-22.37	NS
200713_s_at	MAPRE1	microtubule-associated protein, RP/EB family, member 1	BP: cell growth and maintenance, MF: structural molecule activity, binding	NS	2.16	NS
224896_s_at, 244078_at	TTL	tubulin tyrosine ligase	BP: cell growth and maintenance, MF: structural molecule activity, binding	NS	4.23	NS
1557073_s_at	TTBK2	Tau tubulin kinase 2	BP: cell growth and maintenance, MF: structural molecule activity, binding, catalytic activity	NS	3.95	NS
203715_at	TBCE	tubulin-specific chaperone e	BP: cell growth and maintenance, MF: structural molecule activity, binding, catalytic activity	NS	3.83	NS
221047_s_at	MARK1	MAP/microtubule affinity-regulating kinase 1	BP: cell growth and maintenance, MF: structural molecule activity, binding, catalytic activity	NS	3.19	NS
215660_s_at	MAST2	microtubule associated serine/threonine kinase 2	BP: cell growth and maintenance, MF: structural molecule activity, binding, catalytic activity	NS	2.81	NS
221326_s_at, 231853_at	TUBD1	tubulin, delta 1	BP: cell growth and maintenance, MF: structural molecule activity, binding	NS	-13.14	-11.98

3.7 Cross–resistance Studies

The results suggested that the resistant sublines developed varying degree of cross-resistance to different anticancer agents and irradiation. Similar findings were aso reported in clinical studies for chemotherapy during development of multidrug resistance (Kröger *et al.*, 1999; Yonemari *et al.*, 2005). In clinic, development of cross-resistance affects the success of chemotherapy and some patients become refractory to treatment (Marty *et al.*, 1997; Adamo *et al.*, 2007). According to Table 3.15, MCF-7/120nM DOC cells developed 13- and 2-fold cross-resistance to vincristine and tamoxifen, respectively. MCF-7/1000nM DOX cells developed 109.03-, 9.63-, 2.36- and 2.54-fold cross-resistance to paclitaxel, docetaxel, tamoxifen and ATRA respectively. The resistance indices were significantly different and lower than the resistance developed by MCF-7/1000nM DOX to doxorubicin. Both sublines expressed *MDR1* so resistant cells can also develop cross-resistance to other P-gp substrates like paclitaxel, docetaxel and vincristine. Nevertheless, it is probable that senstive MCF-7 cell line became resistant to different drugs through diverse mechanisms, so that the sublines might have responded differently. Tamoxifen and ATRA are not substrates of P-gp and it may be the major cause for the sublines developing no or very low level of cross resistance to these agents. Despite the known anticarcinogenic activity of ATRA, it exhibits its short plasma half-life during repeated oral administration due to the acute retinoid resistance (Choi *et al.*, 2006). Concordantly, resistance to ATRA was previously correlated with high levels of CRABP1 (cellular retinoic acid binding protein 1) which fastens metabolism of retinoic acid resulting in decreased ATRA intracellular concentrations (Boylan *et al.,* 1992). Same report also demonstrated that reduced CRABP1 levels caused higher sensitivity to ATRA. In another study emerging leukemic cells of AML3 patients in relapse after ATRA therapy harbored high levels of CRABP2 (Delva *et al.,* 1993). Interestingly, according to microarray results (Table 3.10), MCF-7/120nM DOC cells, but not MCF-7/1000nM DOX, had reduced *CRABP2* expression (5-fold). Moreover, RA hydroxylation enzyme CYP26A1, previously discussed in section 3.4.2, was also 2.9-fold upregulated in MCF-7/1000nM DOX cells (Table 3.7). So together with reduced *CRABP2* levels elevated *CYP26A1* may explain development of ATRA cross-resistance in doxorubicin resistant cells but not in docetaxel resistant cells. Drug resistance to tamoxifen is a significant clinical problem but the mechanism through which this occurs was not well

understood (Riggins *et al.,* 2007). Tamoxifen is a synthetic non-steroidal anti-estrogen that is used in the treatment of estrogen receptor-positive breast cancer patients (Wu *et al.*, 1997). However, approximately 30% of estrogen receptor α-positive breast cancers do not respond to tamoxifen treatment. In addition, the majority of tumors that initially respond to treatment develop resistance over time (Schafer *et al.,* 2002; Riggins *et al.,* 2007). Both docetaxel and doxorubicin resistant cells developed croos-resistance to tamoxifen. Tamoxifen exert its antiproliferative effect on estrogen receptor-positive breast cancer since it also binds to estrogen receptor like estrogen. Microarray results demonstrated that resistant subline had significantly lower estrogen receptor gene expression levels when compared with sensitive cells (76.92- and 71.94-fold in MCF-7/120nM DOC and MCF-7/1000nM DOX, respectively). Downregulated estrogen receptor levels might be correlated to lower tamoxifen responsiveness in these cells. Secondly, high levels of tenascin C (*TNC*) levels were also found in microarray analysis (7.73- and 3.97-fold in MCF-7/120nM DOC and MCF-7/1000nM DOX, respectively; data not shown). Tenascin C is an adhesion-modulating ECM protein which have also role in cell proliferation, invasion and metastasis. Helleman *et al*. (Helleman *et al.*, 2008) described a significant association between increased *TNC* levels and tamoxifen resistance in relapsed breast cancer patients which can be correlated to generation of proliferative estrogen receptor independent signals through integrin and/or EGFR binding. Relation of ECM proteins to drug resistance is overwieved in detail in microarray data analyis (Section 3.4.3).

Table 3.15 Antiproliferative effects of anticancer drug and irradiation applications on sensitive and resistant MCF-7 cell lines and resistance indices.

Cells	Application	Mean $IC_{50}^{\dagger} \pm SEM^{\gamma}$	R
MCF-7	Paclitaxel	2.12 ± 0.23	-
	Docetaxel	3.49 ± 1.55	-
	Vincristine	5.45 ± 0.66	-
	Doxorubicin	1.14 ± 0.38	-
	Tamoxifen	6.02 ± 1.30	-
	ATRA	40.78±9.42	-
	Irradiation	967 ± 63.98	-
MCF-7/120nM DOC	Docetaxel	163.21 ± 11.19	46.77*
	Vincristine	66.21 ± 9.4	12.15*
	Doxorubicin	1.55 ± 0.44	1.40
	Tamoxifen	12.09 ± 1.48	2.01*
	ATRA	45.80 ± 11.50	1.12
	Irradiation	1858.33 ± 51.94	1.92 *
MCF-7/1000nM DOX	Doxorubicin	183.11 ± 23.63	160.62*
	Paclitaxel	231.15 ± 49.15	109.03*
	Docetaxel	33.61 ± 7.42	9.63*
	Tamoxifen	14.18 ± 0.50	2.36*
	ATRA	103.40 ± 20.11	2.54*
	Irradiation	974.67 ± 21.4	1.01

†Mean IC_{50} values were given in μM for anticancer drug applications and in cGy for irradiation treatment.

$^{\gamma}$SEM values were derived from the IC_{50} values of three independent experiments.

*Represents significant difference between groups with $p<0.05$.

In clinical applications, development of cross-resistance affects the success of both chemotherapy and radiotherapy, and some patients become refractory to radiotharpy as well (Marty *et al.*, 1997; Adamo *et al.*, 2007). In order to evaluate dose dependent cytotoxic effect of γ-radiation on docetaxel and doxorubicin resistant cells and development of cross resistance to irradiation, cells were irradiated with doses of 200 and 800 cGy. Irradiation doses caused significant reduction in cell proliferation of sensitive and resistant MCF-7 cells (Figure 3.38). Inhibitory doses of radiation in cGy for sensitive and resistant cells

were calculated to evaluate antiproliferative effects of irradiation on cells and express resistance indices for irradiation. IC_{50} values and resistance indices are summarized in Table 3.14. According to the table, MCF-7/120nM DOC cells were significantly cross-resistant to irradiation (1.92-fold) compared to sensitive MCF-7. Although MCF-7/1000nM DOX subline was more chemoresistant than MCF-7/120nM DOC (Table 3.14) it did not develop radioresistance. Some of the genes that are involved in DNA repair and/or cell cycle regulation may have been induced in MCF-7/120nM DOC. For instance in a previous report, levels of *DDB2* (involved in DNA repair) and *CDKN1A* (cell cycle regulator) genes were significantly induced by irradiation in breast cancer tissue samples (Helland *et al.*, 2006). The respective study also proposed that these genes were modulated by p53 and altered the radiosensitivity/resistance profiles in tissues following radiotherapy. In addition, both *DDB2* and *CDKN1A* were previously identified as radiation-induced in peripheral white blood cells (Amundson *et al.*, 2004) and fibroblasts (Rodningen *et al.*, 2005)

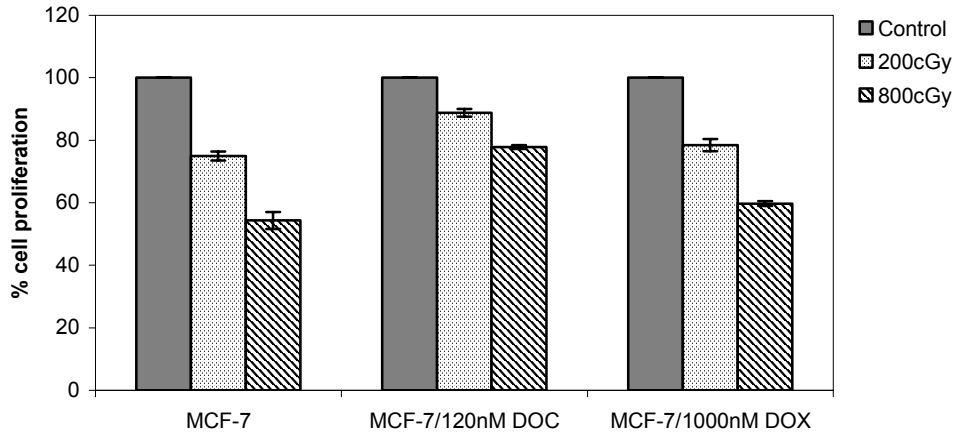

Figure 3.38 Antiproliferative effects of different doses of irradiation on sensitive and resistant cells.

3.8 Drug Interactions

Drug-drug ineractions were evaluated and characterized as synergic, additive, indifferent and antagonist by checkerboard microplate method. Synergism is a positive interaction, that is, combined effect of two compounds is significantly greater than expected results based on their independent effects when they are used separately. Antagonism is a negative interaction, that is, combined effect of two drugs being examined is significantly less than their independent effects when they are measured separately (Kars *et al.,* 2008). The application of two anticancer drugs may be acceptable if the drug interaction is synergistic, but not acceptable if the interaction is antagonistic. According to fractional inhibitory indices, combinations of doxorubicin with docetaxel exerted significant synergic antiproliferative effects on the docetaxel resistant cells (Table 3.16). Tamoxifen exerted additive antiproliferative effects with docetaxel on these cells where vincristine and all-trans retinoic acid (ATRA) had indifferent effects in combined applications with docetaxel. According to Table 3.16, combinations of paclitaxel, docetaxel and tamoxifen with doxorubicin exerted significant synergic effects on the doxorubicin resistant cells. On the

other hand, ATRA had indifferent effects on MCF-7/1000nM DOX. Results demonstrated that tamoxifen can be used in combination with both docetaxel and doxorubicin. Similarly, paclitaxel and tamoxifen were previously applied in combination in-vivo (Fine *et al*., 2006). Also effective combinations of doxorubicin with paclitaxel and docetaxel combination *in vitro* may be good models for *in vivo* combined chemotherapy. Different sensitivities of the sublines to combined applications of anticancer agents can be explained by cellular differences in the resistance mechanisms and differences in the expression levels of the resistance related genes in the sublines. Antiproliferative effects of paclitaxel-doxorubicin, docetaxel-doxorubicin, docetaxel-tamoxifen and doxorubicin-tamoxifen pairs may also be related to the independent effects of anticancer agents on different pathways in the resistant sublines and their combined cytotoxic effects.

Table 3.16 Effects of combined anticancer drug applications on MCF-7 sublines.

Cells	**Anticancer Drug**	**FIX ± SEM[¥]**	**Interaction**
MCF-7/120nM DOC	Docetaxel (+)	-	-
	Vincristine	1.19 ± 0.21	Indifferent
	Doxorubicin	0.43 ± 0.10	Synergism
	Tamoxifen	0.87 ± 0.09	Additive
	ATRA	1.43 ± 0.20	Indifferent
MCF-7/1000nM DOX	Doxorubicin (+)	-	-
	Paclitaxel	0.22 ± 0.07	Synergic
	Docetaxel	0.43 ± 0.07	Synergic
	Tamoxifen	0.15 ± 0.06	Synergic
	ATRA	1.14 ± 0.18	Indifferent

[¥] SEM were derived from the SEM of at least three FIX values.

3.9 Reversal of MDR

Verapamil is a clinically used calcium ion influx inhibitor (calcium entry blocker or calcium ion antagonist) and it is one of the substrates and modifiers of P-gp pump (Taub *et al.*, 2005). Promethazine, a phenothiazine derivative, is clinically used as oral antihistamine that mimics the effects of the naturally occurring histamine. It was previously reported that phenothiazines could be used as P-gp suppressor MDR reversal agents (Motohashi *et al*.,

2001). Effects of verapamil and promethazine on cell proliferation and *MDR1* and *MRP1* gene expression levels were evaluated in order assess modulator efficiency on docetaxel and doxorubicin resistant cells.

3.9.1 Proliferation Studies

Cytotoxicity of verapamil and promethazine were evaluated on sensitive MCF-7, and docetaxel and doxorubicin resistant sublines with highest resistant indices (MCF-7/120nM DOC and MCF-7/1000nM DOX, respectively) (Figures 3.39 and 3.40) and IC_{50} values were calculated (Table 3.17). IC_{50} values demonstrated that cytotoxicity of promethazine was greater than verapamil on both docetaxel and doxorubicin resistant cells. Neither verapamil nor promethazine showed significant difference on cytotoxicity of MCF-7, MCF-7/120nM DOC and MCF-7/1000nM DOX.

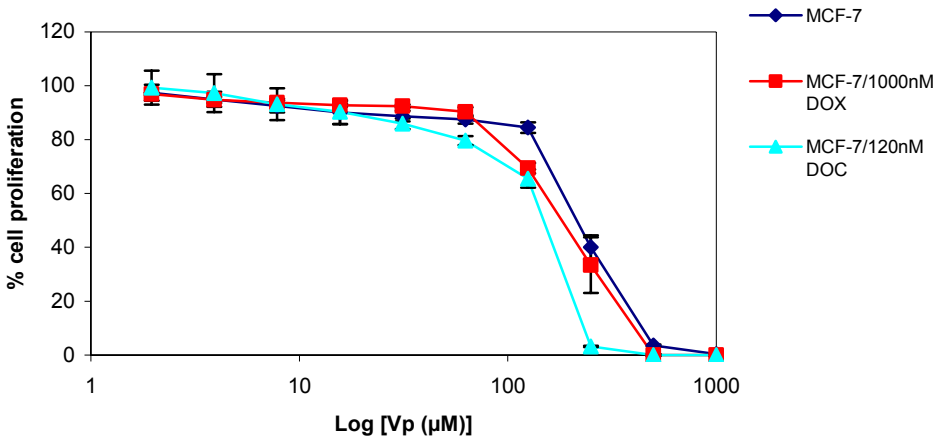

Figure 3.39 Antiproliferative effects of verapamil on MCF-7, MCF-7/1000nM DOX and MCF-7/120nM DOC sublines.

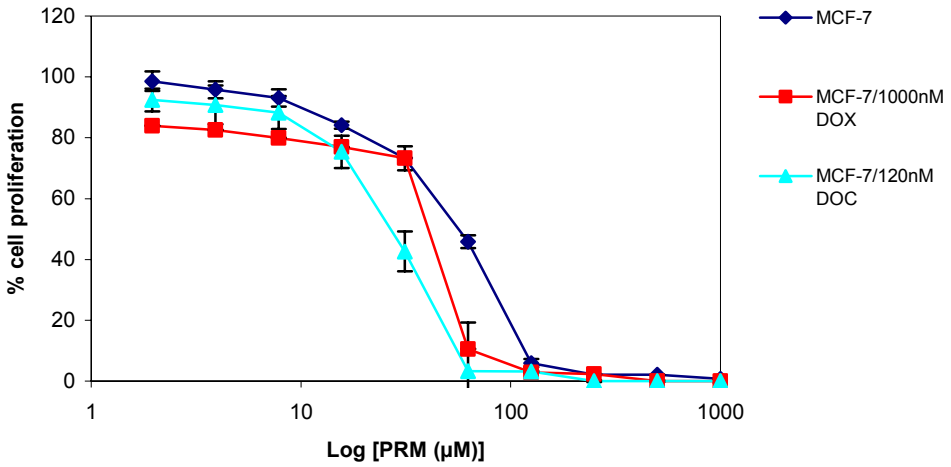

Figure 3.40 Antiproliferative effects of promethazine on MCF-7, MCF-7/1000nM DOX and MCF-7/120nM DOC sublines.

Combined antiproliferative effects of verapamil and promethazine with docetaxel and doxorubicin were also studied by XTT based checkerboard microplate method. Figures 3.41 and 3.42 illustrate single and combined antiproliferative effects of modulators. Concordantly, FIX values demonstrated that (Table 3.17) verapamil exerted synergic effects with both docetaxel and doxorubicin on MCF-7/120nM DOC and MCF-7/1000nM DOX, respectively. On the other hand, in combination promethazine was antagonist with docetaxel on MCF-7/120nM DOC and additive with doxorubicin on MCF-7/1000nM DOX.

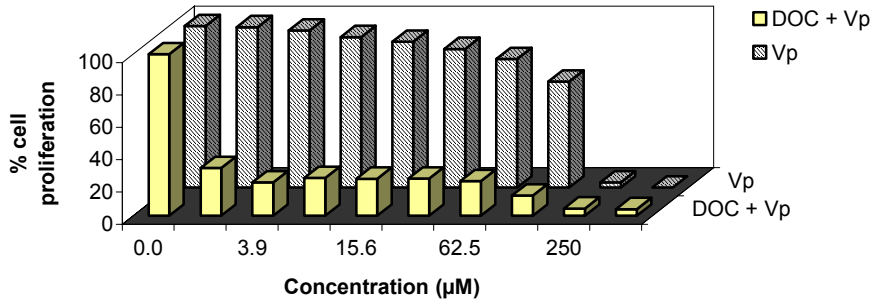

A)

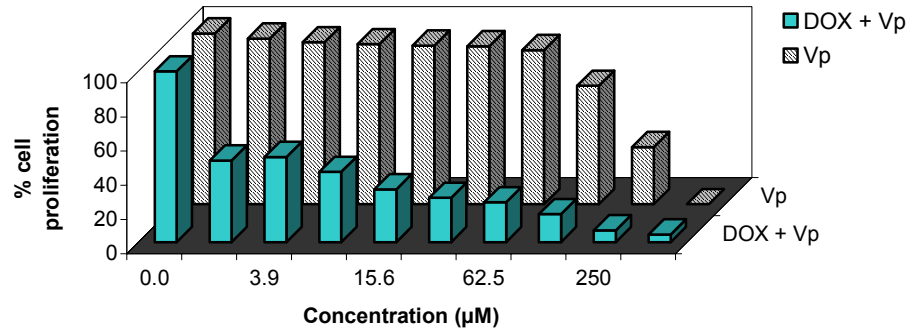

B)

Figure 3.41 Combined antiproliferative effects of verapamil with A) docetaxel on MCF-7/120nM DOC and B) doxorubicin on MCF-7/1000nM DOX.

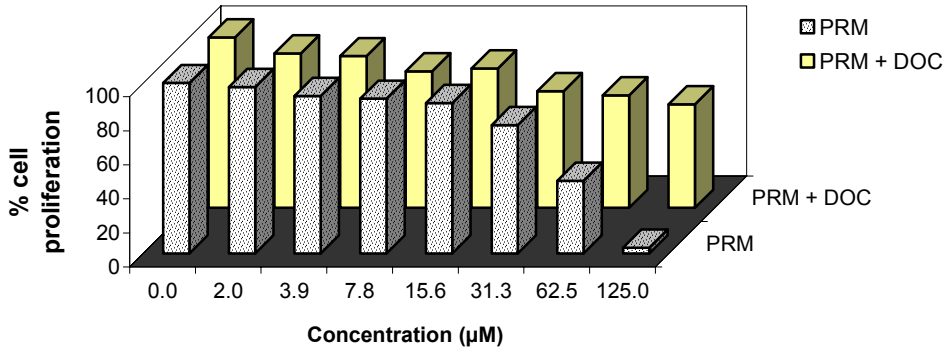

A)

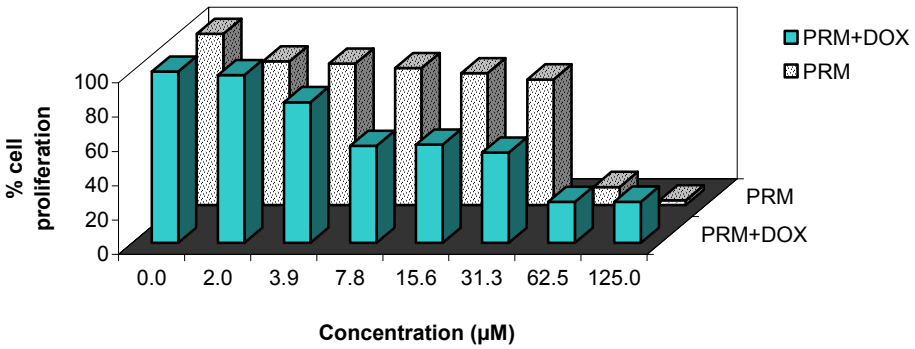

B)

Figure 3.42 Combined antiproliferative effects of promethazine with A) docetaxel on MCF-7/120nM DOC and B) doxorubicin on MCF-7/1000nM DOX.

Table 3.17 Antiproliferative effects of verapamil and promethazine.

Cell Line	Modulator	IC_{50} ± SEM[¥]	FIX ± SEM[γ]	Interaction
MCF-7	Verapamil	138.94 ± 3.79		
	Promethazine	44.64 ± 1.48		
MCF-7/120nM DOC	Docetaxel (+)	163.21 ± 11.19	-	-
	Verapamil	82.86 ± 4.02	0.29 ± 0.11	Synergic
	Promethazine	43.82 ± 1.99	6.23 ± 1.39	Antagonist
MCF-7/1000nM DOX	Doxorubicin (+)	183.11 ± 23.63	-	-
	Verapamil	119.59 ± 12.44	0.50 ± 0.14	Synergic
	Promethazine	27.44 ± 1.66	0.53 ± 0.09	Additive

[¥] SEM were derived from three independent experiments.

[γ] SEM were derived from the SEM of at least three FIX values.

3.9.2 Effects of Verapamil and Promethazine on *MDR1* and *MRP1* Gene Expression

Effects of verapamil and promethazine on gene expression levels of *MDR1* and *MRP1* were evaluated by RT-PCR. 40 and 60μM verapamil was applied to MCF-7/120nM DOC and MCF-7/1000nM DOX, respectively for 48 and 72 h time intervals (Figure 3.43).

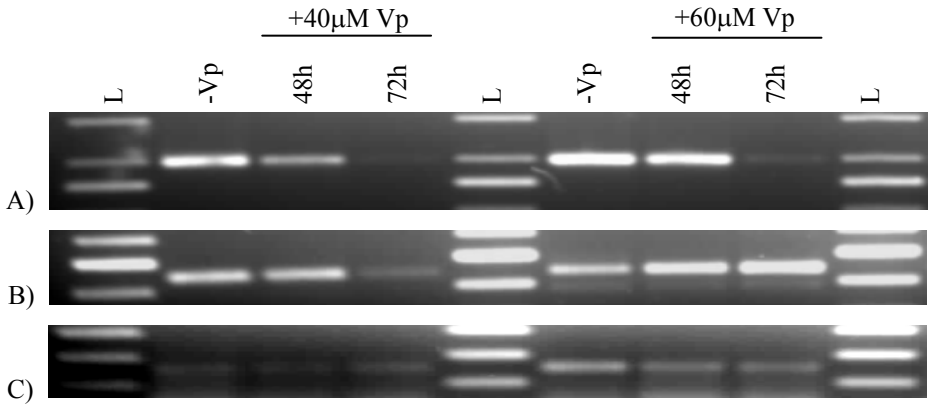

Figure 3.43 RT-PCR results (2% agarose gel); left panel for MCF-7/120nM DOC and right panel for MCF-7/1000nM DOX: A) 295 bp *MDR1*, B) 217 bp *MRP1* and C) 122 bp *β2-microglobulin* products.

RT-PCR results demonstrated that verapamil application caused a decrease in *MDR1* expression (Figure 3.44 A) in docetaxel and doxorubicin resistant cells. There were -1.82- and -3.70-fold decrease for 48 and 72 h verapamil treatment, respectively in MCF-7/120nM DOC cells (Appendix G). Similarly, *MDR1* expression decreased 1.09- and 2.38-fold for 48 and 72 h verapamil treatment, respectively in MCF-7/1000nM DOX. On the other hand, expression of *MRP1* decreased with 48 and 72 h verapamil treatment (1.80- and -2.22-fold, respectively) in MCF-7/120nM DOC (Figure 3.44 B). Interestingly, *MRP1* expression increased with 72 h verapamil treatment (1.15- and 1.41-fold, respectively) in MCF-7/1000nM DOX. Similar expression profile was also observed in the development of doxorubicin resistance (see Figure 3.11 discussed in Section 3.2.2). *MRP1* expression increased with increasing doses of doxorubicin application while it decreased by induction

of *MDR1* expression in doxorubicin resistant sublines. As previously discussed, this seemed to be related to substrate specificity of MRP1 and P-gp pumps *i.e.* doxorubicin is substrate of both of the pumps where docetaxel is substrate of only P-gp.

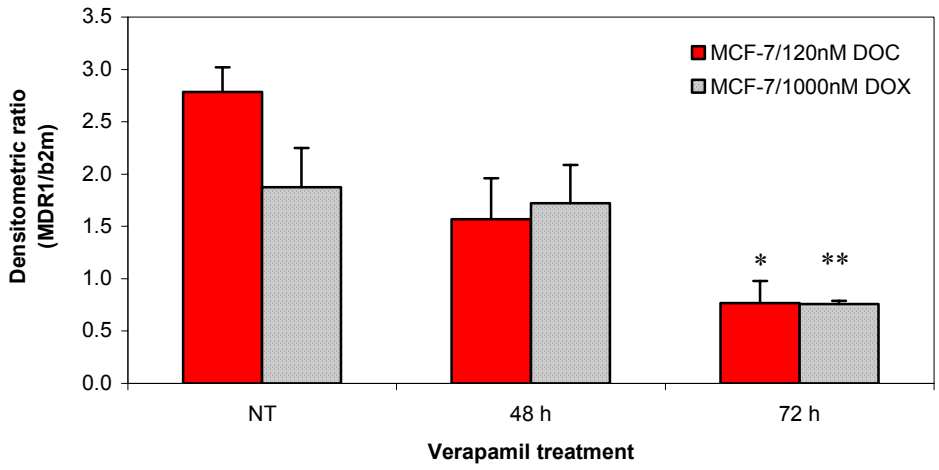

A)

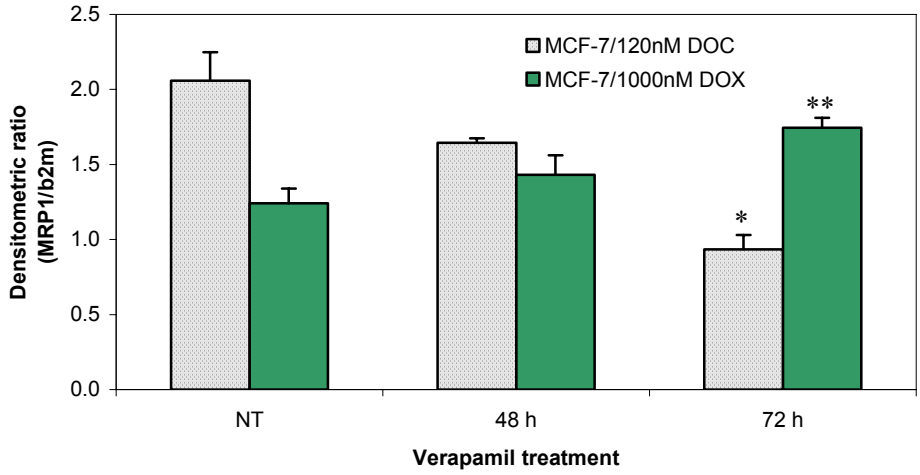

B)

Figure 3.44 Alterations in expression levels of A) *MDR1* and B) *MRP1* genes in MCF-7/120nM DOC and MCF-7/1000nM DOX cells with verapamil treatment. * Represents significant difference in gene expression levels between non treated control and verapamil treatments of MCF-7/120nM DOC ($p < 0.05$), ** represents significant difference in gene expression levels between non treated control and verapamil treatments of MCF-7/1000nM DOX ($p < 0.05$).

Verapamil is a specific first generation P-gp efflux pump inhibitor (Nobili *et al.*, 2006). It exerted synergic effects in combination with docetaxel and doxorubicin on drug resistant MCF-7 cells. Besides its well known MDR modulation function at protein activity level, suppression of *MDR1* and *MRP1* at gene expression level was also demonstrated.

Molnar *et al.* (Molnar *et al.*, 1998) previously described that, *mdr1* gene expression level was reduced due to promethazine application in mouse lymphoma cells and suggested to block gene expression at promoter level. Effect of promethazine on gene expression level of *MDR1* was investigated in docetaxel and doxorubicin resistant cells in dose and time dependent manner. According to RT-PCR results (Appendix G), promethazine application caused either complete loss or decrease in *MDR1* expression in resistant cells depending on time and dose (Figures 3.45 and 3.46). In doxorubicin resistant cells, decrease of expression was concentration dependent for different time intervals *i.e. MDR1* expression was lower in 4.8µM promethazine application when compared to 1.6µM promethazine application (Figure 3.47 B). On the other hand, effect of promethazine increased in MCF-7/120nM DOC with increasing application time due to 4.8µM promethazine application (Figure 3.47 A). Although in docetaxel resistant cells, decrease in *MDR1* expression was less in 72h time interval than in 12, 24 and 48 hours in 1.6µM promethazine applied group, complete *MDR1* blockage was achieved in 72h 4.8µM promethazine application. *MDR1* was not completely blocked in doxorubicin resistant cells. It may be related to differences in MDR1 expression levels in MCF-7/120nM DOC and MCF-7/1000nM DOX. *MDR1* epression level was approximately 3-fold higher in 1000nM DOX resistant cells with respect to 120nM DOC resistant cells according to qPCR results (Appendix G). Concordantly, MCF-7/120nM DOC cells were 46.7-fold resistant to docetaxel where MCF-7/1000 DOX cells were 160.6-fold resistant to doxorubicin (Tables 3.3 A and 3.4 A, respectively).

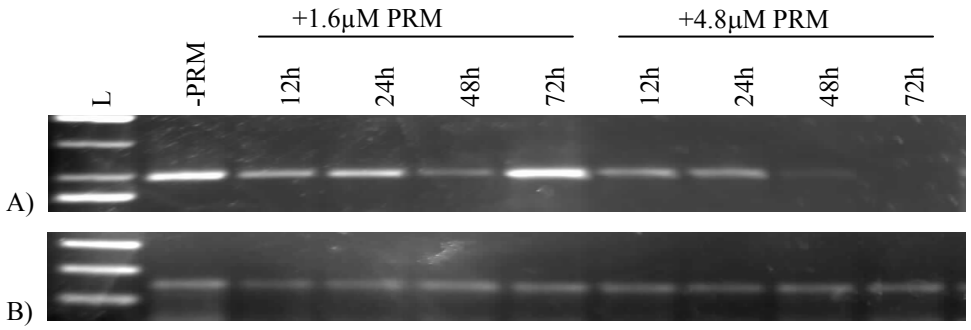

Figure 3.45 RT-PCR results (2% agarose gel) for MCF-7/120nM DOC: A) 295 bp *MDR1* and B) 122 bp *β2-microglobulin* products.

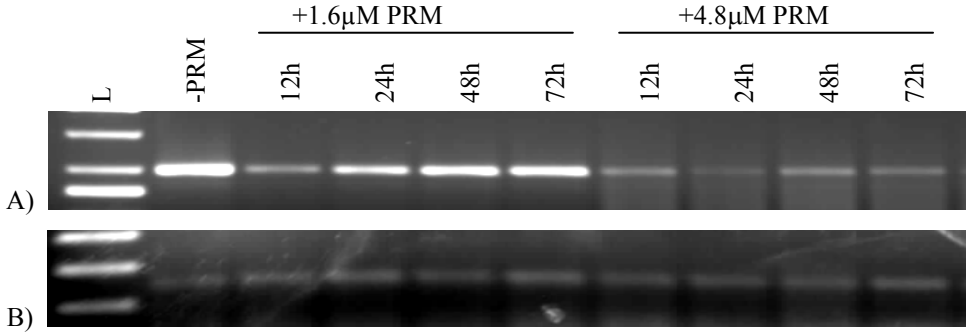

Figure 3.46 RT-PCR results (2% agarose gel) for MCF-7/1000nM DOX: A) 295 bp *MDR1* and B) 122 bp *β2-microglobulin* products.

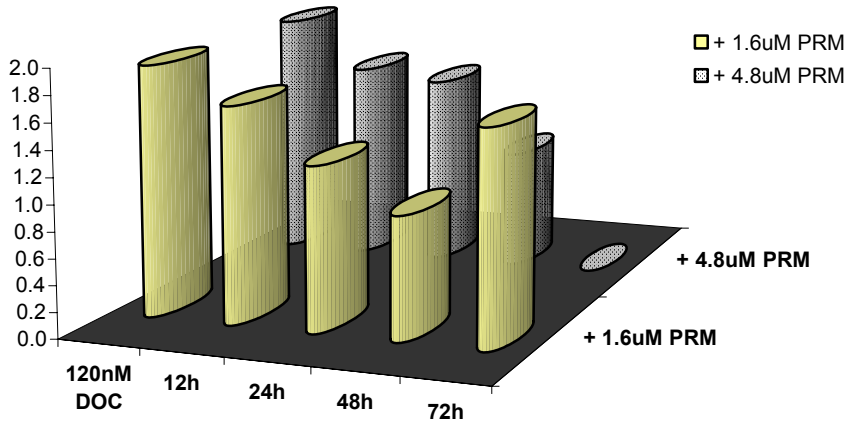

A)

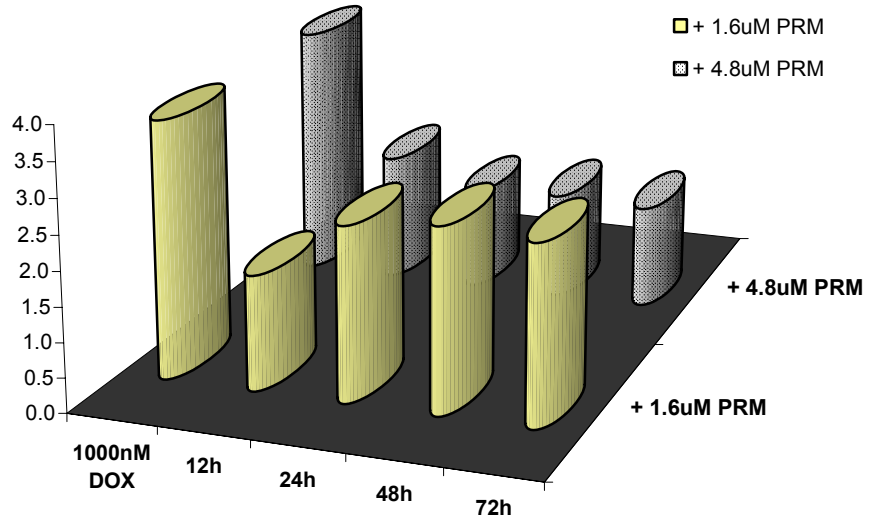

B)

Figure 3.47 Alteration of expression level of *MDR1* gene in A) MCF-7/120nM DOC and B) MCF-7/1000nM DOX with promethazine treatment.

Despite the *MDR1* supressor effects of promethazine, it is not suitable for clinic reversal of docetaxel resistance due to its combined antagonist effect with docetaxel. Conversely, promethazine stil seems to be a candidate resistance modifier of doxorubicin resistance with its combined additive and gene suppressor affects *MDR1* although complete *MDR1* expression inhibition was not achieved.

CHAPTER 4

CONCLUSION

1) Docetaxel and doxorubicin applied cells, having different growth patterns, developed varying degrees of resistance to selective drugs. Degree of resistance increased with drug concentration.

2) According to microarray analysis, expression profiles of MCF-7 and MCF-7/30nM DOC were similar to each other. On the other hand, expression profiles of MCF-7/120nM DOC and MCF-7/1000nM DOX differed from MCF-7 and MCF-7/30nM DOC while the resistant profiles of these two were also similar. This type of expression pattern confirms the gradual increase of resistance during drug selection. Alterations in ABC transporter family and glutathione metabolism related genes, cytochrome P450 family genes, genes encoding the ECM related proteins, genes encoding growth factors and cytokines, cell survival and death genes and genes encoding the EMT related proteins were determined.

3) Induction and overexpression of *MDR1* (P-gp) expression were shown by RT-PCR, qPCR, microarray analysis, Western blot and immunocytochemistry in docetaxel and doxorubicin resistant sublines. P-gp overexpression and drug efflux through P-gp was one of the basic drug resistance mechanisms in docetaxel and doxorubicin resistant sublines.

4) Sensitive MCF-7 cells had intrinsic *MRP1* gene expression at basal level. Sequential increments in *MDR1* and *MRP1* levels (*i.e.* gradual upregulation of *MRP1* untill the emergence of *MDR1*) demonstrated that MRP1 was involved in low levels of doxorubicin resistance while P-gp contributed to intermediate to high levels of resistance since doxorubicin is transported by both P-gp and MRP1. However, MRP1 was not one the mechanisms of doctaxel resistance.

5) Sensitive MCF-7 and doxorubicin resistant cells did not epress *BCRP*. However *BCRP* levels showed a transient increase in 30-60nM docetaxel resistant cells with a progressive downregulation in dose increments and complete loss of expression. BCRP expression pattern might be correlated to estrogen receptor levels since the gene has a putative estrogen response element.

6) Among the genes encoding cytochromes and glutathione metabolism related genes, P450 oxireductase (POR), was noticeably downregulated in MCF-120nM DOC and MCF-7/1000nM DOX. Drastic elevation of *GPX1, GSTP1* genes together with downregulation of POR in MCF-7/120nM DOC and MCF-7/1000nM DOX demonstrated a contribution of ROS defense mechanism in protection from docetaxel and doxorubicin induced cytotoxicity.

7) Genes encoding proteins related to survival and death pathways were altered in drug resistant cells. In particular, TNF superfamily ligands and receptors of extrinsic apoptosis pathways were of great significance. Among this TRAIL (TNFSF10), a selective death ligand of tumor cells for expression of receptors on tumor cells was downregulated in MCF-7/120nM DOC and MCF-7/1000nM DOX. The proteins encoded by *TNFRSF6B* and *TNFRSF10D* genes (decoy TRAIL receptors 2 and 3), protecting cells from apoptosis, were noticibly upregulated in both MCF-7/120nM DOC and MCF-7/1000nM DOX. Similarly, Upregulation of CD40 in both MCF-7/120nM DOC and MCF-7/1000nM DOX seemed to be a common cell survival response. MCF-7/120nM DOC and MCF-7/1000nM DOX showed elevated levels of *AKT3* expression, a downstream activator of PI3K survival signalling. *BIRC5* gene, encoding the surviving protein, was upregulated in doxorubicin resistant cells.

8) Drastic downregulation of estrogen receptor α (ESR1) in MCF-7/120nM DOC and MCF-7/1000nM DOX was observed where it remained unchanged in MCF-7/30nM DOC. Genes related to cell survival like Bcl-2 and Bcl-2-associated athanogene (BAG)-family proteins (*e.g.* BAG-1, BAG-3 and BAG-5) increased in in MCF-7/30nM DOC cells. In evaluation of expression analysis of *Bcl-2* and *Bax*, ratio of antiapoptotic *Bcl-2* to proapoptotic *Bax* expression was considered as a survival parameter which may contribute to drug reistance. Alterations in the ratio were fluctuating among docetaxel resistant sublines with significant changes in between 15 and 30nM docetaxel applications which were also concordant in alterations of Bcl-2 protein levels. These

concentrations may be critical for drug response and regulation of apoptotis. Increased APRIL (*TNFSF13*) level might also be correlated to decreased apoptotic potential of MCF-7/30nM DOC cells. Based on the anti-/apoptotic protein expression profile of MCF-7/30nM DOC, as well as increased Bcl-2/Bax ratio as demonstrated by RT-PCR and western blot, these sublines seemed to be more resistant to apoptosis including both intrinsic and extrinsic pathways. On the other hand, unchanged levels of Bcl-2 decreased expression levels of BAG family proteins in MCF-7/120nM DOC and MCF-7/1000nM DOX cells seems to be related to loss of estrogen receptor in these cells. MCF-7/120nM DOC and MCF-71000nM DOX cells seem to be more sensitive to apoptosis whereas drug resistance in these cells is related to other mechanisms. Thus, variances can be correlated with dose increament responses and stepwise acquirement of resistance.

9) Abberant expression levels of growth factors or their signaling cascades through ligand activation, cause changes in various pathways of cells including cell survival and proliferation or death. *EGFR* was overexpressed in both MCF-7/120nM DOC and MCF-7/1000nM DOX. *CTGF* was drastically upregulated only in MCF-7/120nM DOC cells. Substantial elevation of the gene in MCF-7/120nM DOC adreesses the question whether CTGF or downstream effectors prevent cells from docetaxel induced cytotoxicty.

10) *IL6* and *IL8,* reported for their survival and antiapototic functions in tumor cells were overexpressed in doxorubicin resistant cells. *IL18*, having a PI3K/Akt pathway dependent anti-apoptotic function, was also upregulated in MCF-7/120nM DOC and MCF-7/1000nM DOX.

11) Expression levels of genes related to epithelial-mesenchymal transition were evaluated in drug resistant cells in order to assess their involvement in drug resistance. Among the key regulatory elements of EMT transcription factor Slug was upregulated in both MCF-7/120nM DOC and MCF-7/1000nM DOX. ERα suppresses transcription factor Slug (*SNAI2*) expression by transcriptional repression. Downregulation of ERα in MCF-7/120nM DOC and MCF-7/1000nM DOX might have released transcriptional repression of ERα on Slug which could cause transcriptional activation of key regulatory elements of EMT. Slug gene promoter also contains a Sp1 binding site so it is also one of the downstream mediators of TGFB1 signalling. TGFBR2 together with TGFBR1 form heterodimeric receptor complexes and promote TGFB1 signalling through phosphorylated activation of SMAD2 and 3. Increased expression of TGFBR2 together

with SMAD3 probably enhanced TGFB1 induced EMT in resistant cells. Furthermore, amplified EGF signaling via receptor (EGFR) amplification might have stimulated pathways leading to EMT. Downregulation of E-cadherin and occludins with upregulation of mesenchymal markers like vimentin and N-cadherin are initial determinants of EMT. Accordingly, MCF-7/120nM DOC and MCF-7/1000nM DOX cells had cadherin switch with E-cadherin downregulation and N-cadherin upregulation as well as decreased occludin expression and increased vimentin expression. Since N-cadherin was well correlated to mammary gland development and transformation, as well as its association with FGFR1 stability and expression, it is possible that its upregulation was correlated to cellular proliferation and survival of drug resistant cells.

12) The adhesion of cells to each other or to the ECM is responsible for stimulating signals that regulate migration of immune cells, invasion/metastasis, and angiogenesis in tumor cells. Previous reports demonstrated the association between MDR phenotype with P-gp expression and increased invasive ability. Docetaxel and doxorubicin resistant sublines overexpressed a variety of genes encoding ECM proteins. These include integrins, collagens, laminins, fibronectins, claudin, glypican, keratin, syndecan, and microfibrils (fibrillins and fibulins). Integrin dependent cell attachment elicits integrin-mediated intracellular cell signaling which is among the survival pathways of normal and tumor cells. Laminins, collagens and fibronectins are among attachment proteins that mediate cell survival via integrin interactions and a collective increase in integrin signalling might be one of the mechanisms confering drug resistance. In addition, many ECM proteins (*e.g.* glypican, syndecan, microfibrils) have the function of the regulation of cell proliferation and survival, based on their capacity to modulate the activity of various growth and survival factors. MMPs and ADAMs play role on cell behavior such as cell proliferation, migration, differentiation, angiogenesis, and apoptosis, since they are involved in the cleavage of cell surface receptors, the release of apoptotic ligands, and chemokine in/activation as well as their participitation in integrin signaling. TIMPs specifically inhibit matrix metalloproteinases. MMP upregulation and TIMP downregulation might play role in drug resistance through growth factor and cytokine shedding, promoting survival signals in drug resistant cells and overcoming docetaxel and doxorubicin induced apoptosis, and inducing proliferative pathways of cells.

13) Class II, class III and class V β-tubulin expression level significantly increased in docetaxel resistant cells. These β-tubulin tubulin isotypes with higher microtubule-destabilizing potencies might be correlated to docetaxel resistance.

14) Docetaxel and doxorubicin resistant sublines developed varying degree of cross-resistance to different anticancer agents. MCF-7/120nM DOC cells developed cross-resistance to vincristine and tamoxifen, respectively. On the other hand, MCF-7/1000nM DOX cells developed cross-resistance to paclitaxel, docetaxel, tamoxifen and ATRA respectively. The cross-resistance indices were lower than the resistances developed to selective drugs. Since both sublines expressed *MDR1*, resistant cells development of cross-resistance to other P-gp substrates like paclitaxel, docetaxel and vincristine was expected. Nevertheless, it is probable that senstive MCF-7 cell line might become resistant to different drugs through diverse mechanisms, so that the sublines might have responded differently, such as in tamoxifen and ATRA cross-resistance which are not substrates of P-gp. Interestingly, according to microarray results, MCF-7/120nM DOC cells had reduced *CRABP2* (which fastens metabolism of retinoic acid resulting in decreased ATRA intracellular concentrations) expression. Moreover, RA hydroxylation enzyme CYP26A1, was also upregulated in MCF-7/1000nM DOX cells. So together with reduced *CRABP2* levels, elevated *CYP26A1* may explain development of ATRA cross-resistance in doxorubicin resistant cells but not in docetaxel resistant cells. Both docetaxel and doxorubicin resistant cells developed croos-resistance to tamoxifen. Since, tamoxifen exert its antiproliferative effect on estrogen receptor-positive breast cancer, lower estrogen receptor levels which might be cause of lower tamoxifen responsiveness in these cells.

15) MCF-7/120nM DOC cells were also significantly cross-resistant to irradiation. Although MCF-7/1000nM DOX subline was more chemoresistant than MCF-7/120nM DOC, it did not develop radioresistance. Some of the genes that are involved in repair to radiaition induced damage might have been induced only in docetaxel resistant cells.

16) Combinations of doxorubicin with docetaxel exerted significant synergic antiproliferative effects on the docetaxel resistant cells where tamoxifen exerted additive antiproliferative effects with docetaxel. On the other hand, combinations of paclitaxel, docetaxel and tamoxifen with doxorubicin exerted significant synergic effects on the doxorubicin resistant cells. Accordingly, tamoxifen can be used in combination with

both docetaxel and doxorubicin. Also effective combinations of doxorubicin with paclitaxel and docetaxel combination *in vitro* may be good models for *in vivo* combined chemotherapy in resistant breast tumors.

17) Verapamil, a clinically used calcium ion influx inhibitor and P-gp substrate, and promethazine, a clinically used oral antihistamine, were evaluated in order assess their modulator efficiency on docetaxel and doxorubicin resistant cells. Combined drug applications demonstrated that verapamil exerted synergic effects with both docetaxel and doxorubicin on MCF-7/120nM DOC and MCF-7/1000nM DOX, respectively. On the other hand, in combination promethazine was antagonist with docetaxel on MCF-7/120nM DOC and additive with doxorubicin on MCF-7/1000nM DOX. Verapamil application caused a decrease in *MDR1* expression in docetaxel and doxorubicin resistant cells in a time edepndent schedule. Similarly, expression of *MRP1* decreased verapamil treatment in MCF-7/120nM DOC. However, it increased with verapamil treatment in MCF-7/1000nM DOX as concordant with the expression profile observed in the development of doxorubicin resistance. Therefore, results further confimed the sequential emergence of *MDR1* and *MRP1* in doxorubicin resistant cells. Suppressive effect of verapamil on *MDR1* and *MRP1* at gene expression level besides its well known MDR modulation function at protein activity level was demonstrated. Similarly, regulatory effect of promethazine on gene expression level of *MDR1* was also demonstrated in MCF-7/120nM DOC and MCF-7/1000nM DOX. Promethazine application caused either complete loss or decrease in *MDR1* expression in resistant cells depending on time and concentration. Despite suppressive effects of promethazine on *MDR1*, it is not suitable for clinic reversal of docetaxel resistance for its combined antagonist effect with docetaxel. However, promethazine stil seems to be a candidate resistance modifier of doxorubicin resistance with its combined additive and gene suppressor effects on *MDR1*.

Mechanisms effecting on MCF-7 cells in conferring resistance to docetaxel and doxorubicin are summarized in Figures 4.1, 4.2 and 4.3 (for MCF-7/30nM DOC, MCF-7/120nM DOC and MCF-7/1000nM DOX, respectively).

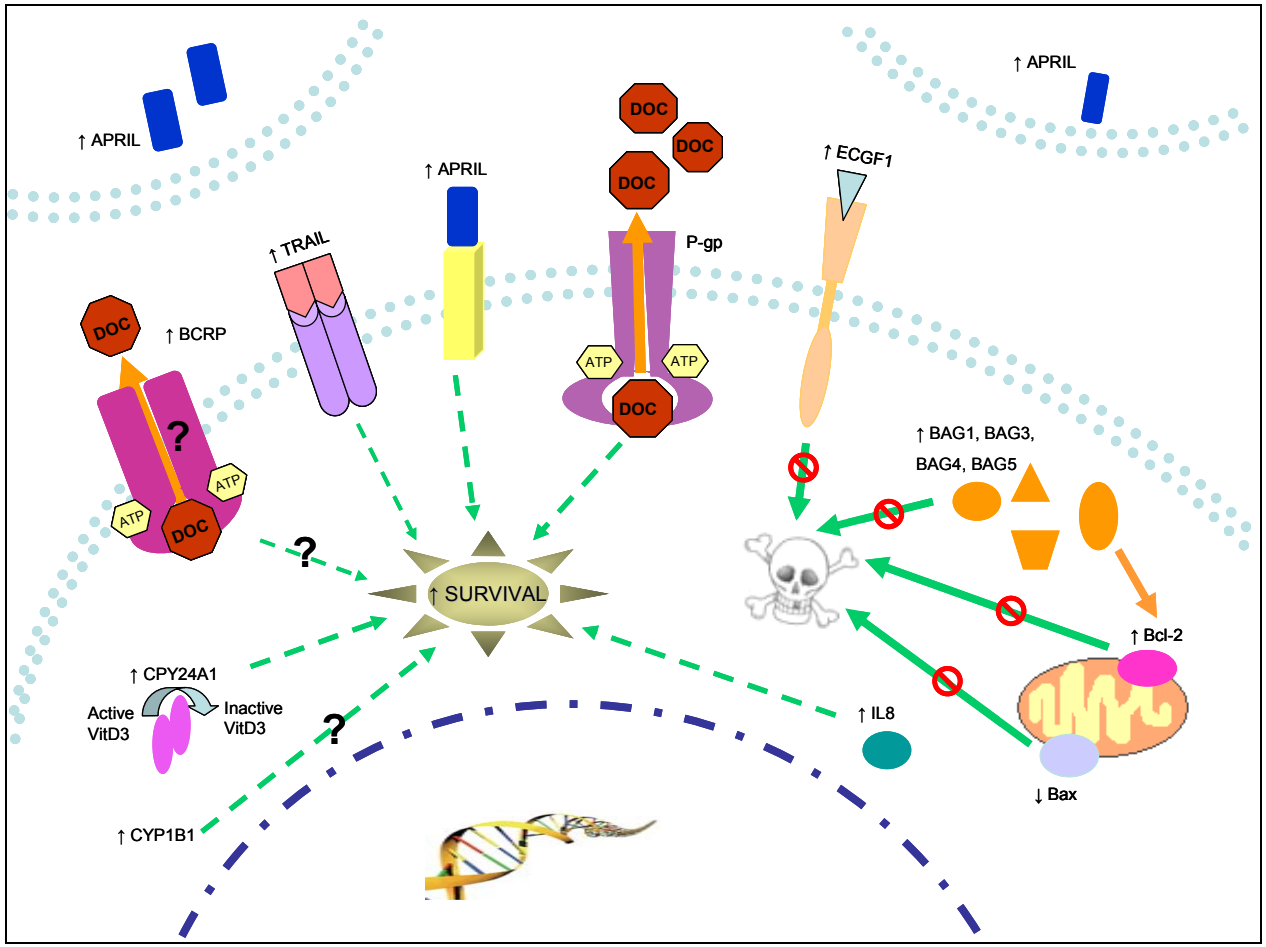

Figure 4.1 Schematic representation of mechanism of docetaxel resistance in MCF-7/30nM DOC.

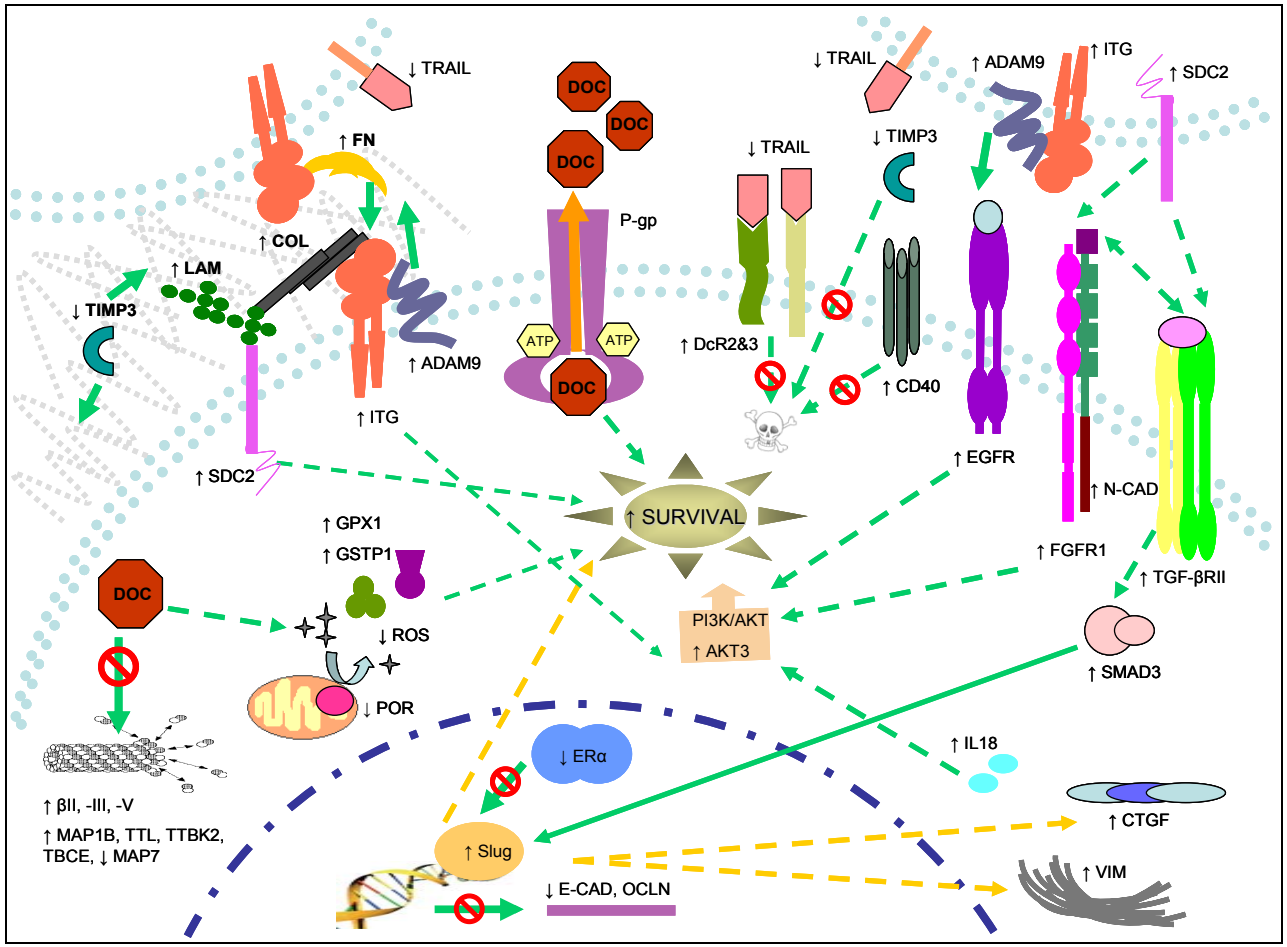

Figure 4.2 Schematic representation of mechanism of docetaxel resistance in MCF-7/120nM DOC.

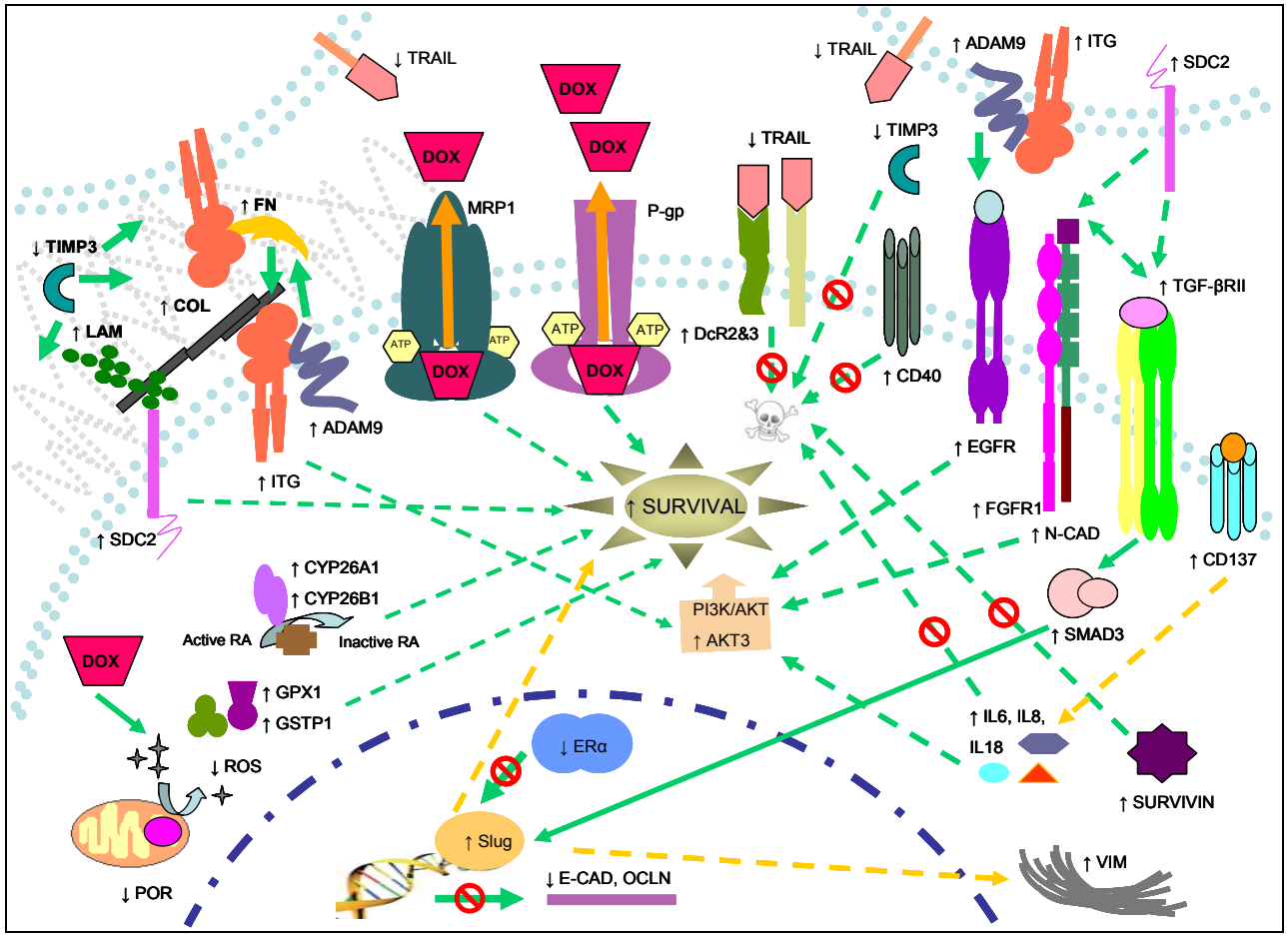

Figure 4.3 Schematic representation of mechanism of doxorubicin resistance in MCF-7/1000nM DOX.

In conclusion, this study elucidated some molecular mechanisms of docetaxel and doxorubicin resistance in breast carcinoma model cell line MCF-7 and evaluated efficacy of reversal agents on resistant sublines. Identification of resistance mechanisms may potentially personalize chemotherapy and increase the efficacy of chemotherapy with life quality of patients.

REFERENCES

21CEP Research Group, Paclitaxel (Taxol) mechanism of action. www.21cecpharm.com/px/action.htm, 10/2/2007.

Adamo V, Iorfida M, Montalto E, Festa V, Garipoli C, Scimone A, Zanghì M, Caristi N. Overview and new strategies in metastatic breast cancer (MBC) for treatment of tamoxifen-resistant patients. Ann Oncol 2007: 18; 53-57.

Affymetrix, GeneChip Human Genome U133 Plus 2.0 Array. www.affymetrix.com/products_services/arrays/specific/hgu133plus.affx, 12/4/2008.

Affymetrix, GeneChip One-Cycle Target Labeling and Control Reagents. www.affymetrix.com/products_services/reagents/specific/one_cycle_target_control.affx, 12/4/2008.

Ahmed N, Riley C, Rice G, Quinn M. Role of integrin receptors for fibronectin, collagen and laminin in the regulation of ovarian carcinoma functions in response to a matrix microenvironment. Clin Exp Metastasis. 2005; 22(5): 391-402.

Ahonen M, Baker AH, Kähäri VM. Adenovirus-mediated gene delivery of tissue inhibitor of metalloproteinases-3 inhibits invasion and induces apoptosis in melanoma cells. Cancer Res 1998; 58(11): 2310-5.

Akiba H, Nakano H, Nishinaka S, Shindo M, Kobata T, Atsuta M, Morimoto C, Ware CF, Malinin NL, Wallach D, Yagita H, Okumura K. CD27, a member of the tumor necrosis factor receptor superfamily, activates NF-kappaB and stress-activated protein kinase/c-Jun N-terminal kinase via TRAF2, TRAF5, and NF-kappaB-inducing kinase. J Biol Chem 1998; 273(21): 13353-8.

Allen JD, Schinkel AH. Multidrug resistance and pharmacological protection mediated by the breast cancer resistance protein (BCRP/ABCG2). Molecular Cancer Therapeutics 2002; 1: 427-34.

Amour A, Slocombe PM, Webster A, Butler M, Knight CG, Smith BJ, Stephens PE, Shelley C, Hutton M, Knäuper V, Docherty AJ, Murphy G. TNF-alpha converting enzyme (TACE) is inhibited by TIMP-3. FEBS Lett. 1998; 435(1): 39-44.

Amundson SA, Grace MB, McLeland CB, Epperly MW, Yeager A, Zhan Q, Greenberger JS, Fornace AJ Jr. Human in vivo radiation-induced biomarkers: gene expression changes in radiotherapy patients. Cancer Res 2004; 64: 6368-71.

Andreadis C, Gimotty PA, Wahl P, Hammond R, Houldsworth J, Schuster SJ, Rebbeck TR. Members of the glutathione and ABC-transporter families are associated with clinical outcome in patients with diffuse large B-cell lymphoma. Blood 2007; 109(8): 3409-3416.

Angus WGR, Larsen MC, Jefcoate CR. Expression of CYP1A1 and CYP1B1 depends on cell-specific factors in human breast cancer cell lines: role of estrogen receptor status. Carcinogenesis 1999; 20(6): 947-955.

Aoudjit F, Vuori K. Integrin signaling inhibits paclitaxel-induced apoptosis in breast cancer cells. Oncogene. 2001; 20(36): 4995-5004.

Bernard-Marty C, Treilleux I, Dumontet C, Cardoso F, Fellous A, Gancberg D, Bissery MC, Paesmans M, Larsimont D, Piccart MJ, Di Leo A. Microtubule-associated parameters as predictive markers of docetaxel activity in advanced breast cancer patients: results of a pilot study. Clin Breast Cancer 2002; 3: 341-345.

Bacus SS, Kiguchi K, Chin D, King CR and Huberman E: Differentiation of cultured human breast cancer cells (AU-565 and MCF-7) associated with loss of cell surface HER-2/neu antigen. Mol Carcinogen 1990; 3(6): 350-362.

Banerjee A. Increased levels of tyrosinated α-, βIII-, and βIV-tubulin isotypes in paclitaxel-resistant MCF-7 breast cancer cell. Biochem Bioph Res Co 2002; 293:598-601.

Banerjee A, Roach MC, Trcka P, Luduena RF. Increased microtubule assembly in bovine brain tubulin lacking the type III isotype of beta-tubulin. J Biol Chem 1990; 265:1794-1799.

Baron BW, Zeleznik-Le N, Baron MJ, Theisler C, Huo D, Krasowski MD, Thirman MJ, Baron RM, Baron JM. Repression of the PDCD2 gene by BCL6 and the implications for the pathogenesis of human B and T cell lymphomas. Proc Natl Acad Sci USA 2007; 104(18): 7449-54.

Baxendale AJ, Dawson CW, Stewart SE, Mudaliar V, Reynolds G, Gordon J, Murray PG, Young LS, Eliopoulos AG. Constitutive activation of the CD40 pathway promotes cell transformation and neoplastic growth. Oncogene 2005; 24: 7913-23.

Beck V, Herold H, Benge A, Luber B, Hutzler P, Tschesche H, Kessler H, Schmitt M, Geppert HG, Reuning U. ADAM15 decreases integrin alphavbeta3/vitronectin-mediated

ovarian cancer cell adhesion and motility in an RGD-dependent fashion. Int J Biochem Cell Biol 2005; 37(3): 590-603.

Bergametti F, Denier C, Labauge P, Arnoult M, Boetto S, Clanet M, Coubes P, Echenne B, Ibrahim R, Irthum B, Jacquet G, Lonjon M, Moreau JJ, Neau JP, Parker F, Tremoulet M, Tournier-Lasserve E; Société Française de Neurochirurgie. Mutations within the programmed cell death 10 gene cause cerebral cavernous malformations. Am J Hum Genet 2005; 76(1): 42-51.

Bergonié J, Tribondeau L. Interpretation of some results from radiotherapy and an attempt to determine a rational treatment technique. 1906. Yale J Biol Med 2003; 76(4-6):181-2.

Bhattacharya R, Cabral F. A ubiquitous β-tubulin distrupts microtubule assembly and inhibits cell proliferation. Mol Biol Cell 2004; 15:3123-3131.

Bialik S, Kimchi A. The death-associated protein kinases: structure, function, and beyond. Annu Rev Biochem 2006; 75: 189-210.

Black MM, Slaughter T, Fischer I. Microtubule-associated protein 1b (MAP1b) is concentrated in the distal region of growing axons. J Neurosci 1994; 14(2): 857-70.

Bloom GS, Luca FC, Vallee RB. Microtubule-associated protein 1B: identification of a major component of the neuronal cytoskeleton. Proc Natl Acad Sci U S A 1985; 82(16): 5404-8

Bodo A, Bakos E, Szeri F, Varadi A, Sarkadi B. The role of multidrug transporters in drug availability, metabolism and toxicity. Toxicol Lett 2003; 140: 133-43.

Borsellino N, Belldegrun A, Bonavida B. Endogenous interleukin 6 is a resistance factor for cis-diamminedichloroplatinum and etoposide-mediated cytotoxicity of human prostate carcinoma cell lines. Cancer Res 1995; 55(20): 4633-9.

Borst J, Hendriks J, Xiao Y. CD27 and CD70 in T cell and B cell activation. Curr Opin Immunol 2005;17(3): 275-81.

Borst P, Evers R, Kool M, Wijnholds J. A family of drug transporters: the multidrug resistance-associated proteins. J Natl Cancer Inst 2000; 92(16): 1295-302.

Bournique B, Lemarie A. Docetaxel (Taxotere) is not metabolized by recombinant human CYP1B1 in vitro, but acts as an effector of this isozyme. Drug Metab Dispos 2002; 30: 1149-1152.

Boylan JF, Gudas LJ. The level of CRABP-I expression influences the amounts and types of all-trans-retinoic acid metabolites in F9 teratocarcinoma stem cells. J Biol Chem 1992; 267(30): 21486-91.

Bradford MM. Rapid and sensitive method for quantitation of microgram quantities of protein utilizing principle of protein-dye binding. Anal Biochem 1976; 72: 248-254.

Brat DJ, Bellail AC, Van Meir EG. The role of interleukin-8 and its receptors in gliomagenesis and tumoral angiogenesis. Neuro-Oncology 2007; 7: 122-133.

Brimmell M, Burns JS, Munson P, McDonald L, O'Hare MJ, Lakhani SR, Packham G. High level expression of differentially localized BAG-1 isoforms in some oestrogen receptor-positive human breast cancers. Br J Cancer 1999; 81(6): 1042-51.

Brock I, Hipfner DR, Nielsen BS, Jensen PB, Deeley RG, Cole SP, Sehested M. Sequential coexpression of the multidrug resistance genes MRP and mdr1 and their products in VP-16 (etoposide)-selected H69 small cell lung cancer cells. Cancer Res 1995; 55(3): 459-62.

Bronstein JM, Chen K, Tiwari-Woodruff S, Kornblum HI. Developmental expression of OSP/claudin-11. J Neurosci Res 2000; 60(3): 284-90.

Burger H, Foekens JA, Look MP, Meijer-van Gelder ME, Klijn JG, Wiemer EA, Stoter G, Nooter K. RNA expression of breast cancer resistance protein, lung resistance-related protein, multidrug resistance-associated proteins 1 and 2, and multidrug resistance gene 1 in breast cancer: correlation with chemotherapeutic response. Clin Cancer Res 2003; 9(2): 827-36.

Caposio P, Gugliesi F, Zannetti C, Sponza S, Mondini M, Medico E, Hiscott J, Young HA, Gribaudo G, Gariglio M, Landolfo S. A novel role of the interferon-inducible protein IFI16 as inducer of proinflammatory molecules in endothelial cells. J Biol Chem 2007; 282(46): 33515-29.

Carrozzino F, Soulié P, Huber D, Mensi N, Orci L, Cano A, Féraille E, Montesano R. Inducible expression of Snail selectively increases paracellular ion permeability and differentially modulates tight junction proteins. Am J Physiol Cell Physiol 2005; 289(4): C1002-14.

Chaudhry SS, Cain SA, Morgan A, Dallas SL, Shuttleworth CA, Kielty CM. Fibrillin-1 regulates the bioavailability of TGFbeta1. J Cell Biol 2007; 176(3): 355-67.

Chen DJ, Nirodi CS. The epidermal growth factor receptor: a role in repair of radiation-induced DNA damage. Clin Cancer Res 2007; 13(22 Pt 1): 6555-60.

Chen L, Klass C, Woods A. Syndecan-2 regulates transforming growth factor-beta signaling. J Biol Chem 2004; 279(16): 15715-8.

Christofori G. Changing neighbours, changing behaviour: cell adhesion molecule-mediated signalling during tumour progression. EMBO J 2003; 22(10): 2318-23.

Choi CH, Kim HS, Rha HS, Jeong JH, Park YH, Min YD, Kee KH, Lim DY. Drug concentration-dependent expression of multidrug resistance-associated protein and P-glycoprotein in the doxorubicin-resistant acute myelogenous leukemia sublines. Mol Cells 1999; 9(3): 314-9.

Choi J, Park SY, Joo CK. Transforming growth factor-beta1 represses E-cadherin production via slug expression in lens epithelial cells. Invest Ophthalmol Vis Sci 2007; 48(6): 2708-18.

Choi Y, Kim SY, Park K, Yang J, Cho KJ, Kwon HJ, Byun Y. Chemopreventive efficacy of all-trans-retinoic acid in biodegradable microspheres against epithelial cancers: results in a 4-nitroquinoline 1-oxide-induced oral carcinogenesis model. Int J Pharm 2006; 320 (1-2): 45-52.

Chomczynski PS: Single step method of RNA isolation by acid guanidium thiocyanate-phenol-chloroform extraction. Anal Biochem 1987; 162: 156-159.

Choubey D, Deka R, Ho SM. Interferon-inducible IFI16 protein in human cancers and autoimmune diseases. Front Biosci 2008; 13: 598-608.

Chun E, Lee KY. Bcl-2 and Bcl-XL are important for the induction of paclitaxel resistance in human hepatocellular carcinoma cells. Biochem Biophys Research Commun 2004; 315: 771-9.

Ciardiello F, Caputo R, Borriello G, Del Bufalo D, Biroccio A, Zupi G, Bianco AR, Tortora G. ZD1839 (IRESSA), an EGFR-selective tyrosine kinase inhibitor, enhances taxane activity in bcl-2 overexpressing, multidrug-resistant MCF-7 ADR human breast cancer cells. Int J Cancer 2002; 98(3): 463-9.

Clarke SJ, Rivory LP. Clinical pharmacokinetics of docetaxel. Clin Pharmacokinet 1999; 36(2): 99-114.

Clemons M, Leahy M, Valle J, Jayson G, Ranson M, Howell A. Clinical Oncology Update, Review of recent trials of chemotherapy for advanced breast cancer: the taxanes. Eur J Cancer 1997; 33: 2183-93.

Cobley JG, Clark AC, Weerasurya S, Queseda FA, Xiao JY, Bandrapali N, D'Silva I, Thounaojam M, Oda JF, Sumiyoshi T, Chu MH: CpeR is an activator required for expression of the phycoerythrin operon (cpeBA) in the cyanobacterium Fremyella diplosiphon and is encoded in the phycoerythrin linker-polypeptide operon (cpeCDESTR). Mol Microbiol 2002; 44(6): 1517-31.

Cole SP, Bhardwaj G, Gerlach JH, Mackie JE, Grant CE, Almquist KC, Stewart AJ, Kurz EU, Duncan AM, Deeley RG. Overexpression of a transporter gene in a multidrug-resistant human lung cancer cell line. Science 1992; 258(5088): 1650-4.

Coleman AB. Positive and negative regulation of cellular sensitivity to anti-cancer drugs by FGF-2. Drug Resist Updat 2003; 6(2): 85-94.

Coley HM. Mechanisms and strategies to overcome chemotherapy resistance in metastatic breast cancer. Cancer Treat Rev 2008; 34(4): 378-90.

Conze D, Weiss L, Regen PS, Bhushan A, Weaver D, Johnson P, Rincón M. Autocrine production of interleukin 6 causes multidrug resistance in breast cancer cells. Cancer Res 2001; 61(24): 8851-8.

Cory S, Huang DC, Adams JM. The Bcl-2 family: roles in cell survival and oncogenesis. Oncogene 2003; 22(53): 8590-607.

Crown J. Docetaxel: Overview of an active drug for breast cancer. The Oncologist 2001; 6: 1-4.

Crown J, O'Leary M, Ooı W-S. Docetaxel and paclitaxel in the treatment of breast cancer: A review of clinical experience. The Oncologist 2004; 9 (suppl 2): 24-32.

Cummings J, Allan L, Willmott N, Riley R, Workman P, Smyth JF. The enzymology of doxorubicin quinone reduction in tumour tissue. Biochem Pharmacol 1992;44(11): 2175-83.

Dalton WS. Mechanisms of drug resistance in hematologic malignancies. Semin Hematol 1997; 34: 3-8.

Danial NN. BCL-2 family proteins: critical checkpoints of apoptotic cell death. Clin Cancer Res 2007; 13(24): 7254-63.

Dean M, Hamon Y, Chiminib G. The human ATP-binding cassette (ABC) transporter superfamily. J Lipid Res 2001; 42: 1007-17.

Dean M, Rzhetsky A, Allikmets R. The human ATP-binding cassette (ABC) transporter superfamily. Genome Res 2001: 11; 1156-66.

Del Bufalo D, Biroccio A, Trisciuoglio D, Bruno T, Floridi A, Aquino A, Zupi G. Bcl-2 has differing effects on the sensitivity of breast cancer cells depending on the antineoplastic drug used. Eur J Cancer 2002; 38(18): 2455-62.

Dell KJB, Hassel B, Doyle LA, Ross DD. Prometer characterization and genomic organization of the human breast cancer resistance protein (ATP-binding cassette transporter G2) gene. BBA 2001; 1520: 234-41.

Delva L, Cornic M, Balitrand N, Guidez F, Micléa JM, Delmer A, Teillet F, Fenaux P, Castaigne S, Degos L, et al. Resistance to all-trans retinoic acid (ATRA) therapy in relapsing acute promyelocytic leukemia: study of in vitro ATRA sensitivity and cellular retinoic acid binding protein levels in leukemic cells. Blood 1993; 82(7): 2175-81.

Dhawan P, Singh AB, Deane NG, No Y, Shiou SR, Schmidt C, Neff J, Washington MK, Beauchamp RD. Claudin-1 regulates cellular transformation and metastatic behavior in colon cancer. J Clin Invest 2005; 115(7): 1765-76.

Dong M, How T, Kirkbride KC, Gordon KJ, Lee JD, Hempel N, Kelly P, Moeller BJ, Marks JR, Blobe GC. The type III TGF-beta receptor suppresses breast cancer progression. J Clin Invest 2007; 117(1): 206-17.

Doong H, Vrailas A, Kohn EC. What's in the 'BAG'?--A functional domain analysis of the BAG-family proteins. Cancer Lett 2002; 188(1-2): 25-32.

Doyle LA, Yang W, Abruzzo LV, Krogmann T, Gao Y, Rishi AK, Ross DD. A multidrug resisrance transporter from human MCF-7 breast cancer cells. Proc Natl Acad Sci 1998; 95: 15665-70.

Dozier JH, Hiser L, Davis JA, Thomas NS, Tucci MA, Benghuzzi HA, Frankfurter A, Correia JJ, Lobert S: β class II tubulin predominates in normal and tumor breast tissues, Breast Cancer Res 2003; 5: R157-R169.

Drewes G, Ebneth A, Preuss U, Mandelkow EM, Mandelkow E. MARK, a novel family of protein kinases that phosphorylate microtubule-associated proteins and trigger microtubule disruption. Cell. 1997; 89(2): 297-308.

Drukman S, Kavallaris M. Microtubule alterations and resistance to tubulin-binding agents (Review). Int J Oncol 2002; 21: 621-8.

Duan Z, Brakora KA, Seiden MV. Inhibition of ABCB1 (MDR1) and ABCB4 (MDR3) expression by small interfering RNA and reversal of paclitaxel resistance in human ovarian cancer cells. Molecular Cancer Theraupetics 2004; 3: 833-8.

Duan Z, Feller AJ, Penson RT, Chabner BA, Seiden MV. Discovery of differentially expressed genes associated with paclitaxel resistance using cDNA array technology: analysis of interleukin (IL) 6, IL-8, and monocyte chemotactic protein 1 in the paclitaxel-resistant phenotype. Clin Cancer Res 1999; 5(11): 3445-53.

Duncan MR, Frazier KS, Abramson S, Williams S, Klapper H, Huang X, Grotendorst GR. Connective tissue growth factor mediates transforming growth factor beta-induced collagen synthesis: down-regulation by cAMP. FASEB J 1999; 13(13): 1774-86.

Dvorák Z, Vrzal R, Ulrichová J, Macejová D, Ondková S, Brtko J. Expression, protein stability and transcriptional activity of retinoic acid receptors are affected by microtubules interfering agents and all-trans-retinoic acid in primary rat hepatocytes. Mol Cell Endocrinol 2007; 267(1-2): 89-96.

Ee PL, Kamalakaran S, Tonetti D, He X, Ross DD, Beck WT. Identification of a novel estrogen response element in the breast cancer resistance protein (ABCG2) gene. Cancer Res 2004; 64(4): 1247-51.

Endicott JA, Ling V. The biochemistry of P-glycoprotein-mediated multidrug resistance. Annu Rev Biochem 1989; 58: 137-71.

Eisenblätter T, Hüwel S, Galla HJ. Characterisation of the brain multidrug resistance protein (BMDP/ABCG2/BCRP) expressed at the blood-brain barrier. Brain Res 2003; 971(2): 221-31.

Eliopoulos GM, Moellering JR RC. Antimicrobial combinations. In: Lorian V, eds. Antibiotics in Laboratory Medicine. USA, Williams and Wilkins. 1980, pp 432-443.

Enju A, Palmieri FM, Perez EA. Weekly administration of docetaxel and paclitaxel in metastatic or advanced breast cancer. Oncologist 2005; 10: 665-685.

Engi H, Gyemant N, Lorand T, Levai A, Ocsovszki I, Molnar J. Cinnamylidene ketones as potential modulators of multidrug resistance in mouse lymphoma and human colon cancer cell lines. In Vivo 2006; 20: 119-124.

Esparza J, Vilardell C, Calvo J, Juan M, Vives J, Urbano-Márquez A, Yagüe J, Cid MC. Fibronectin upregulates gelatinase B (MMP-9) and induces coordinated expression of gelatinase A (MMP-2) and its activator MT1-MMP (MMP-14) by human T lymphocyte

cell lines. A process repressed through RAS/MAP kinase signaling pathways. Blood 1999; 94(8): 2754-66.

Evans DB, Rank KB, Bhattacharya K, Thomsen DR, Gurney ME, Sharma SK. Tau phosphorylation at serine 396 and serine 404 by human recombinant tau protein kinase II inhibits tau's ability to promote microtubule assembly. J Biol Chem 2000; 275(32):24977-83.

Fan CW, Chan CC, Chao CC, Fan HA, Sheu DL, Chan EC. Expression patterns of cell cycle and apoptosis-related genes in a multidrug-resistant human colon carcinoma cell line. Scand J Gastroenterol 2004; 39(5): 464-9.

Faridi J, Wang L, Endemann G, Roth RA. Expression of constitutively active Akt-3 in MCF-7 breast cancer cells reverses the estrogen and tamoxifen responsivity of these cells in vivo. Clin Cancer Res 2003; 9(8): 2933-9.

Fears CY, Gladson CL, Woods A. Syndecan-2 is expressed in the microvasculature of gliomas and regulates angiogenic processes in microvascular endothelial cells. J Biol Chem 2006; 281(21): 14533-6.

Filmus J, Selleck SB. Glypicans: proteoglycans with a surprise. J Clin Invest 2001; 108(4): 497-501.

Fine RL, Chen J, Balmaceda C, Bruce JN, Huang M, Desai M, Sisti MB, McKhann GM, Goodman RR, Bertino JS Jr, Nafziger AN, Fetell MR. Randomized Study of Paclitaxel and Tamoxifen Deposition into Human Brain Tumors: Implications for the Treatment of Metastatic Brain Tumors. Clin Cancer Res 2006; 12: 5770-6.

Finger EC, Turley RS, Dong M, How T, Fields TA, Blobe GC. TbetaRIII suppresses non-small cell lung cancer invasiveness and tumorigenicity. Carcinogenesis 2008; 29(3): 528-35.

Fischer OM, Hart S, Gschwind A, Prenzel N, Ullrich A. Oxidative and Osmotic Stress Signaling in Tumor Cells Is Mediated by ADAM Proteases and Heparin-Binding Epidermal Growth Factor. Mol Cell Biol 2004; 24(12): 5172-83.

Ford JM, Prozialeck WC, Hait WW. Structural features determining activity of phenothiazines and related drugs for inhibition of cell growth and reversal of multidrug resistance. Mol Pharmacol 1989; 35: 105-15.

Giaccone G, Pinedo HM. Drug Resistance. Oncologist 1996; 1(1 & 2): 82-87.

Giannakakau P, Gussio R, Nogales E, Downing K, Fojo T. A common pharmacophore for epothilone and taxanes: Molecular basis of drug resistance conferred by tubulin mutations in human cancer cells. Proc Natl Acad Sci USA 2000; 97: 2904-9.

Giannakakou P, Sackett DL, Kang YK, Zhan Z, Buters JT, Fojo T, Poruchynsky MS. Paclitaxel-resistant human ovarian cancer cells have mutant beta-tubulins that exhibit impaired paclitaxel-driven polymerization. J Biol Chem 1997; 272:17118-17125.

Glavinas H, Krajcsi P, Cserepes J, Sarkadi B. The Role of ABC Transporters in Drug Resistance, Metabolism and Toxicity. Current Drug Delivery 2004; 1: 27-42.

Gowardhan B, Douglas DA, Mathers ME, McKie AB, McCracken SR, Robson CN, Leung HY. Evaluation of the fibroblast growth factor system as a potential target for therapy in human prostate cancer. Br J Cancer 2005; 92(2): 320-7.

Grünert S, Jechlinger M, Beug H. Diverse cellular and molecular mechanisms contribute to epithelial plasticity and metastasis. Nat Rev Mol Cell Biol 2003; 4(8): 657-65.

Gundersen GG, Kalnoski MH, Bulinski JC. Distinct populations of microtubules: tyrosinated and nontyrosinated alpha tubulin are distributed differently in vivo. Cell 1984; 38(3): 779-89.

Hahne M, Kataoka T, Schröter M, Hofmann K, Irmler M, Bodmer JL, Schneider P, Bornand T, Holler N, French LE, Sordat B, Rimoldi D, Tschopp J. APRIL, a new ligand of the tumor necrosis factor family, stimulates tumor cell growth. J Exp Med 1998; 188(6): 1185-90.

Hajra KM, Chen DY, Fearon ER. The SLUG zinc-finger protein represses E-cadherin in breast cancer. Cancer Res 2002; 62(6): 1613-8.

Han Z, Ni J, Smits P, Underhill CB, Xie B, Chen Y, Liu N, Tylzanowski P, Parmelee D, Feng P, Ding I, Gao F, Gentz R, Huylebroeck D, Merregaert J, Zhang L. Extracellular matrix protein 1 (ECM1) has angiogenic properties and is expressed by breast tumor cells. FASEB J 2001; 15(6): 988-94.

Hari M, Yang H, Zeng C, Canizales M, Cabral F. Expression of class III β-tubulin reduces microtubule assembly and confers resistance to paclitaxel. Cell Motil Cytoskel 2003; 56: 45-56.

Hasegawa S, Miyoshi Y, Egawa C, Ishitobi M, Tamaki Y, Monden M, Noguchi S. Mutational analysis of the class I beta-tubulin gene in human breast cancer. Int J Cancer 2002; 101:46-51.

Hasegawa S, Miyoshi Y, Egawa C, Ishitobi M, Taguchi T, Tamaki Y, Monden M, Noguchi S. Prediction of response to docetaxel by quantitative analysis of class I and III beta-tubulin isotype mRNA expression in human breast cancers. Clin Cancer Res 2003; 9: 2992-2997.

Hase H, Kanno Y, Kojima H, Morimoto C, Okumura K, Kobata T. CD27 and CD40 inhibit p53-independent mitochondrial pathways in apoptosis of B cells induced by B cell receptor ligation. J Biol Chem 2002; 277(49): 46950-8.

Helland A, Johnsen H, Frøyland C, Landmark HB, Saetersdal AB, Holmen MM, Gjertsen T, Nesland JM, Ottestad W, Jeffrey SS, Ottestad LO, Rodningen OK, Sherlock G, Børresen-Dale AL. Radiation-induced effects on gene expression: An in vivo study on breast cancer. Radiother Oncol 2006; 80: 230-5.

Helleman J, Jansen MP, Ruigrok-Ritstier K, van Staveren IL, Look MP, Meijer-van Gelder ME, Sieuwerts AM, Klijn JG, Sleijfer S, Foekens JA, Berns EM. Association of an extracellular matrix gene cluster with breast cancer prognosis and endocrine therapy response. Clin Cancer Res 2008; 14(17): 5555-64.

Hempel N, How T, Cooper SJ, Green TR, Dong M, Copland JA, Wood CG, Blobe GC. Expression of the type III TGF-beta receptor is negatively regulated by TGF-beta. Carcinogenesis 2008; 29(5): 905-12.

Ho EA, Piquette-Miller M. Regulation of multidrug resistance by pro-inflammatory cytokines. Curr Cancer Drug Targets 2006; 6(4): 295-311.

Honjo Y, Hrycyna CA, Yan QW, Medina-Pérez WY, Robey RW, van de Laar A, Litman T, Dean M, Bates SE. Acquired mutations in the MXR/BCRP/ABCP gene alter substrate specificity in MXR/BCRP/ABCP-overexpressing cells. Cancer Res 2001; 61(18): 6635-9.

Hosotani Y, Kashiwamura S, Kimura-Shimmyo A, Sekiyama A, Ueda H, Ikeda T, Mimura O, Okamura H. Interleukin-18 prevents apoptosis via PI3K/Akt pathway in normal human keratinocytes. J Dermatol 2008; 35(8): 514-24.

Howell A, Sims AH, Ong KR, Harvie MN, Evans DG, Clarke RB. Mechanisms of Disease: prediction and prevention of breast cancer--cellular and molecular interactions. Nat Clin Pract Oncol 2005; 2(12): 635-46.

Hoyt DG, Rusnak JM, Mannix RJ, Modzelewski RA, Johnson CS, Lazo JS. Integrin activation suppresses etoposide-induced DNA strand breakage in cultured murine tumor-derived endothelial cells. Cancer Res 1996; 56 :4146-4149.

Huang Y, Ray S, Reed JC, Ibrado AM, Tang C, Nawabi A, Bhalla K. Estrogen increases intracellular p26Bcl-2 to p21Bax ratios and inhibits taxol-induced apoptosis of human breast cancer MCF-7 cells. Breast Cancer Res Treat 1997; 42(1): 73-81.

Huesker M, Folmer Y, Schneider M, Fulda C, Blum HE, Hafkemeyer P. Reversal of drug resistance of hepatocellular carcinoma cells by adenoviral delivery of anti-MDR1 ribozymes. Hepatology 2002; 36: 874-84.

Ikeda R, Tajitsu Y, Iwashita K, Che XF, Yoshida K, Ushiyama M, Furukawa T, Komatsu M, Yamaguchi T, Shibayama Y, Yamamoto M, Zhao HY, Arima J, Takeda Y, Akiyama S, Yamada K. Thymidine phosphorylase inhibits the expression of proapoptotic protein BNIP3. Biochem Biophys Res Commun 2008; 370(2): 220-4.

Imaginis, Breast cancer treatment options. www.imaginis.com/breasthealth/staging.asp. 4/5/2008

Imaginis, Staging and Survival Rates of Breast Cancer. www.imaginis.com/breasthealth/treatment.asp. 4/5/2008

Integrative Medical Arts Group, Inc, Adriamycin. home.caregroup.org/clinical/altmed/interactions/Images/Drugs/doxorubi.gif, 23/5/2008.

Irizarry RA, Hobbs B, Collin F, Beazer-Barclay YD, Antonellis KJ, Scherf U, Speed TP. Exploration, normalization, and summaries of high density oligonucleotide array probe level data. Biostatistics 2003; 4(2): 249-64.

Ishimura N, Isomoto H, Bronk SF, Gores GJ. Trail induces cell migration and invasion in apoptosis-resistant cholangiocarcinoma cells. Am J Physiol Gastrointest Liver Physiol 2006; 290(1): G129-36.

Jang CW, Chen CH, Chen CC, Chen JY, Su YH, Chen RH. TGF-beta induces apoptosis through Smad-mediated expression of DAP-kinase. Nat Cell Biol 2002; 4(1): 51-8.

Jethwa P, Naqvi M, Hardy RG, Hotchin NA, Roberts S, Spychal R, Tselepis C. Overexpression of Slug is associated with malignant progression of esophageal adenocarcinoma. World J Gastroenterol 2008; 14(7): 1044-52.

Jiang Y, Wang M, Celiker MY, Liu YE, Sang QX, Goldberg ID, Shi YE. Stimulation of mammary tumorigenesis by systemic tissue inhibitor of matrix metalloproteinase 4 gene delivery. Cancer Res 2001; 61(6): 2365-70.

Jechlinger M, Grunert S, Tamir IH, Janda E, Lüdemann S, Waerner T, Seither P, Weith A, Beug H, Kraut N. Expression profiling of epithelial plasticity in tumor progression. Oncogene 2003; 22(46): 7155-69.

Johnson AL, Ratajczak C, Haugen MJ, Liu HK, Woods DC. Tumor necrosis factor-related apoptosis inducing ligand expression and activity in hen granulosa cells. Reproduction 2007; 133(3): 609-16.

Joza N, Susin SA, Daugas E, Stanford WL, Cho SK, Li CY, Sasaki T, Elia AJ, Cheng HY, Ravagnan L, Ferri KF, Zamzami N, Wakeham A, Hakem R, Yoshida H, Kong YY, Mak TW, Zúñiga-Pflücker JC, Kroemer G, Penninger JM. Essential role of the mitochondrial apoptosis-inducing factor in programmed cell death. Nature 2001; 410(6828): 549-54.

Kajita M, McClinic KN, Wade PA. Aberrant expression of the transcription factors snail and slug alters the response to genotoxic stress. Mol Cell Biol 2004; 24(17): 7559-66.

Kars MD, Iseri OD, Gunduz U, Ural AU, Arpaci F, Molnar J. Development of rational in vitro models for drug resistance in breast cancer and modulation of MDR by selected compounds. Anticancer Research 2006; 26: 4559-4568.

Kars MD, Işeri OD, Gunduz U, Molnar J. Reversal of multidrug resistance by synthetic and natural compounds in drug-resistant MCF-7 cell lines. Chemotherapy 2008; 54(3): 194-200.

Kavallaris M, Dennis Y, Kuo S, Burkhart CA, Regl DL, Norris MD, Haber M, Horwitz SB. Taxol-resistant epithelial ovarian tumors are associated with altered expression of specific β-tubulin isotypes. J Clin Invest 1997; 100:1282-1293.

Kavallaris M, Burkhart CA, Horwitz SB. Antisense oligonucleotides to class III β-tubulin sensitize drug-resistant cells to Taxol. Brit J Cancer 1999; 80:1020-1025.

Kavallaris M, Tait AS, Walsh BJ, He L, Horwitz SB, Norris MD, Haber M. Multiple microtubule alterations are associated with vinca alkaloid resistance in human leukemia cells. Cancer Res 2001; 61:5803-5809.

Keller M, Rüegg A, Werner S, Beer HD. Active caspase-1 is a regulator of unconventional protein secretion. Cell 2008; 132(5): 818-31.

Kern C, Cornuel JF, Billard C, Tang R, Rouillard D, Stenou V, Defrance T, Ajchenbaum-Cymbalista F, Simonin PY, Feldblum S, Kolb JP. Involvement of BAFF and APRIL in the resistance to apoptosis of B-CLL through an autocrine pathway. Blood 2004; 103(2): 679-88.

Kerr JF, Wyllie AH, Currie AR. Apoptosis: a basic biological phenomenon with wide-ranging implications in tissue kinetics. Br J Cancer 1972; 26: 239-57.

Hewitt KJ, Agarwal R, Morin PJ. The claudin gene family: expression in normal and neoplastic tissues. BMC Cancer 2006; 6: 186.

Kitazono M, Takebayashi Y, Ishitsuka K, Takao S, Tani A, Furukawa T, Miyadera K, Yamada Y, Aikou T, Akiyama S. Prevention of hypoxia-induced apoptosis by the angiogenic factor thymidine phosphorylase. Biochem Biophys Res Commun 1998; 253(3): 797-803.

Knowlden JM, Hutcheson IR, Jones HE, Madden T, Gee JM, Harper ME, Barrow D, Wakeling AE, Nicholson RI. Elevated levels of epidermal growth factor receptor/c-erbB2 heterodimers mediate an autocrine growth regulatory pathway in tamoxifen-resistant MCF-7 cells. Endocrinology 2003; 144: 1032–1044.[

Knutsen T, Rao VK, Ried T, Mickley L, Schneider E, Miyake K, Ghadimi BM, Padilla-Nash H, Pack S, Greenberger L, Cowan K, Dean M, Fojo T, Bates S. Amplification of 4q21-q22 and the MXR Gene in independently derived Mitoxantrone-Resistant cell lines. Genes Chromosomes Cancer 2000; 27(1): 110-6.

Kobayashi H, Takemura Y, Wang FS, Oka T, Ohnuma T. Retrovirus-mediated transfer of anti-MDR1 hammerhead ribozymes into multidrug-resistant human leukemia cells: screening for effective target sites. Int J Cancer 1999; 81: 944-50.

Kominsky SL. Claudins: emerging targets for cancer therapy. Expert Rev Mol Med 2006; 8(18): 1-11.

Kong D, Wang Z, Sarkar SH, Li Y, Banerjee S, Saliganan A, Kim HR, Cher ML, Sarkar FH. Platelet-derived growth factor-D overexpression contributes to epithelial-mesenchymal transition of PC3 prostate cancer cells. Stem Cells 2008; 26(6): 1425-35.

Kortazar D, Carranza G, Bellido J, Villegas JC, Fanarraga ML, Zabala JC. Native tubulin-folding cofactor E purified from baculovirus-infected Sf9 cells dissociates tubulin dimers. Protein Expr Purif 2006; 49(2): 196-202.

Kowalski P, Surowiak P, Lage H. Reversal of different drug-resistant phenotypes by an autocatalytic multitarget multiribozyme directed against the transcripts of the ABC transporters MDR1/P-gp, MRP2, and BCRP. Mol Ther 2005; 11: 508-22.

Kraus AC, Ferber I, Bachmann SO, Specht H, Wimmel A, Gross MW, Schlegel J, Suske G, Schuermann M. In vitro chemo-and radio-resistance in small cell lung cancer

correlates with cell adhesion and constitutive activation of AKT and MAP kinase pathways. Oncogene 2002; 21: 8683-8695.

Krätzschmar J, Lum L, Blobel CP. Metargidin, a membrane-anchored metalloprotease-disintegrin protein with an RGD integrin binding sequence. J Biol Chem 1996; 271(9): 4593-6.

Krishan A, Fitz CM, Andritsch I. Drug retention, efflux and resistance in tumor cells. Cytometry 1997; 29: 279-85.

Krishna R, Mayer LD. Multidrug resistance (MDR) in cancer. Mechanisms, reversal using modulators of MDR and the role of MDR modulators in influencing the pharmacokinetics of anticancer drugs. Eur J Pharm Sci 2000; 11(4): 265-83.

Kröger N, Achterrath W, Hegewisch-Becker S, Mross K, Zander AR. Current options in treatment of anthracycline-resistant breast cancer. Cancer Treat Rev 1999; 25: 279-291.

Kruh GD, Belinsky MG. The MRP family of drug efflux pumps. Oncogene 2003; 22: 7537–7552.

Kubo M, Kikuchi K, Nashiro K, Kakinuma T, Hayashi N, Nanko H, Tamaki K. Expression of fibrogenic cytokines in desmoplastic malignant melanoma. Br J Dermatol 1998; 139(2): 192-7.

Kumar N. Taxol-induced polymerization of purified tubulin. Mechanism of action. J Biol Chem 1981; 256: 10435-10441.

Kutuzovaa GD, DeLuca HF. 1,25-Dihydroxyvitamin D3 regulates genes responsible for detoxification in intestine. Toxicology and Applied Pharmacology 2007; 218 (1): 37-44.

Kwak JC, Ongusaha PP, Ouchi T, Lee SW. IFI16 as a negative regulator in the regulation of p53 and p21(Waf1). J Biol Chem 2003; 278(42): 40899-904.

Kwok TT, Mok CH, Menton-Brennan L. Up-regulation of a mutant form of p53 by doxorubicin in human squamous carcinoma cells. Cancer Res 1994; 54: 2834-36.

Kyu-Ho HE, Gehrke L, Tahir SK. Modulation of drug resistance by α tubulin in paclitaxel resistant human lung cancer cell line. Eur J Cancer 2000; 36: 1565-71.

Lage H. Drug resistance in breast cancer. Cancer Therapy 2003; 1: 81-91

Lakshmanan U, Porter AG. Caspase-4 interacts with TNF receptor-associated factor 6 and mediates lipopolysaccharide-induced NF-kappaB-dependent production of IL-8 and CC chemokine ligand 4 (macrophage-inflammatory protein-1). J Immunol 2007; 179(12): 8480-90.

Lee JH, Takahashi T, Yasuhara N, Inazawa J, Kamada S, Tsujimoto Y. Bis, a Bcl-2-binding protein that synergizes with Bcl-2 in preventing cell death. Oncogene 1999; 18(46): 6183-90.

Lee YH, Albig AR, Maryann R, Schiemann BJ, Schiemann WP. Fibulin-5 Initiates Epithelial-Mesenchymal Transition (EMT) and Enhances EMT Induced by TGF-{beta} in Mammary Epithelial Cells Via a MMP-Dependent Mechanism. Carcinogenesis Advance Access published online on August 19, 2008.

Leonard GD, Fojo T, Bates SE. The role of ABC transporters in clinical practice. Oncologist 2003; 8(5): 411-24.

Leotlela PD, Wade MS, Duray PH, Rhode MJ, Brown HF, Rosenthal DT, Dissanayake SK, Earley R, Indig FE, Nickoloff BJ, Taub DD, Kallioniemi OP, Meltzer P, Morin PJ, Weeraratna AT. Claudin-1 overexpression in melanoma is regulated by PKC and contributes to melanoma cell motility. Oncogene 2007; 26(26): 3846-56.

Li J, Yuan J. Caspases in apoptosis and beyond. Oncogene. 2008; 27(48): 6194-206.

Liang Y, Meleady P, Cleary I, McDonnell S, Connolly L, Clynes M. Selection with melphalan or paclitaxel (Taxol) yields variants with different patterns of multidrug resistance, integrin expression and in vitro invasiveness. Eur J Cancer 2001; 37(8): 1041-52.

Lilling G, Hacohen H, Nordenberg J, Livnat T, Rotter V, Sidi Y. Differential sensitivity of MCF-7 and LCC2 cells, to multiple growth inhibitory agents: possible relation to high bcl-2/bax ratio? Cancer Lett 2000; 161: 27-34.

Lin T, Islam O, Heese K. ABC transporters, neural stem cells and neurogenesis--a different perspective. Cell Res 2006; 16(11): 857-71.

Lioni M, Brafford P, Andl C, Rustgi A, El-Deiry W, Herlyn M, Smalley KS. Dysregulation of claudin-7 leads to loss of E-cadherin expression and the increased invasion of esophageal squamous cell carcinoma cells. Am J Pathol 2007; 170(2): 709-21.

Liu B, Staren ED, Iwamura T, Appert HE, Howard JM. Mechanisms of Taxotere-related drug resistance in pancreatic carcinoma. J Surg Res 2001; 99(2): 179-86.

Lo HW, Hung MC. Nuclear EGFR signalling network in cancers: linking EGFR pathway to cell cycle progression, nitric oxide pathway and patient survival. Br J Cancer. 2006; 94(2): 184-8.

Loo TW, Clarke DM. Recent progress in understanding the mechanism of P-glycoprotein-mediated drug efflux. J Membr Biol 2005; 206(3): 173-85.

Lu Q, Luduena RF. Removal of beta III isotype enhances taxol induced microtubule assembly. Cell Struct Funct 1993; 18:173-182.

Ludueña RF. Multiple forms of tubulin: Different gene products and covalent modifications. Int Rev Cytol 1998; 178:207-275.

Luqmani YA. Mechanisms of drug resistance in cancer chemotherapy. Med Princ Pract 2005; 14 Suppl 1: 35-48.

MacFarlane M, Williams AC. Apoptosis and disease: a life or death decision. EMBO Rep 2004; 5(7): 674-8.

Martinez VG, O'Connor R, Liang Y, Clynes M. CYP1B1 expression is induced by docetaxel: effect on cell viability and drug resistance. Br J Cancer 2008; 98(3): 564-70.

Martinez VG, Williams KJ, Stratford IJ, Clynes M, O'Connor R. Overexpression of cytochrome P450 NADPH reductase sensitises MDA 231 breast carcinoma cells to 5-fluorouracil: possible mechanisms involved. Toxicol In Vitro 2008; 22(3): 582-8.

Marty M, Extra JM, Cottu PH, Espie M. Prospects with Docetaxel in the Treatment of Patients with Breast Cancer. Eur J Cancer 1997: 33; 26-29.

McGrogan BT, Gilmartin B, Carney DN, McCann A. Taxanes, microtubules and chemoresistant breast cancer. Biochim Biophys Acta. 2008; 1785(2): 96-132.

Medical College of Wisconsin, Ontology Report. rgd.mcw.edu/tools/ontology/ont_annot.cgi?ont_id=PW:0000232&ontology=wo, 15/9/2008.

Mild G, Bachmann F, Boulay JL, Glatz K, Laffer U, Lowy A, Metzger U, Reuter J, Terracciano L, Herrmann R, Rochlitz C. DCR3 locus is a predictive marker for 5-fluorouracil-based adjuvant chemotherapy in colorectal cancer. Int J Cancer 2002;102(3): 254-7.

Mimnaugh EG, Dusre L, Atwell J, Myers CE. Differential oxygen radical susceptibility of adriamycin-sensitive and -resistant MCF-7 human breast tumor cells. Cancer Res 1989; 49(1): 8-15.

Mitsumoto M, Kamura T, Kobayashi H, Sonoda T, Kaku T, Nakano H. Emergence of higher levels of invasive and metastatic properties in the drug-resistant cancer cell lines after the repeated administration of cisplatin in tumor-bearing mice. J Cancer Res Clin Oncol 1998; 124: 607-14.

Modrowski D, Orosco A, Thévenard J, Fromigué O, Marie PJ. Syndecan-2 overexpression induces osteosarcoma cell apoptosis: Implication of syndecan-2 cytoplasmic domain and JNK signaling. Bone 2005; 37(2): 180-9.

Molnar J, Gyémánt N, Tanaka M, Hohmann J, Bergmann-Leitner E, Molnár P, Deli J, Didiziapetris R, Ferreira MJU. Inhibition of multidrug resistance of cancer cells by natural diterpens, triterpenes and carotenoids. Curr Pharm Design 2006; 12: 287-311.

Molnar J, Nacsa J, Hever A, Gyemant N, Ugocsai K. Hegyes P, Kiessig ST, Gaal D, Lage H, Varga A. New silicon compounds as resistance modifiers against multidrug resistant cancer cells. Anticancer Res 2004; 24: 865-72.

Molnar J, Szabo D, Mandi Y, Mucsi I, Fischer J, Varga A, Konig S, Motohashi N. Multidrug resistance reversal in mouse lymphoma cells by heterocyclic compounds. Anticancer Res 1998; 18: 3033-8.

Morin PJ. Drug resistance and the microenvironment: nature and nurture. Drug Resist Updat 2003; 4: 169-72.

Motohashi N, Kurihara T, Wakabayashi H, Yaji M, Mucsi I, Molnar J, Maruyama S, Sakagami H, Nakashima H, Tani S, Shirataki Y, Kawase M. Biological activity of a fruit vegetable, "Anastasia green", a species of sweet pepper. In Vivo 2001; 5: 437-42.

Motomura S, Motoji T, Takanashi M, Wang YH, Shiozaki H, Sugawara I, Aikawa E, Tomida A, Tsuruo T, Kanda N, Mizoguchi H. Inhibition of P-glycoprotein and recovery of drug sensitivity of human acute leukemic blast cells by multidrug resistance gene (mdr1) antisense oligonucleotides. Blood 1998; 91(9): 3163-71.

Muraoka S, Miura T. Thiol oxidation induced by oxidative action of adriamycin. Free Radic Res 2004; 38(9): 963-8.

Nabholtz J-MA. Docetaxel-anthracycline combinations in metastatic breast cancer. Breast Cancer Res Treat 2003; 79 (suppl 1): S3-S9.

Nakatani K, Thompson DA, Barthel A, Sakaue H, Liu W, Weigel RJ, Roth RA. Up-regulation of Akt3 in estrogen receptor-deficient breast cancers and androgen-independent prostate cancer lines. J Biol Chem 1999; 274(31): 21528-32.

Narita T, Kimura N, Sato M, Matsuura N, Kannagi R. Altered expression of integrins in adriamycin-resistant human breast cancer cells. Anticancer Res 1998; 18(1A): 257-62.

National Cancer Institute, Cancer Facts, Radiotherapy. www.meds.com/pdq/radio.html, 14/8/2008.

National Center for Biotechnology Information. www.ncbi.nlm.nih.gov, 10/12/2008.

Nicholson RI, Hutcheson IR, Hiscox SE, Knowlden JM, Giles M, Barrow D, Gee JM. Growth factor signalling and resistance to selective oestrogen receptor modulators and pure anti-oestrogens: the use of anti-growth factor therapies to treat or delay endocrine resistance in breast cancer. Endocr Relat Cancer 2005; 12 Suppl 1: S29-36.

Nicholson RI, McClelland RA, Finlay P, Eaton CL, Gullick WJ, Dixon AR, Robertson JF, Ellis IO, Blamey RW. Relationship between EGF-R, c-erbB-2 protein expression and Ki-67 immunostaining in breast cancer and hormone sensitivity. Eur J Cancer 1993; 29A: 1018-23.

Nista A, Leonetti C, Bernardini G, Mattioni M, Santoni A. Functional role of alpha4beta1 and alpha5beta1 integrin fibronectin receptors expressed on adriamycin-resistant MCF-7 human mammary carcinoma cells. Int J Cancer 1997; 72(1): 133-41.

Nobili S, Landini I, Giglioni B, Mini E. Pharmacological strategies for overcoming multidrug resistance. Curr Drug Targets 2006; 7(7): 861-79.

Nogales E., Wolf SH, Downing KH. Structure of the αβ tubulin dimer by electron crystallography. Nature 1998; 391: 199-203.

Nozawa H, Tadakuma T, Ono T, Sato M, Hiroi S, Masumoto K, Sato Y. Small interfering RNA targeting epidermal growth factor receptor enhances chemosensitivity to cisplatin, 5-fluorouracil and docetaxel in head and neck squamous cell carcinoma. Cancer Sci 2006; 97(10): 1115-24.

Ohishi Y, Oda Y, Uchiumi T, Kobayashi H, Hirakawa T, Miyamoto S, Kinukawa N, Nakano H, Kuwano M, Tsuneyoshi M. ATP-binding cassette superfamily transporter gene expression in human primary ovarian carcinoma. Clin Cancer Res 2002; 8(12): 3767-75.

Ozben T. Mechanisms and strategies to overcome multiple drug resistance in cancer. FEBS Lett 2006; 580(12): 2903-9.

Pal D, Mitra AK. MDR- and CYP3A4-mediated drug-drug interactions. J Neuroimmune Pharmacol 2006; 1(3): 323-39.

Palamarchuk A, Efanov A, Maximov V, Aqeilan RI, Croce CM, Pekarsky Y. Akt phosphorylates and regulates Pdcd4 tumor suppressor protein. Cancer Res 2005; 65(24): 11282-6.

Palissot V, Morjani H, Belloc F, Cotteret S, Dufer J, Berchem G: From molecular characteristics to cellular events in apoptosis-resistant HL-60 cells. Int J Oncol 2005; 26: 825-34.

Palma C, Binaschi M, Bigioni M, Maggi CA, Goso C. CD137 and CD137 ligand constitutively coexpressed on human T and B leukemia cells signal proliferation and survival. Int J Cancer 2004;108(3): 390-8.

Parkin DM, Bray F, Ferlay J, Pisani P. Global cancer statistics, 2002. CA Cancer J Clin 2005; 55(2): 74-108.

Peng G, Geng-yin Z, Qing-hui Z, Hong L, Yin-ping Y, Jing Z, Bao-heng W. Reversal MDR in breast carcinoma cells by ribozyme designed according the secondary structure of mdr1 Mrna. Chinese J Physiol 2006; 49: 96-103.

Pitti RM, Marsters SA, Lawrence DA, Roy M, Kischkel FC, Dowd P, Huang A, Donahue CJ, Sherwood SW, Baldwin DT, Godowski PJ, Wood WI, Gurney AL, Hillan KJ, Cohen RL, Goddard AD, Botstein D, Ashkenazi A. Genomic amplification of a decoy receptor for Fas ligand in lung and colon cancer. Nature 1998; 396: 699-703.

Plasschaert SL, Vellenga E, de Bont ES, van der Kolk DM, Veerman AJ, Sluiter WJ, Daenen SM, de Vries EG, Kamps WA. High functional P-glycoprotein activity is more often present in T-cell acute lymphoblastic leukaemic cells in adults than in children. Leuk Lymphoma 2003; 44(1): 85-95.

Pryer NK, Walker RA, Skeen VP, Bourns BD, Soboeiro MF, Salmon ED. Brain microtubule-associated proteins modulate microtubule dynamic instability in vitro. Real-time observations using video microscopy. J Cell Sci 1992; 103 (Pt 4): 965-76.

Pupa SM, Giuffré S, Castiglioni F, Bertola L, Cantú M, Bongarzone I, Baldassari P, Mortarini R, Argraves WS, Anichini A, Menard S, Tagliabue E. Regulation of breast cancer response to chemotherapy by fibulin-1. Cancer Res 2007; 67(9): 4271-7.

Reijntjes S, Rodaway A, Maden M. The retinoic acid metabolising gene, CYP26B1, patterns the cartilaginous cranial neural crest in zebrafish. International Journal of Developmental Biology 2007; 51: 351-360.

Ren Y, Zhan X, Wei D, Liu J. In vitro reversal MDR of human carcinoma cell line by an antisense oligodeoxynucleotide-doxorubicin conjugate. Biomed Pharmacother 2004; 58(9): 520-6.

Riddick DS, Lee C, Ramji S, Chinje EC, Cowen RL, Williams KJ, Patterson AV, Stratford IJ, Morrow CS, Townsend AJ, Jounaidi Y, Chen CS, Su T, Lu H, Schwartz PS, Waxman DJ. Cancer chemotherapy and drug metabolism. Drug Metab Dispos 2005; 33(8): 1083-96.

Riggins RB, Schrecengost RS, Guerrero MS, Bouton AH. Pathways to tamoxifen resistance. Cancer Lett 2007; 256: 1-24.

Robert J, Larsen AK. Drug resistance to topoisomerase II inhibitors. Biochimie 1998; 80: 247-54.

Rochat B, Morsman JM, Murray GI, Figg WD, McLeod HL. Human CYP1B1 an anticancer agent metabolism: mechanism for tumor-specific drug inactivation? J Pharmacol Exp Ther 2001; 296: 537-541.

Rodningen OK, Overgaard J, Alsner J, Hastie T and Dale BAL. Microarray analysis of the transcriptional response to single or multiple doses of ionizing radiation in human subcutaneous fibroblasts. Radiother Oncol 2005; 77: 231-40.

Rozen S and Skaletsky HJ: Primer3 on the WWW for general users and for biologist programmers. In: Bioinformatics Methods and Protocols: Methods in Molecular Biology (Krawetz S and Misener S, eds). Totowa, NJ, Humana Press. 2000, pp 365-386.

Sala-Torra O, Gundacker HM, Stirewalt DL, Ladne PA, Pogosova-Agadjanyan EL, Slovak ML, Willman CL, Heimfeld S, Boldt DH, Radich JP. Connective tissue growth factor (CTGF) expression and outcome in adult patients with acute lymphoblastic leukemia. Blood 2007; 109(7): 3080-3.

Sanfilippo O, Ronchi E, De Marco C, Di Fronzo G, Silvestrini R. Expression of P-glycoprotein in breast cancer tissue and in vitro resistance to doxorubicin and vincristine. Eur J Cancer 1991; 27: 155-8.

Sanlioglu AD, Dirice E, Aydin C, Erin N, Koksoy S, Sanlioglu S. Surface TRAIL decoy receptor-4 expression is correlated with TRAIL resistance in MCF7 breast cancer cells. BMC Cancer 2005; 5: 54.

Sanofi-aventis, Clinical pharmacology. www.taxotere.com/oncology/about_Taxotere/clinical_pharmacology.aspx, 27/3/2007.

Sarkadi B, Laczka CÖ, Nemet K, Varadi A. ABCG2 – a transporter for all seasons. FEBS Lett 2004; 567: 116-20.

Sarrió D, Rodriguez-Pinilla SM, Hardisson D, Cano A, Moreno-Bueno G, Palacios J. Epithelial-mesenchymal transition in breast cancer relates to the basal-like phenotype. Cancer Res 2008; 68(4): 989-97.

Sethi T, Rintoul RC, Moore SM, MacKinnon AC, Salter D, Choo C, Chilvers ER, Dransfield I, Donnelly SC, Strieter R, Haslett C. Extracellular matrix proteins protect small cell lung cancer cells against apoptosis: a mechanism for small cell lung cancer growth and drug resistance in vivo. Nat Med 1999; 6: 662-8.

Scambia G, Testa U, Benedetti P, Foti E, Martucci R, Gadducci A, Perillo A, Facchini V, Peschle C, Mancuso S. Prognostic significance of interleukin 6 serum levels in patients with ovarian cancer. Br J Cancer 1995; 71: 354-356.

Schafer JM, Bentrem DJ, Takei H, Gajdos C, Badve S, Jordan VC. A mechanism of drug resistance to tamoxifen in breast cancer. J Steroid Biochem Mol Biol 2002; 83 (1-5):75-83.

Schinkl AH, Jonker JW. Mammalian drug efflux transporters of the ATP binding cassette (ABC) family: an overview. Adv Drug Deliver Rev 2003; 55: 3-29.

Schmidt M, Lichtner RB. EGF receptor targeting in therapy-resistant human tumors. Drug Resist Updat 2002; 5(1): 11-8.

Secchiero P, Gonelli A, Carnevale E, Milani D, Pandolfi A, Zella D, Zauli G. TRAIL promotes the survival and proliferation of primary human vascular endothelial cells by activating the Akt and ERK pathways. Circulation 2003; 107(17): 2250-6.

Secchiero P, Gonelli A, Carnevale E, Corallini F, Rizzardi C, Zacchigna S, Melato M, Zauli G. Evidence for a proangiogenic activity of TNF-related apoptosis-inducing ligand. Neoplasia 2004; 6(4): 364-73.

Shalli K, Brown I, Heys SD, Schofield AC. Alterations of beta-tubulin isotypes in breast cancer cells resistant to docetaxel. FASEB J 2005; 10:1299-1301.

Shibata K, Kikkawa F, Nawa A, Suganuma N, Hamaguchi M. Fibronectin secretion from human peritoneal tissue induces Mr 92,000 type IV collagenase expression and invasion in ovarian cancer cell lines. Cancer Res 1997; 57(23): 5416-20.

Slovak ML, Hoeltge GA, Dalton WS, Trent JM. Pharmacological and biological evidence for differing mechanisms of doxorubicin resistance in two human tumor cell lines. Cancer Res 1988; 48: 2793-7.

Smith MR, Kung H, Durum SK, Colburn NH, Sun Y. TIMP-3 induces cell death by stabilizing TNF-alpha receptors on the surface of human colon carcinoma cells. Cytokine. 1997; 9(10): 770-80.

Somerville RPT, Oblander SA, Apte SS. Matrix metalloproteinases: old dogs with new tricks. Genome Biology 2003; 4(6): Article 216.

Sparreboom A, Danesi R, Ando Y, Chan J, Figg WD. Pharmacogenomics of ABC transporters and its role in cancer chemotherapy. Drug Resist Update 2003; 266: 1-14.

Ševkova J, Poledne R, Hubacek JA. ATP-Binding Cassette (ABC) Transporters in Human Metabolism and Diseases. Physiological Research 2004; 53: 235-243.

Stumm S, Meyer A, Lindner, M, Bastert G, Wallwiener D, Guckel B. Paclitaxel Treatment of Breast Cancer Cell Lines Modulates Fas/Fas Ligand Expression and Induces Apoptosis Which Can Be Inhibited Through the CD40 Receptor. Oncology 2004; 66: 101-111.

Sukhai M, Piquette-Miller M. Regulation of the multidrug resistance genes by stress signals. J Pharm Pharm Sci 2000; 3(2): 268-80.

Suyama K, Shapiro I, Guttman M, Hazan RB. A signaling pathway leading to metastasis is controlled by N-cadherin and the FGF receptor. Cancer Cell 2002; 2(4): 301-14.

Szondy Z, Reichert U, Bernardon JM, Michel S, Tóth R, Ancian P, Ajzner E, Fesus L. Induction of apoptosis by retinoids and retinoic acid receptor gamma-selective compounds in mouse thymocytes through a novel apoptosis pathway. Mol Pharmacol 1997; 51(6): 972-82.

Takahama Y, Yamada Y, Emoto K, Fujimoto H, Takayama T, Ueno M, Uchida H, Hirao S, Mizuno T, Nakajima Y. The prognostic significance of overexpression of the decoy receptor for Fas ligand (DcR3) in patients with gastric carcinomas. Gastric Cancer 2002; 5(2): 61-8.

Takayama S, Sato T, Krajewski S, Kochel K, Irie S, Millan JA, Reed JC. Cloning and functional analysis of BAG-1: a novel Bcl-2-binding protein with anti-cell death activity. Cell 1995; 80(2): 279-84.

Tang SC, Beck J, Murphy S, Chernenko G, Robb D, Watson P, Khalifa M. BAG-1 expression correlates with Bcl-2, p53, differentiation, estrogen and progesterone receptors in invasive breast carcinoma. Breast Cancer Res Treat 2004; 84(3): 203-13.

Taub ME, Podila L, Ely D, Almeida I. Functional assessment of of multiple P-glycoprotein probe substrates: influence of cell and modulator concentration on P-gp activity. Drug Metab Dispos 2005; 33(11): 1679-87.

Teixeira C, Reed JC, Pratt MA. Estrogen promotes chemotherapeutic drug resistance by a mechanism involving Bcl-2 proto-oncogene expression in human breast cancer cells. Cancer Res 1995; 55(17): 3902-7.

The Apoptopedia, www.celldeath.de/encyclo/index.html, 25/6/2007.

Thomas H, Coley HM. Overcoming multidrug resistance in cancer: an update on the clinical strategy of inhibiting p-glycoprotein. Cancer Control 2003; 10: 159-165.

Thompson EW, Newgreen DF, Tarin D. Carcinoma invasion and metastasis: a role for epithelial-mesenchymal transition? Cancer Res 2005; 65(14): 5991-5.

Triller N, Korosec P, Kern I, Kosnik M, Debeljak A. Multidrug resistance in small cell lung cancer: expression of P-glycoprotein, multidrug resistance protein 1 and lung resistance protein in chemo-naive patients and in relapsed disease. Lung Cancer 2006; 54(2): 235-40.

Trochon-Joseph V, Martel-Renoir D, Mir LM, Thomaïdis A, Opolon P, Connault E, Li H, Grenet C, Fauvel-Lafève F, Soria J, Legrand C, Soria C, Perricaudet M, Lu H. Evidence of antiangiogenic and antimetastatic activities of the recombinant disintegrin domain of metargidin. Cancer Res 2004; 64(6): 2062-9.

Tsang WP, Kong SK, Kwok TT. Epidermal growth factor induction of resistance to topoisomerase II toxins in human squamous carcinoma A431 cells. Oncol Rep 2006; 16(4): 789-93.

Ueda J, Semba S, Chiba H, Sawada N, Seo Y, Kasuga M, Yokozaki H. Heterogeneous expression of claudin-4 in human colorectal cancer: decreased claudin-4 expression at the invasive front correlates cancer invasion and metastasis. Pathobiology 2007; 74(1): 32-41.

Ugocsai K, Varga A, Molnar P, Antus S, Molnar J. Effects of selected flovanoids and carotenoids on drug accumulation and apoptosis induction in multidrug-resistant colon cancer cells expressing MDR1/LRP. In Vivo 2005; 19: 433-8.

Umeyama T, Okabe S, Kanai Y, Hirokawa N. Dynamics of microtubules bundled by microtubule associated protein 2C (MAP2C). J Cell Biol 1993; 120(2): 451-65.

Underbrink, M., Pou, A. The Principles of Radiation Oncology. www.utmb.edu/otoref/grnds/Radiation-oncology-2003-1203/Radiation-oncology-2003-1203.htm, 3/12/2007.

Verdier-Pinard P, Shahabi S, Wang F, Burd B, Xiao H, Goldberg GL, Orr GA, Horwitz SB. Detection of human betaV-tubulin expression in epithelial cancer cell lines by tubulin proteomics. Biochemistry 2005; 44:15858-15870.

Verdier-Pinard P, Wang F, Martello L, Burd B, Orr GA, Horwitz SB. Analysis of tubulin isotypes and mutations from taxol-resistant cells by combined isoelectrofocusing and mass spectrometry. Biochem 2003; 42:5349-4357.

Virtual Medical Centre, Breast Cancer (Carcinoma of the Breast). www.virtualcancercentre.com/diseases.asp?did=696, 23/6/2008

Virtual Medical Centre, Breast Cancer (Invasive Ductal Carcinoma of the Breast). www.virtualcancercentre.com/diseases.asp?did=674, 23/6/2008

Virtual Medical Centre, Breast Cancer (Lobular Carcinoma of the Breast). www.virtualcancercentre.com/diseases.asp?did=675, 23/6/2008

Vonderheide RH. Prospect of Targeting the CD40 Pathway for Cancer Therapy. Clinical Cancer Research 2007; 13(4): 1083-8.

Wahab N, Cox D, Witherden A, Mason RM. Connective tissue growth factor (CTGF) promotes activated mesangial cell survival via up-regulation of mitogen-activated protein kinase phosphatase-1 (MKP-1). Biochem J 2007; 406(1): 131-8.

Walker BP, Smith C, Youndale T, Leblane J, Whitfield JF, Sikorska M. Topoisomerase II-reactive chemotherapeutic drugs induce apoptosis in thymocytes. Cancer Res 1991; 51: 1078-85.

Wang LG, Liu XM, Kreis W, Budman DR. The effect of antimicrotubule agents on signal transduction pathways of apoptosis: a review. Cancer Chemother Pharmacol 1999; 44: 355-361.

Wang Q, Zhang P, Zhang Q, Wang X, Li J, Ma C, Sun W, Zhang L. Analysis of CD137 and CD137L expression in human primary tumor tissues. Croat Med J 2008; 49(2): 192-200.

Wang YG, Liu HT, Zhang YM, Ma DL. cDNA cloning and expression of an apoptosis-related gene, human TFAR-15 gene. Science in China series C-life sciences 1999; 42: 323-329.

Wehland J, Weber K. Turnover of the carboxy-terminal tyrosine of alpha-tubulin and means of reaching elevated levels of detyrosination in living cells. J Cell Sci 1987; 88 (Pt 2): 185-203.

Wenger C, Ellenrieder V, Alber B, Lacher U, Menke A, Hameister H, Wilda M, Iwamura T, Beger HG, Adler G, Gress TM. Expression and differential regulation of connective tissue growth factor in pancreatic cancer cells. Oncogene 1999; 18(4): 1073-80.

Wilkins-Port CE, Higgins PJ. Regulation of extracellular matrix remodeling following transforming growth factor-beta1/epidermal growth factor-stimulated epithelial-mesenchymal transition in human premalignant keratinocytes. Cells Tissues Organs 2007; 185(1-3): 116-22.

Wilson C, Purcell C, Seaton A, Oladipo O, Maxwell P, O'Sullivan J, Wilson R, Johnston PG, Waugh D. Chemotherapy-induced CXC-chemokine/CXCR2 signaling in metastatic prostate cancer cells confers resistance to oxaliplatin through potentiation of NF-{kappa}B transcription and evasion of apoptosis. J Pharmacol Exp Ther 2008 (In press).

Wilson L, Jordan MA. Microtubule dynamics: taking aim at a moving target. Chem Biol 1995; 2: 569-573.

World Health Orginisation. Cancer. www.who.int/mediacentre/factsheets/fs297/en, 1/7/2008

Wu Q, Dawson MI, Zheng Y, Hobbs PD, Agadir A, Jong L, Li Y, Liu R, Lin B, Zhang XK. Inhibition of trans-retinoic acid-resistant human breast cancer cell growth by retinoid X receptor-selective retinoids. Mol Cell Biol 1997; 17: 6598-608.

Yabuki N, Sakata K, Yamasaki T, Terashima H, Mio T, Miyazaki Y, Fujii T, Kitada FK. Gene amplification and expression in lung cancer cells with acquired paclitaxel resistance. Cancer Genetics and Cytogenetics 2007; 173: 1-9.

Ye Y, Xiao Y, Wang W, Yearsley K, Gao JX, Barsky SH. ERalpha suppresses slug expression directly by transcriptional repression. Biochem J 2008; 416(2): 179-87.

Yilmaz R, Yücel M, Öktem HA. Quality assessment of gene expression data for an affymetrix platform with the two sample t-tests statistical analysis. International Journal of Biotechnology and Biochemistry. 2008;4:101-108.

Yonemori K, Katsumata N, Uno H, Matsumoto K, Kouno T, Tokunaga S, Yamanaka Y, Shimizu C, Ando M, Takeuchi M, Fujiwara Y. Efficacy of weekly paclitaxel in patients with docetaxel-resistant metastatic breast cancer. Breast Cancer Res Treat 2005; 89(3): 237-41.

Yonish-Rouach E, Resnitzky D, Lotem J, Sachs L, Kimchi A, Oren M. Wild-type p53 induces apoptosis of myeloid leukaemic cells that is inhibited by interleukin-6. Nature 1991; 352(6333):345-7.

Young AM, Allen CE, Audus KL. Efflux transporters of the human placenta, Adv Drug Deliver Rev 2003; 55: 125-132.

Yvon AM, Wadsworth P, Jordan MA. Taxol suppresses dynamics of individual microtubules in living human tumor cells. Mol Biol Cell 1999; 10: 947-959.

Xie D, Nakachi K, Wang H, Elashoff R, Koeffler HP. Elevated levels of connective tissue growth factor, WISP-1, and CYR61 in primary breast cancers associated with more advanced features. Cancer Res 2001; 61(24): 8917-23.

Xian W, Schwertfeger KL, Vargo-Gogola T, Rosen JM. Pleiotropic effects of FGFR1 on cell proliferation, survival, and migration in a 3D mammary epithelial cell model. J Cell Biol 2005; 171(4): 663-73.

Zaffaroni N, Daidone MG. Survivin expression and resistance to anticancer treatments: perspectives for new therapeutic interventions. Drug Resist Updat 2002; 5(2): 65-72.

Zavadil J, Böttinger EP. TGF-beta and epithelial-to-mesenchymal transitions. Oncogene 2005; 24(37): 5764-74.

Zhang S, Yang X, Morris ME. Flavonoids are inhibitors of breast cancer resistance protein (ABCG2)-mediated transport. Mol Pharmacol 2004; 65: 1208-16.

Zhou DC, Ramond S, Viguie F, Faussat AM, Zittoun R, Marie JP. Sequential emergence of MRP- and MDR1-gene over-expression as well as MDR1-gene translocation in homoharringtonine-selected K562 human leukemia cell lines. Int J Cancer 1996; 65(3): 365-71.

Zhu A, Wang X, Guo Z. Study of tea polyphenol as a reversal agent for carcinoma cell lines' multidrug resistance (study of TP as a MDR reversal agent). Nucl Med Biol 2001; 28: 735-40.

APPENDIX A

CELL CULTURE MEDIUM

Table A.1 RPMI 1640 Medium (1X) (Biochrom).

Composition	Concentration (mg/L)	Composition	Concentration (mg/L)
NaCl	6000	L-lysine-HCl	40
KCl	400	L-methionine	15
$Na_2HPO_4 \cdot 7H_2O$	1512	L-phenylalanine	15
$MgSO_4 \cdot 7H_2O$	100	L-proline	20
$Ca(NO_3)_2 \cdot 4H_2O$	100	L-serine	30
D-glucose	2000	L-theronine	20
Phenol red	10	L-trytophane	5
$NaHCO_3$	2000	L-tyrosine	20
L-arginine	200	L-valine	20
L-asparagine	50	Glutathione	1
L-aspartic acid	20	Biotine	0.2
L-cyctine	50	Vitamin B_{12}	0.005
L-glutamine	532	D-Ca-pantothenate	0.25
L-glutamic acid	20	Choline chloride	3
Glycine	10	Folic acid	1
L-histidine	15	Myo-inositol	35
L-hydroxyproline	20	Nictoninamide	1
L-isoleucine	50	p-amino-benzoic-acid	1
L-leucine	50	Pridoxin HCl	1
Riboflavin	0.2	Thiamine-HCl	1

APPENDIX B

DEVELOPMENT OF RESISTANT SUBLINES

For the development of docetaxel and doxorubicin resistant sublines, cells were stepwise selected by increasing drug applications. Prior to dose increaments, adapted cells became confluent in respective drug concentrations and maintained at least for four months (Tables B1 and B2).

Table B.1 Weeks of docetaxel applications for the development of resistant sublines.

[DOC (nM)]	15	17	20	25	30	35	45	60	80	90	120
Weeks	6	4	4	4	8	5	4	6	5	4	5

Table B.2 Weeks of docetaxel applications for the development of resistant sublines.

[DOX (nM)]	140	150	160	180	200	260	400	600	800	1000
Weeks	4	4	4	4	5	5	5	4	5	4

APPENDIX C

BUFFERS AND SOLUTIONS

RNA Isolation

Diethyl pyrocarbonate (DEPC)-treated dH_2O (1 L)

DEPC	100 µL
dH_2O	1 L

DEPC added water was left under hood for overnight and then autoclaved.

Guanidium thiocynate (GTC) Solution (20 mL)

GTC (4 M)	9.45 g
Sarcosyl (0.5% w/v)	0.1 g
Tri-sodium citrate dihydrate (MW: 294.1) (25 mM)	0.147 g

Volume was completed to 20 mL with DEPC-treated dH_2O, pH was adjusted to 7 and the solution was filtered for sterilization.

Sodium Acetate Solution (2M, 10 mL)

Sodium acetate (MW: 82.03)	1.64 g

Volume was completed to 10 mL with DEPC-treated dH_2O, pH was adjusted to 4 and the solution was autoclaved. Solution was stored at RT.

Sodium Citrate Buffer (0.1 M, 150 mL)

Tri-sodium dihydrate (MW: 294.1)	1.146 g
Monohydrated citrate (MW: 210.14)	2.33 g

Volume was completed to 150 mL with DEPC-treated dH_2O, pH was adjusted to 4.3 and the solution was autoclaved. Solution was stored at 4°C.

Citrate Saturated Acid Phenol (100 mL)

Phenol	100 mL
Hydroxyguinoline (MW: 145.16)	0.1 g
Sodium citrate buffer (0.1 M)	100 mL

Mixture was shaked well and the lower clear phenol phase was extracted after the pH became acidic (checked by litmus paper). Solution was kept at dark, at 4°C.

Agarose Gel Electrophoresis

TAE (Tris-Acetate-EDTA) Buffer (50X, 1 L)

Tris-base (MW: 121.14)	242 g
Glacial acetic acid	57.1 mL
EDTA disodium dihydrate (MW: 372.24) (0.5 M)	100 mL

Volume was adjusted to 1 L with dH_2O, pH was adjusted to 8.5 and the solution was autoclaved for sterilization. Solution was stored at 4°C.

Ethidium Bromide (EtBr) Solution

EtBr (MW: 394.31)	10 mg
dH_2O	1 mL

Solution was kept at dark, at 4°C.

Protein Isolation

TrisHCl (1M, 10 mL)

Tris-base (MW: 121.14)	1.21 g

Volume was completed to 10 mL with dH_2O, pH was adjusted to 7.5 by HCl titration and the solution was autoclaved. Solution was stored at 4°C.

EDTA (0.125M, 10 mL)

EDTA (MW: 292.3)	0.37 g

Volume was completed to 10 mL with dH_2O and NaOH was dropped to enhance solubility. Solution was stored at RT.

CHAPS Buffer (5% w/v, 5 mL)

CHAPS (MW: 614.9)	0.25 g

Volume was completed to 5 mL with dH_2O and the solution was stored at 4°C.

PMSF (100mM, 1 mL)

PMSF	0.018 g
EtOH	1 mL

Solution was stored at 4°C.

Aprotinin (0.1 mg/mL, 1mL)

Aprotinin	0.01 g
Physiologic saline	1 mL

10 mg/mL aprotinin solution was diluted 1:100 by physiologic saline to achieve 0.1 mg/ml stock solution and the solution was kept at -20°C.

Pepstatin A (0.2 mg/mL)

Pepstatin	0.002 g
DMSO	1 mL

2 mg/mL aprotinin solution was diluted 1:10 by DMSO to achieve 0.2 mg/ml stock solution and the solution was kept at -20°C.

β-mercaptoethanol (0.5M, 5 mL)

β-mercaptoethanol (14.3 M)	175 µL
dH_2O	4825 µL

Lysis Buffer (300 µL)

TrisHCl (1M)	3 µL
$MgCl_2$ (25mM)	12 µL
EDTA (0125M)	2.4 µL
CHAPS (5% w/v)	30 µL
Glycerol (87% v/v)	34.5 µL
PMSF (100mM)	3 µL
Aprotinin (0.1 mg/mL)	6 µL
Pepstatin A (0.2 mg/mL)	1.5 µL

β-mercaptoethanol (0.5M)	3 μL
dH_2O	204.6 μL

Solution was freshly prepared prior to use at RT.

Bradford Reagent (5X, 1 L)

Coomassie Brillant Blue G250	500 mg
EtOH (95% v/v)	250 mL
Phosphoric acid (85% v/v)	500 mL

Solution was completed to 1 L with dH_2O, filtered from coarse filter and stored at 4°C.

SDS-PAGE and Western Blotting

Gel Solution (30% T, 2.67% C, 50 mL)

Acrylamide	14.6 g
Bis acrylamide	0.4 g

Solution was completed to 50 mL with dH_2O, filtered from coarse filter and stored at dark, at 4°C.

Separating Gel Buffer (1.5M TrisHCl, 100 mL)

Tris-base (MW: 121.14)	18.15 g
dH_2O	60 mL

pH was adjusted to 8.8, volume was completed to 100 mL with dH_2O, and stored at 4°C.

Stacking Gel Buffer (0.5M TrisHCl, 100 mL)

Tris-base (MW: 121.14)	6 g
dH_2O	60 mL

pH was adjusted to 6.8, volume was completed to 100 mL with dH_2O, and stored at 4°C.

SDS (10% w/v, 10 mL)

SDS (MW: 288.38)	1 g

Solution was completed to 10 mL with dH_2O by gentle stirring and stored at RT.

APS (10% w/v, 1 mL)

APS (MW: 228.2)	100 mg
dH_2O	1 mL

Solution was freshly prepared prior to use.

Sample Dilution (SDS Reducing) Buffer (4X, 10 mL)

TrisHCl (1M, pH 6.8)	2.5 mL
Glycerol	4 mL
β-mercaptoethanol	2 mL
SDS (MW: 288.38)	0.8 g
Bromophenol blue	0.001 g

Solution was completed to 10 mL with dH_2O and stored at dark, at 4°C.

Running (Electrode) Buffer (10X, 500 mL)

Tris-base (MW: 121.14)	15 g
Glycine (MW: 75.07)	72 g

Solution was completed to 500 mL with dH_2O and stored at 4°C.

Coomassie Blue Staining Solution (400 mL)

Coomassie Brillant Blue R	0.4 g
MetOH	200 mL
Glacial acetic acid	48 mL

Solution was completed to 400 mL with dH_2O, filtered from coarse filter and stored at dark, at 4°C.

Destain Solution (500 mL)

MetOH	150 mL
Glacial acetic acid	35 mL

Solution was completed to 500 mL with dH_2O, filtered from coarse filter and stored at dark, at 4°C.

Transfer (Blotting) Buffer (4 L)

Tris-base (MW: 121.14)	12.114 g
Glycine (MW: 75.07)	57.65 g

MetOH	800 mL

Solution was completed to 4 L with dH_2O and stored at 4°C.

Equilibration (TBST) Buffer (1 L)

Sodium chloride (MW: 58.44)	29.25 g
TrisHCl (MW: 157.6)	3.16 g
Tween 20 (MW: 1227.7)	500.5 µL

Solution was completed to 1 L with dH_2O and stored at 4°C.

Blocking Buffer (300 mL)

Non fat dry milk	15 g

Solution was freshly prepared prior to use and kept at 4°C. Volume was completed to 300 mL with TBST.

Microarray

MES Stock (12X, 100 mL)

MES free-acid monohydrate	70.4 g
MES sodium salt	193.3g

Volume was completed to 100 mL with DEPC-treated dH_2O, filter sterilized (0.2 µm) and stored at 4 °C.

MES Hybridization Buffer (2X, 500 mL)

Sodium chloride (5M)	200 mL
12X MES stock	82 mL

Volume was completed to 500 mL with DEPC-treated dH_2O, filter sterilized (0.2 µm) and stored at RT.

MES Stain Buffer (2X, 250 mL)

12X MES stock	41.7 mL
Sodium chloride (5M)	92.5 mL
Tween 20 (10% v/v)	2.5 mL

Volume was completed to 250 mL with DEPC-treated dH_2O, filter sterilized (0.2 µm) and stored at RT.

Hybridization Coctail

Fragmented cRNA	30 μL
Control Oligo B2	5 μL
20X Hybridization Controls	15 μL
Herring Sperm DNA	3 μL
BSA (50 mg/mL)	3 μL
2X MES Hybridization Buffer	150 μL
DMSO	30 μL
dH_2O	64 μL

BSA solution was freshly prepared by dissolving 50 mg BSA in 1 mL dH_2O. The solution was freshly prepared prior to use.

SAPE (Streptavidin Phycoerythrin) Solution

2X MES Stain Buffer	600 μL
BSA (50 mg/mL)	48 μL
SAPE (50 mg/mL)	12 μL
DI H_2O	540 μL

The solution was freshly prepared prior to use and kept at dark, at 4°C.

Antibody Solution

2X MES Stain Buffer	300 μL
BSA (50 mg/mL)	24 μL
Normal Goat IgG (10 mg/mL)	6 μL
Biotinylated antibody (0.5 mg/mL)	3.6 μL
DI H_2O	266.4 μL

The solution was freshly prepared prior to use and kept at dark, at 4°C.

APPENDIX D

OPTIMIZATION OF RT-PCR CYCLES

Number of cycles is an important parameter in PCR. In expression analysis, quantification is performed at logarithmic phase of PCR at which band intensity of the PCR products increase linearly with cycles of PCR. Densitometric measurements of band intensities were plotted against cycle numbers and optimum PCR cycle was selected from the increasing phase of the line graph. Genes with cycle optimization results are given below:

- ***β2-microglobulin (β2-m)***

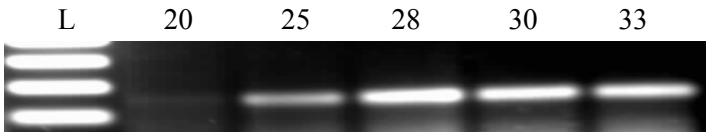

A)

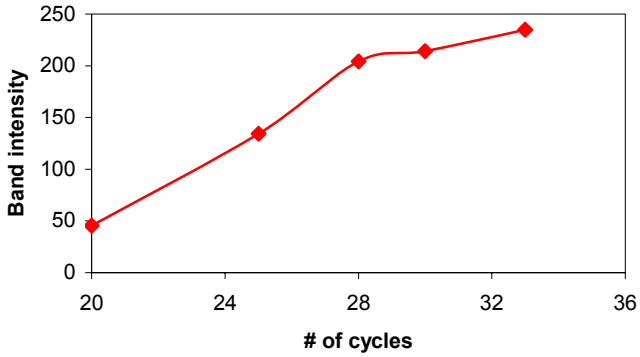

B)

Figure D.1 A) RT-PCR results of *β2-m* gene product (122 bp) on 2% agarose. Lanes: L; 50 bp ladder, 20, 25, 28, 30 and 33; cycles B) Graphic illustration of the results.

PCR condition for expression analysis of *β2-m* was set as 30 cycles.

- ***MDR1***

A)

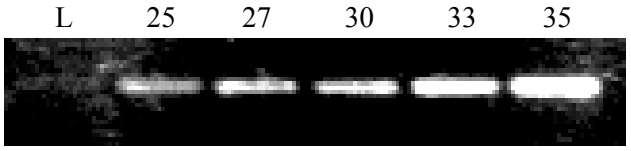

B)

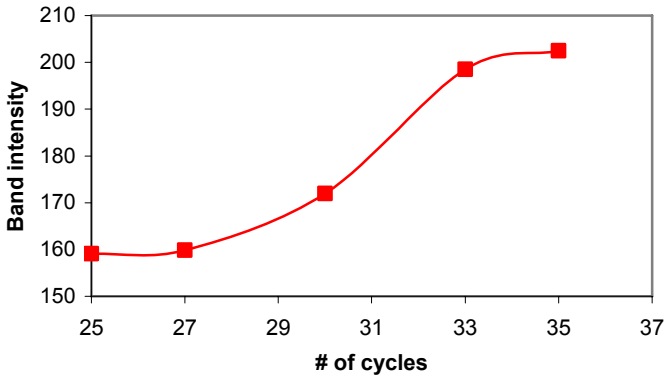

Figure D.2 A) RT-PCR results of *MDR1* gene product (298 bp) on 2% agarose. Lanes: L; 50 bp ladder, 25, 27, 30, 33 and 35; cycles, B) Graphic illustration of the results.

PCR condition for expression analysis of *MDR1* was set as 30 cycles.

- ***MRP1***

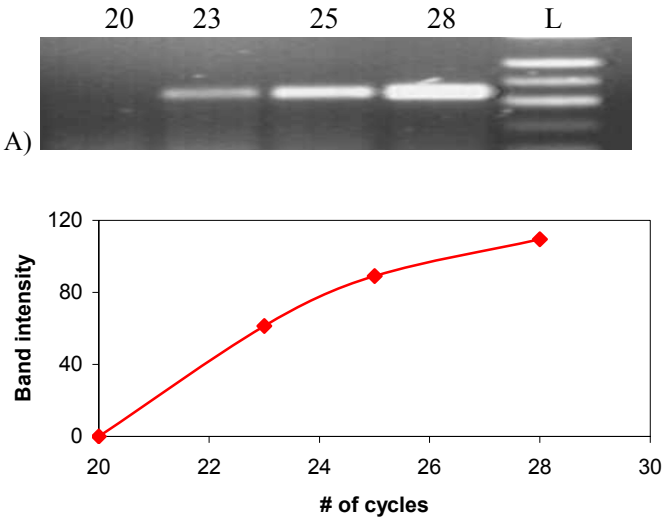

Figure D.3 A) RT-PCR results of *MRP1* gene product (217 bp) on 2% agarose. Lanes: L; 50 bp ladder, 20, 23, 25 and 28; cycles, B) Graphic illustration of the results.

PCR condition for expression analysis of *MRP1* was set as 25 cycles.

- ***Bcl-2***

A)

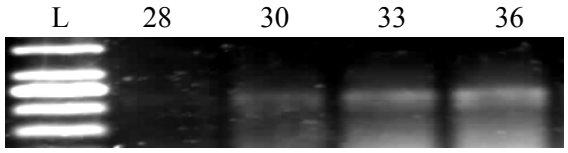

B)

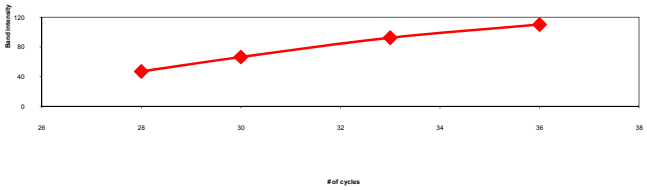

Figure D.4 A) RT-PCR results of *Bcl-2* gene product (219 bp) on 2% agarose. Lanes: L; 50 bp ladder, 28, 30, 33 and 36; cycles, B) Graphic illustration of the results.

PCR condition for expression analysis of *Bcl-2* was set as 30 cycles.

- ***Bax***

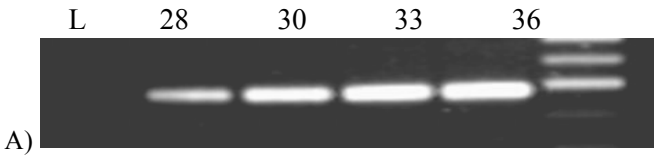

A)

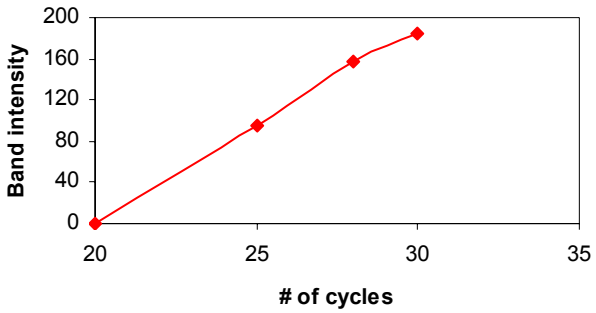

B)

Figure D.5 A) RT-PCR results of *Bcl-2* gene product (188 bp) on 2% agarose. Lanes: L; 50 bp ladder, 20, 23, 28, 30 and 33; cycles, B) Graphic illustration of the results.

PCR condition for expression analysis of *Bax* was set as 28 cycles.

- ***βI tubulin***

A)

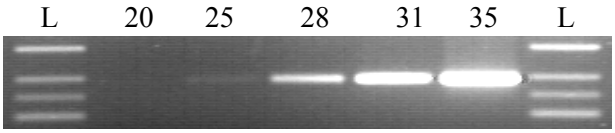

B)

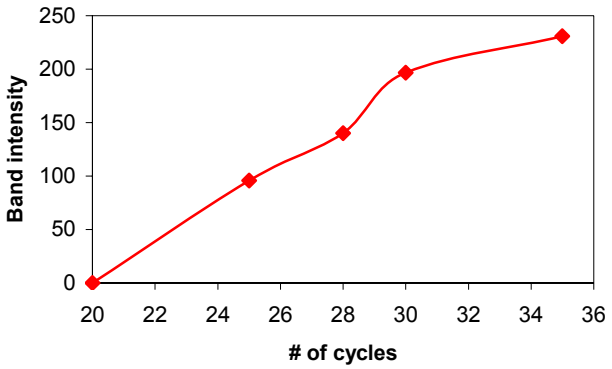

Figure D.6 A) RT-PCR results of *βI tubulin* gene product (289 bp) on 2% agarose. Lanes: L; 50 bp ladder, 20, 25, 28, 31 and 35; cycles, B) Graphic illustration of the results.

PCR condition for expression analysis of *βI tubulin* was set as 31 cycles.

- ***βII tubulin***

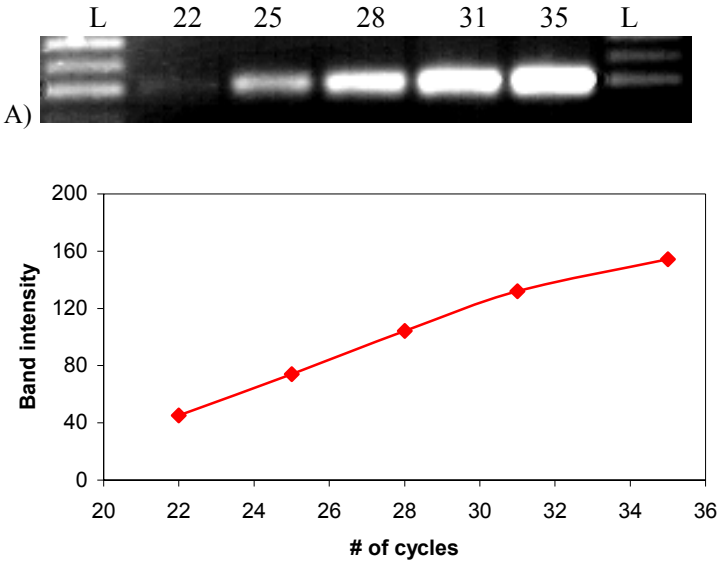

Figure D.7 A) RT-PCR results of *βII tubulin* gene product (200 bp) on 2% agarose. Lanes: L; 50 bp ladder, 22, 25, 28, 31 and 35; cycles, B) Graphic illustration of the results.

PCR condition for expression analysis of *βII tubulin* was set as 31 cycles.

- ***βIII tubulin***

A)

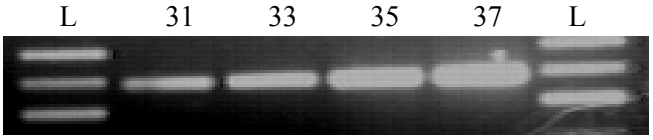

B)

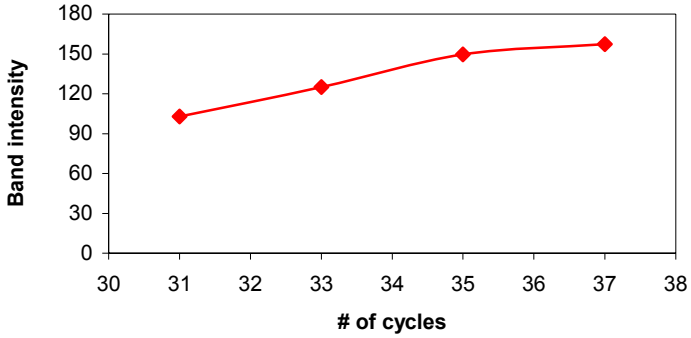

Figure D.8 A) RT-PCR results of *βIII tubulin* gene product (228 bp) on 2% agarose. Lanes: L; 50 bp ladder, 31, 33, 35 and 37; cycles, B) Graphic illustration of the results.

PCR condition for expression analysis of *βII tubulin* was set as 33 cycles.

- ***βIVb tubulin***

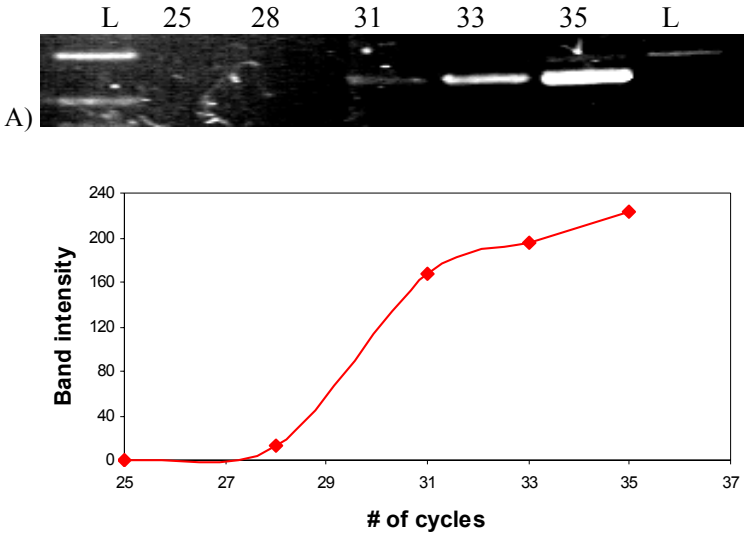

Figure D.9 A) RT-PCR results of *βIVb tubulin* gene product (344 bp) on 2% agarose. Lanes: L; 50 bp ladder, 25, 28, 31, 33 and 35; cycles, B) Graphic illustration of the results.

PCR condition for expression analysis of *βIVb tubulin* was set as 31 cycles.

- ***βV tubulin***

A)

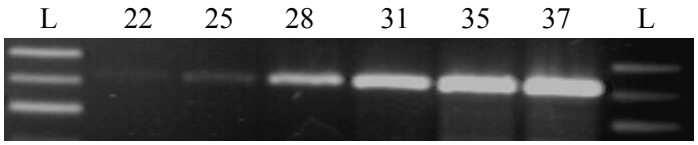

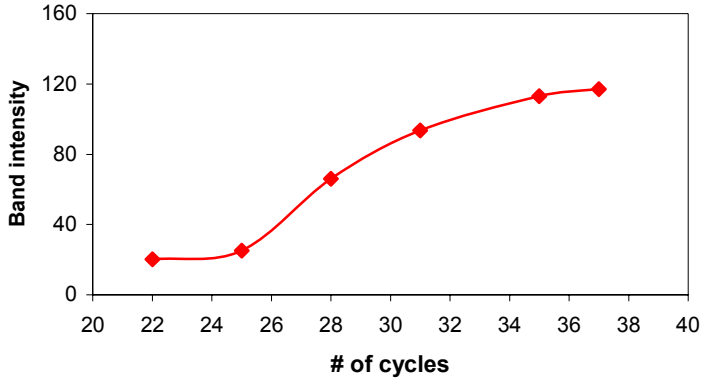

B)

Figure D.10 A) RT-PCR results of *βV tubulin* gene product (256 bp) on 2% agarose. Lanes: L; 50 bp ladder, 22, 25, 28, 31, 35 and 37; cycles, B) Graphic illustration of the results.

PCR condition for expression analysis of *βV tubulin* was set as 31 cycles.

APPENDIX E

ARRAY ATTRIBUTES

Table E.1 Attributes for microarray; part 1.

Attribute name	Attribute unit	Numeric	1000 DOXORUBICIN 1.txt	1000 DOXORUBUCIN 2.txt	120 DOCETAXEL 1.txt	120 DOCETAXEL 2.txt	30 DOCETAXEL 2.txt	30 DOCETAXEL l.txt	NORMAL 1.txt	NORMAL 2.txt
Array Design	Attribute unit	no	HG-U133_Plus_2	HG-U133_Plus_2	HG-U133_Plus_2	HG-U133_Plus_2	HG-U133_Plus_2	HG-U133_Plus_2	HG-U133_Plus_2	HG-U133_Plus_2
Author		no	Iseri	Iseri	Iseri	Iseri	Iseri	Iseri	Iseri	Iseri
CEL File		no	1000 DOXORUBICIN 1.CEL	1000 DOXORUBUCIN 2.CEL	120 DOCETAXEL 1.CEL	120 DOCETAXEL 2.CEL	30 DOCETAXEL 2.CEL	30 DOCETAXEL l.CEL	NORMAL 1.CEL	NORMAL 2.CEL
Analysis Name		no	RMA Percentile	RMA Percentile	RMA Percentile	RMA Percentile	RMA Percentile	RMA Percentile	RMA Percentile	RMA Percentile
Algorithm Parameters		no	Percentile:75;CellMargin:2;OutlierHigh:1.500;OutlierLow:1.004;AlgVersion:6.0;FixedCellSize:TRUE;FullFeature Width:7;FullFeatureHeight:7;IgnoreOutliersInShiftRows:FALSE;FeatureExtraction:TRUE;PoolWidthExtenstion:2; PoolHeightExtension:2;UseSubgrids:FALSE;Ran							
Experiment Type		no	Drug resistance	Drug resistance	Drug resistance	Drug resistance	Drug resistance	Drug resistance	Drug resistance	Drug resistance
Resistance		no	Doxorubicin	Doxorubicin	Docetaxel	Docetaxel	Docetaxel	Docetaxel	Sensitive	Sensitive
n	nM	yes	1000	1000	120	120	30	30	0	0
Diseased/Normal		no	Cancer	Cancer	Cancer	Cancer	Cancer	Cancer	Cancer	Cancer
Treatment type		no	Drug application	Drug application	Drug application	Drug application	Drug application	Drug application	No drug application	No drug application

Table E.2 Attributes for microarray; part 2.

Attribute name	Attribute unit	Numeric	1000 DOXORUBICIN 1.txt	1000 DOXORUBUCIN 2.txt	120 DOCETAXEL 1.txt	120 DOCETAXEL 2.txt	30 DOCETAXEL 2.txt	30 DOCETAXEL l.txt	NORMAL 1.txt	NORMAL 2.txt
Organism		no	Human	Human	Human	Human	Human	Human	Human	Human
RNA type		no	total RNA	total RNA	total RNA	total RNA	total RNA	total RNA	total RNA	total RNA
Tissue Type		no	Breast epithelial	Breast epithelial	Breast epithelial	Breast epithelial	Breast epithelial	Breast epithelial	Breast epithelial	Breast epithelial
Diseased/ Normal		no	Cancer	Cancer	Cancer	Cancer	Cancer	Cancer	Cancer	Cancer
Strain/Cell-line		no	MCF-7	MCF-7	MCF-7	MCF-7	MCF-7	MCF-7	MCF-7	MCF-7
Genetic Characteristic		no	Wild type	Wild type	Wild type	Wild type	Wild type	Wild type	Wild type	Wild type
Growth Conditions		no	RPMI 1640, 10% FBS, 2 mM L-glutamine, 1% Gentamycin							
Sampling Method		no	Cell pellet	Cell pellet	Cell pellet	Cell pellet	Cell pellet	Cell pellet	Cell pellet	Cell pellet
Treatment type		no	Drug application	Drug application	Drug application	Drug application	Drug application	Drug application	No drug application	No drug application
Labeling Protocol		no	IVT labelling	IVT labelling	IVT labelling	IVT labelling	IVT labelling	IVT labelling	IVT labelling	IVT labelling

APPENDIX F

CALCULATIONS

1. T_d

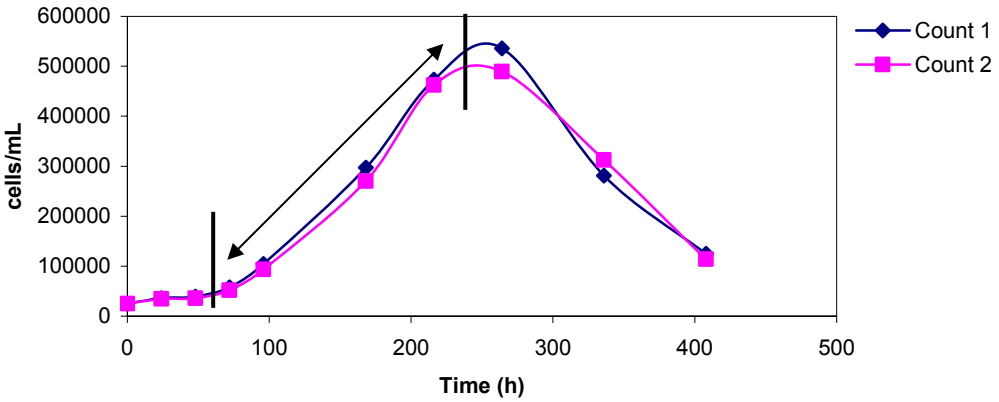

Figure F.1 A representative growth curve; labels represent logarithmic phase of the growth.

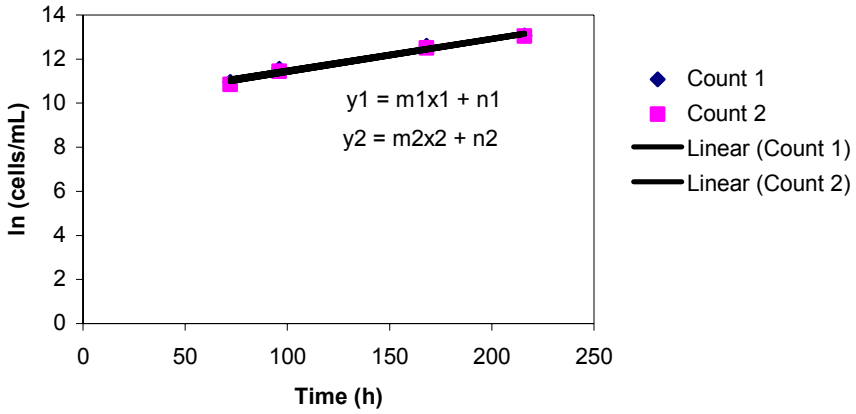

Figure F.2 Linear plot representing the logarithmic growth phase giving the equation for growth rate calculations.

From logarithmic phase of the growth curve (labeled in Figure E.1), a linear growth plot was generated as shown in Figure E.2. Slope of the trend line gives the growth rate (μ) and t_d was calculated by using μ as follows:

μ (Growth rate) = m

$t_d = \ln 2 / \mu$

Since the counts were performed in duplicates, two t_d values were calculated from m_1 and m_2 (corresponding to μ_1 and μ_2, respectively) and average of the two was considered as t_d with standard error of the means.

2. IC_{50}

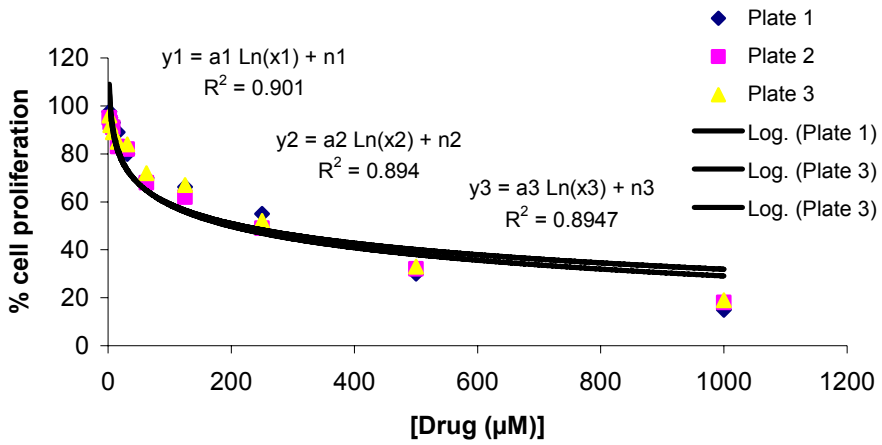

Figure F.3 A representative logarithmic proliferation curve giving the equations for IC_{50} calculations.

IC_{50} values were calculated from equations obtained from logarithmic proliferation versus drug concentration curve (Figure E.3) as follows:

50 = a Ln(x) +n where x is the concentration at which cell proliferation is 50%.

Since the experiments were performed in triplicates, three IC_{50} values were calculated from data obtained from three plates. Average of the three values was considered as IC_{50} with standard error of the means.

3. Protein Concentration Determination by Bradford

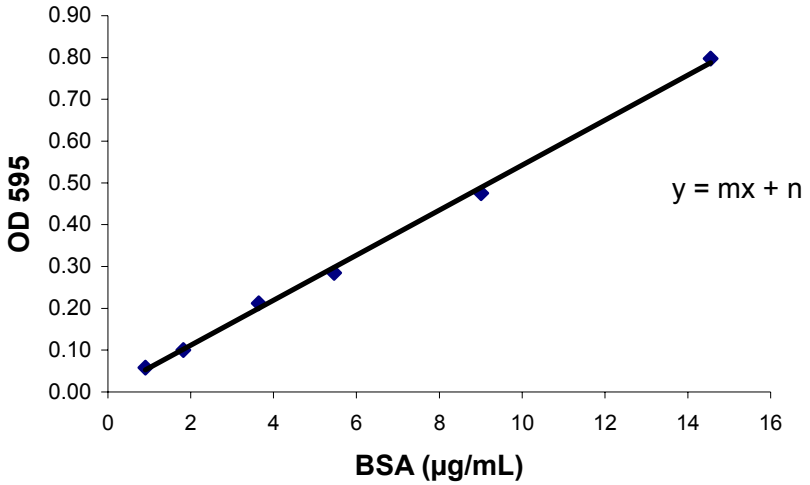

Figure F.4 A Bradford standard curve.

Protein concentration of the samples were determined from standard Bradford curves (Figure E.4). Optical density of the samples were inserted in the equation and concentration of the sample was calculated by solving the equation for x and multiplyin by the dilution factor of the sample.

APPENDIX G

DENSITOMETRY

Table G.1 Densitometric measurement data of *MDR1* RT-PCR products.

Cells	*MDR1* product		*β2-m* product		*MDR1*/*β2-m* ± SEM*	Fold change (FC) ± SEM*
MCF-7	0.00	0.00	191.98	157.23	0.00	-
MCF-7/15nM DOC	0.00	0.00	236.7	208.96	0.00	-
MCF-7/17nM DOC	0.00	0.00	150.26	156.22	0.00	-
MCF-7/20nM DOC	127.1	110.65	163.25	148.97	0.76 ± 0.02	1.00 ± 0.00
MCF-7/25nM DOC	132.64	134.67	122.87	133.78	1.04 ± 0.04	1.37 ± 0.02
MCF-7/30nM DOC	210.16	186.58	193.07	180.16	1.06 ± 0.03	1.40 ± 0.00
MCF-7/35nM DOC	219.28	195.06	211.08	179.3	1.06 ± 0.02	1.40 ± 0.07
MCF-7/45nM DOC	244.36	222.97	228.14	208.8	1.07 ± 0.00	1.41 ± 0.03
MCF-7/60nM DOC	202.32	169.31	179.41	155.45	1.11 ± 0.02	1.46 ± 0.01
MCF-7/80nM DOC	165.96	166.63	131.13	125.35	1.30 ± 0.03	1.71 ± 0.08
MCF-7/90nM DOC	248.45	223.03	189.95	171.68	1.30 ± 0.00	1.71 ± 0.03
MCF-7/120nM DOC	268.71	249.44	122.08	108.61	2.25 ± 0.05	2.96 ± 0.13
MCF7	0.00	0.00	156.95	188.63	0.00	-
MCF-7/140nM DOX	0.00	0.00	131.45	206.94	0.00	-
MCF-7/150nM DOX	0.00	0.00	162.39	207.66	0.00	-
MCF-7/160nM DOX	0.00	0.00	137.17	197.46	0.00	-
MCF-7/180nM DOX	0.00	0.00	123.6	196.34	0.00	-
MCF-7/200nM DOX	0.00	0.00	189.39	206.14	0.00	-
MCF-7/260nM DOX	0.00	0.00	152.49	169.49	0.00	-
MCF-7/400nM DOX	68.08	133.27	198.94	225.73	0.47 ± 0.12	1.00 ± 0.00
MCF-7/600nM DOX	144.33	183.01	126.53	214.68	1.00 ± 0.14	2.39 ± 0.94
MCF-7/800nM DOX	146.49	245.16	115.64	167.12	1.37 ± 0.10	3.09 ± 0.61
MCF-7/1000nM DOX	141.69	232.2	105.57	149.09	1.45 ± 0.11	3.28 ± 0.64

* SEM were derived from two independent experiments.

Table G.2 Densitometric measurement data of *MRP1* RT-PCR products.

Cells	***MRP1* product**		***β2-m* product**		***MRP1*/*β2-m* ± SEM***	**FC ± SEM***
MCF-7	222.09	228.28	157.23	191.98	1.30 ± 0.11	1.00 ± 0.00
MCF-7/15nM DOC	195.03	194.09	208.96	236.7	0.88 ± 0.06	0.68 ± 0.01
MCF-7/17nM DOC	176.37	154.13	156.22	150.26	1.08 ± 0.05	0.83 ± 0.03
MCF-7/20nM DOC	181.54	161.41	148.97	163.25	1.10 ± 0.11	0.85 ± 0.02
MCF-7/25nM DOC	159.65	140.15	133.78	122.87	1.17 ± 0.03	0.90 ± 0.06
MCF-7/30nM DOC	179.82	159.99	180.16	193.07	0.91 ± 0.08	0.70 ± 0.00
MCF-7/35nM DOC	175.32	168.27	179.3	211.08	0.89 ± 0.09	0.68 ± 0.01
MCF-7/45nM DOC	176.98	171.58	208.8	228.14	0.80 ± 0.05	0.62 ± 0.02
MCF-7/60nM DOC	174.28	170.42	155.45	179.41	1.04 ± 0.09	0.80 ± 0.00
MCF-7/80nM DOC	166.75	162.18	125.35	131.13	1.28 ± 0.05	0.99 ± 0.05
MCF-7/90nM DOC	239.47	229.87	171.68	189.95	1.30 ± 0.09	1.00 ± 0.02
MCF-7/120nM DOC	169.26	171.89	108.61	122.08	1.48 ± 0.08	1.14 ± 0.04
MCF7	92.88	150.27	156.95	188.63	0.69 ± 0.10	1.00 ± 0.00
MCF-7/140nM DOX	119.61	141.81	131.45	206.94	0.80 ± 0.11	1.20 ± 0.34
MCF-7/150nM DOX	123.97	209.67	162.39	207.66	0.89 ± 0.12	1.28 ± 0.01
MCF-7/160nM DOX	114.62	196.19	137.17	197.46	0.91 ± 0.08	1.33 ± 0.08
MCF-7/180nM DOX	123.68	176.71	123.6	196.34	0.95 ± 0.05	1.41 ± 0.28
MCF-7/200nM DOX	157.46	239.99	189.39	206.14	1.00 ± 0.17	1.43 ± 0.03
MCF-7/260nM DOX	134.69	226.87	152.49	169.49	1.11 ± 0.23	1.59 ± 0.09
MCF-7/400nM DOX	137.32	243.2	198.94	225.73	0.88 ± 0.19	1.26 ± 0.09
MCF-7/600nM DOX	88.45	165.77	126.53	214.68	0.74 ± 0.04	1.08 ± 0.11
MCF-7/800nM DOX	68.77	148.38	115.64	167.12	0.74 ± 0.15	1.06 ± 0.05
MCF-7/1000nM DOX	61.83	129.21	105.57	149.09	0.73 ± 0.14	1.04 ± 0.05

* SEM were derived from two independent experiments.

Table G.3 Densitometric measurement data of *BCRP* RT-PCR products.

Cells	***BCRP* product**		***β2-m* product**		***BCRP*/*β2-m* ± SEM***	**FC ± SEM***
MCF-7	0.00	0.00	113.8	84.38	0.00	-
MCF-7/15nM DOC	0.00	0.00	144.19	97.53	0.00	-
MCF-7/17nM DOC	0.00	0.00	167.27	109.78	0.00	-
MCF-7/20nM DOC	0.00	0.00	180.78	148.52	0.00	-
MCF-7/25nM DOC	0.00	0.00	131.37	124.82	0.00	-
MCF-7/30nM DOC	235.14	229.44	156.7	107.61	1.82 ± 0.32	1.00 ± 0.00
MCF-7/35nM DOC	85.5	46.39	188.9	92.34	0.48 ± 0.02	0.27 ± 0.03
MCF-7/45nM DOC	84.22	68.18	248.32	155.66	0.39 ± 0.05	0.22 ± 0.01
MCF-7/60nM DOC	81.97	42.82	158.54	102.34	0.47 ± 0.05	0.27 ± 0.07
MCF-7/80nM DOC	0.00	0.00	167.95	111.16	0.00	-
MCF-7/90nM DOC	0.00	0.00	174.65	109.85	0.00	-
MCF-7/120nM DOC	0.00	0.00	143.06	94.22	0.00	-

* SEM were derived from two independent experiments.

Table G.4 Densitometric measurement data of *Bcl-2* and *Bax* RT-PCR products; *SEM were derived from two independent experiments.

A)

Cells	***Bcl-2* product**		***Bax* product**		***β2-m* product**	
MCF-7	182.36	156.05	256.64	246.59	191.98	157.23
MCF-7/15nM DOC	171.73	132.74	149.22	134.99	236.7	208.96
MCF-7/17nM DOC	126.86	115.59	150.14	137.31	150.26	156.22
MCF-7/20nM DOC	122.82	108.7	192.28	200.46	163.25	148.97
MCF-7/25nM DOC	105.66	106.63	189.52	167.14	122.87	133.78
MCF-7/30nM DOC	171.55	132.92	155.42	158.49	193.07	180.16
MCF-7/35nM DOC	175.61	155.04	182.77	171.07	211.08	179.3
MCF-7/45nM DOC	178.79	147.8	175.67	180.11	228.14	208.8
MCF-7/60nM DOC	133.4	114.13	157.67	158.62	179.41	155.45
MCF-7/80nM DOC	106.23	110.06	141.32	142.9	131.13	125.35
MCF-7/90nM DOC	143.28	146.39	205.32	200.86	189.95	171.68
MCF-7/120nM DOC	133.76	95.02	170.77	167.33	122.08	108.61
MCF7	139.91	197.24	235.50	225.36	156.95	188.63
MCF-7/140nM DOX	115.28	100.22	181.13	192.49	131.45	206.94
MCF-7/150nM DOX	133.30	112.1	200.45	225.31	162.39	207.66
MCF-7/160nM DOX	116.85	109.87	151.77	205.57	137.17	197.46
MCF-7/180nM DOX	111.59	103.99	149.33	211.42	123.6	196.34
MCF-7/200nM DOX	141.27	113.65	182.56	218.01	189.39	206.14
MCF-7/260nM DOX	114.99	108.13	143.91	207.1	152.49	169.49
MCF-7/400nM DOX	149.67	117.24	180.83	223.14	198.94	225.73
MCF-7/600nM DOX	131.51	95.7	116.57	225.96	126.53	214.68
MCF-7/800nM DOX	102.26	87.19	114.91	169.08	115.64	167.12
MCF-7/1000nM DOX	100.46	72.72	113.29	164.59	105.57	149.09

Table G.4 (Continued)

B)

Cells	*Bcl-2/β2-m* ± SEM*	Fold change ± SEM*	*Bax/β2-m* ± SEM*	Fold change ± SEM*	*Bcl-2/Bax* ± SEM*	Fold change ± SEM*
MCF-7	0.91 ± 0.08	1.00 ± 0.00	1.37 ± 0.20	1.00 ± 0.00	0.67 ± 0.04	1.00 ± 0.00
MCF-7/15nM DOC	0.68 ± 0.05	0.76 ± 0.12	0.64 ± 0.01	0.48 ± 0.06	1.07 ± 0.08	1.59 ± 0.03
MCF-7/17nM DOC	0.79 ± 0.05	0.88 ± 0.14	0.94 ± 0.06	0.71 ± 0.15	0.84 ± 0.00	1.26 ± 0.07
MCF-7/20nM DOC	0.74 ± 0.01	0.82 ± 0.09	1.26 ± 0.08	0.93 ± 0.08	0.59 ± 0.05	0.88 ± 0.02
MCF-7/25nM DOC	0.83 ± 0.03	0.92 ± 0.12	1.40 ± 0.15	1.06 ± 0.26	0.60 ± 0.04	0.90 ± 0.11
MCF-7/30nM DOC	0.90 ± 0.01	0.91 ± 0.16	0.84 ± 0.04	0.63 ± 0.06	0.97 ± 0.13	1.44 ± 0.11
MCF-7/35nM DOC	0.85 ± 0.02	0.94 ± 0.07	0.91 ± 0.04	0.68 ± 0.07	0.93 ± 0.03	1.39 ± 0.04
MCF-7/45nM DOC	0.75 ± 0.04	0.83 ± 0.12	0.82 ± 0.05	0.61 ± 0.06	0.92 ± 0.10	1.36 ± 0.07
MCF-7/60nM DOC	0.74 ± 0.00	0.82 ± 0.08	0.95 ± 0.07	0.70 ± 0.05	0.78 ± 0.06	1.16 ± 0.03
MCF-7/80nM DOC	0.84 ± 0.03	0.93 ± 0.05	1.11 ± 0.03	0.83 ± 0.10	0.76 ± 0.01	1.14 ± 0.08
MCF-7/90nM DOC	0.80 ± 0.05	0.88 ± 0.03	1.13 ± 0.04	0.84 ± 0.09	0.71 ± 0.02	1.07 ± 0.08
MCF-7/120nM DOC	0.99 ± 0.11	1.10 ± 0.22	1.47 ± 0.07	1.09 ± 0.11	0.68 ± 0.11	1.00 ± 0.10
MCF7	1.00 ± 0.26	1.00 ± 0.00	1.35 ± 0.15	1.00 ± 0.00	0.77 ± 0.28	1.00 ± 0.00
MCF-7/140nM DOX	0.64 ± 0.13	0.65 ± 0.04	1.11 ± 0.26	0.81 ± 0.10	0.63 ± 0.27	0.80 ± 0.05
MCF-7/150nM DOX	0.63 ± 0.06	0.65 ± 0.10	1.09 ± 0.14	0.81 ± 0.01	0.59 ± 0.14	0.81 ± 0.11
MCF-7/160nM DOX	0.70 ± 0.10	0.72 ± 0.08	1.07 ± 0.03	0.80 ± 0.07	0.65 ± 0.12	0.91 ± 0.18
MCF-7/180nM DOX	0.70 ± 0.14	0.72 ± 0.05	1.14 ± 0.07	0.85 ± 0.05	0.63 ± 0.16	0.85 ± 0.10
MCF-7/200nM DOX	0.64 ± 0.04	0.70 ± 0.22	1.01 ± 0.05	0.76 ± 0.12	0.64 ± 0.07	0.99 ± 0.45
MCF-7/260nM DOX	0.69 ± 0.02	0.74 ± 0.18	1.08 ± 0.14	0.83 ± 0.20	0.65 ± 0.07	1.00 ± 0.45
MCF-7/400nM DOX	0.63 ± 0.04	0.68 ± 0.21	0.95 ± 0.04	0.72 ± 0.11	0.66 ± 0.07	1.02 ± 0.45
MCF-7/600nM DOX	0.68 ± 0.07	0.71 ± 0.11	0.99 ± 0.07	0.75 ± 0.13	0.69 ± 0.03	1.01 ± 0.33
MCF-7/800nM DOX	0.68 ± 0.07	0.71 ± 0.11	1.00 ± 0.01	0.75 ± 0.09	0.68 ± 0.06	0.98 ± 0.27
MCF-7/1000nM DOX	0.68 ± 0.01	0.73 ± 0.18	1.09 ± 0.02	0.82 ± 0.10	0.63 ± 0.00	0.93 ± 0.34

Table G.5 Densitometric measurement data of *β-tubulin* isotypes.

Cells	***βI***		***βII***		***βIII***		***βIVa***		***βIVb***		***βIV***		***β2-m***	
MCF-7	220.88	231.23	239.17	181.11	79.44	74.51	235.51	198.81	237.15	221.4	181.02	157.56	113.8	84.38
15nM DOC	0.00	0.00	217.69	115.36	92.22	73.47	109.33	59.21	0.00	0.00	160.52	139.95	144.19	97.53
17nM DOC	34.67	129.38	175.67	88.01	116.47	67.13	108.55	55.07	0.00	0.00	125.79	99.95	167.27	109.78
20nM DOC	33.93	132.42	176.46	105.46	87.52	58.66	113.54	57.27	0.00	0.00	139.56	143.83	180.78	148.52
25nM DOC	0.00	0.00	136.91	101.28	104.64	68.71	113.54	84.12	0.00	0.00	137.37	129.82	131.37	124.82
30nM DOC	69.03	192.76	206.36	143.1	156.31	91.61	219.67	217.29	81.2	69.8	173.35	175.75	156.7	107.61
35nM DOC	120.27	223.68	227.42	165.49	186.44	124.31	147.53	92.77	163.94	152.86	197.84	209.75	188.9	92.34
45nM DOC	242.33	232.35	244.42	203.61	252.71	224.28	213.39	103.83	228.03	225.57	231.56	279.32	248.32	155.66
60nM DOC	101.2	190.49	209.2	193.62	209.29	110.13	152.71	59.65	173.67	135.07	199.98	181.55	158.54	102.34
80nM DOC	46.36	146.63	170.55	165.09	197.42	133.89	112	53.83	155.43	144.91	179.87	192.56	167.95	111.16
90nM DOC	81.44	172.84	229.32	225.16	204.49	138.26	93.19	43.96	146.45	142.23	262.18	252.64	174.65	109.85
120nM DOC	106.33	145.67	215.96	217.75	219.63	133.05	99.26	56.44	172.71	133.99	238.18	233.92	143.06	94.22

Table G.6 Densitometric measurement ratios of *β-tubulin* isotypes to *β2-m*.

Cells	***CI/β2-m*** **± SEM***	***CII/β2-m*** **± SEM***	***CIII/β2-m*** **± SEM***	***CIVa/β2-m*** **± SEM***	***CIVb/β2-m*** **± SEM***	***CV/β2-m*** **± SEM***
MCF-7	2.32 ± 0.29	1.12 ± 0.03	0.79 ± 0.09	2.21 ± 0.14	2.35 ± 0.27	0.93 ± 0.22
MCF-7/15nM DOC	0.00	0.74 ± 0.18	0.70 ± 0.06	0.68 ± 0.08	0.00	0.68 ± 0.09
MCF-7/17nM DOC	0.54 ± 0.23	0.87 ± 0.30	0.65 ± 0.04	0.58 ± 0.07	0.00	0.74 ± 0.07
MCF-7/20nM DOC	0.48 ± 0.25	0.89 ± 0.19	0.44 ± 0.04	0.51 ± 0.12	0.00	0.91 ± 0.03
MCF-7/25nM DOC	0.00	0.94 ± 0.18	0.67 ± 0.12	0.77 ± 0.10	0.00	1.04 ± 0.01
MCF-7/30nM DOC	0.94 ± 0.29	0.93 ± 0.14	0.92 ± 0.07	1.71 ± 0.31	0.58 ± 0.07	0.94 ± 0.03
MCF-7/35nM DOC	1.24 ± 0.06	1.00 ± 0.08	1.17 ± 0.18	0.89 ± 0.11	1.26 ± 0.39	1.05 ± 0.05
MCF-7/45nM DOC	1.25 ± 0.31	1.02 ± 0.05	1.23 ± 0.21	0.76 ± 0.10	1.18 ± 0.27	1.17 ± 0.06
MCF-7/60nM DOC	1.10 ± 0.11	1.21 ± 0.04	1.20 ± 0.12	0.77 ± 0.19	1.21 ± 0.11	1.15 ± 0.14
MCF-7/80nM DOC	0.65 ± 0.23	1.31 ± 0.01	1.19 ± 0.01	0.58 ± 0.09	1.11 ± 0.19	1.45 ± 0.02
MCF-7/90nM DOC	0.87 ± 0.12	1.26 ± 0.05	1.21 ± 0.04	0.47 ± 0.07	1.07 ± 0.23	1.43 ± 0.10
MCF-7/120nMDOC	1.07 ± 0.06	1.89 ± 0.12	1.47 ± 0.06	0.65 ± 0.05	1.31 ± 0.11	2.05 ± 0.14

***** SEM were derived from two independent experiments.

Table G.7 Fold changes (FC) in *β-tubulin* isotype expressions.

Cells	**FC of βI ± SEM***	**FC of βII ± SEM***	**FC of βIII ± SEM***	**FC of βIVa ± SEM***	**FC of βIVb ± SEM***	**FC of βV ± SEM***
MCF-7	1.00 ± 0.00	1.00 ± 0.00	1.00 ± 0.00	1.00 ± 0.00	1.00 ± 0.00	1.00 ± 0.00
MCF-7/15nM DOC	0.00	0.66 ± 0.18	0.88 ± 0.03	0.31 ± 0.05	0.00	0.75 ± 0.08
MCF-7/17nM DOC	0.25 ± 0.13	0.78 ± 0.29	0.84 ± 0.15	0.26 ± 0.05	0.00	0.81 ± 0.11
MCF-7/20nM DOC	0.22 ± 0.14	0.80 ± 0.19	0.57 ± 0.12	0.23 ± 0.07	0.00	1.02 ± 0.21
MCF-7/25nM DOC	0.00	0.84 ± 0.18	0.88 ± 0.26	0.35 ± 0.07	0.00	1.18 ± 0.29
MCF-7/30nM DOC	0.43 ± 0.18	0.84 ± 0.15	1.20 ± 0.23	0.77 ± 0.09	0.25 ± 0.00	1.05 ± 0.22
MCF-7/35nM DOC	0.54 ± 0.04	0.90 ± 0.09	1.47 ± 0.06	0.40 ± 0.02	0.52 ± 0.11	1.17 ± 0.21
MCF-7/45nM DOC	0.53 ± 0.07	0.92 ± 0.07	1.54 ± 0.06	0.35 ± 0.07	0.50 ± 0.06	1.34 ± 0.37
MCF-7/60nM DOC	0.48 ± 0.11	1.08 ± 0.00	1.55 ± 0.34	0.36 ± 0.11	0.51 ± 0.01	1.27 ± 0.15
MCF-7/80nM DOC	0.29 ± 0.14	1.17 ± 0.03	1.52 ± 0.16	0.26 ± 0.06	0.47 ± 0.03	1.65 ± 0.40
MCF-7/90nM DOC	0.39 ± 0.10	1.12 ± 0.01	1.55 ± 0.13	0.21 ± 0.04	0.45 ± 0.05	1.59 ± 0.27
MCF-7/120nM DOC	0.47 ± 0.04	1.68 ± 0.06	1.90 ± 0.30	0.29 ± 0.04	0.56 ± 0.02	2.29 ± 0.39

***** SEM were derived from two independent experiments.

Table G.8 QPCR results for *MDR1*.

Cells	Mean Cp	STD Cp	Mean Concentration (MC)	STD of MC	SEM of MC	FC
MCF-7	34.40	1.00	0.0043×10^7	0.0049×10^7	0.0035×10^7	1
MCF-7/30nM DOC	28.22	0.38	0.58×10^7	0.14×10^7	0.1×10^7	134.88
MCF-7/120nM DOC	24.02	0.03	7.58×10^7	0.14×10^7	0.1×10^7	1762.79
MCF-7/400nM DOX	29.71	0.03	0.23×10^7	0.0043×10^7	0.003×10^7	53.49
MCF-7/1000nM DOX	22.48	0.02	19.6×10^7	0.29×10^7	0.21×10^7	4558.14

Table G.9 QPCR results for *MRP1*.

Cells	Mean Cp	STD Cp	Mean Concentration (MC)	STD of MC	SEM of MC	FC
MCF-7	20.34	0.34	13×10^6	3.39×10^6	2.4×10^6	1
MCF-7/30nM DOC	21.14	0.11	7.65×10^6	0.58×10^6	0.41×10^6	0.59
MCF-7/120nM DOC	21.65	0.13	5.3×10^6	0.48×10^6	0.34×10^6	0.41
MCF-7/400nM DOX	19.41	0.31	27×10^6	5.97×10^6	4.22×10^6	2.08
MCF-7/1000nM DOX	22.29	0.34	3.4×10^6	0.82×10^6	0.58×10^6	0.26

Table G.10 Densitometric measurements of Western blot results.

Cells	Bcl-2	Bax	GAPDH	Bcl-2/ GAPDH	FC	Bax/ GAPDH	FC
MCF-7	133.22	75.04	87.08	1.53	1.00	0.86	1.00
MCF-7/15nM DOC	147.16	70.79	94.67	1.55	1.02	0.75	0.87
MCF-7/17nM DOC	103.56	68.66	81.79	1.27	0.83	0.84	0.97
MCF-7/20nM DOC	103.78	56.41	101.14	1.03	0.67	0.62	0.72
MCF-7/25nM DOC	96.15	58.55	99	0.97	0.63	0.74	0.85
MCF-7/30nM DOC	97.92	58.77	111.31	0.88	0.58	0.44	0.51
MCF-7/35nM DOC	108.86	-	94.58	1.15	0.75	-	-
MCF-7/45nM DOC	118.67	-	130.67	0.91	0.59	-	-
MCF-7/60nM DOC	113.09	-	115.12	0.98	0.64	-	-
MCF-7/80nM DOC	122.02	-	129.1	0.95	0.62	-	-
MCF-7/90nM DOC	131.21	-	133.53	0.98	0.64	-	-
MCF-7/120nM DOC	148.76	-	117.16	1.27	0.83	-	-
MCF7	141.05	94.57	158.19	0.89	1.00	0.60	1.00
MCF-7/140nM DOX	127.16	91.09	172.34	0.74	0.83	0.53	0.88
MCF-7/150nM DOX	113.3	82.13	162.6	0.70	0.78	0.51	0.84
MCF-7/160nM DOX	82.68	87.03	117	0.71	0.79	0.74	1.24
MCF-7/180nM DOX	76.92	82.54	145.84	0.53	0.59	0.57	0.95
MCF-7/200nM DOX	71.68	88	146.29	0.49	0.55	0.60	1.01
MCF-7/260nM DOX	66.02	90.57	143.58	0.46	0.52	0.63	1.06
MCF-7/400nM DOX	65	-	121.47	0.54	0.60	-	-
MCF-7/600nM DOX	73.26	-	147.11	0.50	0.56	-	-
MCF-7/800nM DOX	79.43	-	147.25	0.54	0.60	-	-
MCF-7/1000nM DOX	93.57	-	153.9	0.61	0.68	-	-

Table G.11 Densitometric measurements of verapamil applications; * SEM were derived from two independent experiments.

A)

Cells	**MCF-7/120nM DOC -Vp**		**MCF-7/120nM DOC 48h Vp**		**MCF-7/120nM DOC 72h Vp**	
***MDR1* product**	192.95	203.41	123	123.16	64.02	67.81
***B2-m* product**	63.86	79.74	62.75	104.92	65.46	122.13
MDR1*/*β2-m* ± SEM	2.79 ± 0.24		1.57 ± 0.39		0.77 ± 0.21	
FC ± SEM*	1.0		0.55 ± 0.09		0.27 ± 0.05	
***MRP1* product**	119.35	179.31	101.24	175.63	54.94	125.84
***B2-m* product**	63.86	79.74	62.75	104.92	65.46	122.13
MRP1*/*β2-m* ± SEM	2.06 ± 0.19		1.64 ± 0.03		0.93 ± 0.10	
FC ± SEM*	1.0		0.80 ± 0.06		0.45 ± 0.00	

B)

Cells	**MCF-7/1000nM DOX -Vp**		**MCF-7/1000nM DOX 48h Vp**		**MCF-7/1000nM DOX 72h Vp**	
***MDR1* product**	225.65	210.41	197.78	**185.74**	75.1	91.75
***B2-m* product**	100.29	140.66	94.8	**137.32**	95.11	125.92
MDR1*/*β2-m* ± SEM	1.87 ± 0.38		1.72 ± 0.37		0.76 ± 0.03	
FC ± SEM*	1.0		0.92 ± 0.01		0.42 ± 0.07	
***MRP1* product**	114.75	188.38	**123.44**	214.43	159.54	228.02
***B2-m* product**	100.29	140.66	94.8	**137.32**	95.11	125.92
MRP1*/*β2-m* ± SEM	1.24 ± 0.10		1.43 ± 0.13		1.74 ± 0.07	
FC ± SEM*	1.0		1.15 ± 0.01		1.41 ± 0.06	

Table G.12 Densitometric measurements of promethazine applications.

Cels	Application	*MDR1*	*β2-m*	*MDR1/β2 -m*	FC
MCF-7/120nM DOC	-PRM	186.39	96.82	1.93	1.00
	+1.6µM PRM (12 h)	122.54	73.84	1.66	0.86
	+1.6µM PRM (24 h)	117.59	93.39	1.26	0.65
	+1.6µM PRM (48 h)	96.8	102.73	0.94	0.49
	+1.6µM PRM (72 h)	174.59	106.98	1.63	0.85
	+4.8µM PRM (12 h)	117.08	75.41	1.55	0.81
	+4.8µM PRM (24 h)	111.56	75.23	1.48	0.77
	+4.8µM PRM (48 h)	69	74.88	0.92	0.48
	+4.8µM PRM (72 h)	0	73.53	0	0
MCF-7/1000nM DOX	-PRM	238.54	64.25	3.71	1.00
	+1.6µM PRM (12 h)	124.3	74.46	1.67	0.45
	+1.6µM PRM (24 h)	181.7	72.08	2.52	0.68
	+1.6µM PRM (48 h)	209.76	78.77	2.66	0.72
	+1.6µM PRM (72 h)	210.97	81.63	2.58	0.70
	+4.8µM PRM (12 h)	115.74	61.77	1.87	0.50
	+4.8µM PRM (24 h)	91.37	61.51	1.49	0.40
	+4.8µM PRM (48 h)	105.61	67.96	1.55	0.42
	+4.8µM PRM (72 h)	102.98	68.6	1.50	0.40

CURRICULUM VITAE

PERSONAL INFORMATION

Surname, Name:	Darcansoy İşeri, Özlem
Nationality:	Turkish Republic
Date and Place of Birth:	9 March 1980, Ankara
Martial Status:	Married
Phone:	+90 532 6438749
e-mail :	dozlem@metu.edu.tr, oiseri@gmail.com

EDUCATION

Degree	Institution	Year of Graduation
PhD	METU Biotechnology	2009
MS	METU Biotechnology	2004
BS (High honors)	METU Biology	2002
High school	TED Ankara College	1998

WORK EXPERIENCE

Year	Place	Enrollment
October 2002- January 2009	METU Biological Sciences	Research-Teaching assistant
2001 (July-September)	TÜBİTAK DNA/Cell Bank & Gene Research Laboratory	Intern researcher

TEACHING EXPERIENCE

Year and Enrollment	Courses
2002-2009, Teaching assistant	Molecular and Transmission Genetics Laboratory, Microbiology Laboratory, Cell Biology Laboratory, General Biology Laboratory

FOREIGN LANGUAGES

Advanced English

PUBLICATIONS

Papers Published in International Journals

1. İşeri ÖD, Kars MD, Eroğlu S, Gündüz U. Cross-resistance Development and Combined Applications of Anticancer Agents in Drug Resistant MCF-7 Cell Lines. International Journal of Hematology and Oncology 2009 (In press).
2. Eskiocak U, İşeri ÖD, Kars MD, Biçer A, Gündüz U. Effect of Doxorubicin on Telomerase Activity and Apoptotic Gene Expression in Doxorubicin Resistant and Sensitive MCF-7 Cells. Chemotherapy 2008; 54: 209-216.
3. Kars MD, Iseri OD, Gunduz U, Molnar J. Reversal of MDR by Synthetic and Natural Compounds in Drug Resistant MCF-7 Cell Lines. Chemotherapy 2008; 54: 194-200.
4. Sakin V, Eskiocak U, Kars MD, İşeri ÖD, Gündüz U. hTERT Gene Expression Levels and Telomerase Activity in Drug Resistant MCF-7 Cells. Experimental Oncology 2008; 30(3): 1-4.
5. Kars MD, İşeri ÖD, Ural AU, Gündüz U. In Vitro Evaluation of Zoledronic Acid Resistance Developed in MCF-7 Cells. Anticancer Research 2007; 27: 4031-4038.
6. Kars MD, Iseri OD, Gunduz U, Ural AU, Arpaci F, Molnar J. Development of rational in vitro models for drug resistance in breast cancer and modulation of MDR by selected compounds. Anticancer Research 2006; 26: 4559-4568.
7. İşeri ÖD, Mutlu PK, Kars MD, Avcu F, Ural AU, Gündüz U: Expression of multidrug resistance 1, lung resistance protein and breast cancer resistance protein genes in chronic leukemias. Biological Research (Under review).
8. İşeri ÖD, Kars MD, Gündüz U: Antimicrotubule Resistant MCF-7 Cells Have Altered β-Tubulin Isotype mRNA Levels and Possess Single Base Substitutions in TUBB Gene. Journal of Chemotherapy (Under review).
9. İşeri ÖD, Kars MD, Arpaci F, Gündüz U: Gene Expression Analysis of Drug Resistant MCF-7 Cells: Implications for Relation to Extracellular Matrix Proteins. Cancer Science (Under review)
10. Kars MD, Iseri ÖD, Ural AU, Avcu F, Beyzadeoglu M, Dirican B, Gündüz U: Development of Radioresistance in Drug Resistant Human MCF-7 Breast Cancer Cells. Journal of Radiotherapy in Practice (Under review)

Full Papers Published in International Conferences

1. İşeri ÖD, Kars MD, Gündüz U: Promethazine inhibits MDR1 gene expression in drug resistant MCF-7 cell lines. Poster presentation, 2nd Congress of Molecular Medicine 24-26 March 2007, İstanbul-TURKEY, p308.
2. Kars MD, İşeri ÖD, Ural AU, Gündüz U: In-vitro evaluation of zoledronic acid resistance developed in MCF-7 cells. Poster presentation, 2nd Congress of Molecular Medicine, 24-26 March 2007, İstanbul-TURKEY, p304.

3. Sakin V, Eskiocak U, Kars MD, İşeri ÖD, Gündüz U: Investigation of hTERT mRNA levels and telomarase activity in drug resistant MCF-7 cells. Poster presentation, II. Congress of Molecular Medicine 24-26 March 2007, İstanbul-TURKEY, p310.

Abstracts Published in International Conferences

1. İşeri ÖD, Kars MD, Arpacı F, Gündüz U: Drug Resistant MCF-7 Cells Have Altered mRNA Levels for ECM Related Proteins. Poster presentation, 33rd FEBS Congress Biochemmistry of Cell Regulation, June 28-July 7 2008, Athens-GREECE, FEBS Journal.
2. İşeri ÖD, Kars MD, Arpacı F, Gündüz U: Alterations in β-tubulin Isotypes and AntiMicrotubule Drug Resistance in MCF-7 Cells. Poster presentation, 33rd FEBS Congress Biochemmistry of Cell Regulation, June 28-July 7 2008, Athens-GREECE, FEBS Journal.
3. Dönmez Y, İşeri ÖD, Kars MD, Gündüz U: Analysis of β-tubulin isotypes and apoptotic gene expression in response to paclitaxel treatment in MCF-7 breast carcinoma cell lines. Poster presentation, EMBO Young Scientists Forum, February 20-22 2008, İstanbul-TURKEY.
4. İşeri ÖD, Kars MD, Arpacı F, Gündüz U: Analysis of Expression of β-tubulin Isotypes and Mutations of Class I β-tubulin Gene In Docetaxel Resistant MCF-7 Cells. Poster presentation, 32nd FEBS Congress Molecular Machines, July 7-12 2007, Vienna-AUSTRIA, FEBS Journal, Vol 274 p 234.
5. Kars MD, İşeri ÖD, Gündüz U, Molnár J: Reversal of MDR by Synthetic and Natural Compounds in Drug Resistant MCF-7 Cell Lines. Poster presentation, 32nd FEBS Congress Molecular Machines, July 7-12 2007, Vienna-AUSTRIA, FEBS Journal, Vol 274 p 233.
6. Eskiocak U, İşeri ÖD, Kars MD, Biçer A, Gündüz U: Effect of Doxorubicin on Telomerase Activity and Apoptotic Gene Expression in Doxorubicin Resistant and Sensitive MCF-7 Cells. Poster presentation, 32nd FEBS Congress Molecular Machines, July 7-12 2007, Vienna-AUSTRIA, FEBS Journal, Vol 274 p 156.
7. Eroğlu S, Kars MD, İşeri ÖD, Gündüz U: Cross-resistance Development and Combined Applications of Anticancer Agents in Drug Resistant MCF-7 Cell Lines. Poster presentation, 3rd International Meeting on Medicinal and Pharmaceutical Cehmistry, 16-21 October 2007, Antalya- TÜRKİYE, p 136.
8. Ural AU, Iseri OD, Mutlu PK, Kars MD, Avcu F, Gunduz U: Expression of multidrug resistace 1, lung resistance protein and breast cancer resistance protein genes in chronic lymphocytic and chronic myelogeneous leukemia. Oral presentation, American Society of Hematology 48th Annual Meeting, 9-12 December 2006 Orlando-Florida-USA, Blood Journal of American Society of Hematology Vol. 108 No: 11 Part 2 p169b.
9. Güç E, Gündüz G, Şen P, İşeri ÖD, Kars MD, Gündüz U: Synthesis and Characterization of Dendritic Polymers and PLGA Microcapsules for Anti-Cancer Drug Release. Poster presentation, 13th International Pharmaceutical Technology Symposium, 10-13 September 2006 Antalya-TURKEY, p73.

10. Kars MD, Iseri ÖD, Gündüz U, Doleschall Z, Csuka O, Bak M, Molnár J: Analysis of Multidrug Resistance (MDR) Related Gene Expression Profiles in MCF-7 Cell Lines: Poster presentation, 19th Meeting of the European Association For Cancer Research, 1-4 July 2006, Budapest–HUNGARY, p86.
11. Kars MD, Iseri ÖD, Gündüz U, Ural AU, Molnár J: Modulation of Multidrug Resistance in Paclitaxel and Vincristine Resistant MCF-7 Cell Lines. Oral and poster presentation (Selected for presentation at Young Scientist Forum). 31st FEBS Congress, 24-29 June 2006, Istanbul-Turkey, FEBS Journal, Vol 273, p278.
12. Iseri ÖD, Kars MD, Gündüz U, Arpacı F: Investigation of Multidrug Resistance in Docetaxel and Doxorubicin Resistant MCF-7 Cell Lines. Oral presentation. 31st FEBS Congress, 24-29 June 2006, Istanbul-Turkey, FEBS Journal Vol 273, p43.
13. Iseri ÖD, Kars MD, Gündüz U: Investigation of Apoptotic Gene Expression Levels in Multidrug Resistant MCF-7 Cell Lines. Poster presentation. 31st FEBS Congress, 24-29 June 2006, Istanbul-Turkey, FEBS Journal, Vol 273 p80.
14. Kars MD, Iseri ÖD, Kücük B, Sen P, Gündüz U: An Improved Technique for Preparation of Doxorubicin Loaded PLGA Microspheres for Drug Release Studies.Poster presentation, 31st FEBS Congress, 24-29 June 2006, Istanbul-TURKEY, FEBS Journal, Vol 273 p281.
15. Kars MD, Iseri ÖD, Gündüz U, Engi H, Molnár J: Investigation of Molecular Mechanisms of Multiple Drug Resistance in MCF-7 Cell Line and Reversal of MDR. Poster presentation. 17th International Congress on Anticancer Treatment, 30 January-02 February 2006, Paris-FRANCE, p328.
16. Kars MD, Iseri ÖD, Gündüz U, Molnár J: Reversal of Multiple Drug Resistance in Anticancer Drug Selected Resistant MCF-7 Cell Lines. Oral presentation, International Seminar on Drug Resistance in Cancer, 5 December 2005, Szeged-HUNGARY, p23.
17. Demirel M, İşeri ÖD, Atalay C, Baran Y, Kaya P, Gündüz U: Investigation of molecular mechanisms of multiple drug resistance. Poster presentation, European 11th COST ACTION B16 Symposium on Multi-drug Resistance Reversal, Belek-TURKEY, 2005.
18. İşeri ÖD, Demirel M, Arpacı F, Gündüz U: Investigation of multidrug resistance gene expression in mammary carcinoma tissue samples. Poster presentation, Hellenic Association of Medical Geneticists and Aristotle University of Thessaloniki, 6th Balkan Meeting on Human Genetics, GREECE, 2004, p13.
19. Demirel M, İşeri ÖD, Ural AU, Gündüz U: Cytotoxicity and multidrug resistance gene expression analysis in MCF-7 breast carcinoma cell. Oral presentation, Hellenic Association of Medical Geneticists and Aristotle University of Thessaloniki, 6th Balkan Meeting on Human Genetics, GREECE, 2004, p76.

Abstracts Published in National Conferences

1. Dönmez Y, İşeri ÖD, Kars MD, Gündüz U: Paklitaksel Uygulanan MCF-7 Hücrelerinde Apoptotik Gen Ekspresyonu Düzeylerinin İncelenmesi. Poster sunumu, 15. Biyoteknoloji Kongresi, 28-31 Ekim 2007, Antalya- TÜRKİYE, p 63.
2. Dönmez Y, Akçay İM, İşeri ÖD, Kars MD, Gündüz U: Paklitaksel ve Vinkristin Uygulanan MCF-7 Hücrelerinde β-tubulin İzotip Ekspresyonlarının İncelenmesi. Poster sunumu, 15. Biyoteknoloji Kongresi, 28-31 Ekim 2007, Antalya- TÜRKİYE, p 64.
3. Ural AU, Iseri OD, Mutlu PK, Kars MD, Avcu F, Gunduz U: Kronik lenfositik lösemi ve kronik miyelositer lösemi vakalarında çoklu ilaç direnç 1, akciğer direnç protein ve meme kanseri direnç protein genlerinin tanımlanması. Poster sunumu, Türk Hematoloji Derneği 32. Hematoloji Kongresi, 8-12 Kasım 2006, Antalya-TÜRKİYE, Turkish Journal of Hematology Vol. 23 No:3 p131.
4. Iseri ÖD, Kars MD, Gündüz U: ATP Bağımlı Taşıyıcı Poteinlerinin Gen Ekspresyon Düzeylerinin MCF-7 Meme Kanseri Hücre Hatlarında İncelenmesi. Poster sunumu. Multidisipliner Kanser Araştırma Sempozyumu 12-15 Mart 2006, Uludağ-TÜRKİYE, p200.
5. Iseri ÖD, Kars MD, Gündüz U: Dosetaksel ve Doksorubisine Dirençli MCF-7 Meme Kanseri Hücre Hatlarında Bcl-2 ve Bax Gen Ekspresyonlarının İncelenmesi. Sözlü sunum. Multidisipliner Kanser Araştırma Sempozyumu 12-15 Mart 2006, Uludağ-TÜRKİYE, p115.
6. Eskiocak U, İşeri ÖD, Kars MD, Gündüz U: Telomeraz aktivitesinin TRAP yöntemiyle incelenmesi. Poster sunumu, 14. Ulusal Biyoteknoloji Kongresi, 31 Ağustos-2 Eylül 2005 Eskişehir-TÜRKİYE, p 545.
7. İşeri ÖD, Demirel M, Arpacı F, Gündüz U: Meme kanseri doku örneklerinde ve MCF-7 model hücre hattında ilaç dirençliliği genlerinin ekspresyon analizi. Sözlü ve poster sunumu, Türk Biyokimya Derneği Moleküler Kanser Sempozyumu, 6-7 Nisan 2004, İzmir-TÜRKİYE, p 26.
8. Demirel M, İşeri ÖD, Ünal N, Ural AU, Gündüz U: Taksoid grubu ilaçların MCF-7 meme kanseri hücre hattında sitotoksisite ve gen ekspresyonu analizleri. Poster sunumu (Special Poster Award), Klinik Biyokimya Uzmanları Derneği 1. Ulusal Kongresi, 1-4 Ekim 2003, Kapadokya-TÜRKİYE, p173.

PROJECTS INVOLVED

1. METU-Gülhane Military School of Medicine Partner Project (Reseacher): 'Investigation of Multidrug Resistance Mechanisms in Multiple Myeloma Cell Lines by Microarray Analysis (Multipl Myeloma Hücre Hatlarında İlaç Dirençliliği Mekanizmalarının Mikroarray Analizi ile İncelenmesi)' BAP2008-R-08-11-11, September 2008-On going.
2. TÜBİTAK (Reseacher): 'Synthesis of Dendritic Polymers for Anticancer Drug Release and Applications in Cell Cultures (Anti-Kanser İlaç Salımına Yönelik Dendritik Polimer Sentezi ve Hücre Kültürlerinde Uygulanması)' 107T179, July 2007-January 2009.

3. TÜBİTAK (Reseacher): 'Investigation of Mechanisms of Drug Resistance and Reversal In Different Model Cancer Cell Lines By Molecular Biology Techniques (Farklı Kanser Tiplerine Model Hücre Hatlarında İlaç Dirençlilik Mekanizmalarının Moleküler Yöntemlerle İncelenmesi ve Geri Çevirilmesi)' 106S019, June 2006-June 2008.
4. DPT (Reseacher): 'Investigation of Anticancer Drug Resistance Mechanisms and Drug Targeting in Mammary Carcinoma (Meme Kanserinde Antikanser İlaçlara Karşı Dirençlilik Mekanizmalarının İncelenmesi ve İlaç Hedeflenmesi)' BAP 07-02-DPT.02K120540-14, June 2002-June 2005.
5. METU Research Foundation Project: 'Investigation of MRP1 and BCRP Gene Expression Levels in Anticancer Drug Applied Resistant MCF-7 Cell Line' BAP-2003-07-0200-64, June 2003-April 2006.

COURSES PARTICIPATED

1. Principles in Cell Culture Technology and Artificial Organs (Hücre Kültürü Teknolojisinde Temel Prensipler ve Yapay Organlar). November 24-26, 2004, Ege University Applied Science-Technology Research Institute

SCHOLARSHIPS

1. TÜBİTAK, Doktorate Scholar in Turkey (2005-2006)
2. Türkish Society of Biochemistry FEBS Scholar (31st FEBS Congress, 2006, İstanbul-TURKEY)
3. FEBS Scholar (32nd FEBS Congress, 2007, Vienn-AUSTURIA)

AWARDS

1. Turkish Society of Hematology 32nd National Hematology Congress, November 8-12, 2006, Antalya-TURKEY, Industry Award
2. Turkish Society of Clinical Biochemists 1st National Congress, October 1-4, 2003, Kapadocia-TURKEY, Poster Special Award

MEMBERSHIPS

1. Turkish Society of Biotechnology
2. Turkish Society of Biochemistry
3. Society of Molecular Canser Research